THE UNIVERSITY OF WARWICK

Library Declaration and Deposit Agreement

1. STUDENT DETAILS

Please complete the following:

Full name: Jiamiao Hu

University ID number: 1256073

2. THESIS DEPOSIT

2.1 Under your registration at the University, you are required to deposit your thesis with the University in BOTH hard copy and in digital format. The digital copy should normally be saved as a single pdf file.

2.2 The hard copy will be housed in the University Library. The digital copy will be deposited in the University's Institutional Repository (WRAP). Unless otherwise indicated (see 2.6 below), this will be made immediately openly accessible on the Internet and will be supplied to the British Library to be made available online via its Electronic Theses Online Service (EThOS) service.
[At present, theses submitted for a Master's degree by Research (MA, MSc, LLM, MS or MMedSci) are not being deposited in WRAP and not being made available via EthOS. This may change in future.]

2.3 In exceptional circumstances, the Chair of the Board of Graduate Studies may grant permission for an embargo to be placed on public access to the thesis **in excess of two years**. This must be applied for when submitting the thesis for examination (further information is available in the *Guide to Examinations for Higher Degrees by Research*.)

2.4 If you are depositing a thesis for a Master's degree by Research, the options below only relate to the hard copy thesis.

2.5 If your thesis contains material protected by third party copyright, you should consult with your department, and if appropriate, deposit an abridged hard and/or digital copy thesis.

2.6 Please tick one of the following options for the availability of your thesis (guidance is available in the *Guide to Examinations for Higher Degrees by Research)***:**

☑ Both the hard and digital copy thesis can be made publicly available immediately

☐ The hard copy thesis can be made publicly available immediately and the digital copy thesis can be made publicly available after a period of two years (*should you subsequently wish to reduce the embargo period please inform the Library*)

☐ Both the hard and digital copy thesis can be made publicly available after a period of two years (*should you subsequently wish to reduce the embargo period please inform the Library*)

☐ Both the hard copy and digital copy thesis can be made publicly available after _____ (insert time period in excess of two years). **This option requires the prior approval of the Chair of the Board of Graduate Studies (see 2.3 above)**

The University encourages users of the Library to utilise theses as much as possible, and unless indicated below users will be able to photocopy your thesis.

☐ I **do not** wish for my thesis to be photocopied

3. GRANTING OF NON-EXCLUSIVE RIGHTS

Whether I deposit my Work personally or through an assistant or other agent, I agree to the following:

- Rights granted to the University of Warwick and the British Library and the user of the thesis through this agreement are non-exclusive. I retain all rights in the thesis in its present version or future versions. I agree that the institutional repository administrators and the British Library or their agents may, without changing content, digitise and migrate the thesis to any medium or format for the purpose of future preservation and accessibility.

4. DECLARATIONS

I DECLARE THAT:

- I am the author and owner of the copyright in the thesis and/or I have the authority of the authors and owners of the copyright in the thesis to make this agreement. Reproduction of any part of this thesis for teaching or in academic or other forms of publication is subject to the normal limitations on the use of copyrighted materials and to the proper and full acknowledgement of its source.

- The digital version of the thesis I am supplying is either the same version as the final, hard-bound copy submitted in completion of my degree once any minor corrections have been completed, or is an abridged version (see 2.5 above).

- I have exercised reasonable care to ensure that the thesis is original, and does not to the best of my knowledge break any UK law or other Intellectual Property Right, or contain any confidential material.

- I understand that, through the medium of the Internet, files will be available to automated agents, and may be searched and copied by, for example, text mining and plagiarism detection software.

- At such time that my thesis will be made publically available digitally (see 2.6 above), I grant the University of Warwick and the British Library a licence to make available on the Internet the thesis in digitised format through the Institutional Repository and through the British Library via the EThOS service.

- If my thesis does include any substantial subsidiary material owned by third-party copyright holders, I have sought and obtained permission to include it in any version of my thesis available in digital format and that this permission encompasses the rights that I have granted to the University of Warwick and to the British Library.

5. LEGAL INFRINGEMENTS

I understand that neither the University of Warwick nor the British Library have any obligation to take legal action on behalf of myself, or other rights holders, in the event of infringement of intellectual property rights, breach of contract or of any other right, in the thesis.

Please sign this agreement and ensure it is bound into the final hard bound copy of your thesis, which should be submitted to Student Reception, Senate House.

Student's signature: .....…… Date: .....

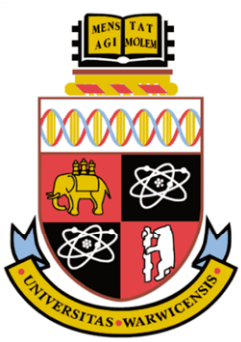

THE UNIVERSITY OF WARWICK

THE EFFECTS OF SHORT-CHAIN FATTY ACID ACETATE ON BROWN ADIPOCYTES DIFFERENTIATION AND METABOLISM

By

Jiamiao Hu, MSc.

A thesis submitted in fulfilment of the requirements for the degree of Doctor of Philosophy in Medical Sciences

Warwick Medical School

University of Warwick, United Kingdom

March, 2016

Supervisors

Dr. Jing Chen & Dr. Harpal S. Randeva

Contents

List of Tables

List of Figures

Acknowledgement

First, I would like to express my sincere gratitude to my supervisor(s) Dr. Jing Chen & Dr. Harpal S. Randeva, for their invaluable support and guidance throughout all the time of my research and writing of this thesis. I appreciate their vast knowledge and skills in laboratory work, as well as their assistance in writing and presenting this thesis.

I am also indebted to Dr. Ioannis Kyrou, Dr. Manjunath Ramanjaney, Dr. Gyanendra Tripathi, Mr. Sean James, Dr. Vanlata Patel, Dr. Mingzhan Xue, Prof. Bo Bai, Prof. Bo Ban, Dr. Xiaoyu Chen, Msc. Xin Cai, Msc. Sarah Hamzah and Dr. Adya Raghu for their sound advice, kindly help and excellent guidance in my research. Especially I want thank Dr. Ioannis Kyrou and Dr. Manjunath Ramanjaney, for their hard questions that incented me to widen my research from various perspectives. I also would like to acknowledge Prof. Bo Bai, Dr. Xiaoyu Chen and Msc. Xin Cai, for obtaining ethical approval for animal research as well as caring the animals and collecting the samples.

Besides, I also gratefully acknowledge Coventry General Charities, who fully provided the fund for this project. Meanwhile, I am also grateful to Diabetic Fund and University of Warwick Departmental S'SHIPS/BURS'S for providing me with financial support during my study.

In addition, I also would like to express my appreciation to my parents and my wife, for their continuous financial support, indispensable help, enthusiastic love, encouragement and sacrifice in the past few years. This thesis would not have been finished without their blessing.

Finally, I would like to thank everybody who helped me, as well as express my sincere apology that I could not mention personally one-by-one.

Declaration

Hereby I declare that this thesis is submitted to the University of Warwick in support of my application for the degree of Doctor of Philosophy. It has been composed by myself and has not been submitted in any previous application for any degree. The work presented (including data generated and data analysis) was carried out by the author except in the cases outlined below:

Construction of IM-BAT cells was carried out by Dr. Mark Christian (Warwick Medical School, University of Warwick);

Preparation of formalin-fixed, paraffin-embedded brown adipose tissues sections was carried out by Mr. Sean James (West Midlands Genomic Medical Centre, UHCW NHS Trust)

Animals care and tissue samples collection were carried out with the help from Dr. Xiaoyu Chen and Msc. Xin Cai (Institute of Neurobiology, Jining Medical University)

Parts of this thesis have been submitted to *Endocrinology* and accepted for publication.

All the research has been undertaken in accordance with University Safety Policy; Guidelines on Ethical Practice and the Guide for the Care and Use of Laboratory Animals.

Jiamiao Hu

List of Publications

1. Hu J, Kyrou I, Tan BK, Dimitriadis GK, Ramanjaneya M, Tripathi G, Patel VH, James S, Kawan M, Chen J, Randeva HS. Short-chain Fatty Acid Acetate Stimulates Adipogenesis and Mitochondrial Biogenesis via GPR43 in Brown Adipocytes. *Endocrinology.* 2016 May;157(5):1881-94. doi: 10.1210/en.2015-1944. Epub 2016 Mar 18. PubMed PMID: 26990063.

2. Ramanjaneya M, Tan BK, Rucinski M, Kawan M, Hu J, Kaur J, Patel VH, Malendowicz LK, Komarowska H, Lehnert H, Randeva HS. Nesfatin-1 inhibits proliferation and enhances apoptosis of human adrenocortical H295R cells. *J Endocrinol.* 2015 Jul;226(1):1-11. doi: 10.1530/JOE-14-0496. Epub 2015 Apr 13. PubMed PMID: 25869615.

3. Ban B, Bai B, Zhang M, Hu J, Ramanjaneya M, Tan BK, Chen J. Low serum cartonectin/CTRP3 concentrations in newly diagnosed type 2 diabetes mellitus: in vivo regulation of cartonectin by glucose. *PLoS One.* 2014 Nov 19;9(11):e112931. doi: 10.1371/journal.pone.0112931. eCollection 2014. PubMed PMID: 25409499; PubMed Central PMCID: PMC4237345.

4. Tan BK, Chen J, Hu J, Amar O, Mattu HS, Ramanjaneya M, Patel V, Lehnert H, Randeva HS. Circulatory changes of the novel adipokine adipolin/CTRP12 in response to metformin treatment and an oral glucose challenge in humans. *Clin Endocrinol (Oxf).* 2014 Dec;81(6):841-6. doi: 10.1111/cen.12438. Epub 2014 Mar 19. PubMed PMID: 24612181.

5. Tan BK, Chen J, Hu J, Amar O, Mattu HS, Adya R, Patel V, Ramanjaneya M, Lehnert H, Randeva HS. Metformin increases the novel adipokine cartonectin/CTRP3 in women with polycystic ovary syndrome. *J Clin Endocrinol Metab.* 2013 Dec;98(12):E1891-900. doi: 10.1210/jc.2013-2227. Epub 2013 Oct 23. PubMed PMID: 24152681.

Summary

Short-chain fatty acids (SCFA) are a sub-group of fatty acids including formic acid, acetic acid, propionic acid, isobutyric acid, butyric acid, isovaleric acid and valeric acid. Acetate, propionate and butyrate are three major short-chain fatty acids, which are mainly formed in the gastrointestinal tract *via* colonic bacteria fermentation of carbohydrates, especially resistant starches and dietary fibre. There has been increasing interest in the idea that the short-chain fatty acids play crucial roles in a range of physiological functions. Recently, increasing evidence suggested there is a strong link between short-chain fatty acids and energy homeostasis. Several studies highlighted the protective effects of the short-chain fatty acids on high-fat diet induced obesity and other harmful metabolic disorders in mice. However, the coherent understanding of the multi-level network in which short-chain fatty acids exert their effects still needs to be elucidated. Up to date, it has been demonstrated that short-chain fatty acids can mediate energy balance *via* affecting appetite control in brain, increasing adipogenesis in white adipocyte, and regulating insulin sensitivities in white adipose tissue and muscle, etc.. However, the effects of short-chain fatty acids on brown adipocytes have not been fully investigated.

In this study, we examined the roles of short-chain fatty acid acetate and its receptor(s) in the regulation of brown adipocyte differentiation and metabolism. Firstly, we identified the expression of short-chain fatty acids sensing GPR43 in brown adipose tissue and immortalized brown adipocytes

by real-time PCR, Western blots and immunohistochemistry. Moreover, GPR43 expression was found to increase during the adipogenesis of cultured brown adipocytes. Pro-adipogenic reagent PPARγ agonist stimulation led to a further augment of GPR43 expression while anti-adipogenic reagents such as PPARγ antagonist, RXR antagonist and STAT5 inhibitor played the opposite role on GPR43 expression. Transcription factors such as XBP1 and STAT5 were identified to be involved in GPR43 expression regulation in brown adipocytes.

Furthermore, we also examined the role of acetate in the regulation of brown adipogenesis. Our results showed that acetate treatment during adipogenesis up-regulated AP2, PGC-1α and UCP1 expression and affected the morphological changes of brown adipocytes. Moreover, an increase in mitochondrial biogenesis was observed after acetate treatment. Acetate also elicited the activation of ERK and CREB, and these responses were sensitive to $G_{(i/o)}$-type G-protein inactivator, Gβγ-subunit inhibitor, PLC inhibitor and MEK inhibitor, indicating a role for the $G_{(i/o)}$βγ/PLC/PKC/MEK signalling pathway in these responses. These effects of acetate were mimicked by treatment with 4-CMTB, a synthetic GPR43 agonist, and were impaired in GPR43 knock-down cells, further supported the hypothesis that GPR43 mediates the pro-adipogenic effects of acetate in brown adipocytes. Furthermore, the effects of acetate treatment on brown adipose tissue were also measured *in vivo*. Mice fed with acetate demonstrated increased PGC-1α in brown adipose tissue, which was in agreement with the results obtained from immortalized brown adipocytes.

In addition, we also measured the effects of acetate on lipid metabolism in differentiated brown adipocytes. The results showed effects of acetate treatment on lipolysis were different in white adipocytes and brown adipocytes. Acetate treatment significantly decreased the lipolysis in white adipocytes while had little effects on lipolysis in brown adipocytes. Besides, acetate treatment was also found to decrease TF2-C12 fatty acid uptake in differentiated IM-BAT cells, suggesting acetate may affect many aspects of lipid metabolism in brown adipocytes.

Collectively, our results indicated that acetate might have important physiological roles in brown adipocytes. Short-chain fatty acids may serve to regulate brown adipose tissue functions and therefore improve metabolic health.

Abbreviations

˚C: degree Celsius

4-CMTB: 4-chloro-α-(1-methylethyl)-N-2-thiaz-olylbenzeneacetamide

APS: ammonium persulfate

Akt: RAC-alpha serine/threonine-protein kinase

AMPK: AMP-activated protein kinase

ATP: adenosine triphosphate

BAT: brown adipose tissue

BCA: bicinchoninic acid

bp: base pairs

BSA: bovine serum albumin

cAMP: cyclic adenosine monophosphate

cDNA: complementary Deoxyribonucleic Acid

CHOP: C/EBP homologous protein

Ct: threshold cycle

Da: Daltons

DMEM: Dulbecco’s modified Eagle's medium

DNase: deocyribonuclease

dNTP: deoxynucleoside triphosphate

ECL: enhanced chemiluminescence

EDTA: ethylenediamine tetra-acetate

ERK: extracellular signal Regulated Kinases

FAD: flavin adenine dinucleotide

$FADH_2$: flavin adenine dinucleotide, reduced

FCCP: Carbonyl cyanide-4-(trifluoromethoxy)phenylhydrazone

FFA: free fatty acids

GAPDH: glyceraldehyde-3-Phosohate Dehydrogenase

g: gram

gDNA: genomic deoxyribonucleic acid

GLP-1: glucagon-like peptide-1

GPCR: G Protein-coupled Receptors

h: hour

IHC: immunohistochemistry

LCFA: long-chain fatty acids

M: Molar

MAPKKK: mitogen-activated protein kinase kinase kinase

MAPKK: mitogen-activated protein kinase kinase

MAPK: mitogen-activated protein kinase

MEM: minimal essential medium

mA: milliampere

min: minutes

mg: milligram

mL: millilitre

mM: millimolar

mRNA: messenger ribonucleic acid

mtDNA: mitochondrial deoxyribonucleic acid

MTT: 3-(4,5-dimethylthiazol-2-yl)-2,5-diphenyltetrazolium bromide

MTS: 3-(4,5-dimethylthiazol-2-yl)-5-(3-carboxymethoxyphenyl)-2-(4-

sulfophenyl)-2H-tetrazolium

NAD: Nicotinamide adenine dinucleotide

NADH: Nicotinamide adenine dinucleotide, reduced

PBS: phosphate buffer saline

PCR: polymerase chain reaction

Pen/Strep: penicillin/streptomycin

PYY: peptide YY

real-time PCR: real-time quantitative reverse transcription PCR

RNase: ribonuclease

RT-PCR: reverse transcription polymerase chain reaction

shRNA: small hairpin ribonucleic acid

siRNA: small interfering ribonucleic acid

TAE: tris-acetate-EDTA

TBS: tris-buffered saline

TEMED: tetramethylethylenediamine

UV: ultraviolet

V: volts

WAT: white adipose tissue

WB: Western blot

XBP1: X-box binding protein 1

Chapter 1: Introduction

1.1 Free fatty acids

Free fatty acids (FFAs) are a group of carboxylic acids with a long aliphatic chain, which can be categorized according to their chemical properties or metabolism profiles (Calder, 2015)

For example, according to the absence or existence of the carbon-carbon double bond within fatty acid chain, fatty acids can be divided into saturated and unsaturated fatty acids (figure 1-1) (Lobb and Chow, 2007); while according to the aliphatic chain length, the fatty acids can be categorized into short-chain fatty acids (with aliphatic chain shorter than 6 carbons), medium-chain fatty acids (with aliphatic chain of 6-12 carbons), and long-chain fatty acids (with aliphatic chain longer than 13 carbons) (Gunstone, 1996)

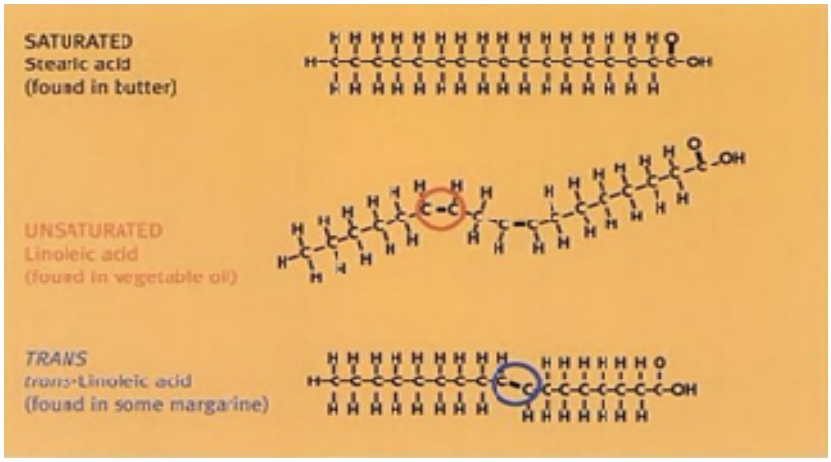

Figure 1-1 Difference in structures of saturated and unsaturated fatty acids. Red circle represents the *cis* double bonds in aliphatic chain of linoleic acid, while blue circles shows the *trans* double bond in aliphatic chain of trans-linoleic acid. (Watson, 2008).

Besides, fatty acids also can be classified into essential fatty acids and non-essential fatty acids according to their dietary necessity (Elkins, 1999). The essential fatty acids are fatty acids required for biological processes but can

not be synthesized in the body and must be obtained from diet (Kaur et al., 2014). Until now, two fatty acids: alpha-linolenic acid and linoleic acid are recognized as essential fatty acids for human beings (Kaur et al., 2014). Besides, several other fatty acids such as docosahexaenoic acid (DHA) and eicosapentaenoic acid (EPA) are needed under certain developmental or disease conditions, therefore sometimes are defined as conditionally essential fatty acids (Cunnane, 2003).

The major role of fatty acids is producing energy, especially in the negative energy balance status (Calder, 2015). Due to the advantage that the same amount of fats (esterified fatty acids) can release more stored chemical energy in the form of ATP compared to carbohydrates and proteins, fatty acids are the most effective way to store excess energy in the form of triglycerides (Numa, 1984). However, fatty acids not only function as energy sources but also act to influence cell and tissue metabolism. Increasing evidence supports the hypothesis that free fatty acids and their receptors function as nutrient sensors to regulate a variety of physiological homeostasis, including energy homeostasis (Ichimura et al., 2009). It is now clear that fatty acids are linked with a range of diseases such as obesity, type 2 diabetes, hypertension, atherogenic dyslipidaemia, and non-alcoholic fatty liver disease (Boden, 2011). For example, plasma free fatty acids levels are up-regulated in obesity patient (Opie and Walfish, 1963). Increased free fatty acids level leads to the insulin resistance in skeletal muscle and liver (DeFronzo et al., 1981, Boden et al., 2002). Besides, free fatty acids have also been proved to level up NF-γB activation and pro-inflammatory cytokines expression in human skeletal muscle (Itani et al., 2002) and

adipocyte (Chung et al., 2005). Furthermore, free fatty acids were also found to induce ER stress in adipocyte (Guo et al., 2007), liver cells, and pancreatic β-cells (Urano et al., 2000). Indeed, a better understanding of fatty acids functions may provide potential therapeutic avenues to tackle many diseases.

1.1.1 Long-chain fatty acids and medium-chain fatty acids

Long-chain fatty acids contain more than 13 carbon atoms on their aliphatic chains. Both saturated and unsaturated long-chain fatty acids have been found to be vital for normal physical functions. Palmitic acid (16:0) and stearic acid (18:0) are two most abundant saturated fatty acids in nature. They widely exist in animal products of diets. Several studies have shown that intake of these two fatty acids leads to the rise of cholesterol in blood, which was thought to be the risk factor for cardiovascular disease. However, recent evidence showed that there is no significant direct association between saturated long-chain fatty acids consumption and heart disease (Felton et al., 1994, Siri-Tarino et al., 2010). In contrast, saturated fat and dietary cholesterol display protective functions in the heart and reduce endothelial inflammation. It is now believed that combination of high-sugar diet, *trans* fat and long-chain saturated fat contributes to the development of cardiovascular disease more than long-chain saturated fat itself.

Besides, circulating concentrations of saturated long-chain fatty acids can also reflect the risk of type 2 diabetes. A study including 12,403 people with incident type 2 diabetes and 16,154 comparator individuals demonstrated an interesting finding that plasma palmitic, and stearic acids were positively associated with incident type 2 diabetes while pentadecanoic acid (15:0),

heptadecanoic acid (17:0), arachidic acid (20:0), behenic acid (22:0), tricosanoic acid (23:0), and lignoceric acid (24:0) were inversely associated with incident type 2 diabetes, suggesting the saturated long-chain fatty acids might be not homogeneous in their metabolic effects (Forouhi et al., 2014). Polyunsaturated long-chain fatty acids, especially the long-chain omega-3 polyunsaturated fatty acids such as eicosapentaenoic acid (EPA, 20:5, n-3) and docosahexaenoic acid (DHA, 22:6, n-3), have demonstrated a range of beneficial effects including lowering blood pressure, treating depression and decreasing the risk of heart attacks (Miyajima et al., 2001, Grosso et al., 2014, Marik and Varon, 2009). In addition, EPA and DHA play crucial roles in central nervous system and visual function development in infants (Innis, 2007). Studies have demonstrated that exposure to higher levels of DHA promoted cognitive development in human infants such as increased scores on the Fagan test of novelty preference at 6 months of age (O'Connor et al., 2001); better problem solving abilities at 9 (Willatts et al., 1998b) and 10 (Willatts et al., 1998a) months of age; more rapid information processing at 6.5, 9 and 12 months of age (Werkman and Carlson, 1996); and more development of attention at 12 and 18 months of age (Colombo et al., 2004). Because of its crucial role in the growth and development of infants, DHA is also regarded as a conditionally essential fatty acid and added as supplement to most infant formula (Cunnane, 2003).

Medium-chain fatty acids have between 6 and 12 carbon atoms. The major medium-chain fatty acids in edible oils and diet include caproic acid (6:0), caprylic acid (8:0), capric acid (10:0) and lauric acid (12:0). In a double-blind,

controlled human trial, the results demonstrated that medium-chain fatty acids decreased body weight and suppressed fat deposition, suggesting medium-chain fatty acids might own health beneficial properties on metabolic disorders (Tsuji et al., 2001). Meanwhile, as ketogenic diet, medium-chain saturated fatty acids and their esterified form (medium-chain triglycerides) were found to alleviate neurodegenerative disorders such as Alzheimer's disease (Maalouf et al., 2009). A randomized, double-blind, placebo-controlled, multicenter trial showed that ketogenic agent AC-1202 (a commercial form of medium-chain triglycerides) improved ADAS-Cog scores in mild to moderate Alzheimer's disease (Henderson et al., 2009). Medium-chain saturated fatty acids are also linked to the control of immune responses. Lauric acid (12:0) and its monoglyceride (monolaurin) are considered to offer wide-spectrum anti-viral, anti-bacterial and anti-fungal properties (Lieberman et al., 2006). Indeed, monolaurin exists in breast milk and plays important roles for infant immunity.

In addition to these discovered functions of long-chain fatty acids and medium-chain fatty acids, future studies can provide more information about the functions of these fatty acids and may provide nutrient and therapeutic benefits for humans.

1.1.2 Short-chain fatty acids

Short-chain fatty acids (SCFAs) are a sub-group of fatty acids containing less than 6 carbon atoms, including formic acid, acetic acid, propionic acid, isobutyric acid, butyric acid, isovaleric acid and valeric acid.

Short-chain fatty acids are the major by-products formed in the gastrointestinal tract *via* colonic bacteria fermentation of carbohydrates, especially resistant starch and dietary fibre (Andoh et al., 2003). It has been recognised for a long history that dietary fibre would benefit the digestive system healthy and contribute to other health issues, such as lowering cholesterol level and controlling blood glucose level (Brown et al., 1999, Causey et al., 2000). Recently, studies have revealed that these beneficial effects of high-fibre diets are, at least partly, attributed to its end-products by digestion as short-chain fatty acids (Canfora et al., 2015). It has been suggested that dietary intake of resistant starch in excess of 30 g per day leads to high-peripheral circulating acetate in blood (Robertson et al., 2005).

In human, acetate, propionate and butyrate are three major short-chain fatty acids, which account for 83% of short-chain fatty acids produced in gut (Velazquez et al., 1997). Because substrate for colonic fermentation is at highest level in proximal colon (including ascending colon and transverse colon), the colonic fermentation mainly occurs in proximal colon. Therefore, the total amount of short-chain fatty acids in the proximal colon is higher (at around 70 to 140 mM) than that in the distal colon (ranged from 20 to 70 mM) (Topping and Clifton, 2001).

After produced in gastrointestinal tract, short-chain fatty acids are absorbed by colon rapidly and efficiently. It is estimated that only less than 10% of short-chain fatty acids produced in colon would be excreted in human feces. Butyrate is largely absorbed in colon and plays as the major energy source for colonocytes (Wong et al., 2006). Butyrate oxidation has been shown to

make up around 70% and 60% of the oxygen consumed in human descending colon and ascending colon when physiological levels of glucose and butyrate was present (Roediger, 1980). Liver is another organ which can absorb the short-chain fatty acids. Propionate is mainly absorbed in the liver (Wong et al., 2006). Recently, a research to measure short-chain fatty acids exchange across the gut and liver in humans at surgery showed little intestinal produced butyrate and propionate escaped the splanchnic area because of highly efficient hepatic uptake of propionate (Bloemen et al., 2009).

Followed by colonic fermentation, most of acetate enters the peripheral circulation to be metabolized by peripheral tissues (Wong et al., 2006). Usual short-chain fatty acids concentration in the bloodstream are 100-150 μM for acetate, 4-5 μM for propionate and 1-3 μM for butyrate (Wolever et al., 1997), indicating the majority of short-chain fatty acids functions in peripheral tissues are attribute to the acetate. Indeed, recent research shows this blood concentration of acetate is in the range for activating its receptors such as GPR43 and GPR41 (Brown et al., 2003).

Clinical studies have found that short-chain fatty acids administration positively influenced the treatment of ulcerative colitis, Crohn's disease, and antibiotic-associated diarrhea (Harig et al., 1989, Vernia et al., 1995, Di Sabatino et al., 2005, Binder, 2010), which highlighted the involvment of short-chain fatty acids in a wide range of biological functions. Besides, short-chain fatty acids also showed significant anti-proliferative activity on colon cancer both in *in vitro* and *in vivo* studies, among which butyrate displayed

most potential (Goncalves and Martel, 2013). Indeed, it has been indicated that incidence rates of bowel cancer, diabetes and coronary heart disease are much lower in countries with traditionally high-fibre diets (Slavin, 2013). Recent studies also showed that short-chain fatty acids are important regulators in metabolism and energy homeostasis. For example, acetate may cross the blood-brain barrier and lead to appetite suppression *via* mediating neuropeptides in appetite regulation, indicating short-chain fatty acids can affect energy intake *via* central appetite regulation (Frost et al., 2014). Also, dietary supplementation of butyrate improved insulin sensitivity and increased energy expenditure in adipose tissue, muscle and liver of dietary-obese C57BL/6J mice, suggesting short-chain fatty acids may have potential application in the treatment of metabolic syndrome *via* peripheral organs (Gao et al., 2009). Indeed, a better understanding towards the roles of short-chain fatty acids in metabolism may provide useful information for keeping energy homeostasis.

1.2 Free fatty acids-sensing G protein-coupled receptors

1.2.1 G-Protein coupled receptor

G-Protein coupled receptors, also known as GPCRs, constitute the largest family of cell membrane receptors in eukaryotes and play significant roles in a diversity of cellular physiology (Salon et al., 2011). Although GPCRs function diversely and sense various ligands with different structures, they share a common structure called seven-transmembrane domain (Lu et al., 2002). GPCRs are thus also described as seven-transmembrane domain

receptors or 7-TM receptors (figure 1-2) (Pierce et al., 2002). Besides, most GPCRs (Class 1 GPCRs) also have a common palmitoylated cysteine at C-terminus or intracellular loops (Goddard and Watts, 2012). In contrast, GPCRs show great multiplicity in the regions of extracellular N-terminus, intracellular C-terminus, intra- and extra-cellular loops, which could be the structure basis for its diversity functions.

According sequence homology, GPCRs are classically divided into three main classes: Class 1 (aka Class A, Rhodopsin-like), Class 2 (aka Class B, Secretin-like), Class 3 (aka Class C, Glutamate Receptor-like). Three distinct GPCR families display their own characteristic sequence and evolutionary relationship.

Majority (approximately 90%) of GPCRs belongs to Class 1 (Class A) GPCRs (Davenport et al., 2013), which can be further classified into 19 sub-families (Subfamily A1 – A19) according to a phylogenetic analysis (Joost and Methner, 2002).

The Class 2 (Class B) GPCRs feature a globular N-terminal extracellular domain (ECD) with conserved disulfide bonds and a characteristic seven-transmembrane signature (Hollenstein et al., 2014).

The Class 3 (Class C) GPCRs normally contain a unique large hydrophilic extracellular agonist-binding regions and several conserved cysteine residues (Brauner-Osborne et al., 2007).

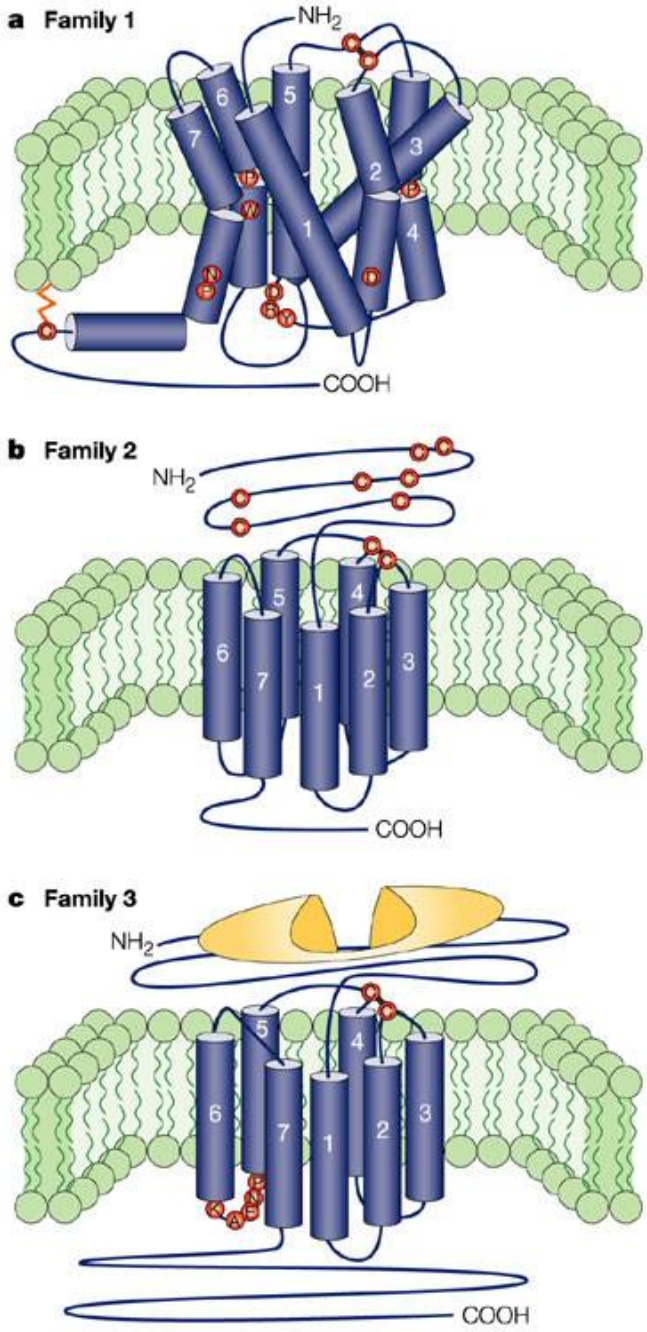

Figure 1-2 The structures of G-protein coupled receptors families. Family 1 (family A) GPCRs: red circles show highly conserved amino acids; black line represents a disulfide bridge connecting the first and second extracellular loops; orange zigzag show the palmitoylation of carboxyl-terminal tail, which serves as an anchor to the membrane. Family 2 (family B) GPCRs: red circles show cysteines located in the N-terminal extracellular domain, which normally form conserved disulfide bridges. Family 3 (family C) GPCRs: yellow shows an example of

hydrophilic extracellular agonist-binding regions of family 3 GPCRs. (EllisClare, 2004) .

Due to their involvement in multiple physiological functions, GPCRs have been the centre of drug discovery (Salon et al., 2011). It is estimated that currently nearly 40% of the drugs on the market function through GPCRs (Overington et al., 2006).

Despite no detectable shared sequence homology between classes, all GPCRs have a common mechanism of signal transduction. GPCRs transmit signals into cell through its coupled guanine nucleotide-binding proteins (G proteins). G proteins, also known as heterotrimeric G proteins complexes, are composed of Gα, Gβ and Gγ subunits (Cabrera-Vera et al., 2003). The standard model of G protein signalling is shown in figure 1-3 (EllisClare, 2004). In the inactive state of GPCRs, the Gα subunit binds to a molecular of GDP and forms a tight association with Gβγ heterodimer at the inside surface of cell membrane (Conklin and Bourne, 1993). Once GPCRs are activated by ligands, the Gα subunit undergoes a conformational change leading to an exchange of GTP for GDP, allowing it dissociating from Gβγ heterodimer (McCudden et al., 2005). Both dissociated Gα subunit and Gβγ heterodimer can transduce the downstream signals, respectively (Clapham and Neer, 1993). The signals will be terminated by intrinsic GTPase activity of Gα subunit, which catalyses the hydrolysis of bound GTP into GDT and leads to the re-association of Gα subunit and Gβγ heterodimer (Kleuss et al., 1994).

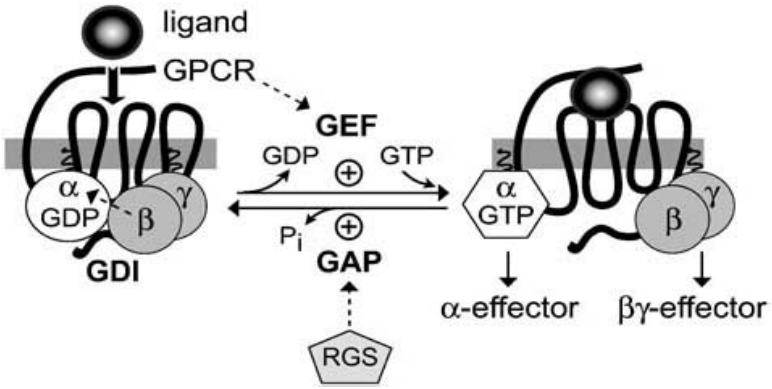

Figure 1-3 Standard model of GDP/GTP cycle in GPCR signalling pathways. In the resting state, Gα subunit is GDP bound and closely associated with the Gβγ heterodimer to form heterotrimeric G proteins, which interacts with the cytosolic loops of GPCRs located on cell membrane. Gβγ stabilizes Gα coupling to GPCR and also functions as a guanine nucleotide dissociation inhibitor (GDI) to inhibiting the spontaneous exchange of GDP for GTP on Gα subunit. When ligand binds to GPCR, the receptor act as guanine nucleotide exchange factors (GEFs) and induces a GDP to GTP exchange in the Gα subunit and the dissociation from Gβγ heterodimer. Both Gα subunit and Gβγ heterodimer trigger downstream effects. The cycle returns to the resting state when Gα hydrolyses GTP back to GDP. GTPase-accelerating proteins (GAPs), such as the Regulator of G-protein Signalling (RGS) proteins, could accelerate this process (McCudden et al., 2005).

According to their sequence homology and functional similarity, the Gα subunits can be divided into four major catalogues including $G\alpha_s$ family ($G\alpha_{(s/olf)}$), $G\alpha_{(i/o)}$ family ($G\alpha_{(i1/i2/i3/o/t\text{-}rod/t\text{-}cone/gust/z)}$), $G\alpha_q$ family ($G\alpha_{(q/11/14/16)}$), and $G\alpha_{(12/13)}$ family (Simon et al., 1991). $G\alpha_s$ subunits mainly stimulate adenylyl cyclase (AC) and increase cellular levels of cAMP, which is an important second messenger in cells (Hanoune and Defer, 2001). In contrast, $G\alpha_i$ subunits play an opposite role to $G\alpha_s$ subunits, which inhibit adenylyl cyclase (AC) and decrease cellular levels of cAMP (Simonds, 1999, Hanoune and Defer, 2001). $G\alpha_q$ subunits activate phospholipase C (PLC), which then

cleave phosphatidylinositol 4,5-bisphosphate (PIP2) into diacyl glycerol (DAG) and inositol 1,4,5-triphosphate (IP_3), followed by Ca^{2+} release from endoplasmic reticulum (ER) and protein kinase C (PKC) activation (Ross, 2011). Compared to widely studied $G\alpha_s$, $G\alpha_i$ and $G\alpha_q$ signals, $G\alpha_{(12/13)}$ signal was less understood. Up to date, it has been found that $G\alpha_{(12/13)}$ subunits mainly regulate small G-protein Rho activity (Riobo and Manning, 2005). Besides, dissociated Gβγ heterodimer also regulates large number of downstream effectors including PI3Kγ, MAPKs, and Ion channels, etc.. (Tilley, 2011).

A range of selective inhibitors have been discovered to differentiate the signalling pathways elicited by different G protein subunits. For example, pertussis toxin (PTX) catalyses the ADP-ribosylation of the $G\alpha_{(i/o)}$ subunits and prevents the G proteins interacting with GPCRs on the cell membrane, thus interfering the downstream signalling (Mangmool and Kurose, 2011). Therefore, PTX has become a widely used biochemical tool to study the signal transduction of $G\alpha_{(i/o)}$-coupled receptor signalling. Meanwhile, NF 449 and NF 503 were found to be selective $G\alpha_s$ antagonists, with little effects on $G\alpha_{(i/o)}$ and $G\alpha_{(q/11)}$-coupled receptors (Hohenegger et al., 1998). Recently, $G\alpha_{(q/11)}$-selective inhibitors such as YM-254890 and WU-07047 have also been reported, which blocks the exchange of GDP for GTP in $G\alpha_{(q/11)}$ activation (Rensing et al., 2015). Besides, Gallein, a cell-permeable xanthene compound, binds to Gβγ with high affinity and effectively blocks Gβγ-dependent cellular activities (Lehmann et al., 2008). Taken together,

these specific inhibitors and loss-of-function G-proteins mutants can be used to determine the downstream signalling after GPCRs activation.

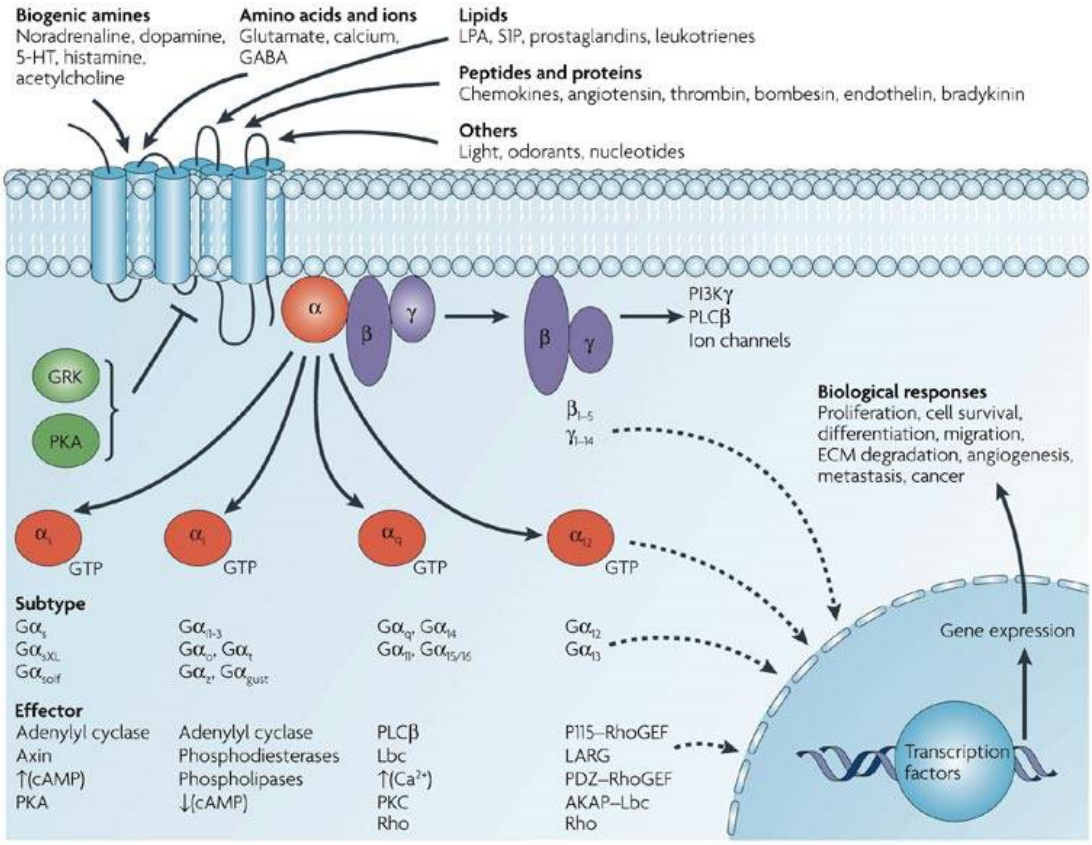

Figure 1-4 Diversity of G-protein-coupled receptor signalling. GPCRs interact with heterotrimeric G proteins composed of Gα subunit and Gβγ heterodimer that are GDP bound in the absence of ligands. Following activation by ligands, GPCRs catalyses the exchange of GDP to GTP in the Gα subunit and the dissociation of Gα subunit from Gβγ heterodimer. Dissociated Gα subunits trigger distinct downstream effectors (such as adenylyl cyclase (AC), phospholipase C (PLC)) and cause the changes of secondary messengers (such as cAMP, IP3 or Ca2+). In addition to the regulation of these classical secondary messenger generating systems, Gβγ heterodimer also activate signalling molecules, including phospholipases, ion channels and lipid kinases. Ultimately, the integrated G-protein-regulated signalling mediates target genes expression and generate diverse biological responses (Dorsam and Gutkind, 2007).

GPCRs are widely and essentially involved in the regulation of energy homeostasis. For example, olfactory, visual and taste GPCRs play crucial roles in sensing the palatability of the food and regulating the appetite (Gaillard et al., 2004, Loper et al., 2015). A range of energy regulating hormones, such as gastric inhibitory polypeptide / glucose-dependent insulinotropic peptide (GIP), glucagon-like peptide-1 (GLP-1), pancreatic polypeptide (PYY) and cholecystokinin (CCK) also target GPCRs (e.g. GIP receptor; GLP-1 receptor; Y1 receptor, Y2 receptor, Y5 receptor; CCK receptors) respectively and regulate energy balance *via* appetite control, insulin and glucagon release, and gastrointestinal motility (Meier and Nauck, 2005, Kjems et al., 2003, Batterham et al., 2003, Fink et al., 1998). Furthermore, several GPCRs such as CRHR1 (corticotropin-releasing hormone receptor 1), CRHR2, GPR24 have been identified as genes causing monogenic obesity. Loss or mutation any of these genes leads to severe obesity in humans (Farooqi and O'Rahilly, 2005), highlighting the importance of these GPCRs in energy homeostasis.

1.2.2 Free fatty acids-sensing GPCRs

There has been more than one decade since the discovery of free fatty acids as the ligands of several G-protein coupled receptors, including GPR40, GPR41, GPR43, GPR84, GPR119 and GPR120 (Ichimura et al., 2009). The deorphanization of these free fatty acids sensing GPCRs has revealed that extracellular free fatty acids not only function as energy source for cells, but also serve as signalling molecules to mediate wide range of biological processes.

1) GPR40

Human GPR40 gene was firstly identified as putative GPCR gene during the search for novel galanin receptor (GALR) subtypes (Sawzdargo et al., 1997). Human GPR40 gene, also known as free fatty acid receptor 1 gene or FFAR1 gene, together with GPR41, GPR42 and GPR43 are localized on chromosome 19q13.1 (figure 1-5) (Sawzdargo et al., 1997). Interestingly, only homologous genes of GPR40, GPR41 and GPR43 are found in rodent species. Furthermore, no free fatty acid has been found to activate human GPR42 receptor, indicating human GPR42 might be a pseudo gene formed by a duplication of human GPR41 gene during the evolution (Liaw and Connolly, 2009).

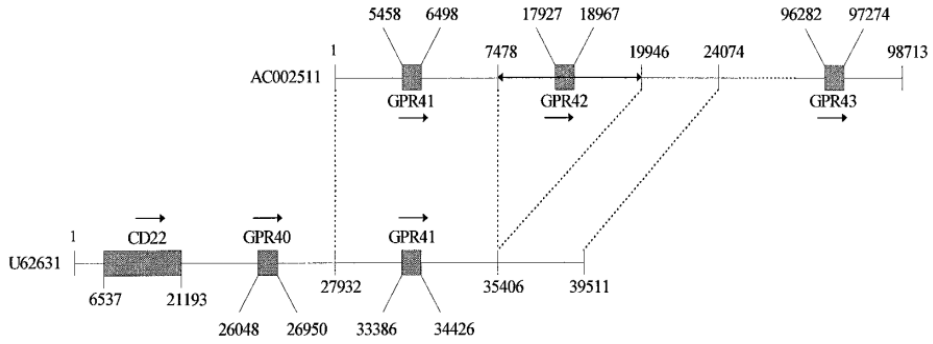

Figure 1-5 The relative localizations of GPR40, GPR41, GPR42, and GPR43 genes in human genome. The relative localizations of GPR40, GPR41, GPR42, and GPR43 genes in relation to the human CD22 gene on the sequences of two overlapping clones under the GenBank accession numbers U62631 and AC002511 (Sawzdargo et al., 1997).

The predominant expression sites of GPR40 are pancreatic β-cells and enteroendocrine cells, where GPR40 regulates glucose-stimulated insulin

and GLP-1, GIP release, respectively (Itoh et al., 2003, Tomita et al., 2006, Edfalk et al., 2008). Besides, GPR40 was also found in pancreatic α-cells, type I cells of taste bud, and breast cancer cell line MCF-7 (Yonezawa et al., 2004, Flodgren et al., 2007, Cartoni et al., 2010).

GPR40 can be activated by medium- and long-chain fatty acids. Approximately 42 different saturated and unsaturated free fatty acids with more than six carbons have been proved with the potency of activating human GPR40 in HEK293 cells, with 5,8.11-eicosatriynoic acid being the most potent (Briscoe et al., 2003).

GPR40 is coupled to pertussis toxin (PTX) insensitive $G\alpha_{(q/11)}$ G-protein, leading to the activation of phospholipase C and elevation of intracellular Ca^{2+} concentration; meanwhile, the ERK1/2 phosphorylation was also observed after GPR40 agonist stimulation (Briscoe et al., 2003). Besides, it was also found that activation of human GPR40 slightly decreased cAMP production in forskolin-stimulated CHO cells expressing human GPR40, suggesting that human GPR40 might also couple to $G\alpha_{(i/o)}$ G-protein partially, however, this finding was not observed in the cells expressing mouse GPR40 (Briscoe et al., 2003).

Due to the potential of stimulating both insulin secretion in β-cells and GLP-1 secretion in L-cells simultaneously (Briscoe et al., 2006, Edfalk et al., 2008), a number of synthetic agonists and antagonist of GPR40 have been discovered (Garrido et al., 2006). Thiazolidinedione (TZDs), a kind of drugs developed in the late 1990s as PPARγ ligand, was also identified as GPR40 agonist using high-throughput reporter assay with clone election

(HighTRACE) system (Kotarsky et al., 2003a, Kotarsky et al., 2003b). Another anti-diabetogenic drug MEDICA16 also selectively activates GPR40 and elevates intracellular Ca^{2+} concentration in cells expressing GPR40 (Hara et al., 2009, Takeuchi et al., 2013). Meanwhile, pharmacy companies also showed great interest in finding novel GPR40 agonists due to the potential of GPR40 as the target of diabetes treatment. A number of GPR40 agonists or antagonists have been discovered. For example, GW9508 (agonist of GPR40) and GW1100 (antagonist of GPR40) were firstly reported by GSK (Briscoe et al., 2006). Merck also reported 5-aryloxy-2,4-thiazolidinediones (Compound C) (Zhou et al., 2010) and 3-substituted 3-(4-aryloxyaryl)-propanoic acids (Walsh et al., 2011) as GPR40 agonist based on their systematic structure-activity relationship (SAR) studies. Moreover, the key sites of GPR40 for the agonist GW9508 and linoleate binding were successfully illustrated (figure 1-6). These findings laid a solid foundation for the development of novel GPR40 agonists with higher potential and selectivity (Sum et al., 2007).

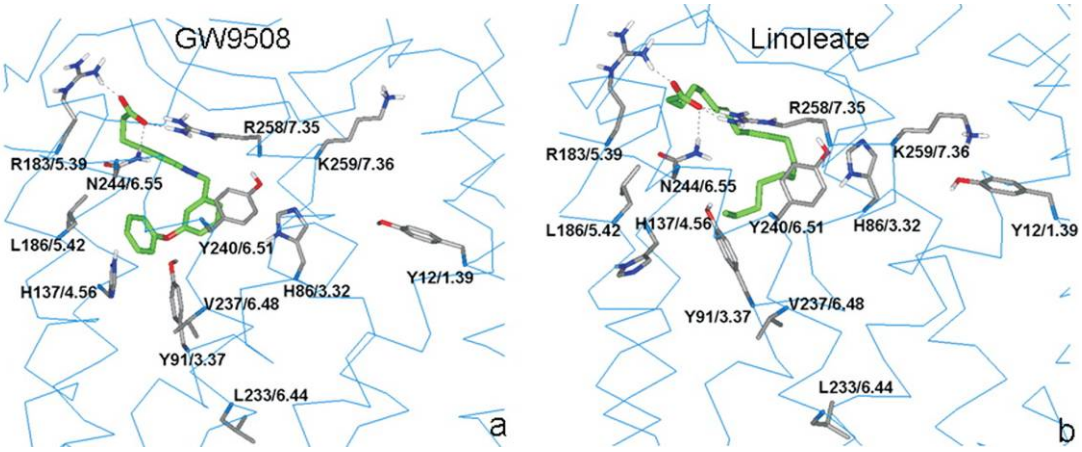

Figure 1-6 Binding pocket of GPR40 in complex with GW9508 and linoleic acid. The ligands are labelled in green. The hydrogen bond between ligands and Arg183,

Asn244, and Arg258 are marked as dash line. Transmembrane helices of receptor are shown as blue wires. Key residues in binding pocket are shown with their position and the Ballesteros Weinstein GPCR numbering. (Sum et al., 2007)

Recently, potent GPR40 agonists (AMG837 and TAK-875) with oral bioavailability were reported by independent groups (Lin et al., 2011, Houze et al., 2012). The evidence from *in vitro* assay, animal model assay and phase III clinical trials on Japanese type 2 diabetes patients indicated TAK-875 is a promising drug to improve the insulin and glucagon secretion to treat type 2 diabetes (Kaku et al., 2013).

Taken together, GPR40 is a very promising therapeutic target for the treatment of type 2 diabetes.

2) GPR41

Human GPR41 gene also locates at GPR40-43 genes cluster. Strikingly, GPR41 mRNA transcription shares the same promoter of GPR40 gene, and its protein translation is mediated by internal ribosome entry site (IRSE) (Bahar Halpern et al., 2012). GPR41 have been deorphanizated by paired with short-chain fatty acids, with propionate, butyrate, and pentanonate as the preference (Brown et al., 2003).

Since GPR41 shares the promoter of GPR40 gene, GPR41 is also highly expressed in pancreatic β-cells and enteroendocrine L-cells (Bahar Halpern et al., 2012). Although it has been reported that short-chain fatty acids stimulated glucagon-like peptide-1 secretion was decreased in GPR41 knock-out mice, however, there is no conclusive evidence showing GPR41

directly regulates GLP-1 secretion since loss of GPR41 caused a decrease in GPR43 expression, which also controls short-chain fatty acids induced GLP-1 secretion (Tolhurst et al., 2012).

Interestingly, the expression and functions of GPR41 in adipocytes are also controversial. It was firstly reported that GPR41 is highly expressed in adipose tissue and stimulates leptin secretion after short-chain fatty acids simulation (Xiong et al., 2004). Over expression of GPR41 led to an increase in leptin production, which was abolished by knockdown of GPR41 (Xiong et al., 2004). In contrast, recent studies claimed GPR41 is not detectable in adipocytes, while the effects of short-chain fatty acids on leptin secretion might go through GPR43 instead of GPR41 (Zaibi et al., 2010). Further investigation is needed to resolve this discrepancy.

Recent studies also showed GPR41 might associate with inflammatory and metabolic diseases. Stimulation with butyrate attenuated inflammation and lipolysis in macrophages and white adipocytes, which is abolished by blocking GPR41 (Ohira et al., 2013). Interestingly, GPR41 knock-out mice showed attenuated inflammatory responses in intestinal epithelial cells following ethanol or 2, 4, 6-trinitrobenzene sulfonic-acid (TNBS) treatment (Kim et al., 2013). Therefore, further investigation is still needed to illustrate the link between GPR41 and inflammation. Besides, male mice with GPR41 knock-out also showed low energy expenditure and increased body fat content (Bellahcene et al., 2013).

GPR41 is exclusively coupled to pertussis toxin (PTX) sensitive $G\alpha_{(i/o)}$ G-protein (Brown et al., 2003). Upon activation, GPR41 inhibits intracellular cAMP accumulation.

Up to date, there is only β-hydroxybutyrate reported as antagonist for GPR41, a ketone body produced during starvation or diabetes (Kimura et al., 2011). Interestingly, short-chain fatty acids increased sympathetic nervous system (SNS) activities *via* GPR41 while β-hydroxybutyrate suppressed SNS activity by antagonizing GPR41, suggesting a mechanism by which dietary status can directly mediate energy expenditure by regulating the activity of the sympathetic nervous system (Kimura et al., 2011).

3) GPR43

Similar to GPR41 gene, human GPR43 gene also locates at GPR40-43 gene cluster on chromosome 19q13.1 (Sawzdargo et al., 1997). However, unlike GPR41, it has its own promoter; therefore, GPR43 has a distinct expression pattern wider than GPR40 and GPR41 (Bahar Halpern et al., 2012). GPR43 has been reported to be present in adipocytes, immune cells, enteroendocrine L-cells and islets cells (Cornall et al., 2011, Karaki et al., 2006, Karaki et al., 2008). Besides, GPR43 was also identified in cancer cells including MCF7 cells (Yonezawa et al., 2007), BaF3 cells (Bindels et al., 2012), and colon cancer cells (Tang et al., 2011). However, the roles of GPR43 in the proliferation of cancer cells are still controversial.

Although GPR43 possesses affinities for short-chain fatty acids overlapping with GPR41, acetate is 100-fold less potent on GPR41 as compared with

propionate and butyrate, whereas acetate activates GPR43 with a strongest potency (Le Poul et al., 2003). Considering the fact that concentration of acetate reaches 100-150 μM in blood while concentration of propionate and butyrate are only 1-3 μM and 4-5 μM, respectively (Wolever et al., 1997), the GPR43 in peripheral tissues could be activated by acetate in blood. However, the average concentration of propionate and butyrate in blood are considered too low to activate GPR41 or GPR43 (Le Poul et al., 2003).

Interestingly, increasing evidence showed the expression of GPR43 is regulated by a range of factors. For example, co-culture bovine muscle satellite cells dramatically increased GPR43 expression in white adipocytes (Choi et al., 2013). Besides, high-fat diet also increased GPR43 expression in adipose tissue, liver and soleus and EDL skeletal muscles (Cornall et al., 2011, Dewulf et al., 2011). These findings suggested GPR43 might link with adipose tissue metabolism. Recent studies also supported this hypothesis. It has been demonstrated that stimulation with short-chain fatty acids significantly decreased lipolysis in white adipose tissue (Ge et al., 2008) and promoted leptin secretion in white adipocytes (Zaibi et al., 2010). However, the overall effects of GPR43 on metabolism *in vivo* is still unclear. The knock-out of GPR43 was found to improve glucose homeostasis and reduce body fat mass under a high-fat diet feeding in mice (Bjursell et al., 2011). However, another study showed GPR43 knock-out mice exhibited obesity on a normal diet while over-expressing GPR43 in adipose tissue kept mice lean when fed a high-fat diet (Kimura et al., 2013).

Similar to GPR40 and GPR41, GPR43 has been proved to affect GLP-1 secretion both *in vitro* and *in vivo* (Tolhurst et al., 2012). Therefore, it also draws attention to identify selective GPR43 agonists as a therapeutic strategy for obesity and diabetes treatment.

GPR43 also profoundly affects inflammatory response. GPR43 has been proved to mediate neutrophil chemotaxis (Vinolo et al., 2011) and recruitment (Sina et al., 2009). GPR43 is also involved in polymorphonuclear cell activation, recruitment of polymorphonuclear cell populations toward sites of bacterial infection (Le Poul et al., 2003). Furthermore, GPR43 deficient mice also demonstrated significant alteration of inflammatory responses *in vivo* (Maslowski et al., 2009).

GPR43 is mainly coupled to $G\alpha_q$ and $G\alpha_{(i/o)}$ G-proteins (Brown et al., 2003). Upon stimulation, GPR43 activates intracellular signalling such as cytoplasmic Ca^{2+} increase, p38 and ERK activation and inhibition of cAMP production (Seljeset and Siehler, 2012).

Both GPR43 agonists and antagonists have been reported. For example, orthosteric agonist (2-methylacrylic acid), allosteric agonists (Compound 58, Compound 34), inverse agonists (Compound 4) have been discovered (figure 1-7) (Bindels et al., 2013). Meanwhile, GLPG0974, a potent and selective antagonist of GPR43, which inhibits GPR43 mediated activation and migration of neutrophils, has demonstrated favourable safety profile and good pharmacokinetic and pharmacodynamic properties in Phase I clinical trial to treat patients with mild-to-moderate ulcerative colitis (Pizzonero et al., 2014, Vermeire et al., 2015).

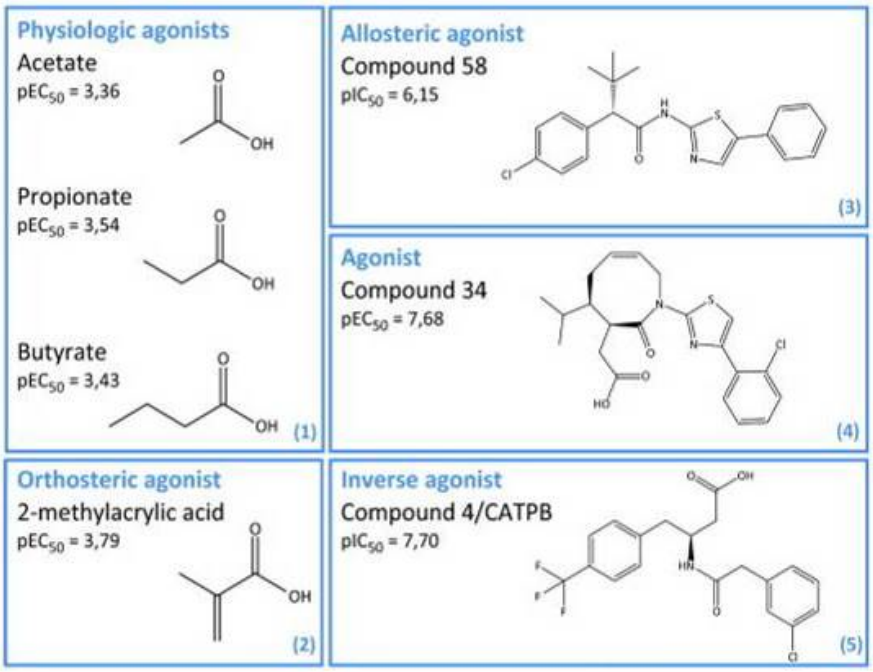

Figure 1-7 Chemical structures of physiological and synthetic ligands of GPR43. pEC_{50} and pIC_{50} represent the negative log of the half maximal effective concentration, and half maximal inhibitory concentration, respectively (Bindels et al., 2013).

4) GPR84

Human GPR84 gene was identified nearly simultaneously by two independent groups in 2001 using different approaches (Wittenberger et al., 2001, Yousefi et al., 2001). Wittenberger *et al.*, firstly reported five putative G-protein coupled receptors including GPR84 by expressed sequence tag (EST) database mining strategy. Using northern blots, the expression of human GPR84 and murine GPR84 were confirmed in brain, heart, muscle, colon, thymus, spleen, kidney, liver, intestine, placenta, lung, and leukocytes (Wittenberger et al., 2001). Subsequently, Yousefi *et al.*, also reported a novel G-protein-coupled receptor identified as GPR84 expressed on granulocytes (Yousefi et al., 2001).

Human GPR84 gene localized on chromosome 12q13.13, while murine GPR84 gene is identified on chromosome 15, the encoded proteins of which share 85% amino acid identity, suggesting they are ortholog of each other (Wittenberger et al., 2001). Notably, the coding sequence of human GPR84 gene contains no introns (Wittenberger et al., 2001).

To identify the endogenous ligands of GPR84, saturated and unsaturated free fatty acids from C1 to C22 in length have been tested. The results demonstrated that only medium-chain saturated free fatty acids (C9-C14) selectively activated GPR84 in CHO cells expressing human GPR84, with capric acid (C10:0), undecanoic acid (C11:0) and lauric acid (C12:0) being the most potent (Wang et al., 2006). Interestingly, no unsaturated free fatty acids showed the potency to activate GPR84. (Wang et al., 2006).

Besides, two synthetic small molecules (diinodrylmethane and indol-3-calbinol) were identified as GPR84 agonists with EC_{50} at 11μM and 100 μM, respectively, by [^{35}S]GTPαS binding assay (figure 1-8) (Takeda et al., 2003). Galapagos also presented pre-clinical evidence for GPR84 inhibitor GLPG1205 as novel treatment for inflammatory bowel diseases, however, no further details were disclosed.

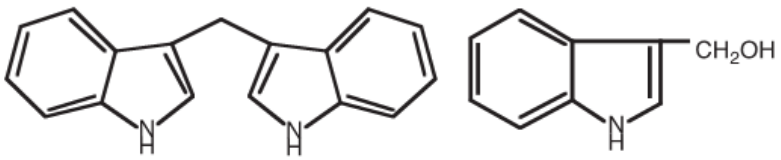

Diindorylmethane Indol-3-calbinol

Figure 1-8 Chemical structures of GPR84 surrogate agonists. Diindorylmethane and indol-3-calbinol were identified as GPR84 agonist with EC_{50} at 11 μM and 100 μM, respectively (Takeda et al., 2003).

GPR84 predominantly expresses in immune cells, including various leukocytes, macrophages, microglia, T lymphocytes, and B lymphocytes (Wang et al., 2006, Lattin et al., 2008). Besides, northern blots analysis also revealed GPR84 mRNA in brain, heart, muscle, colon, thymus, spleen, kidney, liver, intestine, placenta, lung and leucocytes (Wittenberger et al., 2001). Recently, GPR84 was also found in murine white adipose tissue and white adipocyte 3T3-L1 (Nagasaki et al., 2012). Evidence about GPR84 expression suggested the involvement of GPR84 in inflammatory response in immune system. For example, lipopolysaccharides or pro-inflammatory cytokines stimulation could increase GPR84 expression in neutrophils, macrophage and neutrophil granulocytes (Wang et al., 2006, Bouchard et al., 2007, Nagasaki et al., 2012).

Using CHO cells expressing human GPR84, GPR84 was demonstrated almost exclusively binding to pertussis toxin (PTX)-sensitive $G\alpha_{(i/o)}$ G-protein. Stimulating GPR84 with its agonist diindolylmethane also dramatically lower intracellular cyclic AMP (cAMP) production after forskolin stimulation (Wang et al., 2006).

Besides, GPR84 was also considered as a necessary receptor for eye development in *Xenopus laevis*. Knock-down of GPR84 could significantly modulate the proliferation and apoptosis of eye tissues and cause deficient

of retina and lens development (Perry et al., 2010). Due to the fact that *X. laevis* GPR84 distantly resembles human, mouse and rat GPR84, the relationship between GPR84 and eye development in human and rodent species still need more investigation.

5) GPR119

Human GPR119 gene was firstly identified by Fredriksson *et al.*, by searching human genome database and analysing expressed sequence tag database (Fredriksson et al., 2003). The orthologues of GPR119 have been identified in a number of species, including mouse, rat, hamsters, chimpanzees, rhesus monkey, cattle, dog, and fugu (pufferfish) (Zhu et al., 2013). Human GPR119 gene localizes on chromosome Xp26.1, while mouse GPR119 gene localizes on chromosome chrX: 34322403-34323407 (Zhu et al., 2013).

GPR119 was firstly deorphanized to be the receptor of oleoylethanolamide (OEA, C18:1) with EC_{50} at 3.2 μM for human GPR119 and 2.9 μM for mouse GPR119 (Overton et al., 2006). Additionally, previous studies also reported that N-oleoyldopamine (OLDA) and lysophosphatidylcholine (LPC) could stimulate GPR119 in the cells over-expressing GPR119 (Chu et al., 2010).

Similar to the expression profiles of GPR40, human GPR119 gene expresses abundantly only in a limited range of cells, including pancreatic β-cells and enteroendocrine cells in the small intestine (Chu et al., 2010). Recently, the evidence of GPR119 expression in cultured skeletal muscle myotubes was reported (Cornall et al., 2013).

Stimulation of GPR119 leads to an enhancement of both glucose-induced insulin secretion and GLP-1 secretion as GPR40 (Fyfe et al., 2008). However, the detailed mechanism seems to be different. GPR119 is coupled to $G\alpha_s$ G-protein. Upon activation, GPR119 increases intracellular cAMP levels, followed by increased glucose-dependent insulin release in β-cells, GLP-1 release in L-cells and GIP release in K-cells (figure 1-9) (Overton et al., 2008).

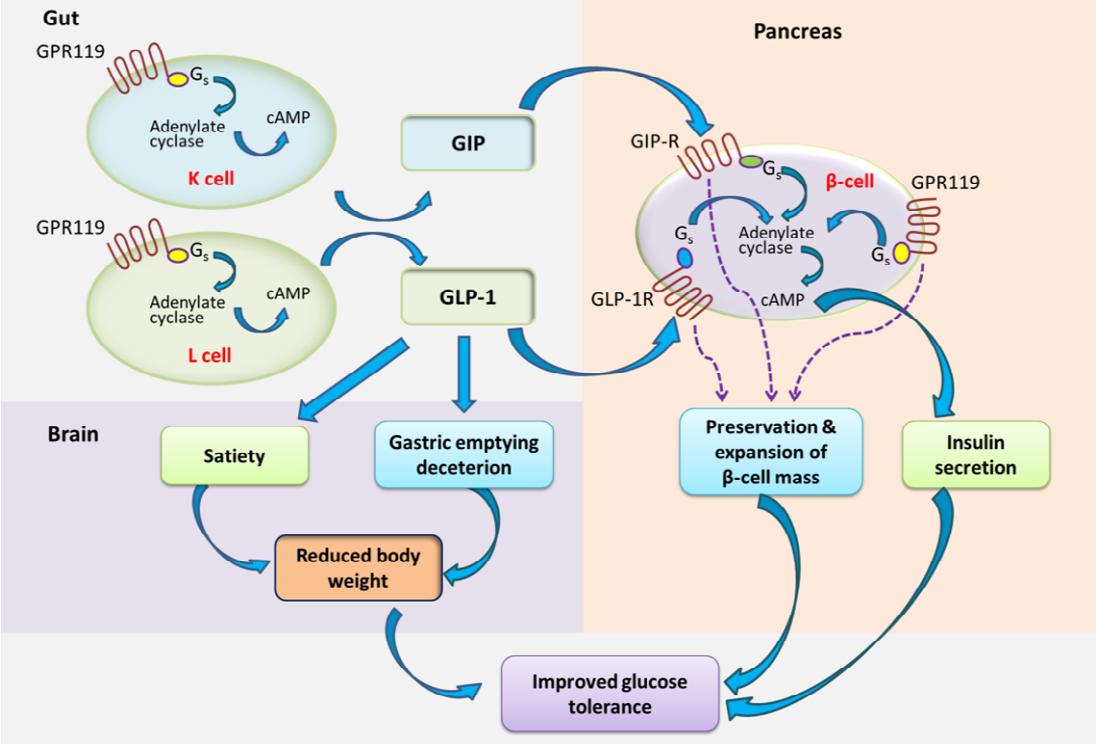

Figure 1-9 Proposed mechanisms of GPR119-mediated glucose metabolism. GPR119 is coupled to $G\alpha_s$ G-protein and increases cAMP levels *via* activation of adenylate cyclase in L and K cells in guts and β cells in islets, which leads to the increase in the release of glucagon-like peptide 1 (GLP-1), glucose-dependent insulinotropic peptide (GIP) or insulin in L, K cells and β cells, respectively. Besides, GLP-1 and GIP secreted from L, and K cells can also further trigger insulin secretion in β cells *via* their receptors, respectively, to mediate glucose metabolism. (Ohishi and Yoshida, 2012, Zhu et al., 2013)

Combining the abilities of promotion of glucose-stimulated insulin secretion and GLP1 release, a number of synthetic agonists of GPR119 have been investigated. Since the first synthetic GPR119 agonist (PSN375963) was reported, more than dozens of GPR119 agonists have been identified. Furthermore, because of the clear therapeutic potential for treating type 2 diabetes, efforts have been made to optimize GPR119 agonists with oral availability. Up to date, several GPR119 agonists including MBX-2982, GSK-1292263 and PSN-821 have been tested in Phase II clinical trials and shown a promising prospect for type 2 diabetes treatment (figure 1-10) (Jones et al., 2009).

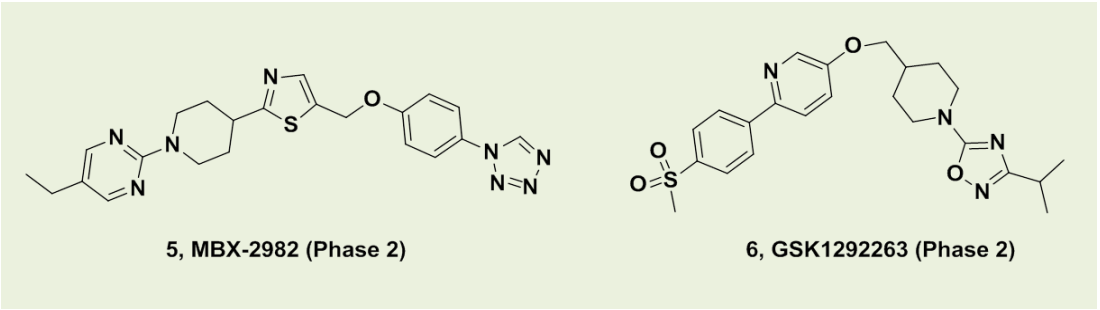

Figure 1-10 Chemical structures of GPR119 agonists used in phase 2 clinical trials. The structure of PSN-821, another GPR119 agonist in phase 2 clinical trials has not been revealed from Prosidion (Hansen et al., 2012, Zhu et al., 2013).

6) GPR120

Human GPR120 gene was firstly reported by Fredriksson *et al.*, in 2003, which is located on human chromosome 10q23.33 (Fredriksson et al., 2003). GPR120 is highly conserved in many species, such as mouse, rat and fugu (pufferfish) (Fredriksson et al., 2003). Interestingly, human GPR120 shares

10% identity with human GPR40, which is another GPCR recognizing medium- and long-chain fatty acids.

A series of medium- and long- chain free fatty acids, including saturated free fatty acids with C14 - C18 and unsaturated free fatty acids with C16 - C22, were identified as endogenous ligands of GPR120. This similarity also reflects on the synthetic agonists. Several GPR40 agonists were also found as the agonists of GPR120 (Suzuki et al., 2008, Hara et al., 2009).

The expression distribution of GPR120 also shares a somewhat similarity to GPR40. Pancreatic β-cells and enteroendocrine L-cells have been identified as the sites of GPR120 expression (Hirasawa et al., 2005). Besides, the expression of GPR120 was also found in taste buds, indicating GPR120 may function in taste sense (Martin et al., 2012). Notably, extensive tissue expression analysis also demonstrated GPR120 is highly expressed both in macrophages and mature adipocytes (Talukdar et al., 2011). The functions of GPR120 both in macrophages and adipocytes (including anti-inflammatory and glucose transport regulation) have been extensively studied (figure 1-11) (Gotoh et al., 2007, Oh et al., 2010).

Recently, a genetic analysis conducted in obese children and adults revealed a striking finding. About 3% of obese patients carry a loss-of-function, nonsynonymous GPR120 mutation (R270H), which was believed as a factor causing obesity and insulin resistance (Oh and Olefsky, 2012). Therefore, GPR120 selective agonists have become potential drugs to improve insulin resistance and treat obesity related diseases.

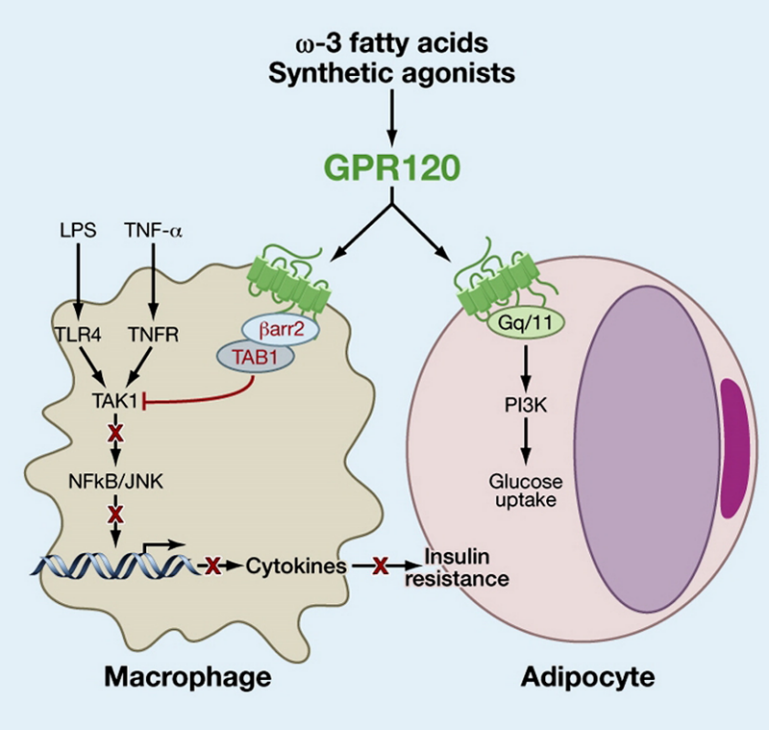

Figure 1-11 Proposed mechanisms of GPR120-mediated insulin sensitization and anti-inflammatory mechanism. GPR120 activates $G\alpha_{(q/11)}$ G-protein and increases glucose uptake *via* PI3K / Akt pathway in white adipocytes, while GPR120 also inhibits TLR and TNF-α inflammatory signalling pathways after forming internalized GPR120-β-arrestin 2 complex in macrophages (Oh et al., 2010).

1.3 Energy Homeostasis

The balance of energy storage and release, also known as energy homeostasis is crucial for overall health and even survival (Woods et al., 1998). It has been well characterized that obesity, the result of long-term positive energy balance, increases the risk for many diseases such as type 2 diabetes, heart disease, hypertension, stroke, liver disease, colon cancer, and osteoarthritis (Must et al., 1999). Similarly, long-term negative energy balance also contributes to several severe body-disorders, including decline in metabolism, loss of bone mass, decreases in thyroid hormones, and

reduction in physical performance (Pollock et al., 2010). Therefore, the ability to adapt to variety of energy intakes and outputs is vital. Currently, the widely accepted model of energy homeostasis consists that fluctuation of energy status generates complex peripheral signals, which become integrated in neural systems; and in turn, regulate behavioural and endocrine output to balance the nutrients intake, storage and expenditure for given environmental conditions (Gale et al., 2004).

Due to the high importance of energy homeostasis, it is estimated that thousands of genes are involved in this process. Several genes coding energy 'homeostatic' regulators have been discovered by investigating monogenic obesity models. Up to date, mutations in 11 different genes, including leptin, leptin receptor, POMC (Proopiomelanocortin), PC1 (proconvertase 1), MC4R (Melanocortin-4-receptor), SIM1 (Single-minded homolog 1), NTRK2 (Neurotropic tyrosine kinase receptor type 2), CRHR1 (corticotropin-releasing hormone receptor 1), CRHR2, GPR24, MC3R (Melanocortin-3-recptor) have been identified to cause monogenic obesity (Farooqi and O'Rahilly, 2005). Among them, the most striking example appears to be the discovery of leptin, which presents a good model that how the peripheral tissue (white adipose tissue) send signals (status of energy storage) to central nervous system (hypothalamus) to decrease energy intake *via* inhibiting neuropeptide Y (NPY) / Agouti-related peptide (AgRP) and activating proopiomelanoortin (POMC) / cocaine- and amphetamine-regulated transcript (CART) neurons (Jang et al., 2000, Cowley et al., 2001, Elias et al., 1998). In addition to the monogenic obesity, there is another

rarely-occurred syndromic obesity, which arise from discrete genetic defects or chromosomal abnormalities, such as Prader-Willi syndrome (PWS), Bardet-Biedl syndrome (BBS), and Alström syndrome (Chung, 2012). In human, polygenic obesity occurs more commonly, which is the synergistic effect of individual's genetic makeup and obesogenic environment that promotes energy intake over energy expenditure (Hinney and Hebebrand, 2008).

Appetite regulation is a major part of energy homeostasis regulation (Woods et al., 1998). Since the efficiency of energy digestion and absorbance has evolved into a very high level (normally more than 90%), therefore, in all higher life-forms, the way to regulate energy intake mainly relies on the appetite regulation, which is controlled by a complicated interplay between adipose tissue, pancreas and gastrointestinal tract and the brain (mainly hypothalamus) (Calder, 2015). The hypothalamus play a pivotal role in controlling appetite, where the complex peripheral signals are integrated and the neuropeptides are send out to stimulate (orexigenic) or inhibit (anorexigenic) appetite and regulate metabolism of peripheral organs, including adipose tissues, the gastrointestinal tract, the pancreas, the liver and the muscle (Liao et al., 2012). Dozens of peptides / proteins have been demonstrated to be involved in this process (figure 1-12). Hypothalamic nuclei play central roles in the control of both hunger and satiety. Several nuclei in hypothalamic (including the arcuate nucleus (ARC), paraventricular nucleus (PVN), dorsomedial hypothalamic nucleus (DMH), lateral

hypothalamic area (LHA) and the ventromedial hypothalamic nucleus (VMH)) are key areas responsible for appetite regulation (Yeo and Heisler, 2012).

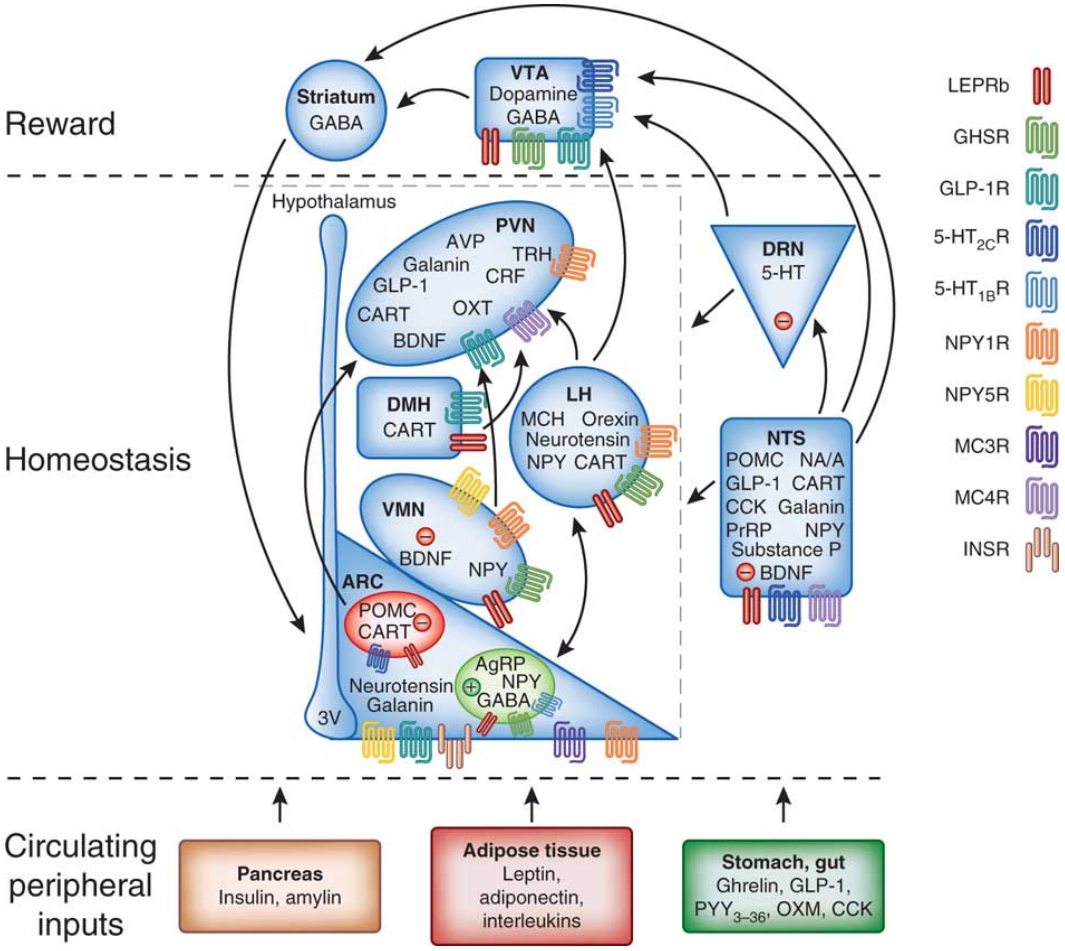

Figure 1-12 Schematic diagram of the hypothalamic nuclei and other relevant higher brain regions in appetite regulation. The ARC (arcuate nucleus) is the crucial nuclei for the regulation of appetite. The ARC in hypothalamus lies immediately above the medianeminence where peripheral peptides and proteins can cross the specially modified blood-brain barrier. The ARC contains two discrete populations of neurones expressing orexigenic neuropeptides (including AGRP (agouti-related peptide), NPY (neuropeptide Y), and GABA (*gamma*-Aminobutyric acid)) or anorexigenic neuropeptides (including POMC (proopiomelanocortin) and CART (cocaine and amphetamine- regulated transcript)), respectively. The ARC has extensive reciprocal connections with other hypothalamic appetite regulating regions including the VMN (ventromedial nucleus), DMH (dorsomedial hypothalamus), PVN (paraventricular nucleus), and LH (lateral hypothalamus). NTS

(nucleus of the solitary tract), DRN (Dorsal raphe nucleus) in the brainstem, VTA (ventral tegmental area) in the midbrain and Striatum also mediate appetite by projections to other nuclei in hypothalamus. Projections between nuclei are indicated with arrows (Yeo and Heisler, 2012).

Notably, in addition to homeostatic eating, which primarily keeps energy balance and meets the energy requirement, hedonic eating also contributes to the energy intake, which arise from anticipation of eating for pleasure instead of energy or nutrient requirement (Lowe and Butryn, 2007). Activation of dopamine-containing neurons in the ventral tegmental area is believed to be involved in many aspects of hedonic eating (figure 1-12) (Lowe and Butryn, 2007). However, it is still difficult to draw a clear-cut line separating “homeostatic” and “hedonic” eating.

Similar to the regulation of appetite, the energy expenditure, another aspect of energy homeostasis regulation, also could be divided into basal and adaptive energy expenditure (Bianco et al., 2005). The basal expenditure is vital for maintaining basic metabolic and physiologic activities, such as maintenance of body temperature, blood flow, ionic and substrate cycles, and basal glands secretion, etc.; while the adaptive energy expenditure mainly consists of physical activity and adaptive thermogenesis (Rosenbaum and Leibel, 2010). Besides, excess energy will be stored. Triglyceride is the most common format to store excess energy in body, while glycogen also serves as a form of energy storage in liver and muscle (Dashty, 2013). In the overfeeding experiment, almost two thirds of the weight gain is stored as

increased fat mass in body (Bouchard et al., 1990, Diaz et al., 1992, Tremblay et al., 1992, Lammert et al., 2000).

Although the detailed mechanism is still vague, however, the energy expenditure also participates in the body weight maintenance and energy balance regulation. As shown by underfeeding or overfeeding studies in rodents, certain energy expenditure mechanisms, such as diet-induced thermogenesis and leptin-induced thermogenesis, contribute to burning up of excess energy as a specific response to increased body weight and fat storage (Dulloo et al., 2002, Westerterp, 2004, Ukropec et al., 2006). In human, overfeeding or obesity also leads to increased energy expenditure *via* increasing sympathetic nervous system (SNS) activity and non-exercise activity thermogenesis (NEAT), together with decreasing parasympathetic nervous system activity (Welle and Campbell, 1983, Levine et al., 1999). However, there is still not decisive evidence to support the hypothesis that relatively low energy expenditure is main cause of the development of obesity, since the controversial results have reported (Ramsey et al., 1998, Brehm et al., 2005, Hamilton et al., 2007).

Regulation of energy expenditure is a complex system involving endocrinological and biochemical mechanisms (Bukowiecki, 1985). Up to date, many factors have been found to affect the energy expenditure, such as physical activity, diet intake, body energy status, hormones (e.g. thyroid hormones) levels, sympathetic nervous system and parasympathetic nervous system activities, futile cycles, and intermediary metabolism genes

(Westerterp, 2013, Reed and Hill, 1996, McAninch and Bianco, 2014, Messina et al., 2013, Qian and Beard, 2006).

Many peripheral tissues have the metabolic potential to mediate thermogenesis. For example, brown adipose tissue, a key thermogenic tissue involved in energy expenditure regulation, contribute to the energy expenditure *via* heat production (Dawkins and Scopes, 1965). Besides, brown adipose also shows obvious hypertrophy and increased energy expenditure in response to high fat feeding, suggesting a role of brown adipose tissue in resisting obesity *via* mediating adaptive thermogenesis (Mercer and Trayhurn, 1987). Indeed, the rats with interscapular brown adipose tissue being lesioned had abnormal body weight (Connolly et al., 1982). Leptin was also found to have direct effects on brown adipose tissue such as increasing glucose utilization and lipolysis, also suggesting brown adipose tissue responses to body energy status (Siegrist-Kaiser et al., 1997).

Short-chain fatty acids have been found to widely mediate energy homeostasis through multiple mechanisms. For example, Frost et al., found short-chain fatty acid acetate reduces appetite *via* a central homeostatic mechanism (Frost et al., 2014). Meanwhile, den Besten et al., reported protective effects of short-chain fatty acids against HFD-induced obesity in mice; which comes from a PPARγ-dependent switch from lipogenesis to oxidation in liver (den Besten et al., 2015). Up to date, there are increasing evidence to support the hypothesis that serum level of short-chain fatty acids reflects nutrient status, thereby, which might feedback regulates the energy metabolism according to body nutrient status. Therefore, it is worthy to

investigate the effects of short-chain fatty acids on other aspects of energy homeostasis, such as brown adipose tissue activities.

1.4 White adipose tissue

White adipose tissue is major form of adipose tissues in human, which accounts for 10% - 25% of total body weight in a non-obese young adult; and this number can reach to nearly 50% in an obesity patient (Heymsfield, 2005). WAT is mainly composed by large number of white adipocytes and other cell types including macrophage, leukocytes, fibroblast, endothelia cells, and adipocyte progenitor cells (Caspar-Bauguil et al., 2009). The main function of white adipose tissue is the storage of excess energy in the form of triglycerides in white adipocytes. Meanwhile, it also serves as the thermal insulation layer of the body and physical protection pad around important internal organ (Anderson and Martin, 1994). However, with the discovery of hormones and adipokines secreted by white adipocytes, the perspective towards white adipose tissue has been profoundly updated (Scherer, 2006). Nowadays, the white adipose tissue is regarded as an endocrine organ (Fonseca-Alaniz et al., 2007).

To maximum the lipid conservation, white adipocytes have a distinctive morphology with a single lipid droplet occupying nearly 90% cell volume and squeezing the nucleus and mitochondria into the periphery of the cell (Napolitano, 1963). Other organelles such as Golgi complex, rough endoplasmic reticulum, smooth endoplasmic reticulum, and lysosomes also stay at poorly development status in mature white adipocytes (Cinti, 2009).

White adipocytes appear in a bright colour, which is believed related with their low mitochondria density (Mescher, 2009). Besides, the mitochondria in white adipocytes do not contain UCP1 protein, which is a distinguishing feature of brown adipocytes (Lean and James, 1983, Pecqueur et al., 2001, Ricquier and Bouillaud, 2000). However, recent studies showed mitochondria in white adipocytes also played an important role in biochemical processes including preadipocyte differentiation (adipogenesis) and lipid metabolism (lipogenesis, lipolysis and fatty acids re-esterification). The enhanced mitochondrial metabolism during the early stage of adipogenesis increases cellular reactive oxygen species (ROS) levels, which is vital for the adipocyte differentiation *via* an mTORC1-dependant pathway (Tormos et al., 2011). Besides, mitochondria in white adipocytes also provide sufficient energy for adipocyte differentiation. Furthermore, the results from clinical research also highlighted the significance of mitochondria in white adipocytes. The abundance of mitochondria and mtDNA in white adipocytes showed a significant decrease in severe obesity and type 2 diabetes patients (Yuzefovych et al., 2013); this phenomenon was also observed in ob/ob mice, db/db mice, diabetic mice, and high-fat diet (HFD)-fed mice (Choo et al., 2006, Rong et al., 2007). *In vitro* experiments prompted the hypothesis that excessive glucose or free fatty acids causes mitochondria dysfunction, which in turns severely impairs the function of white adipocytes (Gao et al., 2010).

As the pool of lipid in body, the lipid metabolism in white adipocytes plays an important role in body energy homeostasis maintenance. The lipid storage

and release are tightly controlled to keep the balance of energy intake and expense of the body (figure 1-13).

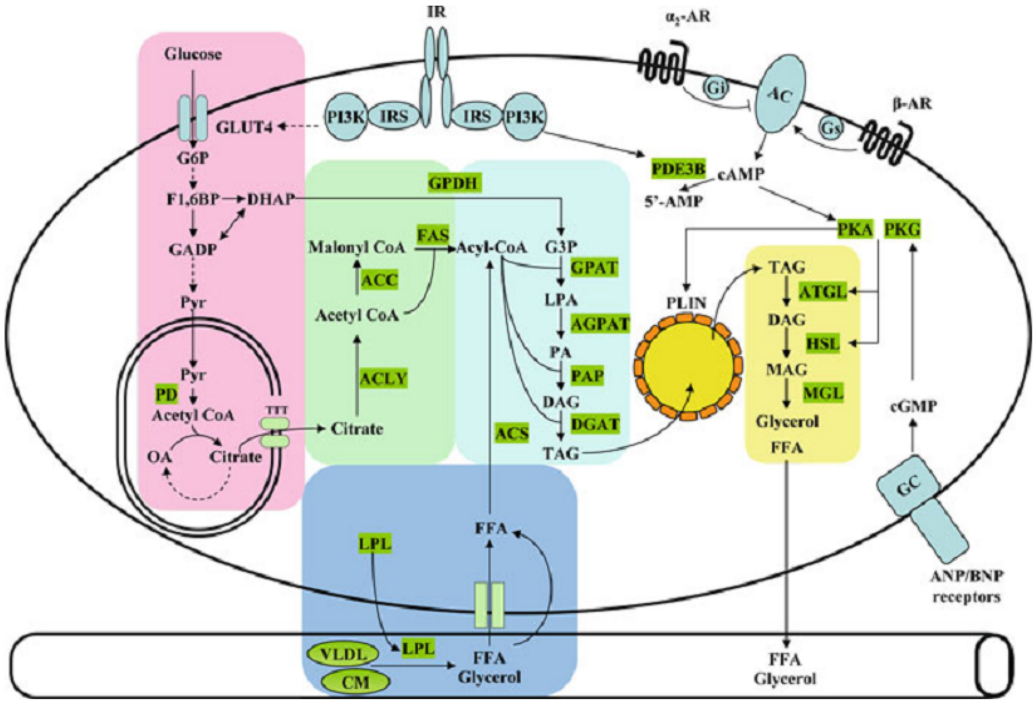

Figure 1-13 Schematic diagram of lipid metabolisms in white adipose tissue. White adipocytes take up fatty acids mainly from chylomicron or VLDL in the plasma *via* fatty acid transporters. Lipoprotein lipase hydrolyses triglycerides in chylomicrons and VLDL into free fatty acids and glycerol. White adipocytes also can synthesize triacylglycerol from carbohydrates *via* lipogenesis. To release the energy from triacylglycerol, triacylglycerol is mobilized through lipolysis process, which is mainly dependent on three lipase including ATGL, HSL, and MGL. The key factors and signalling pathways involved in lipid metabolisms regulation, such as insulin signalling, adrenergic receptors signalling, PKA and PKG activities, GLUT4 expression and location have also been marked. (Gesta and Kahn, 2012)

Synthesis of fatty acids from glucose begins with excess glucose entering into white adipocytes mainly through GLUT4, followed by glycolysis process into pyruvate (Mashima et al., 2009). In mitochondria, pyruvate is oxidized into acetyl-CoA by pyruvate dehydrogenase (Kersten, 2001). Acetyl-CoA is

then transported back into cytosol in the form of citrate, which will be broken down into acetyl-CoA again and catalysed by acetyl-CoA carboxylase into malonyl-CoA (Kersten, 2001). Afterwards, fatty acids synthesis will be catalysed in a cascade from malonyl-CoA (Ganguly, 1960). However, this *de novo* lipogenesis in adipocytes is not main source for lipid storage in white adipose tissue in human. Main source for lipid storage in white adipocytes comes from chylomicron and very-low-density lipoproteins (VLDL) in the plasma.

During the gap between meals or the period of fasting, white adipocytes utilize triglycerides as energy source by mobilizing stored triglycerides. The triglycerides can be broken down into free fatty acids and glycerol in a cascade by a series of enzymes named lipases. The key lipases involved in these hydrolysis steps consist of adipose triglyceride lipase (ATGL), hormone-sensitive lipase (HSL), and monoacyl glycerol lipase (MGL).

Adipose triglyceride lipase (ATGL) was discovered as a novel TAG lipase in 2004 (Jenkins et al., 2004, Villena et al., 2004, Zimmermann et al., 2004). Interestingly, adipose tissue is the only site with abundant expression of ATGL gene (Kershaw et al., 2006). Besides, ATGL expression was also found to be induced by fasting or glucocorticoids stimulation while to be suppressed by feeding or insulin stimulation (Nielsen et al., 2011, Kershaw et al., 2006). Furthermore, ATGL knock-out mice show massive accumulation of triglycerides (Lammers et al., 2011). These evidences together suggest ATGL might be a key lipase for triglycerides hydrolysis *in vivo*.

Hormone-sensitive lipase is the first identified lipase in 1960s, which can catalyse both diglycerides and triglycerides hydrolysis *in vivo*, with 10-fold higher activity for the diglycerides (Vaughan et al., 1964, Strand et al., 1964, Fredrikson et al., 1986). Furthermore, evidence from HSL knock-out mice showed deletion of HSL gene could not abolish the triglyceride hydrolysis (Osuga et al., 2000, Wang et al., 2001) but cause a significant accumulation of diglycerides in many organs in mice, which indicated HSL play a central role in diglycerides catabolism as rate-limiting enzyme (Yeaman, 2004). HSL activity is tightly regulated by hormones. The hormones such as catecholamine, which levels up intracellular cAMP concentration and activates cAMP-dependent PKA activity, leads to the phosphorylation of HSL at three serine residues (Ser563, Ser659, and Ser660) (Krintel et al., 2009).

Monoacylglycerol lipase (MGL) is the lipase in charge of monoglycerides breakdown (Karlsson et al., 1997). MGL is abundant expressed in adipose tissue (Karlsson et al., 1997). Studies have demonstrated this step of monoglycerides breakdown is less regulated compared to diglycerides and triglycerides hydrolysis.

Since the discovery of leptin, more than dozens of adipokines have been identified in white adipocytes (Fonseca-Alaniz et al., 2007). The adipokines appear to be involved in a wide range of physiological processes including metabolism, immunity, insulin sensitivity and angiogenesis.

Short-chain fatty acids have been found to mediate both lipid metabolism and adipokines secretion in white adipose tissue. For example, Hong *et al*. have demonstrated that short-chain fatty acids acetate and propionate

stimulated adipogenesis of 3T3-L1 cells *via* GPR43 (Hong et al., 2005). Besides, it has been found that activation of GPR43 by short-chain fatty acids led to inhibition of lipolysis in white adipocytes *in vitro*. *In vivo* studies also suggested acetate treatment suppressed plasma free fatty acids without inducing the flushing side effect *via* GPR43 (Ge et al., 2008). Short-chain fatty acids were also found to stimulate the expression of leptin in white adipocytes (Xiong et al., 2004, Zaibi et al., 2010). Studies also indicated propionate significantly stimulated leptin expression and decreased resistin expression in human adipose tissue depots, suggesting short-chain fatty acids are involved in adipokines secretion in human (Al-Lahham et al., 2010). Recent study also revealed acetate modulated cytoplasmic leptin in bovine pre-adipocyte (Yonekura et al., 2014).

1.5 Brown adipose tissue

Brown adipose tissue, also known as BAT or brown fat, is another type of adipose tissues firstly found in rodents and human infants. In a long history, it was thought brown adipose tissue was lost quickly after birth, however, both molecular and histological evidence discovered recently supported brown adipose tissue is present in adult humans. Brown adipose tissue has drawn attention as a novel preventive and therapeutic target for the treatment of obesity and other metabolic diseases due to its ability to generate heat by burning calories. In both rodents models and adult humans, increase in brown adipose tissue has been associated with a lean and healthy phenotype (Kopecky et al., 1995, Ghorbani et al., 1997, Guerra et al., 1998,

Cypess et al., 2009, Virtanen et al., 2009). The mass of brown adipose tissue negatively correlates with body mass index and positively with metabolism in resting state, making stimulation of brown adipose tissue in humans to be a possible approach for anti-obesity therapy (Pfannenberg et al., 2010, Yoneshiro et al., 2011, Matsushita et al., 2014).

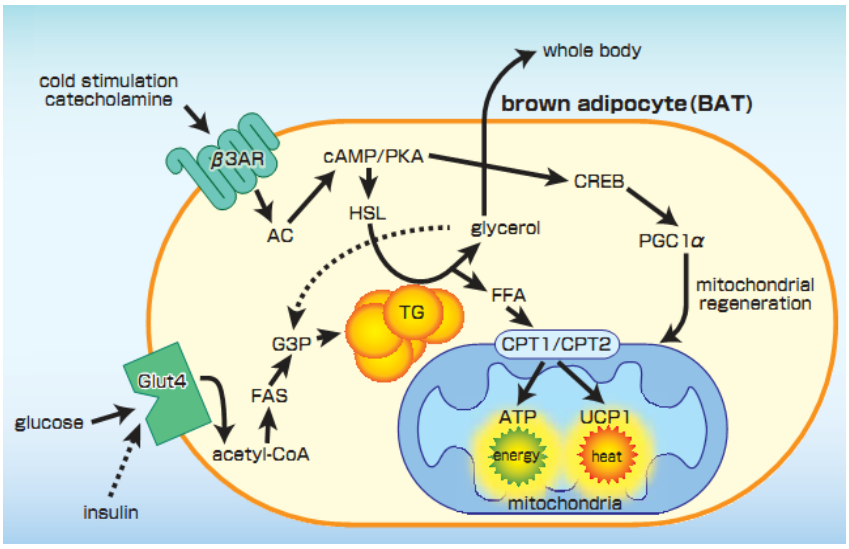

Figure 1-14 Schematic diagram of thermogenesis in brown adipocytes. Upon stimulation by cold or β-adrenergic receptor ligands, triglyceride is broken down into glycerol and free fatty acids, the latter one then enter into mitochondria and oxidized *via* β-oxidation to release the energy. The PKA-CREB-PGC1α signalling pathway activated by β-adrenergic receptor mainly mediates the mitochondrial regeneration in brown adipocytes. Glucose uptake by brown adipocytes *via* Glut4 can also be converted into triglyceride for energy-generation. Besides used for normal ATP production, majority energy released from oxidation is used to produce heat through UCP1 (COSMO Bio Co., Ltd).

In contrast to white adipocytes which originate from myf5- precursors, brown adipocytes stem from myf5+ embryonic precursors (figure 1-15) (Stephens et al., 2011). However, a revised myf5 lineage model has been proposed recently that white adipocytes, especially in retroperitoneal white adipose

tissue (rWAT) and anterior subcutaneous white adipose tissue (asWAT) develop from both myf5- and myf5+ lineage (Sanchez-Gurmaches and Guertin, 2014).

Up to date, it has been reported that adipogenesis of brown adipocytes is highly controlled by several transcription factors. BMP7 and PRDM16 have been identified as the key regulators of brown adipocytes differentiation in the early stage (Stephens et al., 2011), followed by C/EBPs and PPARs continually promoting brown adipogenesis, which finally leads to the induction of thermogenic genes expression (figure 1-15) (Seale, 2010). A set of co-activators also play vital roles in the regulation of this process through their interaction with transcription factors (Rosen et al., 2000). Of note, PPARγ coactivator-1α (PGC-1α) interacts with the transcription receptor PPARγ and regulates the genes expression involved in adipogenesis of brown adipocytes (Liang and Ward, 2006).

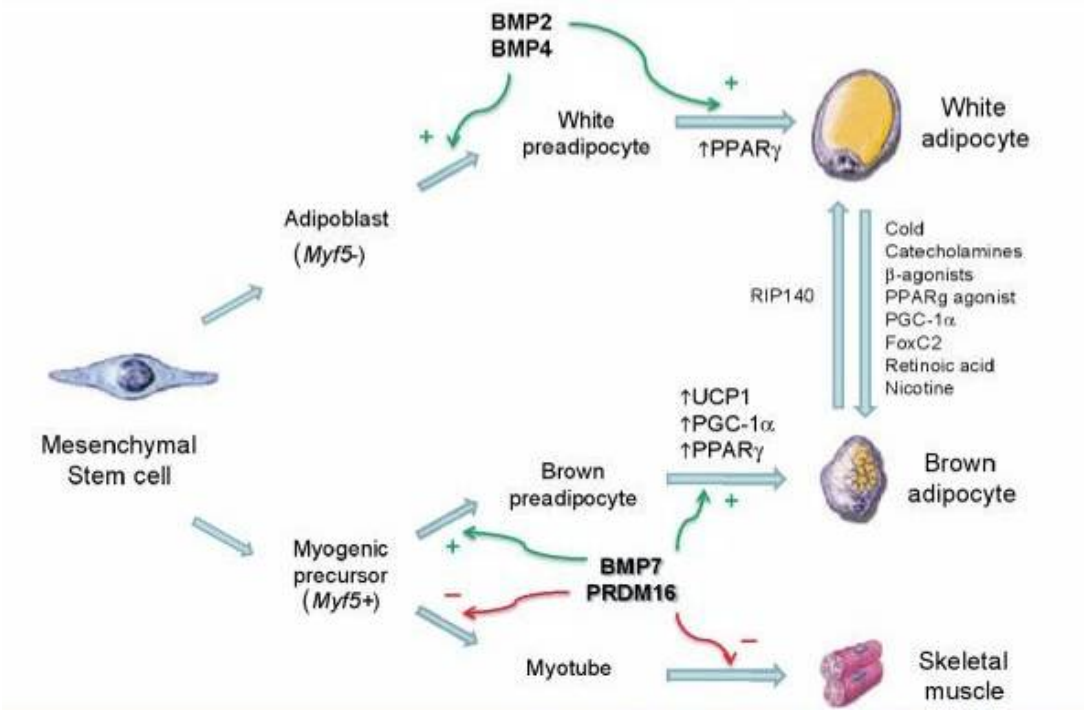

Figure 1-15 Schematic diagram of developmental pathway of white adipocytes, brown adipocytes and skeletal muscle cells differentiation from mesenchymal stem cells. Stimulatory effects are labelled with green arrows while red arrows represent inhibitory effects. BMP2 and BMP4 are crucial for white adipocyte differentiation, while BMP7 and PRDM16 decided the fate of brown adipocyte and skeletal muscle cells. PPARγ is one of the master regulators for both types of adipocytes differentiation. (Stephens et al., 2011)

The increase in mitochondria numbers (mitochondrial biogenesis), is also one major event during the brown adipogenesis. Indeed, the mitochondrial density of brown adipocytes ranks highest among any cell type in mammals (Lindberg et al., 1967). PGC-1α was found to be the major regulator of mitochondrial biogenesis, likely through the co-activation of a non-nuclear hormone receptor transcription factor, nuclear respiratory factor-1 (NRF-1) in brown adipocytes (Wu et al., 1999a). Since data from clinical trials have suggested that increased PPARγ activity reduced hyperglycaemia in type 2 diabetic patients, therefore, increasing the amount and/or activity of PGC-1α is considered as a potential pharmacologic strategy for the treatment of obesity-related diseases (Puigserver, 2005).

The brown adipose tissue possesses several unique structures to perform its non-shivering thermogenesis function. In contrast to one giant lipid drop and small amount of mitochondria, brown adipocytes contain many small lipid droplets and large number of mitochondria, which contribute to its special dark red to tan colour (Vlachakis, 2007). Besides, brown adipose tissue also has more capillaries and unmyelinated nerves than white adipose tissue due

to the oxygen and sympathetic stimulation needed during thermogenesis (Henrikson et al., 1997).

The most striking character of brown adipocytes is its capability of generating heat by non-shivering thermogenesis (Cinti, 2012). Mitochondrial uncoupling protein 1 (UCP1) has been found to be responsible for this process (Matthias et al., 2000). UCP1 protein locates at inner mitochondrial membrane, playing a role as a channel transporting proton from mitochondrial intermembrane space to mitochondrial matrix (Collins et al., 2010). UCP1 mediated proton transport uncouples the respiratory chain, allowing energy being released as large amount of heat instead of ATP (Fedorenko et al., 2012).

The browning of white adipocytes, also known as beige adipocytes or brite adipocytes, also possess thermogenic activities which can suppress weight gain (Sanchez-Gurmaches and Guertin, 2014). In rodent, cold challenge or adrenergic agonist stimulation led to the appearance of beige adipose in white adipose pads (Young et al., 1984). Further study indicated these new-formed brown adipocytes stemmed from existing white adipocytes, not traditional myf5+ preadipocytes, confirming the existence of white adipocytes browning (Shan et al., 2013). Interestingly, the beige adipocytes also showed a direct link with obesity in humans. Carey Al, *et al* found beige adipocytes derived from preadipocytes of subcutaneous white adipose tissue of obese human contains reduced UCP-1 (Carey et al., 2014).

In conclusion, increasing evidence has shown the importance of brown adipose tissue in human, therefore, better understanding of the functions of

brown adipose tissue might open up an exciting new opportunity to combat obesity and other related diseases.

1.6 Mitochondrial respiration

In eukaryotes, mitochondria are the key organelle to produce ATP *via* ATP synthase (complex V) on its inner membrane. The process that ATP synthase produce ATP relies on the H^+ ions gradient from mitochondrial matrix to intermembrane space (Fillingame, 1997). To generate H^+ ions gradient, complex I, complex III and complex IV move the H^+ ions across the inner membrane coupled with the electron transport chains (oxidative phosphorylation) pathway, by which electron was transferred from donor (NADH or succinate) generated in citric acid cycle (TCA) cycles to receptor (molecular oxygen) *via* NADH → Complex I → Q → Complex III → Cytochrome c → Complex IV → O_2 or Succinate → Complex II → FAD → Q → Complex III → Cytochrome c → Complex IV → O_2 (figure 1-16). ATP synthase joins ADP and inorganic phosphate (Pi) together into ATP(Nakamoto et al., 2008). ATP synthase consists of 2 regions, the F_O portion locates within the inner mitochondrial membrane and the F_1 portion locates inside the matrix of the mitochondria (Kagawa and Racker, 1966). X-ray crystallography further revealed that F_1 portion contains three alpha subunits and three beta subunits, which surround an asymmetrical gamma subunit (Fillingame, 1997). According to the current understanding of ATP synthesis model, the proton flows into mitochondrial matrix *via* F_O region and drives the subunit C of F_O portion rotates. The subunit C is tightly attached to

the gamma subunit of F_1 portion, which rotates within three alpha - beta subunits of F_1 portion and leads to ATP synthesis (Nakamoto et al., 2008).

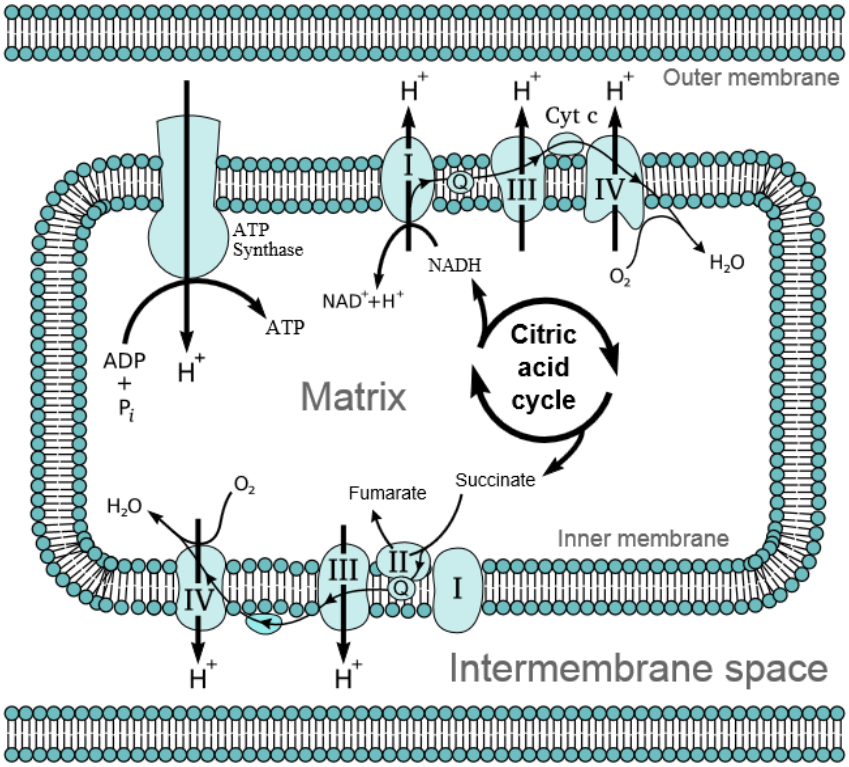

Figure 1-16 Schematic diagram of electron transport chain and oxidative phosphorylation. The electrons are passed from citric acid cycle products (NADH or succinate) to mitochondrial redox carriers until they finally reach molecular oxygen resulting in the production of H_2O. As the Complex I, Complex III, and Complex IV pass the electrons, H^+ ions are transported into the intermembrane space. The gradient of H^+ ions concentration across the intermembrane can be used to drive ATP synthase (Complex V) to produce ATP.

In brown adipocytes, mitochondria possess a unique uncoupling protein to provide a mechanism for its enormous heat-generating capacity (Valverde et al., 2005). Large number of uncoupling protein 1 (UCP1) has been found only in mitochondria in brown adipocytes as well as beige adipocytes (Keipert and Jastroch, 2014), which short circuits the electrochemical (H^+)

gradient across the intermembrane and thereby dissipate the large amounts of chemical energy in the form of heat instead of cellular ATP (Rousset et al., 2004, Keipert and Jastroch, 2014). Therefore, understanding parameters of mitochondria respiration in brown adipocytes is important to investigate its metabolic functions.

By using specific modulators of respiration which target components of the electron transport chain in the mitochondria, it is possible to interrogate several key parameters of mitochondria respiration, including basal respiration (oxygen consumption used to meet energetic demand of the cell under baseline conditions); ATP production (oxygen consumption used to produce ATP by the mitochondria); proton leak (remaining basal mitochondrial respiration not coupled to ATP production); maximal respiration (the maximum rate of respiration that the cell can achieve upon metabolic challenge.); spare respiratory capacity (the capability of the cell to respond to an energetic demand as well as how closely the cell is to respiring to its theoretical maximum) and non-mitochondrial respiration (oxygen consumption that persists due to a subset of cellular enzymes that continue to consume oxygen) (figure 1-17) (Wang et al., 2013a).

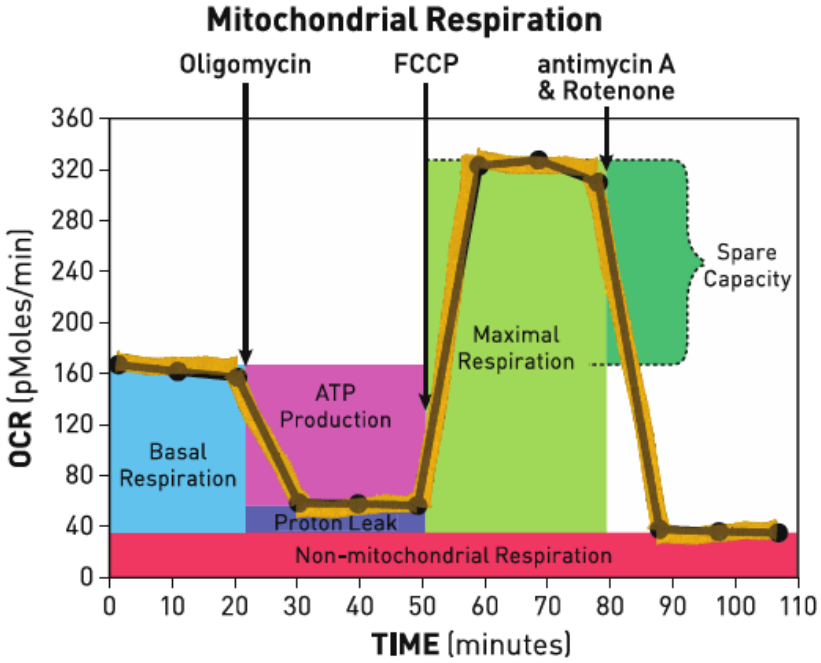

Figure 1-17 The key parameters of mitochondrial respiration measured by Seahorse XF24 Analyser with XF Cell Mito Stress Test Kit. The sequential compounds injections (Oligomycin; FCCP; antimycin A & Rotenone) were indicated with black arrows. Oligomycin blocks ATP synthesis against Complex V, therefore, the decrease of OCR represents the ATP production; FCCP acts as an uncoupling agent, therefore, the maximum OCR recorded after FCCP injection represents the maximum mitochondrial respiration ability. Finally, antimycin A and rotenone totally block the mitochondrial respiration *via* inhibiting mitochondrial Complex I and Complex III, respectively. Therefore, the non-mitochondrial respiration can be measured by the remaining OCR (Wang et al., 2013a).

Take XF Cell Mito Stress Test kit as an example, the compounds used in XF Cell Mito Stress Test Kit include oligomycin, FCCP, and a mix of rotenone and antimycin A. As demonstrated in figure 1-18, oligomycin targets Complex V, which joins inorganic phosphate and ADP into ATP (Kagawa and Racker, 1966). Therefore, measuring the decrease in oxygen consumption following oligomycin injection can reveal mitochondrial

respiration used for ATP production. FCCP (Carbonyl cyanide-4-(trifluoromethoxy)phenylhydrazone) is an uncoupling agent that disrupts Complex V and collapses the H^+ gradient across the intermembrane (Heytler and Prichard, 1962). Consequently, electron flow through the electron transport chain and oxygen consumption reach maximum after FCCP injection. Therefore, FCCP-stimulated oxygen consumption can be measured as maximal respiration and the spare capacity can be calculated as the difference between maximal respiration and basal respiration. Rotenone and antimycin A inhibit the Complex I and complex III, respectively (Teeter et al., 1969). Combination of these two reagents totally blocks the electron transport chain and mitochondrial respiration. Therefore, remaining oxygen consumption after injection of rotenone and antimycin A represents the non-mitochondrial respiration. The proton leak then can be calculated as the difference between respiration after oligomycin injection and respiration after rotenone and antimycin A injection.

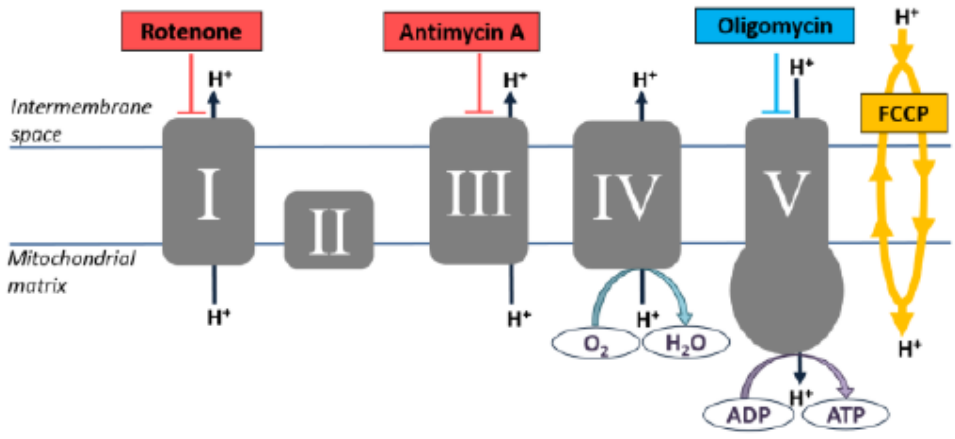

Figure 1-18 The targets of compounds used in XF Cell Mito Stress Test Kit. Oligomycin inhibits ATP synthase (complex V), FCCP dissipate the proton gradient without ATP production, rotenone and antimycin A inhibit complexes I and III, respectively (Wang et al., 2013a).

1.7 Endoplasmic reticulum stress

Endoplasmic reticulum (ER) stress, as a cell self-protective mechanism, is conserved between all mammalian species (Yang et al., 2014). As an organelle for folding and sorting of protein inside the cells, ER possess large number of endoplasmic reticulum chaperone proteins to help the newly made proteins correct folding (Ma and Hendershot, 2004). However, upon accumulation of malfolded proteins in the ER, cells activate a defence mechanism called the ER stress response (Ma and Hendershot, 2004). A wide range of factors have been identified as the causes of ER stress such as aging, genetic deficiency, viral infection or the over-expression of proteins (Yoshida, 2007). It has been revealed that three independent unfolded protein response sensors (protein kinase RNA (PKR)-like ER kinase (PERK); inositol-requiring protein-1 (IRE1α); and activating transcription factor-6 (ATF6)) separately regulate induction unfolded protein response (UPR) (Kaufman et al., 2010). In unstressed state, BiP/glucose-regulated protein 78 (BiP/GRP78) binds to PERK, IRE1α, and ATF6. Upon activation of unfolded protein response, BiP binds to unfolded proteins and dissociates with these three ER sensors PERK, IRE1α, and ATF6, results in phosphorylation of PERK and IRE1α and cleavage of ATF6 (Lee, 2005). Phosphorylated PERK then induces phosphorylation of eIF2α, which attenuates global translation and selectively induces ATF4 translation (Harding et al., 2000). ATF4 induces expression of ER stress-associated molecules, including chaperones, amino acid (AA) transporters, ER-associated degradation (ERAD), CHOP and GADD34 (Harding et al., 2000, Harding et al., 2003, Ma and Hendershot, 2003). Phosphorylation of IRE1α leads to the splicing of X

box binding protein-1 (XBP1) mRNA, which is translated into XBP1s isoform and increases transcription of chaperones, foldases and ERAD genes (Yoshida et al., 2001, Acosta-Alvear et al., 2007). ATF6 is activated by site 1 protease and site 2 protease (S1P/S2P) in the Golgi, which then translocates to the nucleus to activate transcription of chaperones and ERAD genes (Shen and Prywes, 2004). Recently, studies also suggested that these three unfolded protein response sensors can form regulatory networks upon unfolded protein response. For example, PERK/eIF2α/ATF4 pathway is also required for activation of ATF6 and its target genes (Teske et al., 2011).

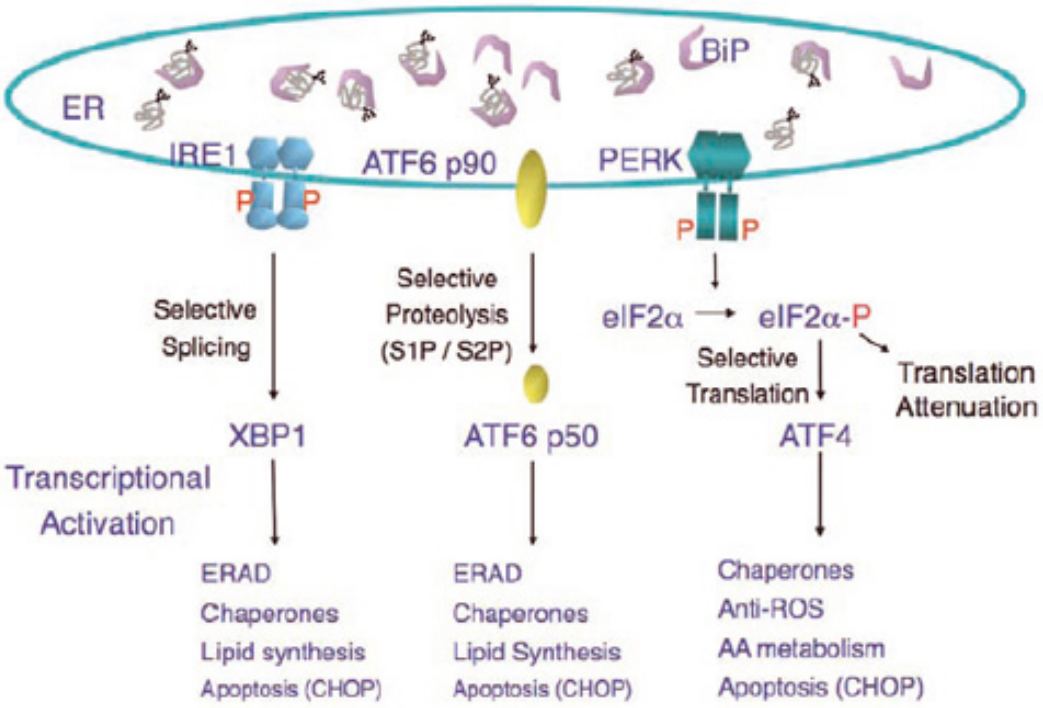

Figure 1-19 The unfolded protein response signalling pathways. In unstressed conditions, the BiP binds to three unfolded protein response sensors (PERK, IRE1, and ATF6) to inhibit their activation. Upon accumulation of unfolded proteins, BiP dissociates with these unfolded protein response sensors and interacts with unfolded proteins, leading to the activation of PERK, IRE1, and ATF6. PERK undergoes homodimerization and autophosphorylation, and phosphorylates eIF2α. Phosphorylated eIF2α decreases global translation but selectively increases

translation of ATF4. ATF4 regulates the transcription of genes involved in antioxidant response and amino acid transporter synthesis, as well as chaperones, CHOP and GADD34. IRE1 also autophosphorylates *via* homodimerization, which results in the splicing of the XBP1 mRNA to form the transcription factor XBP1s, which induces expression of ERAD proteins, chaperones and CHOP. ATF6 is proteolysed by site 1 and site 2 proteases (S1P and S2P). The N-terminal domain of ATF6 induces expression of chaperones, ERAD proteins and CHOP (Kaufman et al., 2010).

ER stress has been identified as a characteristic in adipose tissue of obese individuals, which is believed as one reason to cause chronic inflammation (Kawasaki et al., 2012). Studies have revealed addition of chemical chaperones could restore glucose homeostasis in a mouse model of type 2 diabetes *via* reducing ER stress, suggesting ER stress is a promising target to treat obesity related diseases such as type 2 diabetes (Ozcan et al., 2006). ER stress also mediates adipocytes differentiation. Using *in vitro* models, Han *et al*., demonstrated ER stress suppressed adipocyte differentiation in 3T3-L1 cells (Han et al., 2013). ER stress was also found to affect adipokines expression in adipose tissue. Mondal *et al*., found the induction of ER stress was accompanied by a decrease in adiponectin and Iκβ-α expression as well as increase in TNF-α mRNA in adult-derived human adipocyte stem (ADHAS) cells (Mondal et al., 2012). High-fat diet induced overexpression of GPR43 in tissues such as white adipose tissue, muscle and liver (Dewulf et al., 2011, Cornall et al., 2011), suggesting high-fat diet induced ER stress might also be involved in the regulation of GPR43 (Dewulf et al., 2011).

1.8 MAPK signalling pathway

Mitogen-activated protein kinases (MAPKs) are a highly conserved family of serine/threonine protein kinases. The classical MAPK signalling pathways are regulated by a three-tiered phosphorylation cascade: MAPKKK→MAPKK→MAPK (Seger and Krebs, 1995). When cells are exposed to wide range of extracellular stimuli including mitogens, cytokines, growth factors, and cellular stressors, etc., MAPKKK will be activated and phosphorylate a downstream MAPKK, which will further activate a specific MAPK by phosphorylation (Goldsmith and Dhanasekaran, 2007). In human, at least 19 MAPKKK (MAP3K1, MAP3K2, MAP3K3, MAP3K4, MAP3K5(aka ASK1), MAP3K6(aka ASK2), MAP3K7(aka TAK1), MAP3K8(aka TPL2), MAP3K9, MAP3K10, MAP3K11(aka MLK3), MAP3K12(aka MUK), MAP3K13(aka LZK), MAP3K14, MAP3K15(aka TAO1), MAP3K16(aka TAO2), MAP3K17, RAF1, BRAF, ARAF, ZAK) and 7 MAPKK (MAP2K1, MAP2K2, MAP2K3, MAP2K4, MAP2K5, MAP2K6, MAP2K7) have been discovered. Conventional MAPKs include the extracellular signal-regulated kinase 1 and 2 (ERK1/2), c-Jun N-terminal kinases 1-3 (JNK1-3), p38 isoforms (p38α, β, γ and δ) and ERK5 (figure 1-20) (Cargnello and Roux, 2011). There are also atypical MAPK including ERK3/4, ERK7/8 and Nemo-like kinase (NLK) being discovered in recent years (Cargnello and Roux, 2011). Not all atypical MAPKs follow the classical three-tiered MAPK pathways. For example, ERK3/4 was recently shown to be directly phosphorylated and activated by PAK kinases (Deleris et al., 2011). This two-tiered system was believed to be a more ancient system. Although the details of NLK and ERK7/8 activation remain vague, however, recent studies

suggested that Thr286 is predicted to be key phosphorylation site in the activation loop of NLK. Mutation of Thr286 abolished the autophosphorylation of NLK and downstream c-Myb degradation (Brott et al., 1998). Meanwhile, ERK7/8 was found to physically associate with c-Src. Activated c-Src kinases phosphorylate and activate ERK7/8 in Cos7 cells (Abe et al., 2002, Jin et al., 2015).

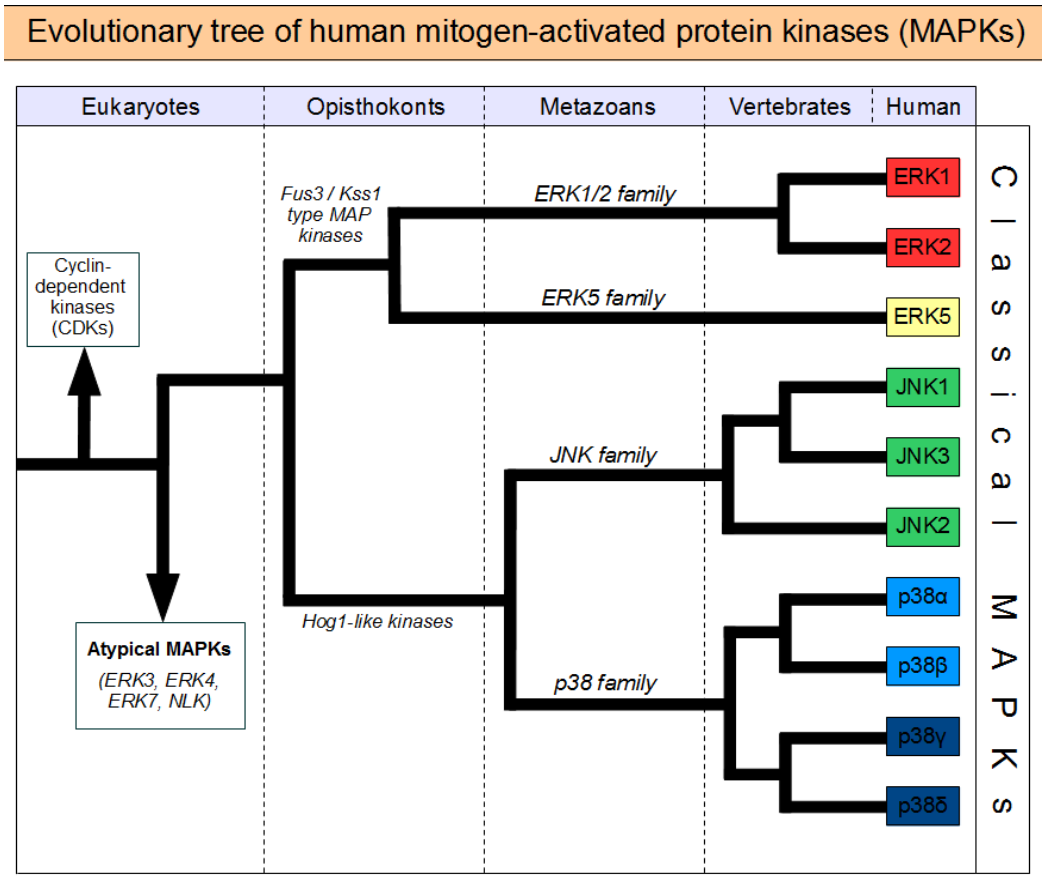

Figure 1-20 The cladogram for mitogen-activated protein kinases. Cladograms were calculated based on the sequences of kinase domains for MAPKs indexed in KinBase (kinase database) (Glatz et al., 2013).

The MAPKKKs activate MAPKKs in a very diversity way. Many MAPKKKs own capacity to phosphorylate multiple MAPKKs *in vitro* and activate many MAPKs when overexpressed (figure 1-21). Only MAPKKK Raf isoforms

phosphorylate MEKs in a highly specific way (Rafs→MEK1/2) (Kyriakis et al., 1992). There are also plenty of crosstalk and signalling switches in MAPKs phosphorylation by MAPKKs, except MEK1/2 was only found to activate ERK1/2 (Wortzel and Seger, 2011). Due to this selectivity, MEK1/2 inhibitors serve as useful tools to investigate the effects of ERK1/2 activation on various downstream effectors and further illustrate the roles of ERK1/2 pathway in cellular regulation. For example, U0126 directly inhibits MEK1 activity, and greatly impairs ERK1/2 activation *in vitro* (Favata et al., 1998*)*. While another widely used MEK1/2 inhibitor PD098059 indirectly blocks MEK1/2 activation by binding to the inactive enzyme and also deactivates ERK1/2 (Dudley et al., 1995).

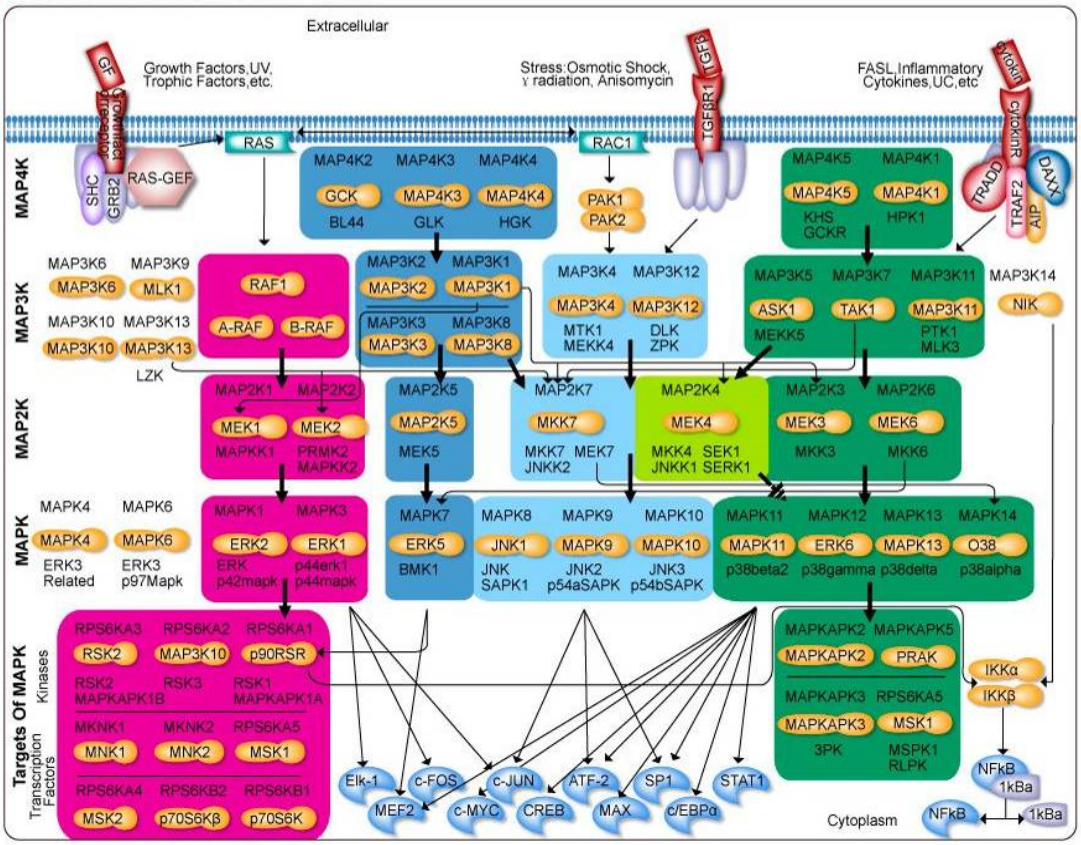

Figure 1-21 Schematic diagram of MAPK cascade. Activated by a diverse array of stimulus, MAPKK kinases (MAPKKKs) phosphorylate and activate a downstream

MAPK kinase (MAPKKs), which then phosphorylates and activates MAPKs. Activated MAPKs leads to the phosphorylation and activation of specific targets of MAPK, such as members of the RSK, MSK, or MNK family, or induced the activation of transcription factors including c-Fos, c-Jun, c-Myc, CREB, STAT1, etc.. (GeneCopoeia).

The kinase cascade that transmits signals from MAPKKK to MAPK provides molecular mechanisms underlying signalling amplification and feedback regulation. Analysis on the computational model has suggested multi-level signalling cascades such as MAPK cascades attenuate input signal noise (Thattai and van Oudenaarden, 2002), and amplify signal transduction specificity (Swain and Siggia, 2002). MAPK cascades amplifying signalling relies on the high efficiency of mitogen-activated protein kinases, which can phosphorylate much more downstream effectors (Khokhlatchev et al., 1997). Therefore, MAPK signalling cascade easily transmits the signals from small number of activated receptors to widespread responses in the cells.

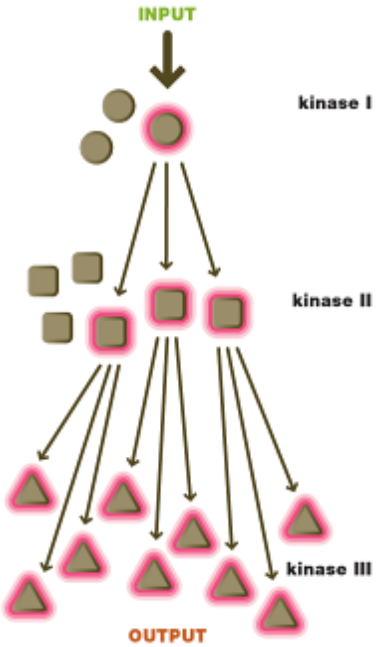

Figure 1-22 Schematic diagram of amplification in signalling cascades. Small number of upstream kinases are activated by input signals and induce the activation of more downstream kinases, resulting in the amplified signals and widespread responses in the cells.

To make MAPK signalling pathways to be controllable, MAPK signalling cascades normally also contain negative feedback loops, which allows excessive input signals can be ignored when the effects have reached the desirable output levels (Katz et al., 2007). Take Raf-MEK-ERK cascade as an example, activated ERK feeds back to MEK by phosphorylation of MEK1 at Thr292, which inhibits the MEK-ERK complex formation, and thereby interferes the MEK phosphorylating ERK (Eblen et al., 2004, Shin et al., 2009).

MAPKs are necessary to modulate adipogenesis in adipose tissue (Bost et al., 2005a). For example, ERK1 was found to be required for proliferative stage of adipogenesis. The ERK1 knock-out mice showed decreased adipose tissue and less adipocytes compared to wild-type mice. Moreover, the preadipocytes from ERK1 knock-out mice demonstrated impaired adipogenesis (Bost et al., 2005b). Although the precise mechanisms underlying the indispensable effects of ERK on adipogenesis is still not fully understood, however, C/EBPβ, an ERK phosphorylation target, might account for the ERK effect on adipocyte differentiation (Park et al., 2004). Meanwhile, increasing evidence also proved the inhibitory effects of p38 selective inhibitor on adipogenesis, suggesting the indispensable role of p38 in adipogenesis (Engelman et al., 1998). Indeed, p38 is also a key kinase for the activation of thermogenesis in brown adipocytes (Cao et al., 2004).

cAMP- and PKA-dependent activation of p38 is an indispensable step in the transcription of the UCP1 gene in brown adipose tissue in mice (Cao et al., 2004).

Indeed, it has been found that numerous metabolic regulators mediate brown adipocyte functions *via* MAPKs. For example, irisin promotes browning of white adipocytes *via* activating p38 and ERK signalling pathway (Wu and Spiegelman, 2014, Zhang et al., 2014). Cardiac natriuretic peptides such as atrial NP (ANP) and ventricular NP (BNP) induce PGC-1α and UCP1 expression in human adipocytes in a p38 MAPK-dependent manner (Bordicchia et al., 2012). GADD45γ regulates the thermogenic capacity and UCP-1 expression in brown adipocytes by activating p38 (Gantner et al., 2014). These findings highlighted the involvement of MAPKs activation, especially the ERK and p38 activation, in the regulation of brown adipocyte.

Recently, receptor-specific regulation of ERK1/2 activation by members of free-fatty acids receptor family has been investigated (Seljeset and Siehler, 2012). The results demonstrated activation of free-fatty acids receptor GPR40, GPR41 and GPR43 all leads to ERK1/2 activation in HEK293 cells stable-transfected with these receptors, respectively. Besides, studies on functions of free-fatty acids receptors also supported that MAPK signalling pathways was involved in free fatty acids mediated effects. For example, it has been found that short-chain fatty acids induce acute phosphorylation of the p38 in MCF-7 human breast cancer cell line *via* GPR43 and in bovine mammary epithelial cells *via* GPR41 and GPR43 (Yonezawa et al., 2007,

Yonezawa et al., 2009). Collectively, MAPK signalling pathways may play important roles in short-chain fatty acids mediated effects.

1.9 CREB signalling pathway

CREB, also known as cAMP response element-binding protein, is a cellular transcription factor (Altarejos and Montminy, 2011). CREB is closely related in structure and function to CREM (cAMP response element modulator) and ATF-1 (activating transcription factor-1), which all belong to ATF/CREB protein family. CREB contains two glutamate-rich domains (Q1 and Q2), a central kinase-inducible domain (KID), and a carboxyl-terminal basic leucine zipper (bZip) domain (figure 1-23). The phosphorylation at Ser133 inside the KID domain mediates the interaction between CREB and CREB-binding protein (CBP) / p300 (Vo and Goodman, 2001). bZip domain promotes CREB - DNA binding (Sharma et al., 2007). CREB also can form homo-dimers as well as hetero-dimers with other members of ATF/CREB family through their bZip domains (Shaywitz and Greenberg, 1999). Q1 and Q2 domains interact with various co-factors to regulate CREB activity. For example, Q1 and Q2 domains can interact with TATA binding protein-associated factor II 135 (TAFII135), which in turn recruits a polymerase complex and stimulates transcription (Felinski and Quinn, 2001).

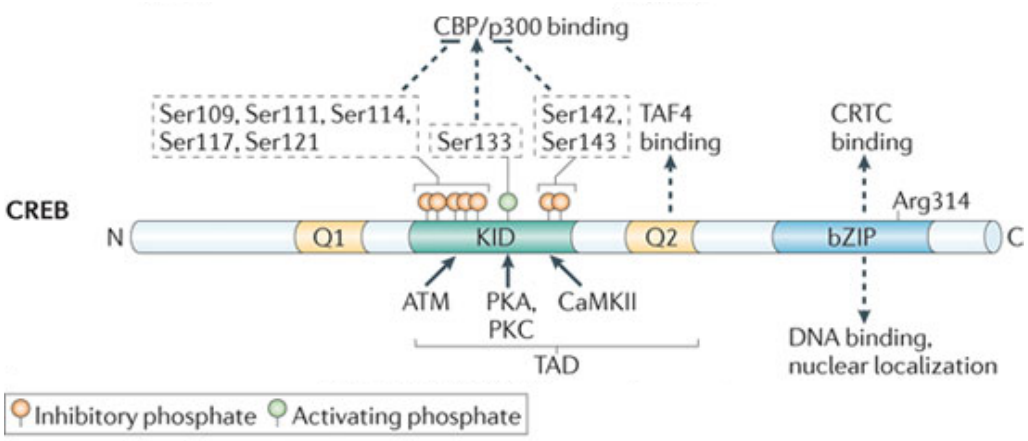

Figure 1-23 Modular organization of CREB. Yellow regions represent two Glu-rich domains (Q1 and Q2); green region shows a central kinase-inducible domain (KID) and blue region demonstrates a carboxyl-terminal basic Leu zipper (bZIP) domain. The amino-terminal transactivation (TAD) domain consist of the KID domain and the Q2 domain. Phosphorylation of Ser residues in the KID domain mainly mediates the interaction with CREB-binding protein (CBP) and its paralogue p300. Phosphorylation at Ser133 promotes this interaction while phosphorylation of other Ser residues flanking Ser133 acts inhibitory effects. The Q2 domain binds to TBP-associated factor 4 (TAF4); The bZIP domain mediates CREB binding to DNA and cAMP-regulated transcriptional co-activators (CRTCs). Arg314 is key residue for the CRTC binding (Altarejos and Montminy, 2011).

CREB is phosphorylated in response to a wide variety of signals (Mayr and Montminy, 2001). Ser133 in KID domain is a key residue to stimulate CREB activity, which could be phosphorylated by numbers of kinases, including CaMK II, PKA, PKC, MSK, RSK, Akt and MAPKAP kinase 2, etc. (Alberts et al., 1994, Andrisani, 1999). CREB phosphorylation at Ser133 leads to the recruitment of CBP/ p300, followed by binding to gene promoters containing cAMP response element (CRE) (Clark et al., 2015). The typical sequence of CRE is ‘TGACGTCA’, while half-site ‘TGACG or CGTCA’ are also found to possess transcriptional activities (Loeken, 1993).

CREB is a crucial regulator to modulate metabolism (Altarejos and Montminy, 2011). Studies have highlighted the diverse functions of CREB in metabolic tissues, including the liver, pancreatic islets, skeletal muscle and adipose tissue. For example, CREB was found to promote β-cell survival. Disruption of CREB function in β-cells leads to decreased islet mass (Jhala et al., 2003). CREB is also important for skeletal muscle. Overexpression of dominant-negative CREB in skeletal muscle causes progressive muscle wasting, muscle inflammation and myonecrosis (Berdeaux et al., 2007). In adipocyte, CREB activation leads to an increased expression of ATF3, which inhibits the expression of insulin-sensitive GLUT4 (Qi et al., 2009). Mutation of adipocyte-CREB in mice increased the expression of GLUT4 in adipocytes and showed protective effects from development of insulin resistance (Qi et al., 2009).

CREB has also been found to play crucial roles in adipogenesis and mitochondrial biogenesis. In 3T3-L1 cells, Reusch *et al.* found conventional differentiation inducing agents such as insulin, dexamethasone, and dibutyryl cAMP stimulated CREB activation throughout the differentiation process (Reusch et al., 2000). Furthermore, constitutively activation of CREB in preadipocytes was sufficient to induce adipogenesis while expression of dominant-negative CREB blocked the differentiation, indicating CREB is necessary to induce adipogenesis (Reusch et al., 2000). Besides, CREB was also found to regulate several adipocyte-specific genes transcriptions *via* binding to putative CRE sequences in the promoters, such as PEPCK, FAS, and FABP, etc.. (Reusch et al., 2000). CREB is also a key regulator for

adipogenesis and thermogenesis in brown adipocytes. Upon activation of β-adrenergic receptor, intracellular cAMP level, as well as cAMP-dependent PKA activity are elevated, leading to the phosphorylation of CREB at Ser133. Activated CREB up-regulates the expression of PGC-1α, which further increases the mitochondria biogenesis and brown adipogenesis (Scarpulla, 2011). Activated CERB also directly increases thermogenic genes transcription such as UCP1 (Xue et al., 2005). In liver, CREB also controls hepatic lipid metabolism *via* stimulating expression of PGC-1α. Mice with deficiency in CREB activity show a fatty liver phenotype (Herzig et al., 2003). Collectively, these studies highlight the importance of CREB signalling pathway in the control of energy homeostasis.

1.10 PPAR signalling pathway

PPARs (Peroxisome proliferator-activated receptors) are a group of nuclear receptors activated by peroxisome proliferators (Moreno et al., 2010). Until now, four PPAR isoforms (α; β/δ; γ1; γ2) have been identified in humans (Berry et al., 2003, Yanase et al., 1997). They share a similar structure which contains the following functional domains: N-terminal region; DBD (DNA-binding domain); flexible hinge region; LBD (ligand binding domain) and C-terminal region (figure 1-24) (Wadosky and Willis, 2012).

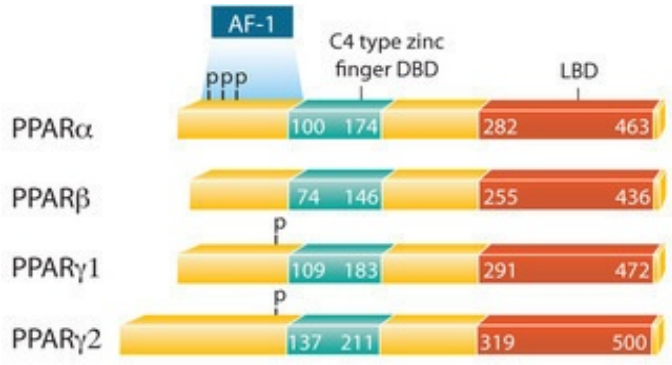

Figure 1-24 Modular organization of PPAR isoforms. Green region shows DBD (DNA-binding domain); while orange region demonstrates LBD (ligand binding domain). The key phosphorylation sites are marked as -P. (Wadosky and Willis, 2012)

PPARs activation requires the formation of heterodimers with another nuclear receptor: retinoid X receptors (RXRs). Both DBD and LBD of PPARs are involved in the dimerization with RXRs. (Bourguet et al., 1995). The PPAR/RXR heterodimers recognize and bind to PPAR-responsive elements (PPREs) in promoters. The typical PPRE contains direct repeats (DRs) DNA sequence of AGG(T/A)CA separated by single or two intervening base-pairs (Miyamoto et al., 1997).

The activation of PPAR/RXR heterodimers normally also requires the recruitment of coactivators, such as PPARγ coactivator 1 (PGC-1), the histone acetyltransferase p300, and the CREB binding protein (CBP), to induce the transcription of target genes (Viswakarma et al., 2010). This process often occurs with the histone modification such as acetylation (figure 1-25).

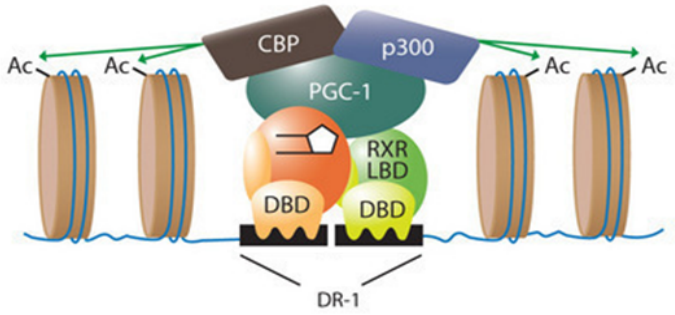

Figure 1-25 Model of PPAR-RXR coactivator complex. The transcription factors PPAR and RXR form the heterodimerization *via* their DBD and LBD domains. After ligand binding to PPAR, coactivators are assembled into transcription factor complex and induce histone modifications such as acetylation, which activates the transcription of target genes (Viswakarma et al., 2010).

Although PPAR isoforms are similar in structure and all play essential roles in metabolism regulation, however, they have relatively distinct tissue distribution and functions. For example, PPARα mainly expresses in liver and controls cholesterol metabolism and fatty acids oxidation (Burri et al., 2010); while PPARγ is abundant in adipose tissue and regulates adipocyte differentiation (Siersbaek et al., 2010); PPARβ/δ is important for fatty acids transport and oxidation, mitochondrial respiration and thermogenesis in skeletal muscles (Erol, 2007). However, recent studies also revealed that there are overlaps across the functions of PPAR isoforms. For example, PPARα also expresses in adipose tissues and promotes adipogenesis (Goto et al., 2011). PPARβ/δ activation also promotes triglyceride metabolism and UCP1 expression in white and brown adipocytes (Wang et al., 2003).

Although it is widely accepted that PPARγ is one of the master regulators for the differentiation of both white and brown adipocytes (Lee et al., 2008). However, these two types of adipocytes exhibit distinct properties and

transcriptome, indicating the existence of complex regulation of genes expression during the differentiation of white and brown adipocytes. Recent studies have highlighted the importance of coregulators of PPARγ (such as PGC-1α) in this process (Viswakarma et al., 2010).

Due to its important roles in energy metabolism, PPARs, especially PPARγ, have become novel drug targets to treat obesity and diabetes. PPARγ agonist thiazolidinediones (e.g. rosiglitazone) have been demonstrated to be effective insulin sensitizers in type 2 diabetes patients (Bailey and Day, 2001). However, due to its side effects on cardiovascular system, rosiglitazone has been withdrawn from the market in European (Singh et al., 2007). Similarly, several other thiazolidinediones, such as pioglitazone, and troglitazone, has also been suspended in some country due to their risks of causing bladder cancer and hepatitis, respectively (Turner et al., 2014, Bonkovsky et al., 2002). Although most of the first generation of thiazolidinediones have been abandoned in clinical treatment due to their unneglectable side effects, however, because of their significant effects on improving insulin resistance in type 2 diabetes patients, search for the novel PPARγ agonists without severe side effects continues. Furthermore, several new investigated PPARα/γ dual agonists, such as ragaglitazar (Skrumsager et al., 2003), muraglitazar (Nissen et al., 2005), tesaglitazar (Oakes et al., 2005), LSN862 (Reifel-Miller et al., 2005), naveglitazar (Yi et al., 2007), and netoglitazone(MCC-555) (Imchen et al., 2013) are reported to improve insulin resistance as well as decrease atherogenic triglycerides and increase

cardioprotective HDL levels, which seems to be a promising strategy to develop anti-diabetic drugs.

Both *in vivo* and *in vitro* studies have linked short-chain fatty acids with PPARγ activity. For example, den Besten *et al.*, found dietary supplement with short-chain fatty acids induced a PPARγ-dependent switch from lipid synthesis to utilization in mice liver (den Besten et al., 2015). Alex *et al.*, reported short-chain fatty acids increased angiopoietin-like 4 synthesis in human colon adenocarcinoma cells by activating PPARγ (Alex et al., 2013). Due to the importance of PPARγ in adipocytes, it is reasonable to speculate that short-chain fatty acids may also mediate functions of adipocytes.

1.11 PI3K/Akt signalling pathway

Akt, also known as Protein Kinase B (PKB), is a serine/threonine-specific protein kinase (Yang et al., 2004). Akt consists of three domains: the PH (pleckstrin homology) domain at N-terminal, the kinase domain and the regulatory domain at C-terminal (Hanada et al., 2004).

Figure 1-26 Modular organization of the AKT. AKT possesses three domains: the PH (pleckstrin homology) domain, the kinase domain and the C-terminal regulatory domain. The PH domain and the kinase domain are linked with a helix structure.

The residues Thr308 in kinase domain and Ser473 in the hydrophobic motif of regulatory domain are phosphorylated when AKT become active (Song et al., 2012).

Akt is mainly involved in the PI3K/AKT pathway (Downward, 1998). Activated PI3K catalyses the phosphorylation of phosphatidylinositol into phosphatidylinositol 3,4,5-trisphosphate ($PI(3,4,5)P_3$) (King et al., 1997). PI(3,4,5)P3 binds to Akt PH domain and induces conformational changes of Akt, followed by exposure of phosphorylation sites Thr308 and Ser473 (Hanada et al., 2004). Phosphorylation of these two residues leads to fully activation of Akt.

Phosphatase and tensin homolog (PTEN) antagonises PI3K functions by converting PI(3,4,5)P3 into PI(4,5)P2. Because PI(3,4,5)P3 is the key secondary message to activate Akt (Maehama and Dixon, 1999), therefore PTEN also inhibits PI3K/Akt signalling pathway (Stambolic et al., 1998).

The PI3K-Akt pathway plays important roles in multiple cellular processes, including brown adipogenesis. Recently, it has been demonstrated that Akt pathway negatively regulated UCP1 transcription in brown adipocytes (Ortega-Molina et al., 2012). Increasing PTEN activity or attenuating Akt activity was found to up-regulate expression of brown adipocyte markers UCP1 in brown adipocytes (Ortega-Molina et al., 2012). However, *in vivo* experiment also demonstrated the necessity of Akt for the normal differentiation of brown adipocytes. Akt1/2 knock-out mice displayed impaired brown adipogenesis. (Peng et al., 2003). Akt was also found to regulate adipocyte differentiation in very early stage (mitotic clonal expansion)

(Nogueira et al., 2012). Therefore, the relationship between Akt and brown adipogenesis still need more work to explore.

1.12 XBP1 signalling pathway

XBP1, the abbreviation for X-box binding protein 1, is a transcription factor that regulates the mammalian unfolded protein response (He et al., 2010). XBP1 contains a bZIP domain allowing it binds to the *cis*-acting X box present in the promoter regions of human major histocompatibility complex class II genes (Liou et al., 1990). Moreover, XBP1 also binds to ER stress response element (ERSE) in response to ER stress (Yoshida et al., 2001). The typical sequence of ERSE is CCAAT-N9-CCACG (Yoshida et al., 1998). As discussed above, XBP1 mRNA splicing was induced after activation of IRE1α, resulting in a frame-shift and an isoform XBP1s. Although both XBP1u and XBP1s can bind to ERSE in the presence of NF-Y, however, only spliced form of XBP1 shows significant transcriptional activity and induces target genes expression (Yoshida et al., 2001).

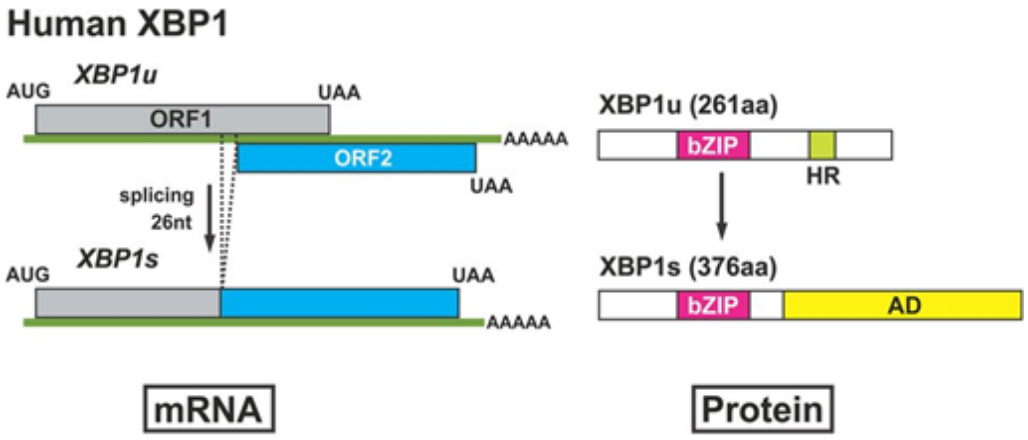

Figure 1-27 mRNA splicing of XBP1 in response to ER Stress. Grey and blue regions represent two ORFs of XBP1; pink region shows a carboxyl-terminal basic Leu zipper (bZIP) domain; green region demonstrates hydrophobic region and yellow region shows transcriptional activator domain. Only the XBP1s form contains the transcriptional activator domain in the C-terminal region when XBP1 mRNA splicing occurs in response to ER Stress (Yoshida et al., 2001, Nagashima et al., 2011).

As a key regulator in ER stress, abnormalities in XBP1 normally link with increased ER stress response and subsequent susceptibility to inflammatory. It has been suggested that XBP1 malfunction contributed to Alzheimer's disease and inflammatory bowel diseases (such as Crohn's disease) (Casas-Tinto et al., 2011, Kaser et al., 2008).

XBP1 is indispensable for the differentiation of various cell types *in vivo*, such as plasma cells, pancreatic and salivary exocrine cells (Reimold et al., 2001, Lee et al., 2005). XBP1 is also crucial for the development of liver cells. Mice lacking XBP1 displayed hypoplastic fetal livers (Reimold et al., 2000). Besides, Xbp1 also mediates lipogenesis in the liver (Lee et al., 2008). Furthermore, XBP1 is also found to be necessary for adipogenesis *in vitro*. Suppressing XBP1 expression in preadipocytes *in vitro* led to severe inhibition of adipogenesis (Sha et al., 2009). However, *in vivo* study showed deletion of adipocyte XBP1 had little effect on adipose tissue formation and metabolic functions in mice, suggesting the complex roles of XBP1 in adipogenesis still need more evidence to elucidate (Gregor et al., 2013).

1.13 STAT signalling pathway

STAT (signal transducer and activator of transcription) proteins are a family of transcription factors. STAT proteins share a highly conserved Src homology2 (SH2) domain, which mediates dimerization of STATs *via* phosphotyrosine. The dimerization of STATs is an essential pre-requisite for the classical STAT signalling pathways. Interestingly, STATs could form both homodimers and heterodimers *via* their SH2 domains. For example, in type I interferon signalling, STAT1-STAT2 heterodimers together with IRF9 can bind to ISRE to induce target genes expression. Several widely-used STAT inhibitors (e.g. 6-Nitrobenzo[b]thiophene-1,1-dioxide, N'-((4-Oxo-4H-chromen-3-yl)methylene) nicotinohydrazide, etc.) target SH2 domain phosphorylation and dimerization events, which also highlights the irreplaceable roles of SH2 domain in STAT signalling.

It has been recognized for more than decades STATs proteins play important roles in the transcriptional control of adipogenesis. The first evidence to support this idea is that increase in expression levels of members of STATs family such as STAT3, STAT5A and STAT5B occurs during differentiation of 3T3-L1 adipocytes and human primary adipocytes (Stephens et al., 1996). Among them, STAT5s has been identified with strong pro-adipogenic activities (Stewart et al., 2011). Knock-out transgenic mice models provide more evidence to support the indispensable role of STATs proteins in adipose tissue *in vivo*. Deletion of STAT5A or STAT5B leads to severe impaired adipose tissue in mice, while double knock-out of STAT5A and STAT5B causes loss of about 80% of fat pad (Teglund et al., 1998).

Interestingly, there are wide cross talk between STAT5 signalling pathway and PPARγ signalling pathway during adipogenesis. In several preadipocyte models, activated STAT5 have been shown to induce PPARγ expression in early stage of adipogenesis, suggesting that STAT5 can promote adipocyte differentiation by regulating PPARγ. Intriguingly, during adipogenesis of human bone marrow-derived stromal cells, PPARγ binds to the STAT5A promoter (Olsen and Haldosen, 2006). Given the tight relationship of PPARγ and adipogenesis, elucidating the complex interplay of STAT5-PPARγ in mediating adipogenesis would advance our understanding towards the transcriptional control of adipogenesis

1.14 Aims of the study

Short-chain fatty acids and their receptors have been proved to play important roles in keeping body metabolic homeostasis. In addition to well-studied function of mediating inflammation, GLP-1 secretion, and appetite, short-chain fatty acids sensing GPCRs, especially GPR43, are also involved in the regulation of white adipocytes differentiation and metabolism. However, the implication of short-chain fatty acids and their receptors in brown adipose tissue is little investigated. This research will focus on the functions of acetate and its receptors in the brown adipose tissue and brown adipocytes and illustrate signalling and biological actions of short-chain fatty acid sensing GPCRs in brown adipocytes. In particular, this study will consist of:

To confirm the expression of short-chain fatty acids sensing GPCRs in brown adipose tissue and brown adipocytes.

To identify the expression pattern of short-chain fatty acids sensing GPCRs in brown adipocytes during differentiation and in response to stimuli.

To investigate the role of acetate in brown adipogenesis and mitochondrial biogenesis.

To illustrate activation of short-chain fatty acids sensing GPCRs induced signalling cascades in brown adipocytes.

To study the role of acetate in lipid metabolism of brown adipocytes.

Chapter 2: Material and methods

2.1 Material

2.1.1 General laboratory reagents

Methanol, Ethanol, Paraformaldehyde: VMR

Isopropanol: Sigma-Aldrich

Tris, SDS, Glycine, EDTA: Fisher Chemical

2.1.2 Molecular biology reagents and kits

Fetal Bovine Serum: Invitrogen

Dimethyl sulfoxide (DMSO): Sigma-Aldrich

Penicillin/Streptomycin (Pen/Strep): Gibco

Trypsin-EDTA solution: Sigma-Aldrich

DEPC-treated water: Invitrogen

Puromycin: Sigma-Aldrich

G-418 Solution: Sigma-Aldrich

*Trans*IT®-2020 Transfection Reagent: Mirus Bio LLC

Lipofectamine® RNAiMAX Reagent: Invitrogen

QIAzol Lysis Reagent: QIAGEN

GenElute Mammalian Total RNA Kit: Sigma-Aldrich

Precision DNase: Primerdesign Ltd

nanoScript 2 Reverse Transcription kit: Primerdesign Ltd

Taq DNA Polymerase: Invitrogen

dNTP Set: Thermo Scientific

SYBR Green PCR Mater Mix: Applied Biosystems

Agarose: VMR

GeneRuler 100 bp Plus DNA Ladder: Thermo Scientific

6 × DNA Loading Dye: Thermo Scientific

Ethidium Bromide: Sigma-Aldrich

ProtoGel 30% (37.5:1 Acrylamide: Bisacrylamide): Geneflow

4 × Resolving Buffer: Geneflow

4 × Stacking Buffer: Geneflow

Ammonium Persulphate (APS): Sigma-Aldrich

N,N,N',N'-Tetramethylethylenediamine (TEMED): Sigma-Aldrich

Radioimmunoprecipitation lysis buffer (RIPA): Millipore

Protease/Phosphatase Inhibitor Cocktail: Roche

Phenylmethanesulfonyl Fluoride (PMSF): Sigma-Aldrich

Bicinchoninic Acid (BCA) Kit: Sigma-Aldrich

PageRuler Prestained Protein Ladder: Thermo Scientific

2× Laemmli Sample Buffer: Bio-rad

Immobilon-P PVDF Transfer Membrane: Millipore

Bovine Serum Albumin (BSA): Sigma-Aldrich

ECL Plus reagents: GE Healthcare

TBST (10X) (Tris buffered saline w/Tween-20): Fisher Scientific

Adipogenesis kit: Millipore

Lipolysis Assay Kit (Fluorometric): Abcam

Free Fatty Acid Uptake Assay Kit (Fluorometric): Abcam

Glucose Uptake Assay Kit (Fluorometric): Abcam

CellTiter 96 Aqueous One Solution Cell Proliferation Assay kit: Promega

Immunohistochemical detection Kit: ImmunoCruz™ rabbit ABC Staining Systems

Gill's formulation #2 hematoxylin: Santa Cruz

2.1.3 Agonist, antangonist and inhibitor

4-CMTB: Tocris Bioscience

Acetate: Sigma-Aldrich

Palmitic Acid: Sigma-Aldrich

Pertussis toxin (PTX): Tocris Bioscience

U0126: Tocris Bioscience

U73122: Tocris Bioscience

Gallein: Tocris Bioscience

N'-((4-Oxo-4H-chromen-3-yl)methylene)nicotinohydrazide: Merck Millipore

GW9662: Tocris Bioscience

HX 531: Tocris Bioscience

Rosiglitazone: Sigma-Aldrich

2.1.4 Antibody

Phospho-p44/42 MAPK (Erk1/2) Rabbit mAb: Cell Signaling (#9101)

P44/42 MAPK (Erk1/2) Rabbit mAb: Cell Signaling (#4695)

Phospho-Akt Rabbit mAb: Cell Signaling (#4060)

Akt Rabbit mAb: Cell Signaling (#9272)

Phospho-CREB (Ser133) Rabbit mAb: Cell Signaling (#9198)

CREB Rabbit mAb: Cell Signaling (#9197)

PGC-1α Rabbit Ab: Santa Cruz (sc-13067)

UCP-1 Rabbit Ab: Sigma-Aldrich (U6382)

Phospho-PTEN (Ser380/Thr382/383) Rabbit Ab: Cell Signaling (#9554)

PTEN Rabbit mAb: Cell Signaling (#9559)

Horseradish peroxidase (HRP) conjugated anti-β-Actin antibody: Santa Cruz (sc-47778 HRP)

2.1.5 Cell culture media

DMEM/Ham's F-12 (1:1) with L-Glutamine, 15 mM Hepes, and 3.151 g/L Glucose: Lonza

DMEM/Ham's F-12 (1:1) w/o L-Glutamine w/o Hepes w/o Glucose: Generon Ltd.

L-glutamine solution (200 mM): Sigma-Aldrich

XF Assay Medium: Seahorse Bioscience

XF Calibrant Solution: Seahorse Bioscience

2.1.6 Primers

All DNA oligos used for real-time PCR were synthesized by Sigma-Aldrich and listed in Table below:

Table 2-1 Primer sequences for real-time PCR

	Sequence (5'-3')	Product length	NCBI Reference Sequence
mGPR43-Forward mGPR43-Reverse	CCACTGTATGGAGTGATCGCTG GGGTGAAGTTCTCGTAGCAGGT	142	NM_146187.4
mBMP7-Forward mBMP7-Reverse	GGAGCGATTTGACAACGAGACC AGTGGTTGCTGGTGGCTGTGAT	158	NM_007557.3
mPRDM16-Forward mPRDM16-Reverse	ATGCGAGGTCTGCCACAAGT CTGCCAGGCGTGTAATGGTT	180	NM_027504.3
mPPARγ-Forward mPPARγ-Reverse	GGCTTCCACTATGGAGTTCA GATCCGGCAGTTAAGATCAC	105	NM_011146.3/
mPGC1a-Forward mPGC1a-Reverse	TGCAGCCAAGACTCTGTATG ATTGGTCGCTACACCACTTC	163	NM_008904.2
mUCP1-Forward mUCP1-Reverse	CACTCAGGATTGGCCTCTAC CTGACCTTCACGACCTCTGT	151	NM_009463.3
mAP2-Forward	ATCACCGCAGACGACAGGAA	132	NM_024406.2

mAP2-Reverse	TTCCACCACCAGCTTGTCAC		
mRPL19-Forward	GGAAAAAGAAGGTCTGGTT	72	NM_009078.2
mRPL19-Reverse	TGATCTGCTGACGGGAGT		

2.1.7 siRNA & shRNA

XBP1 siRNA were purchased from Santa Cruz.

GPR43 shRNA were ordered from Thermo Fisher.

2.1.8 Software

ABI 7500 Software: Applied biosystems

RTCA software: ACEA Biosciences, Inc.

GeneSys: Syngene, Division of Synoptics Ltd.

GeneTool: Syngene, Division of Synoptics Ltd.

GraphPad Prism 6: GraphPad software

2.2 Methods

2.2.1 Animals care

Male C57BL/6J (4 weeks old) mice were purchased from Dakewe Biotech Co., Ltd (Beijing, China). After a 2-week quarantine, the C57BL/6J mice were fed normal diet/chow until 12 weeks of age. For acetate administration, 6-week-old mice were treated with sodium acetate (150 mM) in drinking water for 6 weeks (n = 5 for control, n = 5 for acetate administration). For testing the effect of rosiglitazone on GPR43 expression, mice (12 weeks old) were

intraperitoneally injected daily with 10 mg/kg rosiglitazone for 7 days (n = 5 for control, n = 5 for rosiglitazone injection). All of the mice were housed in the animal facility with a 12 h light/dark cycle and constant temperature (22–24°C). The mice had free access to water and diet. Adipose tissue was isolated as described as previous reports (Mann et al., 2014). All samples were immersed in liquid nitrogen immediately before RNA extraction. The animals care and samples collection were accomplished with the help from Dr. Xiaoyu Chen and Msc. Xin Cai (Jining Medical University, Jining). All procedures were approved by Jining Medical University and met the standards of the Guide for the Care and Use of Laboratory Animals issued by the Ministry of Science and Technology of the People's Republic of China in 2006.-

2.2.2 Cell culture

1) Isolation and immortalization of mice brown adipocyte cell line (IM-BAT)

The immortalized brown adipocyte cell line (IM-BAT) from mice was constructed by Dr. Mark Christian (University of Warwick, Coventry). Briefly, primary cultures of brown adipose tissues were generated by first digesting the interscapular BAT with Tissue Dissociation Buffer (DMEM:F12 medium containing collagenase (10 mg/ml) and DNase (10 mg/ml)) and pelleting the stromal vascular fraction (SVF) by centrifugation at 170 × g for 10 min. Preadipocytes were purified by collecting the cells that passed through 100 μM of mesh. Next, brown preadipocytes were selected by collecting the cells

that passed through 70 μM of mesh and were cultured in DMEM:F12 medium containing 10% fetal bovine serum and 1% antibiotic-antimycotic for 2 days before being immortalized by retroviral-mediated expression of temperature-sensitive SV40 large T antigen H-2kb-tsA58. Cells were continually cultured at 33 ˚C and selected with G418 (100 mg/ml) for 2 weeks.

The established immortalized brown preadipocytes were maintained in DMEM:F12 medium containing 10% fetal bovine serum, 1% Penicillin/Streptomycin, and 50 μg/ml of G418. The mycoplasma contamination was also checked by using kit before the cell line was used for assays.

2) Maintenance and differentiation of IM-BAT cells

The IM-BAT cells were maintained in DMEM:F12 medium containing 10% fetal bovine serum, 1% Penicillin/Streptomycin, and 50 μg/ml of G418. The cells were passaged by using trypsin-EDTA treatment when they reach 80-85% confluent. All experiments were performed between passages 12 and 22.

For differentiation of IM-BAT cells into adipocyte, cells were treated with *differentiation medium I* (DMEM:F12 containing 500 μM 3-isobutyl-1-methylxanthine (IBMX), 250 nM dexamethasone, 170 nM insulin, 1 nM 3,3',5-triiodo-l-thyronine (T3) and 10% fetal bovine serum) for 48 h, followed by incubation with *differentiation medium II* (DMEM:F12 containing 170 nM insulin, 1 nM T3 and 10% fetal bovine serum) until day 7 when lipid droplet

formation was observed. The *differentiation medium II* was replaced every 2-3 days.

3) Maintenance and differentiation of T37i cells

The T37i cells were maintained in DMEM medium containing 10% fetal bovine serum, and 1% Penicillin/Streptomycin. The cells were passaged by using trypsin-EDTA treatment when they reach 70-80% confluent. For differentiation of T37i cells into adipocyte, cells were cultured to confluence and treated with *differentiation medium* (DMEM medium containing 10% fetal bovine serum, 20 nM insulin, 2 nM 3,3',5-triiodo-l-thyronine (T3)) until day 7 when lipid droplet formation was observed. The *differentiation medium* was replaced every 2-3 days (Penfornis et al., 2000).

4) Maintenance and differentiation of 3T3-L1 cells

The 3T3-L1 cells were maintained in DMEM medium containing 10% new-born calf serum, and 1% Penicillin/Streptomycin. The cells were passaged by using trypsin-EDTA treatment when they reach 70-80% confluent. For differentiation of 3T3-L1 cells into adipocyte, cells were cultured to confluence and treated with *differentiation medium* (DMEM medium containing 10% fetal bovine serum, 1.0 µM dexamethasone, 0.5 mM IBMX, 1.0 µg/ml insulin) for 48 h, followed by incubation with *Adipocyte Maintenance Medium* (DMEM medium containing 10% fetal bovine serum and 1.0 µg/ml insulin) until day 7 when lipid droplet formation was observed. The *Adipocyte Maintenance Medium* was replaced every 2-3 days.

2.2.3 siRNA transfection of IM-BAT adipocytes

To introduce siRNA into un-differentiated IM-BAT cells, siRNA were transfected with Lipofectamine RNAiMAX according to manufacturer's manual. Briefly, IM-BAT cells were seeded to be 60-80% confluent at the time of transfection. siRNA-lipid complexes were prepared and incubated at room temperature for 10 min before added into cells. The cell culture medium was changed back into DMEM:F12 containing 10% FBS and 1% Penicillin/Streptomycin after 6h. 24h post transfection, the cells were differentiated as described above.

To introduce siRNA into fully differentiated adipocytes, a modified version of 'reverse transfection' was applied according to the method reported by Kilroy *et al.* (Kilroy et al., 2009). Briefly, adipocytes were differentiated according to the description above and trypsinized to detach from the plate. The detached adipocytes were pelleted and gently resuspended in DMEM:F12 medium containing 10% FBS without antibiotics. The siRNA-lipid complexes were prepared inside the wells of cell culture plates as below: 12 pmol siRNA were diluted in 100 µl Opti-MEM medium and mixed gently. Then, 2 µl Lipofectamine RNAiMAX were added into each well containing the diluted RNAi molecules and mixed gently. After 20 mins incubation at room temperature, 1 ml suspended adipocytes (5×10^5 cells/ml) were plated in wells containing siRNA-lipid complexes. The cells were incubated at 37˚C in a CO_2 incubator for 24 h before down-streaming assays were carried out as indicated. The efficiency of gene knock-down was measured by real-time PCR or Western blots.

2.2.4 Oil Red O staining

Lipid accumulation of differentiated adipocytes was visualized and determined by quantitative Oil Red O staining kit (Millipore ECM950).

Briefly, the preadipocytes were differentiated as described above. Seven days after induction, the medium was carefully discard and the cells were washed with PBS, and fixed by 3.7% formaldehyde for 15 min, followed by stained with Oil Red O solution for 15 min. After staining, plates were washed twice with water and photographed. Oil Red O was eluted using Dye Extraction Solution (100% isopropanol), and absorbance at 490 nm was measured by microplate reader.

2.2.5 Real time analysis using the xCELLigence system

1) xCELLigence System Principle

The xCELLigence system consists of RTCA station (RTCA Analyser and RTCA Control Unit) and E-Plate/CIM-Plate. The E-Plate/CIM-Plate incorporates a gold sensor electrode array that allows cells in the well to be cultured on the top of these electrode while the RTCA station was used to collect and process electrical impedance of sensing electrode signals from E-Plate/CIM-Plate (figure 2-1).

Then, the electrical impedance of gold sensing electrode underneath the cultured cell layer monitored by RTCA station can be calculated as arbitrary cell index (*CI*) units as below:

$CI = (Z_i - Z_0) / 15,$

in which Z_i represents the electrical impedance at given time points and Z_0 means the background of electrical impedance.

Since the electrical impedance is affected by the number, shape, adhesion, or mobility of the adherent cells, therefore, the changes of *CI* could reflect the primary events of adipocyte differentiation.

2) xCELLigence RTCA DP System Set up

The xCELLigence RTCA DP system was calibrated as manufacturer's instructions prior to the measurements. Briefly, the resistor plate was placed into DP station cradle and the Resistor Plate Verification program (-10 sweeps every 30 seconds) was initiated in RTCA software. The results were checked before the start of the experiment. Cell index (CI) value should be lower than 0.063. The raw data should be as below: Row A & Row H: 40.0 ± 2.0; Row B & Row G: 67.5 ± 2.5; Row C & Row F: 93.6 ± 2.9; Row D & Row E: 117.6 ± 3.3.

3) Establish the background reading

E-plate was filled with basal medium (100 µL/ well) and placed into DP station cradle (housed in a humidified incubator at 37 ˚C with a 5% CO_2 atmosphere) to establish the background reading. The program for background measurement was set as Step 1 = 1 sweep for 1min.

4) Real-time monitoring the primary morphological changes in IM-BAT cells differentiation

IM-BAT cells were seed into E-plate at 5 × 10^4 cells per well in 100 µl aliquots. The E-plate was equilibrated at room temperature for 30 min before moved back into DP station cradle. The program was set as 6 sweep every 20 min followed by 100 sweeps every 1 h.

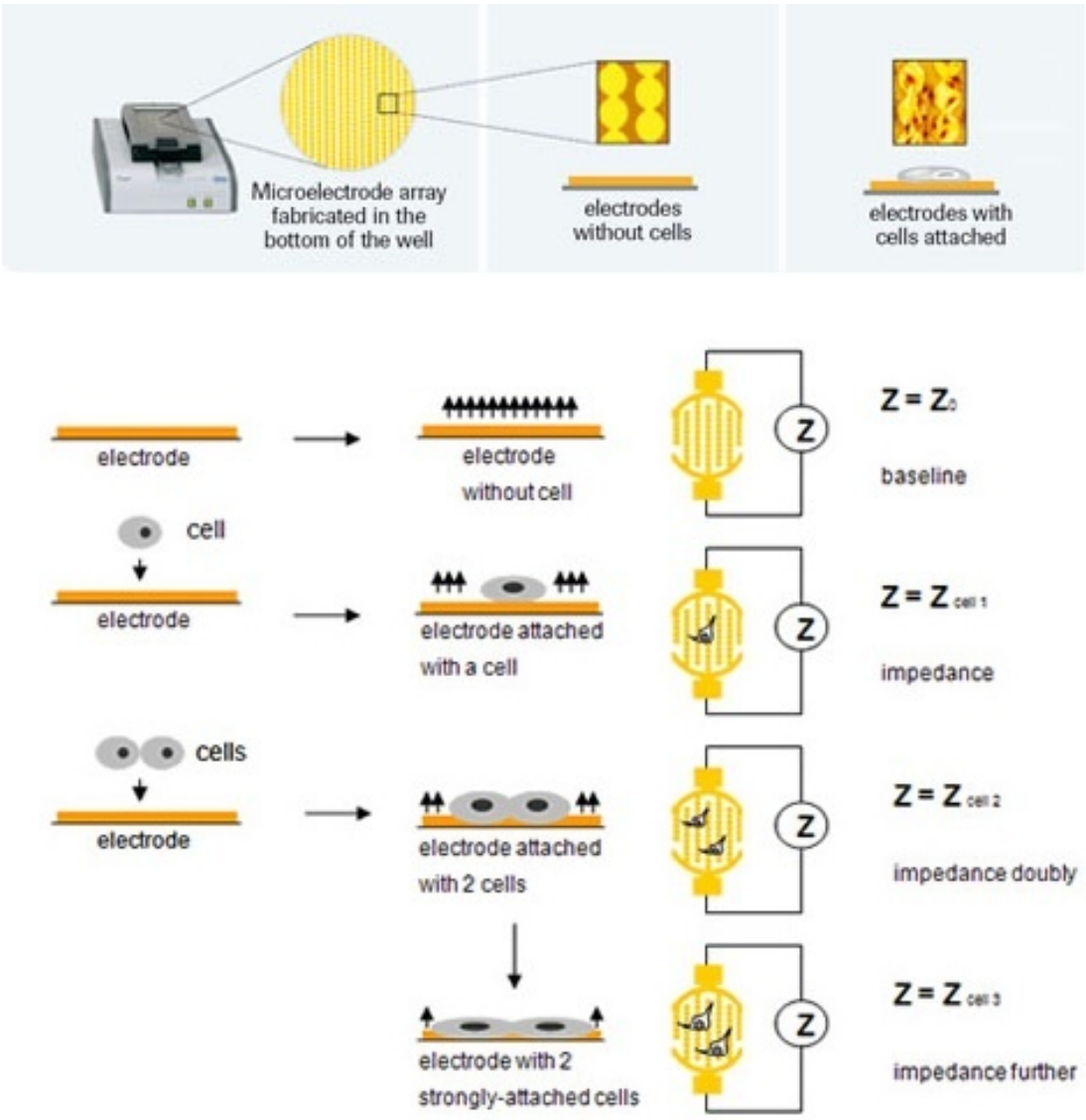

Figure 2-1 The principle of xCELLigence system. The presence of adherent cells on top of the electrodes will affect the local ionic environment at the electrode/solution interface, leading to an increase in the electrode impedance. The increase in electrode impedance is positively correlated to the number of cells attached on the electrodes. Besides, the electrode impedance is also affected by the quality of the cell interaction with the electrodes such as cell adhesion or

spreading. By monitoring electrode impedance, cell viability, number, morphology, and adhesion degree could be measured in a number of cell-based assays.

When cells reached confluence, E-plate were taken out and cells were treated with *Differential medium I* as described above at 36 h post-seeding for 2 days, followed by incubation with *Differential medium II* only or with acetate/ 4-CMTB until days 7 post-induction. The program for each measurement was both set as 6 sweep every 20 min followed by 100 sweeps every 1 h.

The arbitrary Cell Index (CI) was monitored by electrical impedance measurements. The differentiation of IM-BAT cells in E-plate was confirmed by optical microscope observation at days 7 post-induction.

5) Data analysis

After the experiment, the Cell Index (*CI*) curves were normalized to the last time point before the addition of the *differentiation medium* by using the RTCA software included in xCELLigence system. For cooperation of two groups, P values were calculated using Student's t-tests.

2.2.6 Immunohistochemistry

1) IHC staining of differentiated IM-BAT cells

Preparation of coverslips

Circle coverslips were sterilized by 70% ethanol for 30 min and dried in cell culture hood. After sterilization, the cover slips were placed in 12-well plates

and coated with 2% Gelatin solution for 30 min followed by being dried for 15 mins prior to use.

Preparation of cells on coverslips

Preadipocytes were seeded into 12-well plates containing Gelatin coated coverslips at the density of 1×10^5 /well. When cells reached confluence, preadipocytes was treated with *differentiation medium I* for 2 days followed by incubation with *Differential medium II* until days 7 post-induction before staining.

Fixation of cells on coverslips

When adipocytes have reached differentiated status, the culture medium was removed and the cells were washed twice with PBS before incubated with 4% formaldehyde fixative solution for 20 mins at room temperature.

IHC staining for cultured cells on coverslips

The fixed cells were washed twice with PBS. To avoid endogenous peroxidase interference, endogenous peroxidase was neutralized using 0.1% hydrogen peroxide for 5 min. After wash with PBS twice, the cells were blocked with 1.5% blocking serum for 5 min and washed with PBS twice again. The cells were incubated with primary antibodies (anti-GPR43(H-120), Santa Cruz, sc-32906) at 1:100 overnight at 4 ˚C followed by washing with PBS for three times. The cells were incubated with biotin-conjugated secondary antibody and avidin-biotin enzyme reagent (AB enzyme reagent) for 30 mins sequentially with 3 washes for each step. The staining was

developed with DAB chromogen for 2.5 mins followed by counterstaining with Gill's formulation #2 hematoxylin (Santa Cruz, sc-24973) for 10 seconds.

2) IHC staining of Paraffin-embedded mice BAT tissue

Sectioning formalin-fixed, paraffin-embedded mice brown adipose tissues

Formalin-fixed, paraffin-embedded mice brown adipose tissues were kindly provided by Dr. Manjunath Ramanjaney (Hamad Medical Corporation, Doha).

Slides with paraffin-embedded sections were prepared by Mr. Sean James (West Midlands Genomic Medical Centre, Coventry). Briefly, paraffin-embedded adipose tissue was cut into 3 µm thick tissue sections using a rotary microtome Lecia RM2235. The sections were mounted onto histological slides in a 45 °C water bath. Slides with paraffin-embedded sections were dried overnight in oven.

Removal of Paraffin and Rehydration

The paraffin-embedded sections were deparaffinized and rehydrated as follow: 3 × xylenes for 5 mins each, 2 × 100% isopropanol for 3 mins each, 1 × 70% isopropanol for 3 mins.

Antigen Retrieval

The slides were placed in a Slide Chamber filled with 10 mM sodium citrate buffer (pH=6.0) and heated in 2100 Antigen Retriever to unmask antigen.

ABC staining

GPR43 were detected in formalin-fixed, paraffin-embedded human tissue by immunoperoxidase staining using anti-GPR43(H-120) antibody (Santa Cruz, sc-32906) and ImmunoCruz rabbit ABC staining system (Santa Cruz sc-2018) according to the manufacturer's instructions. Briefly, the section was blocked in 1.5% blocking serum for 1 h before incubated with primary antibody (1:100) overnight at 4 ˚C. The sections were washed with PBS three times and stained with biotinylated secondary antibody (1 μg/ml) followed by PBS washes three time for 5 mins each. The staining was developed using DAB chromogen for 2.5 mins followed by hematoxylin (Gill's formulation #2 hematoxylin, Santa Cruz, sc-24973) counterstaining for 10 seconds.

2.2.7 Real-Time Quantitative Reverse Transcription PCR (Two-Step)

1) RNA isolation

For extraction RNA from cultured cells, cells were lysed directly in cell culture plates by adding 500 μl QIAzol lysis reagent per 10^7 cells. Total RNA was purified according to the manual provided by Sigma GenElute Mammalian Total RNA Kit.

For extraction RNA from adipose tissue, the sample was quickly sliced into pieces up to 25 mg followed by addition of 500 μl QIAzol lysis reagent and homogenization immediately until no visible pieces remain. Total RNA was then purified according to manufacturer's instructions.

All RNA samples were quantified by NanoDrop 1000 UV-Vis Spectrophotometer and treated with RNase-free DNase I digestion at 37˚C

for 30 mins to exclude the contamination of genomic DNA before down-streaming assays.

2) Reverse transcription

All the first-strand cDNA synthesis was performed using purified total RNA with nanoScript 2 Reverse Transcription kit by reverse transcription.

For the reverse transcription:
Template RNA (1 μg); 0.5 μl random nonamer primers and 0.5 μl oligo-dT primers were mixed with RNase/DNase free water to final volume of 10 μl, and incubated at 65 ˚C for 5 min, and placed on ice immediately. The RT reaction mix were made up according to total number of reactions as below:

nanoScript2 4 × Buffer (5 μl / reaction); 10 mM dNTP (1 μl / reaction); RNase/DNase free water (3 μl / reaction); nanoScript2 enzyme (1 μl / reaction).

10 μl RT reaction mix were added into samples containing template RNA and random nonamer / oligo-dT primers; and incubated 5 min at 25˚C followed by 20 min at 42˚C. The reaction was terminated by heating at 75˚C for 10 min. The cDNA was stored at -20 ˚C. The cDNA was diluted 1:5 before used for quantitative real-time PCR.

3) Quantitative real-time PCR (qPCR)

The following components (2 × SYBR Green PCR Master Mix: 10 μl /well; Forward Primer (10 μM): 0.5 μl /well; Reverse Primer (10 μM): 0.5 μl /well;

template cDNA: 1 µl / well; RNase/DNase free water: 8 µl /well) were added to an ABI 96-well plate sitting on ice:

The plate was centrifuged at 300 × g for 3 min before put into ABI 7500 fast real-time PCR system. The ABI 7500 software were set as follows:

Holding stage:	Pre-denature:	95˚C 20 s
Cycling Stage:	Denature:	95˚C 3 s
	Extend:	60˚C 30 s
Melt Curve Stage:		95˚C 15 s
		60˚C 1 min

The amplification products were analysed by DNA agarose gel electrophoresis. The gel was loaded with 20 µl DNA samples or DNA ladders in each well. The DNA was separated at 100 V until dye is closed to the end of gel. The results were captured by UV transilluminator equipped inside G:BOX Chemi XX6 system.

2.2.8 Measurement of Mitochondrial DNA

Genomic DNA and mitochondrial DNA were isolated from mature IM-BAT brown adipocytes using QIAamp DNA Mini Kit according to manufacturer's instruction.

The mitochondrial DNA level was determined with primers targeted for mouse mitochondrial D-Loop region and normalized against the genomic

DNA measured with 18S primers using the comparative C_T method with ABI 7500 fast real-time PCR system as described above.

2.2.9 Western Blots

1) Cell / Tissue lysate preparation

For release the protein from cultured cells, cells were lysed directly in cell culture plates by adding 200 µl ice-cold RIPA lysis buffer per 10^7 cells and agitation at 4˚C for 30 min. The cell lysate was then transferred into a 1.5 ml Eppendorf tube followed by 12,000 × g centrifuge at 4 ˚C for 15 min. The supernatant was aspirated into another new 1.5 ml Eppendorf tube before protein quantification.

For extraction protein from tissue, the sample was quickly dissected into pieces followed by addition of 300 µl RIPA lysis buffer per 5 mg and homogenization immediately. The tissue lysates were than agitated at 4˚C for 2 h followed by centrifuge at 12,000 × g for 15 mins. The supernatant was aspirated into another new 1.5 ml Eppendorf tube before protein quantification.

All protein samples were mixed in a 1:1 ration with 2 × Laemmli buffer and denatured by heating at 95 ˚C for 5 min before loading into gels.

2) Protein concentration determination

Protein concentration was measured by bicinchoninic acid (BCA) methods according to the manufacturer's instruction. In brief, the assay based on the reduction of Cu^{2+} to Cu^{1+} from Cu^{2+}-protein complex under alkaline conditions

with the detection of purple-blue Cu^{1+}-BCA complex by reading the absorbance at 562 nm (Olson and Markwell, 2001). The standard curve was drawn by plotting the average absorbance at 562 nm vs. the concentration of BSA standard at each measurement, and the concentration of protein lysate was calculated according to the standard curve.

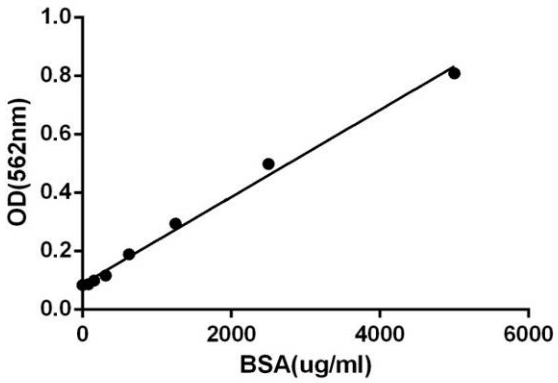

Figure 2-2 A typical standard curve for BSA standards in BCA protein quantification assay. The standard curve was calculated using linear regression and only results with R^2>0.99 will be used to calculate protein concentration.

3) Sodium-dodecyl-sulphate polyacrylamide (SDS-PAGE) gel electrophoresis

The resolving gel (12 % Acrylamide, for separating proteins with 10 -200 kDa MW) was made following the receipt below:

ProtoGel 30% 4.0 ml;

4 × Resolving Buffer 2.5 ml;

Deionized H_2O 3.4 ml;

10% APS 0.1 ml;

TEMED 0.01 ml

The resolving gel casting solution was poured into gel casting cassette and overlaid with distilled water to provide a sharp interface.

After the resolving gel set, the stacking gel was made following the receipt below:

ProtoGel 30% 1.3 ml;

4 × Stacking Buffer 2.5 ml;

Deionized H_2O 6.1 ml;

10% APS 0.1ml;

TEMED 0.01 ml

The stacking gel casting solution was poured into gel casting cassette and inserted with the comb to form the well.

After the stacking gel set, the gel cassette was installed into the tank apparatus. The tank was filled with 1 × SDS Running buffer and load 20 µl protein samples or 1 × Laemmli buffer into each well. The protein was separated at 15 mA per gel until dye is all the way at end of gel.

4) Membrane Transfer

The transfer stack was set up in the following orientation (from top to bottom: Clear clap; Sponge; Filter Paper × 2; PVDF Membrane; Gel; Filter Paper × 2; Sponge; Black clap) and installed into the tank apparatus. The tank was filled with ice-cold 1 × Tris-glycine buffer. The protein was transferred from the gel to the PVDF membrane at 100V for 1 h.

5) Blocking, Antibody incubation, and Detection

After transfer, the PVDF membrane was washed twice in TBST solution and blocked in 5% non-fat milk at room temperature for 1 h. The PVDF membrane was then incubated with relevant primary antibody diluted in 5% BSA solution at optimized dilution overnight at 4 ˚C followed by three times washing with TBST solution before the PVDF membrane was incubated with HRP-conjugated secondary antibody at room temperature for 1 h. ECL Western Blotting Substrate (Pierce) was used to visualize the signal of protein bands. The chemiluminescence were captured by X-ray films (Fujifilm Super RX) or G:BOX Chemi XX6 system. All X-ray films were digitized by Cannon 700F scanner. All the Western blots results were quantitated and analysed by using GeneTools software.

2.2.10 Phospho-Kinase Antibody Array Assay

1) Phospho-Kinase Antibody Array Principle

The Proteome Profiler phospho-kinase array (R&D Systems) were spotted with capture antibodies against 43 different kinases and 2 related total proteins. Cell lysate samples are diluted and incubated with the array. Target proteins are bound by its cognate immobilized capture antibody on the membrane. Detection Antibody Cocktail recognize target proteins and form protein / detection antibody complex. Streptavidin-Horseradish Peroxidase and chemiluminescent detection reagents were added to generate signals which are proportional to the amount of proteins bound. Chemiluminescence is detected in the same manner as Western blots.

2) Screening the effects of acetate treatment on kinases phosphorylation in IM-BAT cells

IM-BAT cells were differentiated and treated with or without acetate (10 mM) for 15 min. Cell lysates were prepared and quantified as described above. After blocked with Array Buffer 1 for 1 h, of cell lysate were applied to phospho-kinase array and incubated at 4˚C overnight. The phospho-kinase array was washed with wash buffer for three times and incubated with Detection Antibody Cocktail at room temperature for 2 h before washed for three times again. The phospho-kinase array was then incubated with Streptavidin-HRP for 30 min at room temperature and washed three times before developed by adding Chemi Reagent Mix. The results were captured by G:BOX Chemi XX6 system (Sysgene) and quantitated using GeneTools software (Sysgene).

2.2.11 Cell viability assay (MTS assay)

The effect of acetate treatment on proliferation of brown adipocytes was measured by CellTiter 96® AQueous One Solution Cell Proliferation Kit. Briefly, cells were seeded into 96 well plate at the density of 5×10^3 cells per well and cultured in the medium free of phenol red with or without acetate for 24 h. Following treatment, 20 µl CellTiter 96 Aqueous One Solution Reagent was add to each well and the plate was incubated at 37 ˚C for 1-4 h. The absorbance was detected at 490 nm using a plate reader.

2.2.12 Oxygen consumption rate (OCR) measurement

The Seahorse Bioscience XF24 extracellular flux analyser was used to determine the cellular oxygen consumption. O_2 tension in an extremely small volume (less than 7 µl) of medium above the monolayer of cells in the XF24 culture microplates were measured by a solid state sensor probes hanging

200μm above the cell. The Oxygen consumption rate (OCR) was calculated by plotting the O_2 tension of the medium in the microenvironment above the cells as a function of time. Baseline (Basal) OCRs were measured firstly followed by oligomycin, FCCP and rotenone + antimycin A being pneumatically injected into the media in each well sequentially through an integrated drug delivery system to assess the ATP turnover, maximum respiratory capacity and non-mitochondrial respiration, respectively. Total protein was extracted by RIPA buffer directly in XF24 culture microplates after OCR measurement. The protein content was quantified by BCA assay as described above and used to normalize the OCR.

2.2.13 Flowcytometry analysis of mitochondrial mass

IM-BAT cell were differentiated as described above for ≥7 days. Acetate or 4-CMTB was supplemented with the *differentiated medium II* from day 2 during differentiation in experimental group.

When IM-BAT cells were fully differentiated, the cells were trypsinized by 0.25% trypsin and pelleted by centrifuge. The supernatant was aspirated and the cell pellet was re-suspended in DMEM:F12 medium with equal volume of the dye-working solution. The cells were then incubated in a 37 ˚C, 5% CO_2 incubator for 30 min before the cells were washed with pre-warmed (37 ˚C) HBBS buffer for three times.

For each measurement, data from 10,000 single-cell events were collected using FC500 flow cytometers (Beckman Coulter), and CytoPainter MitoNIR Indicator Reagent fluorescent intensity was measured in FL4 channel.

2.2.14 Construction of GPR43 knock-down stable cells

1) Optimization of Antibiotic Selection

IM-BAT cells were seeded at 6 × 10^5 cells per well in DMEM/F-12 medium supplemented with 10% fetal bovine serum in a 6-well plate and incubated at 37°C with a humidified atmosphere at 5% CO_2 overnight. On next day, the cell culture medium was replaced with complete media containing puromycin at 6 different concentrations (0, 2, 4, 6, 8 and 10 μg/ml). The cells were continuously cultured for next 7 days with medium being change every 2-3 days. Cell viability in each well was determined by either cell counting on day 7. The minimum concentration of puromycin resulting in complete cell death after 7 days of selection with puromycin would be used for that transduction with shRNA plasmids to construct GPR43 knock-down stable cells.

2) shRNA plasmid DNA transfection

IM-BAT cells were seeded at 3 × 10^5 cells per well in DMEM:F-12 medium supplemented with 10% fetal bovine serum in a 6-well plate and incubated at 37°C with a humidified atmosphere at 5% CO_2 overnight. On next day, GPR43 shRNA plasmids were transfected into IM-BAT preadipocytes by *Trans*IT-2020 Reagent. The *Trans*IT-2020 Reagent: DNA complex was prepared in Opti-MEM I Reduced-Serum Medium and distributed to cells drop-wisely.

The medium was replaced with DMEM:F12 medium containing 10% fetal bovine serum and 8 μg/ml puromycin after 48 h post-transfection and the cells were fed every 3 days with this medium until the colony formation.

3) Validation of GPR43 knock-down

Following selection by puromycin, selected cells were differentiated as described above for 7 days and lysed with Qiazol. The mRNA expression of GPR43 was subjected to real-time PCR analysis.

2.2.15 Lipolysis Assay

IM-BAT cells were differentiated for 7 days and seeded into 96-well clear bottom cell culture plate at 5 × 10^4 cells / well for 4 h before washed with lipolysis wash buffer twice. After wash, the cells were incubated in 150 µl lipolysis assay buffer and treated with test compounds for 3 h. Conditioned medium media was collected and transferred into a new 96-well plate. The final volume was adjusted with lipolysis assay buffer to 50 µl / well. The reaction mix (glycerol assay buffer 42 µl / well; glycerol enzyme mix 2 µl / well; glycerol developer 2 µl / well; picoprobe 4 µl / well) was prepared and added into 96-well plates (50 µl/ well) containing standard and test samples. The plate was incubated at room temperature for 60 mins before the fluorescence (Ex/Em = 535/587 nm) was measured by microplate reader.

2.2.16 Free fatty acids uptake assay

IM-BAT cells were differentiated for 7 days and seeded into 96-well clear bottom cell culture plates at 5 × 10^4 cells / well for 4 h before serum deprived for 1 h. After serum starvation, the cells were treated with test compounds for 30 min followed by incubated with 100 µl fatty acid dye-loading solution (containing TF2-C12 fatty acid). The fluorescence (Ex/Em = 485/515 nm) was measured by microplate reader.

2.2.17 Glucose uptake assay

IM-BAT cell were differentiated for 7 days as described above. Upon differentiation, the cells were starved in DMEM:F12 medium without glucose and FBS for 3 h. The cells were harvest, washed and re-suspended in glucose-free DMEM:F12 medium containing 150 μg/ml 2-NBDG with or without insulin at 1×10^5 cells / ml for 30 min. The 2-NBDG uptake reaction was stopped by removing the incubation medium and washing the cells with pre-cold PBS.

For each measurement, 2-NBDG fluorescent intensity were collected using FC500 flow cytometers (Beckman Coulter) in FL1 channel or plate reader (Ex/Em = 485/535 nm)

2.2.18 Statistical analysis

Results are presented as the mean ± S.E.M of at least triplicate samples in each experimental group; experiments were replicated to ensure consistency. Statistical significance of difference was determined using student t-test when comparing 2 groups or one-way ANOVA followed by post hoc Tukey's multiple comparison test when comparing more than 3 groups. Values were considered to be statistically significant if their P value was lower than 0.05. All statistical calculations were analysed in GraphPad Prism 6.

Chapter 3: Short-chain fatty acid receptor GPR43 expression in brown adipose tissue and brown adipocytes

3.1 Preamble

So far, two GPCRs (GPR41 and GPR43) have been demonstrated to be receptors for short-chain fatty acids (Brown et al., 2003). The expression of GPR43 in white adipocytes and white adipose tissue has been confirmed by real-time PCR, fluorescence in situ hybridization (FISH), and immunohistochemistry in several independent studies (Zaibi et al., 2010, Cornall et al., 2011, Kimura et al., 2013), however, the existence of GPR43 in brown adipose tissue and brown adipocytes were only confirmed by real-time PCR (Zaibi et al., 2010, Regard et al., 2008).

Regarding the controversial reports of GPR41 expression in adipose tissue, Xiong *et al.* showed that short-chain fatty acids stimulate leptin release from white adipose tissue through GPR41 (Xiong et al., 2004), suggesting GPR41 exists in white adipose tissue. However, at least three other studies reported that GPR41 could not be detected in differentiated 3T3-L1 cells or in mouse white adipose tissue (subcutaneous, perirenal, mesenteric, and epididymal fat pads) (Hong et al., 2005, Zaibi et al., 2010, Kimura et al., 2013). GPR43 mRNA, rather than GPR41 mRNA, was found to be detected in these studies. Furthermore, using GPR41 knock-out mice, Zaibi *et al.* further confirmed that short-chain fatty acids induced leptin secretion was only slightly affected after the loss of GPR41, suggesting the promotive effect of short-chain fatty acids on leptin secretion is GPR43-dependenet but not GPR41-dependent (Zaibi et al., 2010). The discrepancies between reports from Xiong *et al.* and Zaibi *et al.* might because the loss of GPR41 also affects GPR43 expression in GPR41 knock-out mice (Zaibi et al., 2010). Indeed, increasing evidence

supports the hypothesis that GPR43 mainly mediates the effects of short-chain fatty acids in adipocytes and adipose tissue (Kimura et al., 2013). However, the implication of GPR41 and GPR43 in brown adipocytes are still not clearly investigated.

Recently, the promoter structure of GPR43 gene in human monocytes has been illustrated. XBP1 was identified as a core *cis* element controlling GPR43 transcription in human monocytes, while several other transcription factors including CREB, CHOP, NFAT and STAT5 act as enhancers in mediating GPR43 expression (Ang et al., 2015). LPS, TNFα, and GM-CSF increase GPR43 expression in human monocytes *via* augment of XBP1s level (Ang et al., 2015). However, the link between XBP1 and GPR43 is still not clear in adipocytes.

To elucidate the biological properties of short-chain fatty acids in brown adipocytes, existence of short-chain fatty acids receptors (GPR41 and / or GPR43) was firstly measured in differentiated IM-BAT cells as well as murine interscapular brown adipose tissue. Furthermore, to investigate the possible roles of short-chain fatty acids in brown adipogenesis, the expression of short-chain fatty acids receptors was also quantified during the adipogenesis of brown adipocytes. Besides, the effects of pro-adipogenic agents (such as PPARγ agonist) and anti-adipogenic agents (such as STAT5 inhibitor) on short-chain fatty acids receptors expression in brown adipocytes and brown adipose tissue were also determined in this study.

3.2 Results

3.2.1 Identification of GPR43 expression in brown adipose tissue

GPR41 and GPR43 have been de-orphaned as short-chain fatty acids receptors in last decades. To test the hypothesis that GPR41 and/or GPR43 mediate the regulatory effects of short-chain fatty acids in brown adipose tissue, reverse transcription PCR analysis was performed on interscapular brown adipose tissue of C57BL/6 mice to measure the mRNA expression levels of GPR41 and GPR43. The results demonstrated that GPR43 mRNA expression reached a clearly detectable level in interscapular brown adipose tissue (figure 3-1(A)). To exclude the possibility of gDNA contamination, the minus-reverse transcriptase '-RT' controls were introduced. The significant decrease of amplification products in -RT controls confirmed the PCR amplification was mostly attributable to the presence of GPR43 cDNA (figure 3-1(A)). To confirm the findings from reverse transcription PCR, real-time PCR was also applied to measure the difference of Ct values between +RT test samples and '-RT' controls. The results also showed a significant increase of Ct values in '-RT' controls group, indicating the gDNA contamination was neglectable (figure 3-1(B)). Besides, in agreement with previous reports, our results also indicated GPR41 were not detected in interscapular brown adipose tissue since the Ct values between test samples and controls were similar.

We also compared the expression levels of GPR43 in subcutaneous white adipose tissues and interscapular brown adipose tissue. Consistent with previous reports, the GPR43 expression level in interscapular brown adipose

tissue was found to be much less (around 10-fold lower) than that in subcutaneous white adipose tissues (figure 3-1 (A) and (C)).

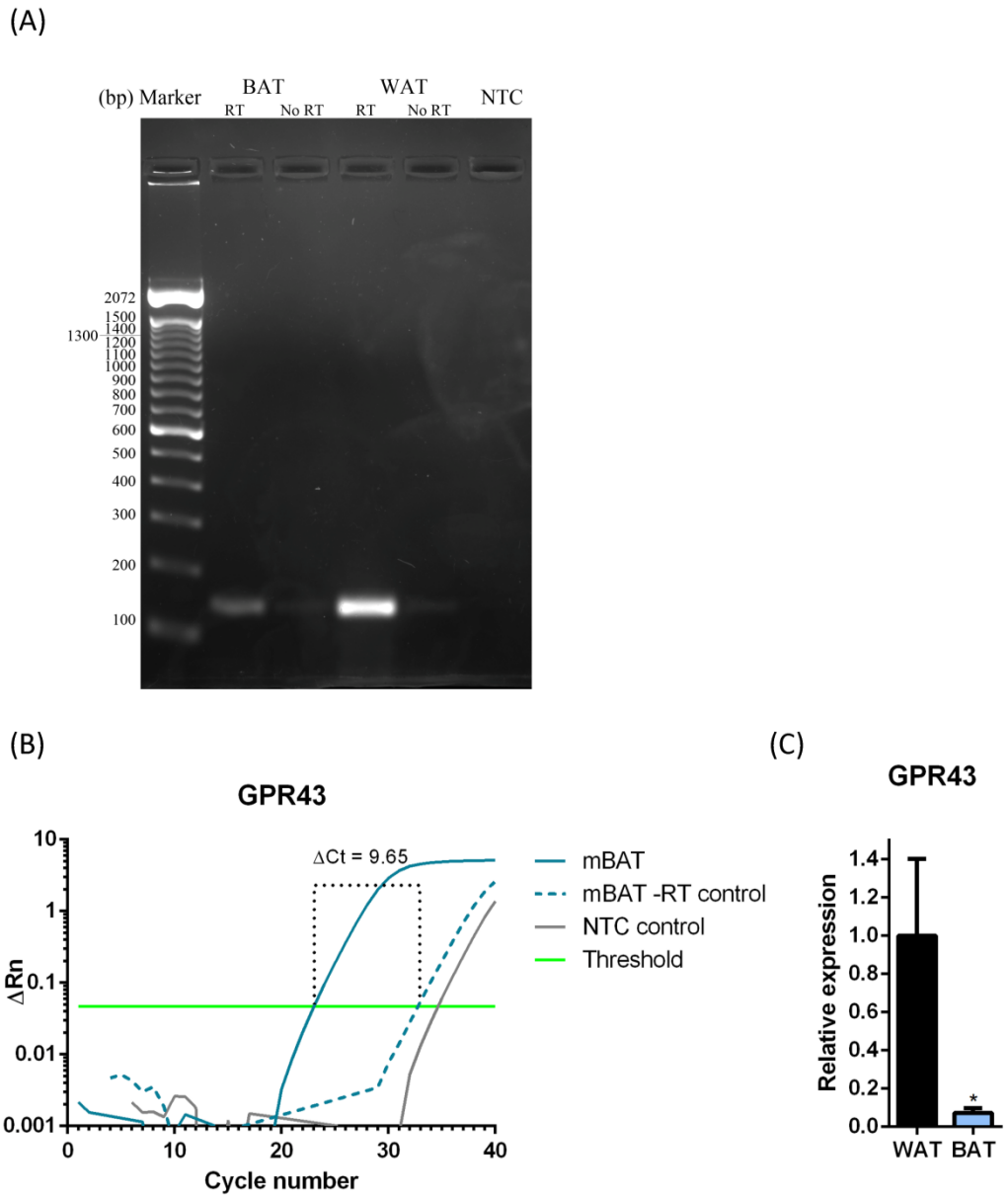

Figure 3-1 Identification of GPR43 mRNA transcription in interscapular brown adipose tissue of C57BL/6 mice. (A) **RT-PCR to envisage GPR43 transcription from interscapular brown adipose tissue.** (B) **Transcription of GPR43 in interscapular brown adipose tissue measured by real-time PCR.** (C) **Transcription level of GPR43 in subcutaneous white adipose tissue and interscapular brown adipose tissue.** Interscapular brown adipose tissue and

white adipose tissue were removed from mice immediately after sacrifice and immersed in RNAlater RNA Stabilization Reagent. RNA was isolated using commercial total RNA isolation kit and used for cDNA synthesis. The target genes transcription was detected by PCR (A) or measured by real-time PCR (B and C). Data presented as mean ± S.E.M.. * P <0.05 compared to control by student's t-test.

Immunohistochemical staining was also used to demonstrate the existence of GPR43 in interscapular brown adipose tissue. As shown in figure 3-2, immunoperoxidase staining of formalin-fixed, paraffin-embedded interscapular brown adipose tissue using anti-GPR43 antibody showed membrane and cytoplasmic staining, while in no primary antibody control, only negligible staining could be found.

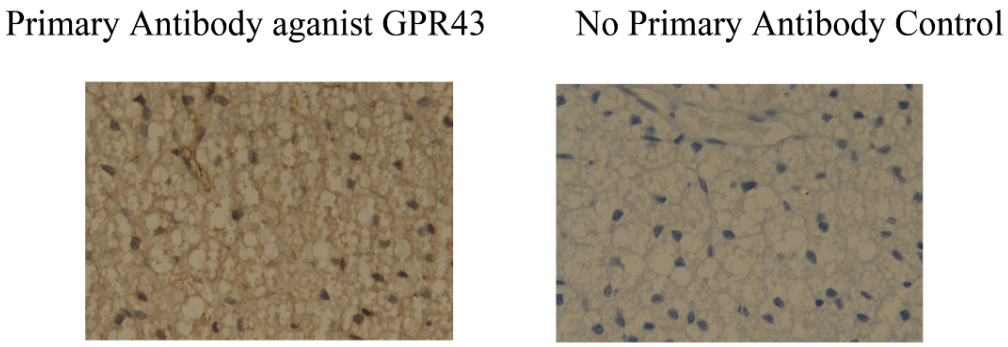

Figure 3-2 Expression of GPR43 in interscapular brown adipose tissue of C57BL/6 mice examined by Immunohistochemistry. Interscapular brown adipose tissue was stained with anti-GPR43 antibody and haematoxylin (40X magnification shown). No primary antibody was served as negative control.

3.2.2 Identification of GPR43 expression in immoralized brown adipocytes

To clarify that GPR43 were expressed in brown adipocytes instead of stromal vascular fraction, immortalized brown adipocytes (IM-BAT) constructed by Dr. Mark Christian (University of Warwick) were differentiated into mature adipocytes as a cell model to analyse the mRNA expression of GPR43 in brown adipocytes.

In keeping with previous report, IM-BAT cells (which have a fibroblast-like appearance under standard culture condition) can differentiate into large, spherical cells, accumulating multiple lipid droplets of various sizes as revealed by the Oil Red O staining after incubated with *differentiation medium I* for 2 days followed by *differentiation medium II* for another 5 days (figure 3-3(A)).

Furthermore, the gene expression of the brown adipocyte marker UCP1 was highly induced in IM-BAT cells after differentiation (figure 3-3(B)). Besides, the UCP1 and mitochondrial DNA levels in differentiated IM-BAT were also significantly higher than differentiated white adipocyte cell line 3T3-L1 (figure 3-3(C))

Moreover, differentiated IM-BAT cells maintained the ability to express large amount of UCP1 after β-adrenergic stimulation; an acute (6 h) treatment with CL-316,243 led to a significant increase of UCP1. A series of functional metabolic assays were also performed to identify and confirm the characteristics of the IM-BAT cells as a brown adipocyte model. Glucose uptake, assessed with a fluorescent glucose analog (2-NBDG), was also

increased after CL-316,243 treatment in mature adipocytes (figure 3-3(E)), indicating that the β3-adrenergic signalling pathway is fully functional in terminal differentiated and full matured IM-BAT cells (figure 3-3(D)).

In addition, Akt phosphorylation was increased by insulin stimulation in differentiated IM-BAT cells, indicating that insulin signalling was also intact in mature IM-BAT adipocytes (figure 3-3(F)).

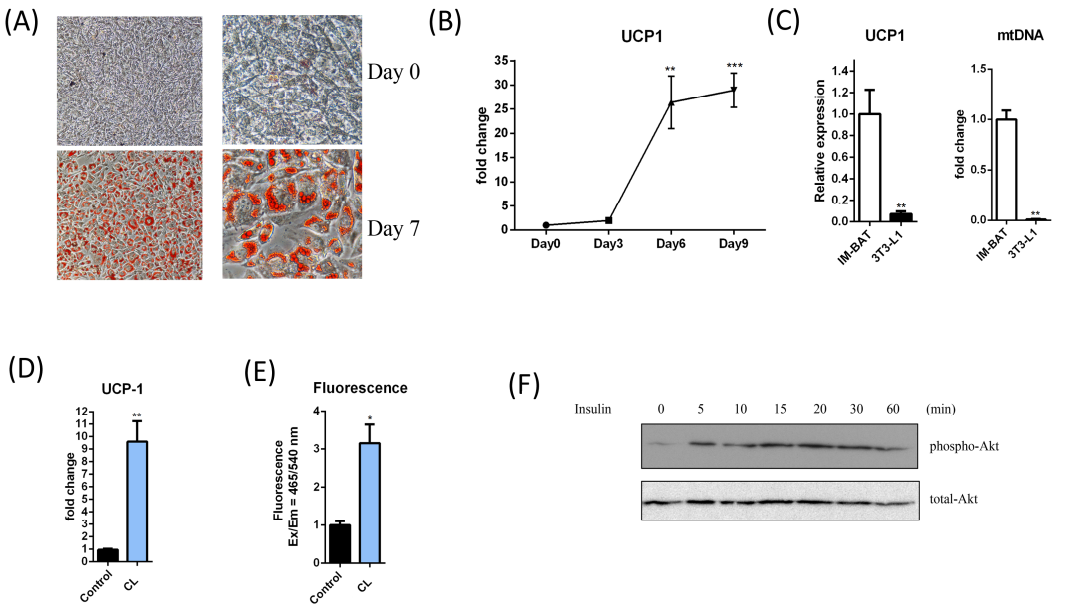

Figure 3-3 Identification of IM-BAT as brown adipocytes model *in vitro*. (A) **Lipid accumulation in differentiated IM-BAT cells visualized by Oil Red-O staining.** Macroscopic pictures of Oil Red-O staining of immortalized BAT (IM-BAT) cells differentiated for 7 days. (B) **Expression levels of UCP1 mRNA in the course of adipogenesis of IM-BAT cells.** IM-BAT cells were differentiated and cell lysate were collected at day 0, day 3, day 6 and day 9. Transcription of UCP-1 was detected by real-time PCR. (C) **UCP-1 and mitochondrial DNA levels in differentiated IM-BAT cells and differentiated 3T3-L1 cells.** IM-BAT and 3T3-L1 cells were differentiated; total RNA and total DNA was isolated by GenElute™ Mammalian Total RNA Miniprep Kit and QIAamp DNA Mini kit, respectively. UCP-1 transcription and mitochondrial DNA to genomic DNA ratio were measured by real-time PCR. (D) **Effects of CL-316,243 (CL) treatment on expression levels of**

UCP1 in differentiated IM-BAT cells. IM-BAT cells were differentiated then treated with CL-316,243 (10 μM) for 6 h. Expression of UCP1 was measured by real-time PCR. (E) Effects of CL-316,243 (CL) treatment on glucose uptake in differentiated IM-BAT cells. IM-BAT cells were differentiated and starved in glucose-free, serum-free DMEM:F12 medium for 3 h. The cells then were treated with CL-316,243 (10 μM) for 3 h and stained with 2-NBDG (150 μg/ml). Fluorescence (Ex/Em = 465/540 nm) was measured by flow cytometry. (F) **Effects of insulin treatment on Akt activation in differentiated IM-BAT cells.** IM-BAT cells were differentiated and serum-starved overnight. The cells then were treated with insulin (1 μM) for 15 min. The phosphorylated Akt and total Akt were measured by Western blots. Data are presented as mean ± S.E.M.. *P <0.05, **P<0.01, ***P<0.001.

After confirmed the IM-BAT cells were able to exhibit the main characteristics of brown adipocytes, next, we measured the GPR43 expression in differentiated IM-BAT cells by real-time PCT. As shown in figure 3-4(A), transcription of GPR43 were clearly detected in differentiated IM-BAT cells, while relatively less expression was found in preadipocytes as well as '-RT' controls. The RT-PCR also visualised the transcription of GPR43 in differentiated IM-BAT cells (figure 3-4(B)).

(A)

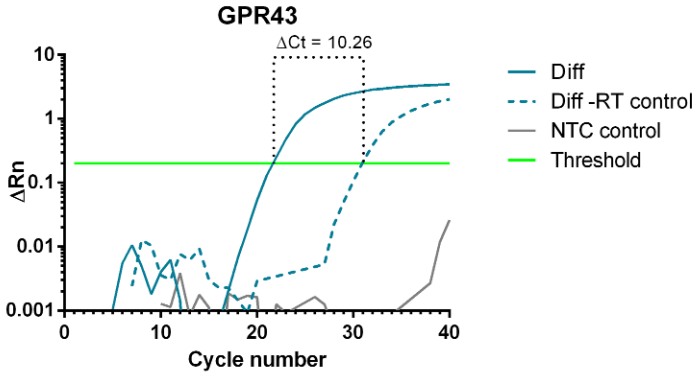

(B)

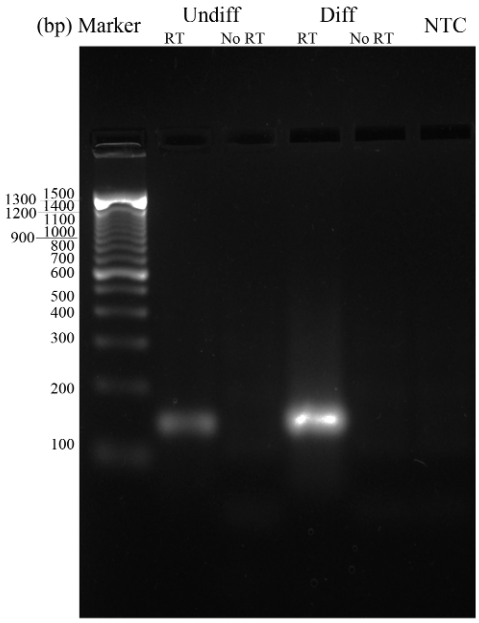

Figure 3-4 Identification of GPR43 mRNA transcription in IM-BAT cells. (A) **Transcription of GPR43 in immortalized brown adipocytes measured by real-time PCR.** (B) **RT-PCR to envisage GPR43 transcription from undifferentiated and differentiated IM-BAT.** Total RNA was isolated from differentiated IM-BAT cells and used for cDNA synthesis. GPR43 transcription was measured by real-time PCR using SYBR green I (A) or visualized by agarose gel electrophoresis after PCR (B).

Western blots were also applied to visualise the protein expression of GPR43 in differentiated immortalized brown adipocytes. As shown in figure 3-5, a distinct band at around 45kD were detected in differentiated IM-BAT cells compared to undifferentiated cells (figure 3-5 (A)), which is close to the theoretical molecular weight of GPR43.

Immunohistochemical staining was also used to demonstrate the existence of GPR43 in IM-BAT cells. Similarly, immunoperoxidase staining of formalin-fixed, differentiated IM-BAT cells using anti-GPR43 antibody showed

membrane and cytoplasmic staining, while in no primary antibody control, only negligible staining could be found (figure 3-5 (B)).

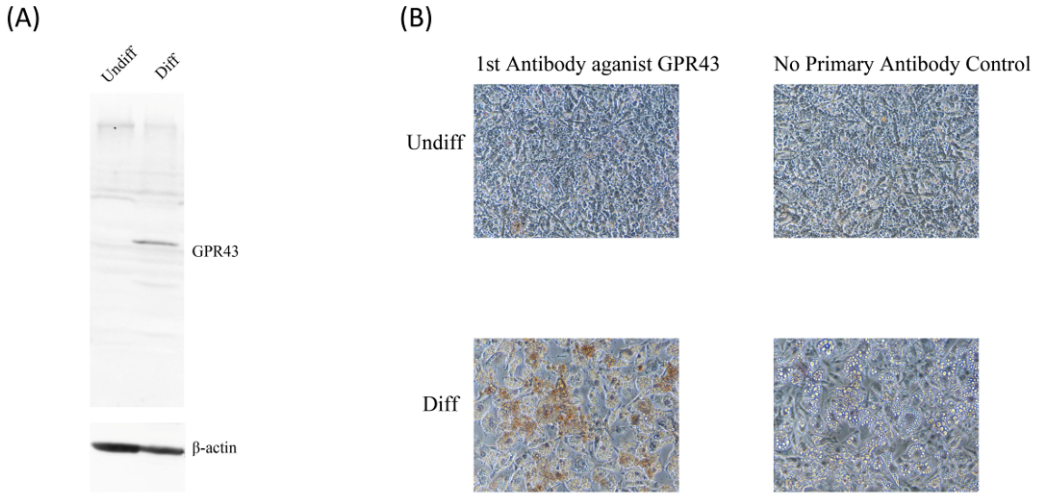

Figure 3-5 Identification of GPR43 protein expression in IM-BAT cells. (A) **Expression of GPR43 in undifferentiated and differentiated IM-BAT adipocytes examined by Western blots.** IM-BAT cells were differentiated then lysed with RIPA buffer. Expression of GPR43 was detected by Western blots using anti-GPR43 antibody. (B) **Expression of GPR43 in IM-BAT cells examined by Immunohistochemistry.** Representative immunohistochemistry staining GPR43 in differentiated IM-BAT cells. No primary antibody group and undifferentiated group were served as negative control (40X and 100X magnification shown).

3.2.3 GPR43 expression pattern during differentiation of brown adipocytes

To better understand the possible role of GPR43 in brown adipocyte differentiation, we began our study by investigating GPR43 expression pattern during the differentiation of cultured brown adipocytes IM-BAT. The mRNA levels of GPR43 were quantified by real-time PCR during the course of adipose differentiation until days 9 post-induction, at which time point the hypertrophic brown adipocytes filled with plenty of lipid droplets. The results

showed that GPR43 mRNA expression was scarcely detected in preadipocytes (Day 0) but clearly escalated at day 3 post-induction, and significantly increased at days 6 after differentiation, and maintained at high expression levels afterwards (Figure 3-6 (A)). These data demonstrated that GPR43 expression increased during brown adipocyte differentiation *in vitro*.

As positive controls, gene expressions of adipogenic-related gene (PGC-1α) and thermogenesis-related gene (UCP1) were also quantified by real-time PCR during the differentiation of IM-BAT cells. The results showed the significant elevation of genes expression reaches significance at day 6 and maintains until day 9 (Figure 3-6 (B) and (C)). These patterns were consistent with previous studies and also demonstrated the successful differentiation of IM-BAT cells.

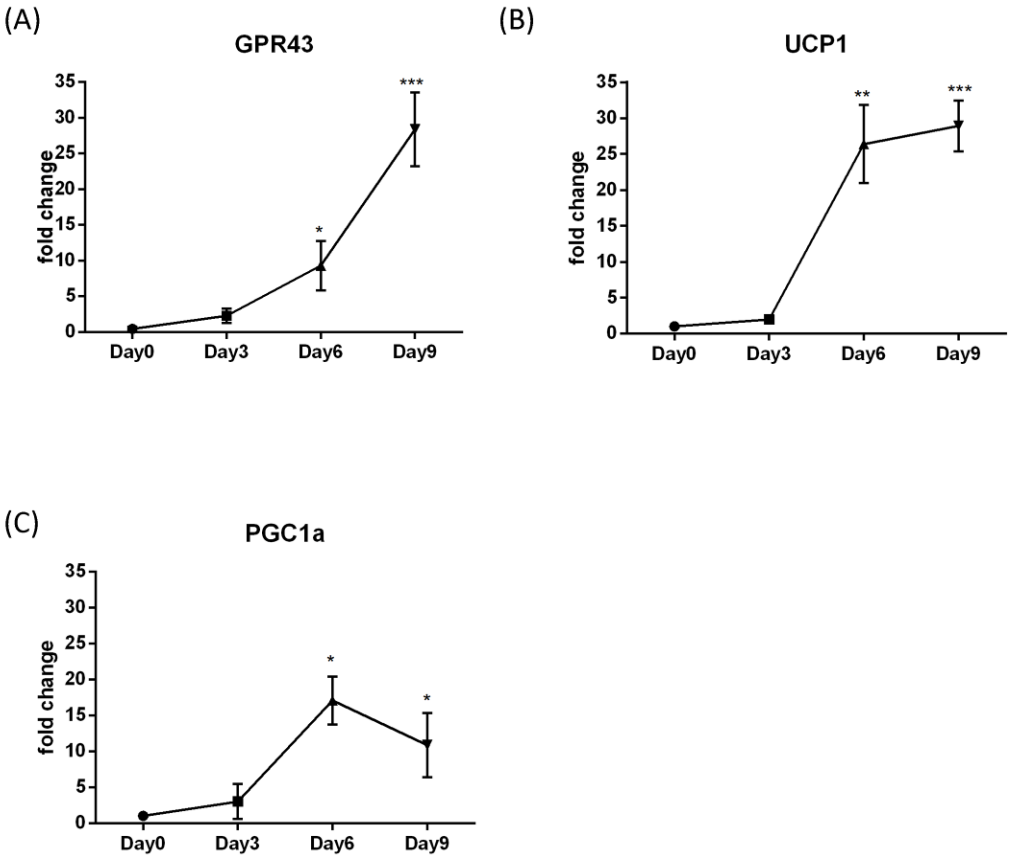

Figure 3-6 Expression patterns of GPR 43 during the differentiation of IM-BAT cells. (A) **Expression levels of GPR43 mRNA in the course of adipogenesis of IM-BAT cells.** (B) **Expression levels of UCP1 mRNA in the course of adipogenesis of IM-BAT cells.** (C) **Expression levels of PGC-1α mRNA in the course of adipogenesis of IM-BAT cells.** IM-BAT cells were differentiated and cell lysate were collected at day 0, day 3, day 6 and day 9. Transcription of target genes were detected by real-time PCR. Data presented as mean ± S.E.M.. * P <0.05, **P<0.01, ***P<0.001 compared to day 0 by one-way ANOVA followed by post-hoc tests.

3.2.4 XBP1 is crucial for GPR43 expression in brown adipocytes

XBP1 has been identified as key regulator of GPR43 transcription in human monocytes (Ang et al., 2015). Interestingly, it has also been reported that both XBP1 and GPR43 expression increase during the adipogenesis of white adipocytes, indicating a possible link between XBP1 and GPR43 expression in adipocytes.

Here, to interrogate the role of XBP1 in GPR43 expression in brown adipocytes, XBP1 expression pattern during brown adipogenesis was initially detected. The results demonstrated XBP1 expression showed a similar increasing trend as GPR43 during differentiation, suggesting the possibility that XBP1 plays an important role in GPR43 expression in brown adipocytes (figure 3-7).

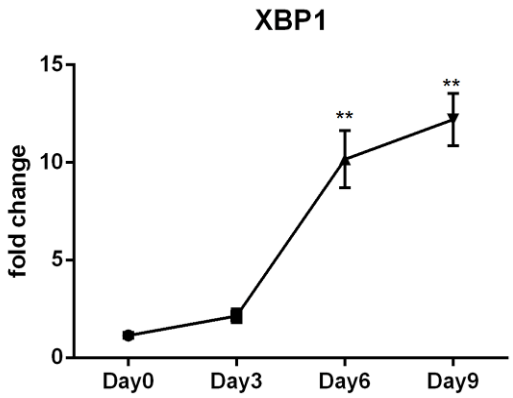

Figure 3-7 Expression levels of XBP1 mRNA in the course of adipogenesis of IM-BAT cells. IM-BAT cells were differentiated and cell lysate were collected at day 0, day 3, day 6 and day 9. Transcription of XBP1 were detected by real-time PCR. Data presented as mean ± S.E.M. **P<0.01 compared to day 0 by one-way ANOVA followed by post-hoc tests.

To further investigate the role of XBP1 in GPR43 expression in brown adipocytes, we knocked-down XBP1 expression by introducing siRNA targeting XBP1 into pre-adipocyte and then differentiated IM-BAT from 24 h post-transfection as described above.

To make sure the duration of silencing after siRNA transfection, the expression of XBP1 was checked from day 1 to day 7 post-differentiation. The XBP1 mRNA transcription levels were checked by real-time PCR and compared to cells transfected with control siRNA. The result showed that the knock-down efficiency reached >60% at 48 h post-transfection (24 h post-differentiation). Moreover, the knock-down efficiency kept at >70% until day 5 post-differentiation and persisted at >70% at day 7 (figure 3-8 (A)), indicating the XBP1 gene silencing effect can last through the differentiation process of IM-BAT cells.

To reach the desirable knock-down efficiency, all the assays were carried out at day 5 post-induction. As expected, knock-down of XBP1 severely impairs the differentiation process. The oil accumulation in IM-BAT cells transfected with XBP1 siRNA was significantly lower after 5 days differentiation compared to the cells transfected with control siRNA (figure 3-8(B)), which is similar to the effect of XBP1 knock-down / knock-out in white adipocytes reported by previous studies. More interestingly, GPR43 expression were also severely decreased in IM-BAT cells transfected with XBP1 siRNA compared to control group (figure 3-8(C)), suggesting XBP1 plays a crucial role in GPR43 expression in brown adipocytes.

(A)

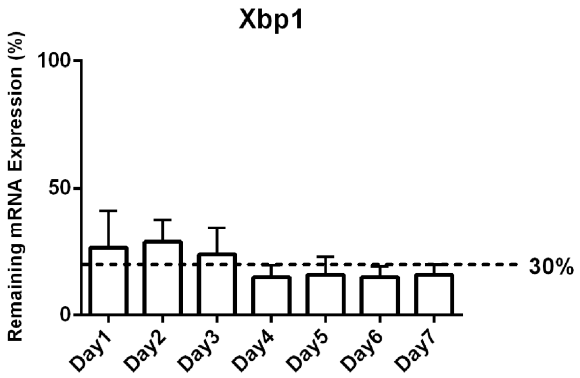

(B)

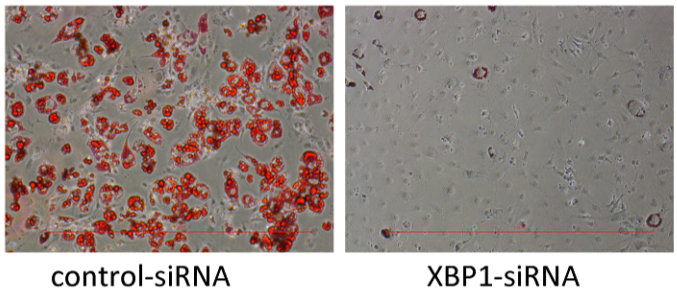

(C)

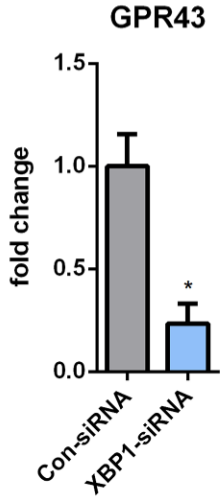

Figure 3-8 Effects of XBP1 knock-down on adipogenesis and GPR43 expression in IM-BAT cells. (A) **Duration of XBP1 silencing after XBP1 siRNA transfection**. IM-BAT cells were transfected with XBP1 siRNAs (Santa Cruz, # sc-38628) or Control siRNA (sc-37007) at 200 nM. The next day, cells were differentiated as indicated. Cells were lysed day 0 through day 7 post-differentiation and XBP1 transcription levels were measured using the real-time PCR. Knock-down efficiency is expressed relative to expression from cells transfected with control siRNA. (B) **XBP1 knock-down impairs the lipid accumulation in IM-BAT cells.** IM-BAT cells were transfected with control siRNA or XBP1 siRNA and differentiated for 5 days. Lipid accumulation was measured with Oil-Red O staining. (C) **Expression levels of GPR43 and XBP1 mRNA in IM-BAT cells transfected with control siRNA or XBP1 siRNA after 5 days differentiation.** IM-BAT cells were transfected with control siRNA or XBP1 siRNA and differentiated for 5 days. Target genes transcription levels were measured by real-time PCR. Data presented as mean ± S.E.M. *P<0.05 compared to control siRNA group by student's t-test.

Similarly, using 'reverse transcription' to knock-down the expression of XBP1 also led to a significant decrease of GPR43 expression. The differentiated IM-BAT cells were trypsinized to detach and transfected with XBP1 siRNA when suspended in DMEM:F12 medium containing 10% FBS without antibiotics. As shown in figure 3-9 (A) and (B), introducing XBP1 siRNA into

differentiated IM-BAT cells led to GPR43 expression decreasing to around 50% after 48h incubation.

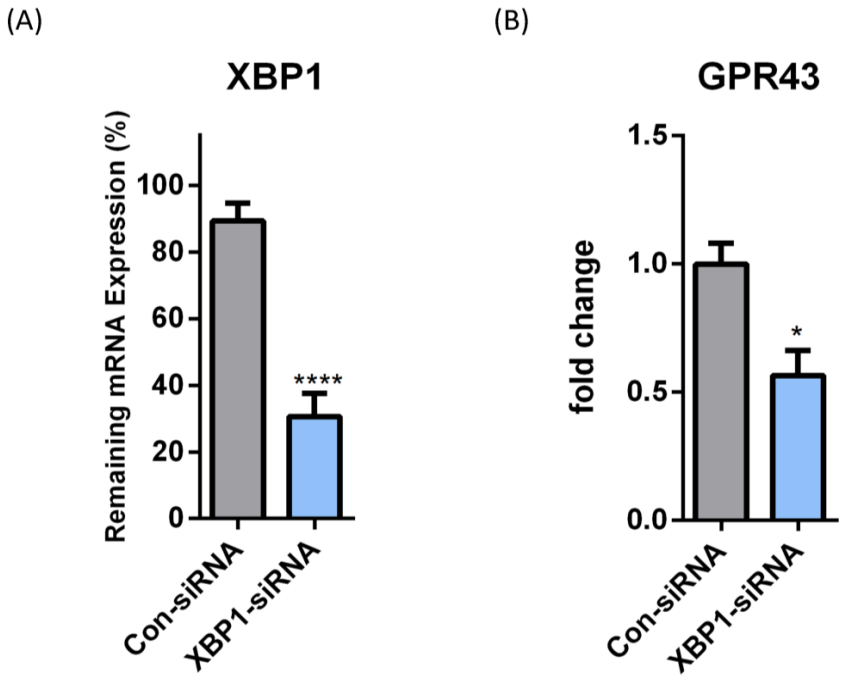

Figure 3-9 Effects of XBP1 knock-down on GPR43 expression in differentiated IM-BAT cells. Expression levels of **XBP1** (A) and **GPR43** (B) mRNA in differentiated IM-BAT cells transfected with control siRNA or XBP1 siRNA. The IM-BAT cells were differentiated for 7 days and transfected with control siRNA or XBP1 siRNA. The cells were lysed after 48 h with QIAzol and the transcription levels of GPR43 and XBP1 were measured by real-time PCR. Data presented as mean ± S.E.M. *P<0.05, ****P<0.0001 compared to control siRNA group by student's t-test.

3.2.5 Rosiglitazone up-regulated GPR43 mRNA expression in brown adipocyte.

To further investigate the links between adipogenesis and GPR43 expression, we also tested the impact of rosiglitazone treatment on GPR43 expression in brown adipocytes *in vitro*. Rosiglitazone, a well-known highly active adipogenic agent increasing PPARγ activity, were supplemented during the differentiation (day 2 to day 7). The results demonstrated that

treatment of rosiglitazone during differentiation significantly increased GPR43 mRNA level up to 3.5-folds as compared to the control condition (figure 3-10(A)). Besides, differentiated IM-BAT cells stimulated with rosiglitazone for short-time (24h) also display significantly augmented GPR43 expression compared to un-treated cells (figure 3- 10(B)).

Meanwhile, we also tested the effects of β-adrenergic receptor agonist and GPR43 agonist on GPR43 expression in differentiated IM-BAT cells. However, treatment with these agonists did not show significant increase in GPR43 expression, although an upward trend was observed when treated with isoproterenol (figure 3- 10(C)).

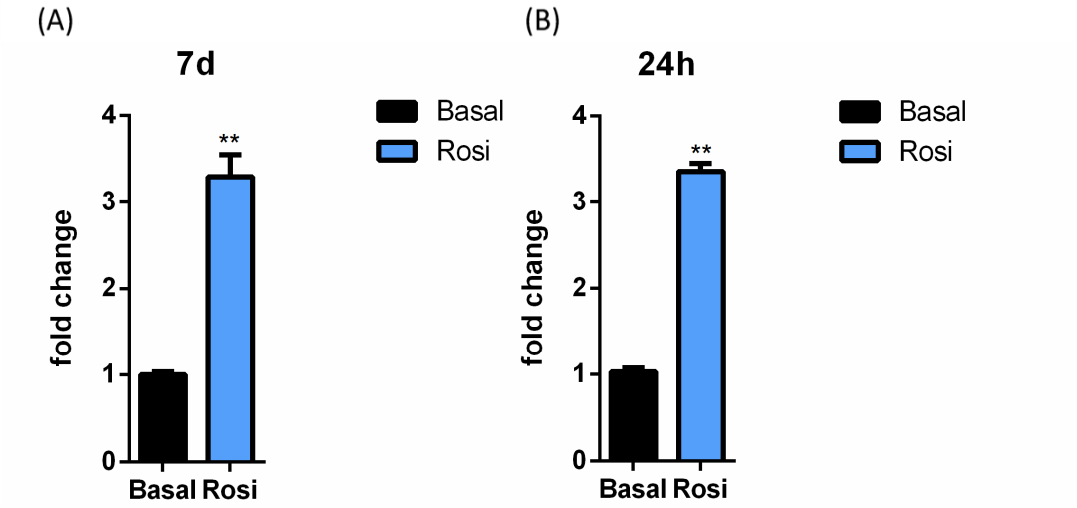

(C)

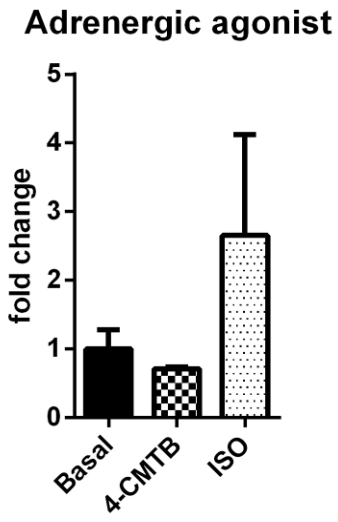

Figure 3-10 Rosiglitazone treatment up-regulates GPR43 expression in IM-BAT cells. (A) **Effects of rosiglitazone treatment on GPR43 mRNA transcription in IM-BAT cells.** The IM-BAT cells were differentiated for 7 days with or without rosiglitazone (1 μM, from day 2 to day 7). The cells were lysed with QIAzol and the transcription levels of GPR43 were measured by real-time PCR. Data presented as mean ± S.E.M. **P<0.01 compared to control siRNA group by student's t-test. (B) **Effects of rosiglitazone treatment on GPR43 mRNA transcription in differentiated IM-BAT cells.** The IM-BAT cells were differentiated for 7 days followed by treated with rosiglitazone (1 μM) for 24 h. The cells were lysed with QIAzol and the transcription levels of GPR43 were measured by real-time PCR. Data presented as mean ± S.E.M. **P<0.01 compared to control siRNA group by student's t-test. (C) **Effects of 4-CMTB and Isoproterenol on GPR43 mRNA transcription in differentiated IM-BAT cells.** The IM-BAT cells were differentiated for 7 days followed by treated with 4-CMTB (1 μM), or isoproterenol (1 μM) for 24 h. The cells were lysed with QIAzol and the transcription levels of GPR43 were measured by real-time PCR. Data presented as mean ± S.E.M.

3.2.6 Rosiglitazone up-regulated GPR43 mRNA expression in brown adipose tissue.

Male C57BL/6J mice (12-week-old) were intraperitoneally injected daily with 10 mg/kg rosiglitazone for 7 days. Brown adipose tissue was isolated immediately after mice were sacrificed. The expression of GPR43 was determined by real-time PCR. The results confirmed the effects of rosiglitazone in IM-BAT cells also applied *in vivo*. GPR43 expression in brown adipose tissue increased around 3-folds compared with control group (figure 3-11(A)). As a positive control, UCP-1 was used to confirm the effects of rosiglitazone on brown adipose tissue. The real-time PCR data showed rosiglitazone significantly up-regulated UCP-1 expression in brown adipose tissue as reported previously (figure3-11 (B)).

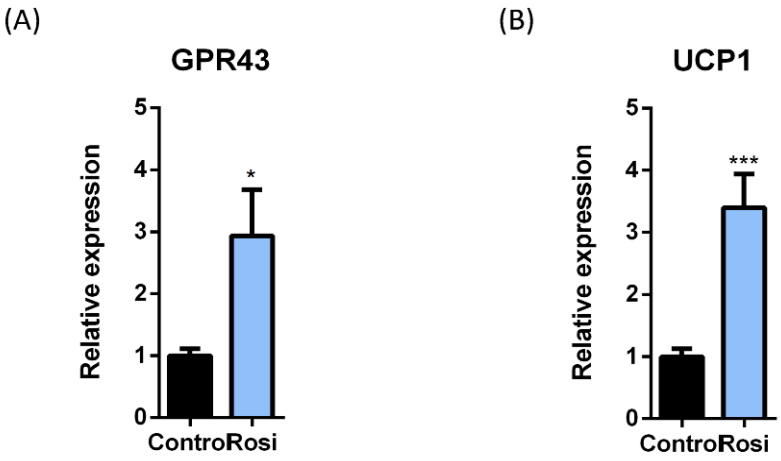

Figure 3-11 Rosiglitazone treatment up-regulates GPR43 expression in interscapular brown adipose tissue of C57BL/6J mice. Effects of rosiglitazone treatment on GPR43 (A) and UCP-1 (B) mRNA transcription in brown adipose tissue of C57BL/6J mice. C57BL/6J mice was bred until 12 week of age before intraperitoneally injected daily with 10 mg/kg rosiglitazone for 7 days. Interscapular brown adipose tissue was immediately sliced into pieces after the mice were sacrificed and immersed into RNAlatter solution. GPR43 and UCP1 mRNA transcription levels were measured by real-time PCR. Data presented as mean ±

S.E.M. *P<0.05, ***P<0.001 compared to control group injected with saline by student's t-test.

3.2.7 PPARγ and RXR involved in rosiglitazone-induced transcriptional upregulation of GPR43 in brown adipocytes

Recent studies have identified that the effects of thiazolidinediones (TZDs) in adipocytes can be categorized into PPARγ-dependent and PPARγ-independent. To elucidate the involvement of PPARγ in rosiglitazone induced increase in GPR43 expression, PPARγ selective antagonist GW9662 was pre-incubated before rosiglitazone treatment for 24 h. The results indicated significant up-regulation of GPR43 expression was only observed in cells treated with rosiglitazone but not in cells pre-treated with GW9662, suggesting rosiglitazone upregulated GPR43 is PPARγ dependent.

Similarly, RXR antagonist HX531 was also applied to test the effects of heterodimerization of PPARγ and RXR on GPR43 expression. The results also showed pre-treatment of HX531 effectively inhibited rosiglitazone induced GPR43 expression in differentiated brown adipocytes.

Taken together, these evidence suggested increase in GPR43 transcription induced by rosiglitazone treatment might require the formation of heterodimerization between PPARγ and RXR.

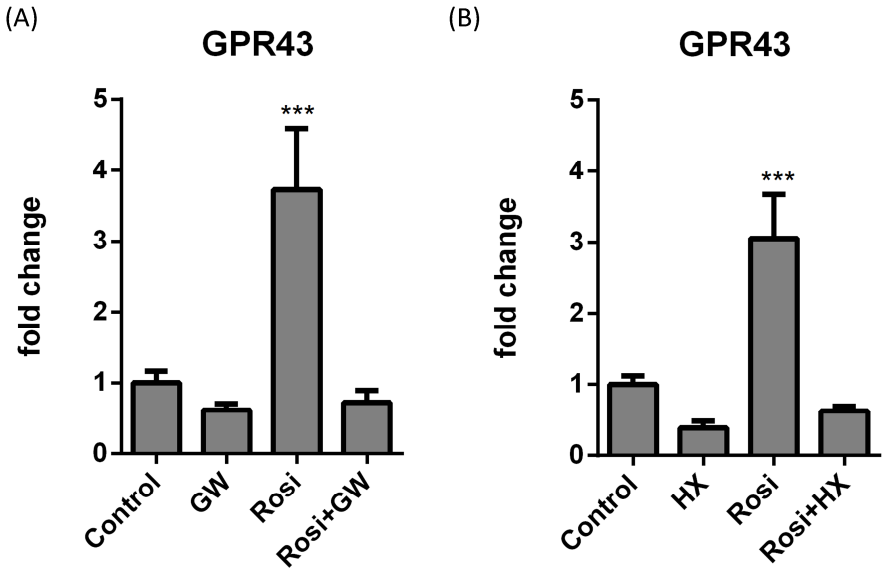

Figure 3-12 PPARγ and RXR are required for rosiglitazone-induced GPR43 expression in IM-BAT cells. (A) **Effects of PPARγ antagonist GW9662 on GPR43 mRNA transcription stimulated by rosiglitazone treatment in IM-BAT cells.** (B) **Effects of RXR antagonist HX531 on GPR43 mRNA transcription stimulated by rosiglitazone treatment in IM-BAT cells.** The IM-BAT cells were differentiated for 7 days. The cells were pre-treated with GW9662 or HX531 for 4 h before treated with or without rosiglitazone (1 μM). The cells were lysed with QIAzol and the transcription levels of GPR43 were measured by real-time PCR Data presented as mean ± S.E.M. ***P<0.001 compared to control siRNA group by one-way ANOVA followed by post-hoc tests.

3.2.8 Rosiglitazone overcame the effects of XBP1 knock-down on GPR43 expression in brown adipocyte.

As we demonstrated above, XBP1 seems to be indispensable for the normal expression of GPR43 in brown adipocytes. In addition, we also observed rosiglitazone significantly up-regulated GPR43 expression in brown adipocytes.

Next, we tried to identify the roles of XBP1 in rosiglitazone-induced transcriptional upregulation of GPR43 in brown adipocytes. We firstly transfected siRNA targeting XBP1 into preadipocytes and differentiated the cells into brown adipocytes with or without the existence of rosiglitazone from day 2 to day 5 post-induction. In accordance to previous findings, the efficiency of XBP1 knock-down could keep at >~70% to day 5 post-induction (figure 3-13 (A)), at which time point GPR43 expression levels were measured by real-time PCR. The results also confirmed that GPR43 mRNA transcription was significantly impaired by the knock-down of XBP1 compared to cells only transfected with control siRNA (figure 3-13 (B)). More interestingly, compared with no rosiglitazone treated cells, the rosiglitazone treated brown adipocytes still showed a significant increase in GPR43 expression at normal level, indicating the promotion effect of rosiglitazone on GPR43 expression is not abolished by XBP1 knock-down.

Besides, since activation of XBP1 requires the splicing of XBP1 mRNA, we also tested the effect of rosiglitazone treatment on XBP1 mRNA splicing by reverse transcription PCR. The results showed that in positive control group, treatment with tunicamycin, a N-linked glycoproteins synthesis inhibitor and commonly used ER stress inducer, led to a clear XBP1 splicing as two bands shown on the gel, while there was no obvious XBP1 mRNA splicing detected after rosiglitazone treatment (figure 3-13 (C)), supporting the hypothesis that XBP1 activation might not involve in rosiglitazone induced GPR43 expression.

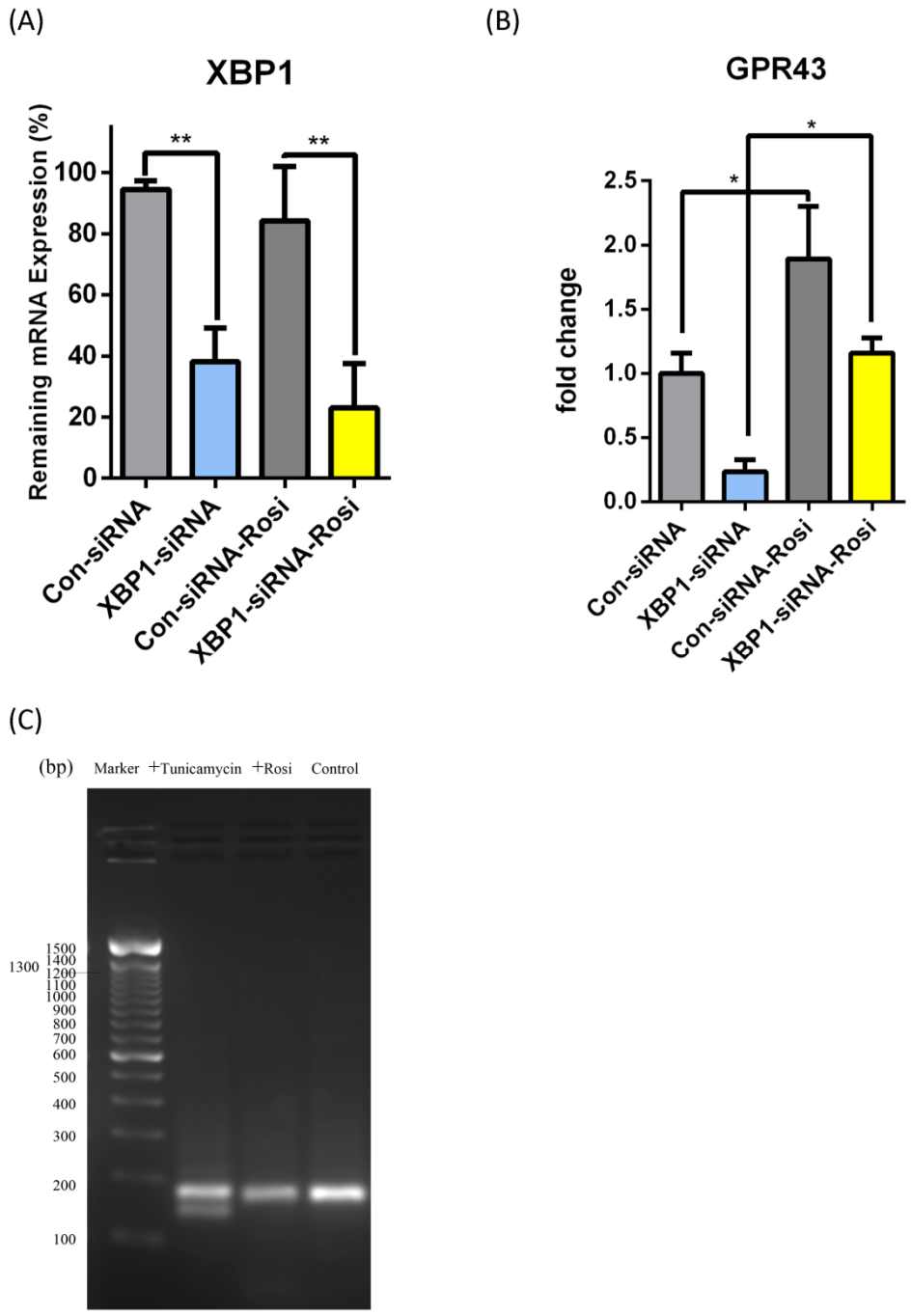

Figure 3-13 Rosiglitazone overcomes the effects of XBP1 knock-down on GPR43 expression in IM-BAT cells. (A) **Validation of shRNA-mediated knock-down of XBP1.** IM-BAT cells were transfected with control siRNA or XBP1 siRNA, on next day, the cells were differentiated for 5 days with or without rosiglitazone (1 μM) from day 2 to day 5. The transcription level of XBP1 was measured at day 5 after differentiation. (B) **Effects of rosiglitazone treatment on GPR43 mRNA transcription in XBP1 knock-down IM-BAT cells.** IM-BAT cells were transfected

with control siRNA or XBP1 siRNA, on next day, the cells were differentiated for 5 days with or without rosiglitazone (1 μM) from day 2 to day 5. The transcription level of GPR43 were measured at day 5 after differentiation. (C) **Effects of rosiglitazone treatment on XBP1 mRNA splicing in differentiated IM-BAT cells.** IM-BAT cells were differentiated and treated with rosiglitazone (1 μM). The splicing of XBP1 were measured by RT-PCR. The cells treated with tunicamycin were used as positive control. Data presented as mean ± S.E.M. *P<0.05, **P<0.01 compared to control siRNA group by one-way ANOVA followed by post-hoc tests.

3.2.9 STAT5 involved in rosiglitazone-induced transcriptional upregulation of GPR43 in brown adipocytes

STAT5 has been identified as an enhancer in GPR43 expression. Besides, STAT5 expression and activation also significantly increased during brown adipogenesis. Previous reports also demonstrated that PPARγ binds to the STAT5A promoter and increase the STAT5A expression, therefore, the rosiglitazone-mediated GPR43 expression might attribute, at least partially, to the increase of STAT5A expression and activation.

To test this hypothesis, we differentiated IM-BAT cells with adipogenic cocktail plus rosiglitazone and / or STAT5 inhibitor. The mRNA levels of GPR43 were examined by real-time PCR at day 5 post-induction. As shown in figure 3-14, rosiglitazone treatment showed an apparent stimulatory effect on GPR43 transcription, while GPR43 expression displayed a significant decrease both in cells treated with STAT5 inhibitor only and cells treated with the combination of rosiglitazone and STAT5 inhibitor. These results suggested STAT5 is indispensable for rosiglitazone induced GPR43 expression in brown adipocytes.

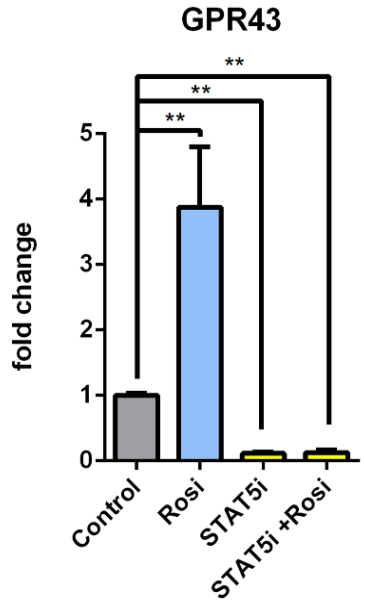

Figure 3-14 Effects of STAT5 inhibitor on rosiglitazone-induced GPR43 expression in IM-BAT cells. IM-BAT cells were differentiated with 1 μM rosiglitazone and or STAT5 inhibitor from day 2 to day 5, GPR43 mRNA transcription in IM-BAT cells was measured by real-time PCR. Data presented as mean ± S.E.M. **P<0.01 compared to control group by one-way ANOVA followed by post-hoc tests.

3.3 Discussion

Brown adipose tissue has emerged as an important endocrine organ in energy homeostasis. Immortalized brown adipocyte is a powerful tool to investigate the functions of brown adipose tissue *in vitro*. Klein *et al.* have proposed several criteria to characterize brown adipose cell lines: 1) expression of a tissue-specific protein UCP-1; 2) high sensitivity to adrenergic stimulation; 3) signalling and metabolic response to insulin stimulation (Klein et al., 2002). Here, our results showed that IM-BAT cells (which have a fibroblast-like appearance under standard culture conditions) can be differentiated into large, spherical cells, accumulating multiple lipid

droplets of various sizes as revealed by the Oil Red O staining and express brown adipocytes marker UCP1. Moreover, differentiated IM-BAT cells maintained the ability to increase UCP1 expression and glucose uptake after β-adrenergic stimulation, while insulin treatment rapidly induced a strong Akt phosphorylation in differentiated IM-BAT cells, indicating that β-adrenergic signalling and insulin signalling were intact in the differentiated IM-BAT adipocytes. Taken together, the above data showed that IM-BAT cells used in our study demonstrated highly phenotypic and functional similarities with brown adipocytes models in previous reports, which have been widely used as a tool to investigate functions of brown adipocytes *in vitro*.

GPR43 shares 38% identity with GPR41 in amino acid sequence and recognizes short-chain fatty acids (Sawzdargo et al., 1997). Based on our experiments, we could not observe GPR41 expression at detectable levels in brown adipocytes as well as in interscapular brown adipose tissue. This finding is consistent with previous data reporting that nearly all identified physiological functions of short-chain fatty acids in white adipocytes were mediated by GPR43 (Kimura et al., 2013).

Although pro-adipogenic and anti-lipolytic properties of GPR43 have been extensively studied in white adipocytes, little information has been known for the implication of this receptor in brown adipocytes. To identify the expression of GPR43 in brown adipose tissue and brown adipocytes, we first utilized real-time PCR, Western blots and immunohistochemistry to explore the expression of GPR43 in brown adipocyte and brown adipose tissue. Our results indicated the GPR43 expression can be detected in interscapular

brown adipose tissue as well as in immortalized brown adipocytes from day 3 post-induction.

Besides, our finding is also consistent with previous reports by Zaibi *et al.* that GPR43 expression is relatively lower in brown adipose tissue than white adipose tissue in mice (Zaibi et al., 2010). However, the expression patterns of GPR43 during differentiation share many similarities in brown adipocytes and white adipocytes. For example, it was found in several white adipocyte models (e.g. 3T3-L1) that GPR43 expression significantly increased in the later stages of differentiation, suggesting the involvement of GPR43 in the process of adipogenesis. Here, our results also demonstrated the GPR43 expression was rapidly and reproducibly increased during the adipogenesis process of IM-BAT cells. Indeed, the fact that GPR43 only being detected in the later phase of adipocyte differentiation makes it a good candidate for a novel adipogenic marker.

Moreover, it has been reported that treatment of PPARγ agonist significantly increased the expression of GPR43 in white adipose tissue *in vivo* and in white adipocytes *in vitro*. Here the promotive effect of PPARγ agonist on GPR43 expression in brown adipose tissue and brown adipocyte was also observed both *in vivo* and *in vitro*. Acute treatment of rosiglitazone led to a rapid increase of GPR43 in differentiated IM-BAT cells and interscapular brown adipose tissue, while treatment of rosiglitazone during the differentiation further up-regulated its expression, which is similar to the effects of thiazolidinedione in white adipocytes in previous studies. This observation also supported the hypothesis that GPR43 exists in brown

adipocytes and shares a similar mechanism of expression control during the adipogenesis.

As transcription factor, PPARγ binds to *cis*-element PPRE in promoter region to directly mediate target genes expression. Although our results clearly demonstrated PPARγ activation led to the up-regulation of GPR43 expression in brown adipocytes as well as brown adipose tissue, however, using computer programme to analyse the structure of GPR43 genes promoter, we could not found putative PPRE. Besides, in report form Ang *et al.*, the PPRE was neither identified in the GPR43 promoter region. Therefore, the promotive effect of PPARγ agonist on GPR43 expression might be attributed to more complex transcription controls during the differentiation of brown adipocytes. However, more evidence is needed to confirm this hypothesis.

Recent studies have shown PPARγ agonists not only function *via* receptor-dependent mechanism at the genomic level, but also may operate *via* receptor-independent effects (Kulkarni et al., 2012). Here, our results revealed that pre-treatment of PPARγ antagonist or PXR antagonist nearly abolished the effect of rosiglitazone on GPR43 expression in IM-BAT cells, suggesting the effect of rosiglitazone on GPR43 expression is PPARγ dependent and requires the dimerization between PPARγ and PXR.

Indeed, XBP1 has been elucidated as core *cis* element controlling the GPR43 transcription in human monocytes by Ang *et al.* (Ang et al., 2015). Here, our results also demonstrated knock-down of XBP1 significantly impaired the expression of GPR43 in brown adipocytes, indicating XBP1 also

plays a crucial role in GPR43 expression in brown adipocytes. Since XBP1 has been identified as an important sensor in ER stress response, it is reasonable to speculate there might be a relationship between ER stress and GPR43 expression. Actually, there has been some evidence to support this hypothesis. It was reported that GPR43 expression was elevated in adipose tissue, muscle and liver in high-fat diet-fed mice (Cornall et al., 2011), while Dr. Manjunath Ramanjaney (Hamad Medical Corporation, Doha, Qatar) also communicated that high-fat diet-fed mice showed augment of GPR43 expression in interscapular brown adipose tissue in mice. Notably, the links between obesity and ER stress, especially in adipose tissues, have been elucidated in both mouse experiments and human studies. Chronic excess nutrient intake has been shown to cause ER stress as well as insulin resistance and inflammation in adipose tissue in mice fed high-fat diets and in ob/ob mice (Kawasaki et al., 2012). Recently, increased ER stress has also been observed in subcutaneous adipose tissue of obese human subjects (Gregor et al., 2009). Hence, based on our findings that XBP1 is an important controller of GPR43 expression in brown adipocyte, the increased activity of XBP1 in ER stress status might be the underlying mechanism by which obesity leads to the increase of GPR43 expression.

Meanwhile, it was also observed that rosiglitazone induced augment of GPR43 was not significantly affected by knock-down of XBP1. Interestingly, although deletion of XBP1 inhibits adipogenesis *in vitro*, Gregor *et al.* found this inhibitory effect could be overcome by stronger pro-adipogenic stimuli, such as thiazolidinedione (Gregor et al., 2013). Deletion of adipocyte-XBP1

in vivo did not affect body weight, adipose tissue mass, serum insulin, or glucose homeostasis, indicating XBP1 might not be an indispensable contributing factor to the formation or expansion of adipose tissue *in vivo* (Gregor et al., 2013). Here, consistent to these findings, our results also suggested rosiglitazone increased GPR43 transcription seems to be XBP1-independent. Studies based on XBP1 knock-out cells or mice may provide more conclusive evidence to prove this hypothesis.

Notably, Choi *et al.* reported that co-culture of adipocytes with myoblasts promoted C/EBPβ and PPARγ gene expression in differentiated myoblasts and GPR43 expression in adipocytes, also suggesting the involvement of GPR43 in adipogenesis *via* mediating PPARγ activity (Choi et al., 2013).

Anti-adipogenic compound STAT5 inhibitor was found to decrease the expression of GPR43, providing more evidence to support the hypothesis that GPR43 might reflect the differentiation status of adipocytes. Furthermore, we also observed that rosiglitazone treatment could not overcome the effects of STAT5 inhibitor on GPR43 expression. Therefore, our findings indicated STAT5 as an important regulator for GPR43 expression in brown adipocytes. Intriguingly, in several pre-adipocyte models, PPARγ was shown to bind to the STAT5A promoter and increase the STAT5A-luciferase reporter expression, while activated STAT5A increased the PPARγ expression during differentiation of adipocytes, indicating a coordinated role between STAT5A and PPARγ in adipogenesis.

Finally, together with the evidence that GPR43 was only detected in differentiated brown adipocytes, as well as the impaired differentiation

caused by knock-down of XBP1 or treatment of STAT5 inhibitor was accompanied by the decrease of GPR43, suggesting GPR43 might be a novel adipogenic marker for brown adipocytes and play important roles in brown adipogenesis.

Chapter 4: Acetate promotes adipogenesis and mitochondrial biogenesis in brown adipose tissue via GPR43

4.1 Preamble

Although it is still not fully understood the molecular mechanism underlying the adipogenesis *in vivo*, however, *in vitro* immortalized cell lines such as 3T3-L1 and 3T3-F442A or primary preadipocytes freshly isolated from stromal vascular fraction of adipose tissue have been widely used as *in vitro* models, which allow researchers to investigate the signalling pathways involved in adipogenesis or to screen the pro-adipogenic and anti-adipogenic potential of hormones, growth factors and various pharmacological compounds.

Based on the findings obtained from *in vitro* models, adipogenesis is recognized as the multi-step process involving a cascade of many different signalling pathways and transcription factors. Up to date, it has been revealed that the adipocytes differentiation was initialized by treatment with adipogenic cocktail (normally includes insulin, dexamethasone and cAMP elevating agents (e.g. IBMX)) when cells reach growth arrest after confluence (Reichert and Eick, 1999). This growth arrest by contact inhibition has been proved to be required for adipocyte differentiation. Within 1 h after the addition of adipogenic cocktail induction, preadipocytes show a transient high expression of c-Fos, c-Jun, JunB, c-Myc until 2-6 h post-induction (Cornelius et al., 1994). These oncogenes promote preadipocytes to re-enter cell cycles and undergo several rounds of cell cycles post-confluent, known as mitotic clonal expansion (Tang et al., 2003). This special mitosis is also indispensable for adipogenesis. Preventing this mitotic clonal expansion by blocking the cell entering S phase at this time point results in the absence of

lipid accumulation and glycerol-3-phosphate dehydrogenase (GPDH) activity, suggesting adipogenesis is severely impaired (Tang et al., 2003). During this step, the genomic DNA is also unwound to allow transcription factors access to regulatory response elements of genes involved in modulating the terminal differentiation (Cornelius et al., 1994). The transcription factors regulated genes expression during adipogenesis is a multi-step cascade. Several key transcription factors in this process have been identified. Among them, members of PPAR family and C/EBP family are found to play central roles (Mandrup and Lane, 1997). Initially, C/EBPβ and CEBPδ transiently increase within 4 h after induction with adipogenic cocktail, which further mediate the expression of PPARγ and C/EBPα (Wu et al., 1999b). PPARγ and C/EBPα expression reach detectable levels from day 2 post-stimulation and peaked at day 2-5 (Christy et al., 1991). Phosphorylated C/EBPα shows strong growth-inhibiting activity and promotes cells to exit cell cycles and start terminal differentiation (Darlington et al., 1998). Interestingly, PPARγ and C/EBPα increase the expression of each other, to amplify the signals of adipogenesis (Shao and Lazar, 1997). PPARγ and C/EBPα are critical for the expression of the late markers of adipogenesis, which consist of lipogenic and lipolytic enzymes, as well as other proteins responsible for modulating the mature adipocyte phenotype (Lefterova et al., 2008). The dramatic morphology changes and formation of lipid droplets inside the cells normally occurred by day 5-7 post-differentiation, by the time cells become terminally differentiated (Fan et al., 1983). Changes of extracellular matrix components and cytoskeletal components are also involved in this morphology changes (Mariman and Wang, 2010). However, there are many

limitations of conventional methods to monitor the cell morphology changes during the differentiation of adipocytes in real-time. Recent studies have shown the potential of xCELLigence system to monitor the differentiation of adipocytes in real-time (Kramer et al., 2014).

Although brown adipogenesis shares plenty of similarities with white adipogenesis, brown adipogenesis also possess its uniquity in many ways, such as large amount of mitochondria biogenesis, transcription of genes for thermogenesis (such as UCP-1), etc.. PPARγ co-activators, especially PGC-1α, are crucial for these unique processes (Farmer, 2008). PGC-1α interacts with the transcription receptor PPARγ and regulates the genes involved in brown adipogenesis. Of note, PGC-1α is highly expressed in brown, but not in white adipocytes (Puigserver et al., 1998). Ectopically expressing PGC-1α in white adipocytes induces ‘browning’ phenotype, indicating that PGC-1α plays an important role in the control of brown adipocyte differentiation and the converting of white adipocytes into beige cells (Bostrom et al., 2012).

Since short-chain fatty acids have been demonstrated to promote white adipogenesis (Hong et al., 2005), therefore, here we aimed to investigate the possible pro-adipogenic effects of short-chain fatty acid acetate in brown adipocytes and in brown adipose tissue. The results may provide useful evidence to understand the links between short-chain fatty acids and brown adipose tissues.

4.2 Results

4.2.1 Acetate showed no significant cytotoxicity towards immortalized brown adipocytes

As an end product of anaerobic fermentation in gut, acetate is expected to show little cytotoxic effects towards brown adipocytes at physiological concentration. To test this hypothesis, the cytotoxicity of acetate was measured by MTS assay using CellTiter 96® AQ_{ueous} One Solution. As can be seen from figure 4-1(A), incubation with acetate ranging from 1 nM to 10 mM showed no significant effect on cell viability in mature adipocytes. Indeed, considering the pH value of DMEM:F12 medium containing 100 mM acetate dramatically changed, the cytotoxicity of acetate at this concentration may attribute, at least partially, to the changes of acidity of the medium.

Meanwhile, to test the effects of long-term treatment of acetate during differentiation, IM-BAT cells were differentiated as described above while acetate was added into *differentiation medium II* from day 2 post-induction at final concentration of 10 mM, which is the same acetate concentrations as Kimura *et al* used for the cellular work in 3T3-L1 cells (Kimura et al., 2013). The cell viability was measured at day 7 after differentiation and compared with the cells differentiated in the absence of acetate. The results also demonstrated no significant changes of cell viability with 10 mM acetate treatment during the differentiation (figure 4-1 (B)). Taken together, these results suggested that in the range of below 10 mM, acetate showed little effects on cell viability or cell proliferation for IM-BAT cells.

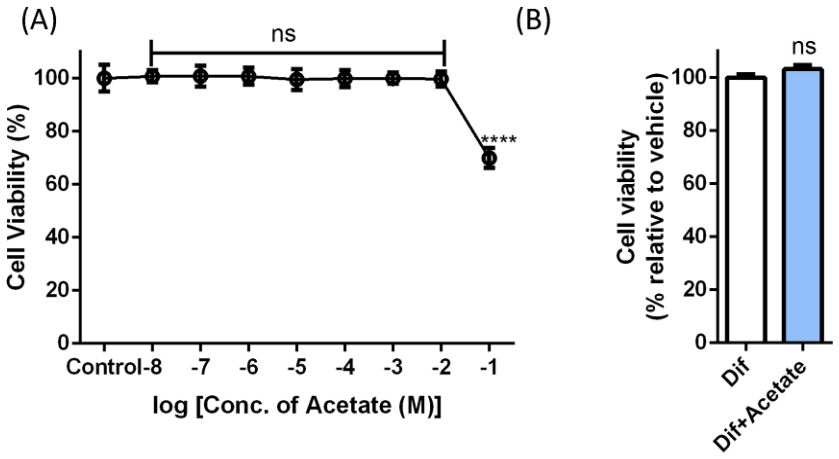

Figure 4-1 The toxicity effects of acetate on IM-BAT cells measured by MTS assay. (A) **The effect of acetate treatment on differentiated IM-BAT cell viability.** IM-BAT cells were differentiated for 7 days and treated with acetate (10 nM to 100 mM) for 24 h. The cell viability was measured by MTS assay and compared with cells without acetate treatment. Data presented as mean ± S.E.M. ****P<0.0001 compared to control by one-way ANOVA followed by post-hoc tests. (B) **The effect of acetate treatment during differentiation on IM-BAT cell viability.** The IM-BAT cells were differentiated for 7 days with or without acetate (10 mM, from day 2 to day 7). The cell viability was measured by MTS assay and compared with cells without acetate treatment. Data presented as mean ± S.E.M. N.S means 'Not Significantly Different'.

4.2.2 Acetate treatment during differentiation increased lipid accumulation of brown adipocytes

In order to examine the effects of acetate on differentiation of brown adipocytes, IM-BAT cells were treated with or without acetate (10 mM) throughout the course of the differentiation process from day 2 until day 7 post-induction, at which time the hypertrophic brown adipocytes filled with plenty of lipid droplets. The differentiated IM-BAT cells were then stained by Oil-Red O (Millipore Oil-Red O staining kit). The lipid accumulation in

differentiated brown adipocyte was then measured semi-quantitatively. As shown in figure 4-2, acetate increased Oil Red O staining of IM-BAT cells after differentiation relative to normally-differentiated control cells, indicating acetate as a positive modulator of brown adipocyte development.

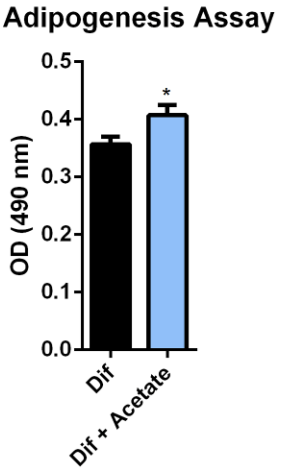

Figure 4-2 Effect of acetate treatment on lipid accumulation in IM-BAT cells measured by adipogenesis kit (Oil-Red O). The IM-BAT cells were differentiated for 7 days with or without acetate (10 mM, from day 2 to day 7). The lipid accumulation was measured by Oil-Red O staining and compared with cells without acetate treatment. Data presented as mean ± S.E.M. *P<0.05 compared to control by student's t-tests.

4.2.3 Acetate treatment during differentiation up-regulated AP2, PPARγ, PGC-1α and UCP1 expression in brown adipocytes

Next, the effects of acetate treatment during differentiation on the expression of several adipogenesis-related and thermogenesis-related genes were also examined by real-time PCR. As shown in figure 4-3 (A), acetate treatment during IM-BAT cells differentiation (from day 2) significantly increases the mRNA transcription levels of AP2, PPARγ, PGC-1α, and UCP1, while no significant changes of BMP7 and PRDM16 mRNA transcription were

observed. The protein expression of PGC-1α and UCP1 in brown adipocytes was also tested after acetate treatment by Western blots. Our results demonstrated that the protein levels of PGC-1α and UCP1 amounts exhibited ~1.9 fold and ~2.3 fold increases, respectively, in acetate treated cells compared to normally-differentiated cells (figure 4-3 (B) and (C)).

Also the concentration-dependent effects of acetate treatment on PGC-1α and UCP1 transcriptions in IM-BAT cells were investigated by real-time PCR. As shown in figure 4-4, compared to the effects of 10 mM acetate treatment during differentiation, acetate at 1 mM also induced a pronounced increase of PGC-1α and UCP1 while lower concentration of acetate induced relatively weaker response on PGC-1α and UCP1 expression (figure 4-4).

Besides, to establish that the observed effects are not cell line dependent, we also performed experiments using an additional brown adipocyte model (T37i) in which we also documented increased AP2, PPARγ, PGC-1α and UCP1 expression upon acetate stimulation (figure 4-5).

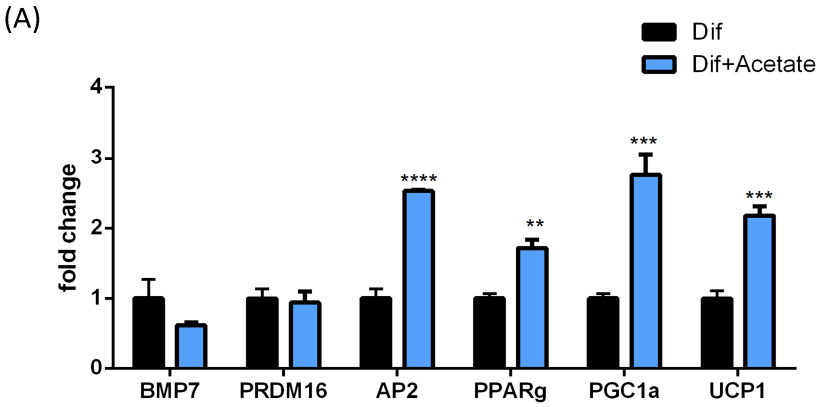

(B)

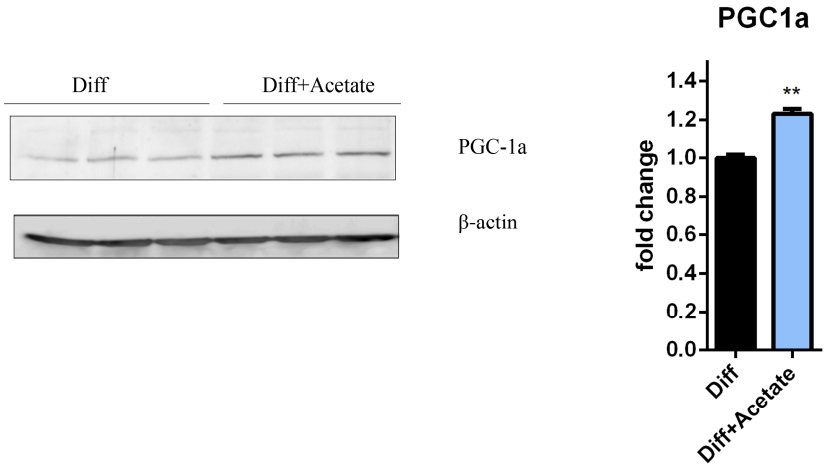

(C)

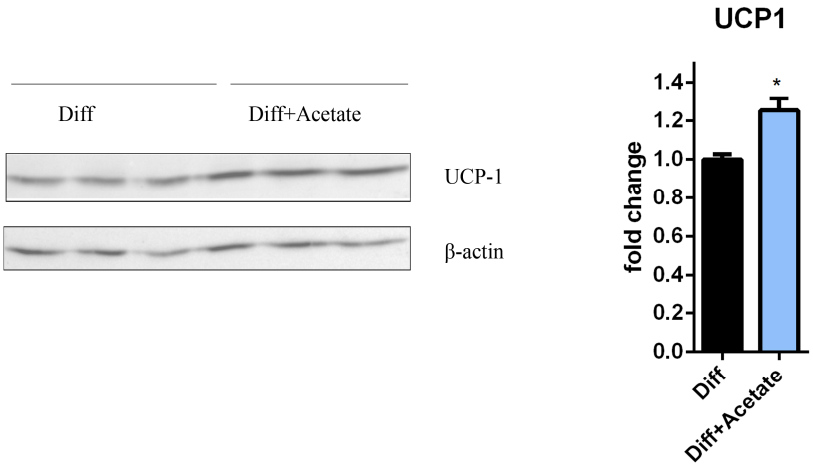

Figure 4-3 Effects of acetate treatment during differentiation on the expression of brown adipogenesis markers in immortalized brown adipocytes. (A) **The effects of acetate treatment on transcription of BMP7, PRDM16, AP2, PPARγ, PGC-1α, and UCP1 in IM-BAT cells detected by real-time PCR.** (B) **The effects of acetate treatment on expression of PGC-1α in IM-BAT cells detected by Western blots.** (C) **The effects of acetate treatment on expression of UCP1 in IM-BAT cells detected by Western blots.** The IM-BAT cells were differentiated for 7 days with or without acetate (10 mM, from day 2 to day 7). The cells were lysed with QIAzol (A) or RIPA buffer (B and C). The transcription levels of BMP7, PRDM16, AP2, PPARγ, PGC-1α, and UCP1 were measured by real-time PCR. The protein expression levels of PGC-1α and UCP1 were measured by western blots. Data are presented as mean ± S.E.M. *P<0.05, **P<0.01, ***P<0.001, ****P<0.0001 compared to control by student's t-tests.

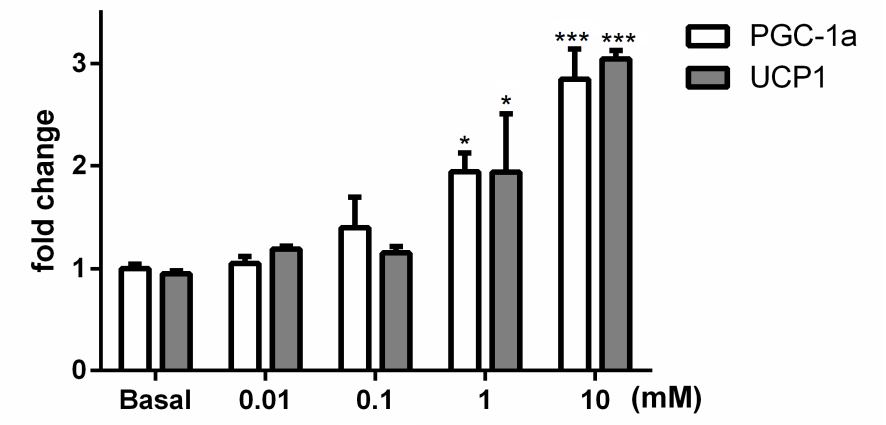

Figure 4-4 Concentration-dependent effects of acetate treatment during differentiation on the expression of PGC-1α and UCP1 in immortalized brown adipocytes. The IM-BAT cells were differentiated for 7 days with or without acetate at different concentrations (0.01 - 10 mM, from day 2 to day 7). The cells were lysed with QIAzol. The transcription levels of PGC-1α, and UCP1 were measured by real-time PCR. Data are presented as mean ± S.E.M. *P<0.05, ***P<0.001 compared to control by student's t-tests.

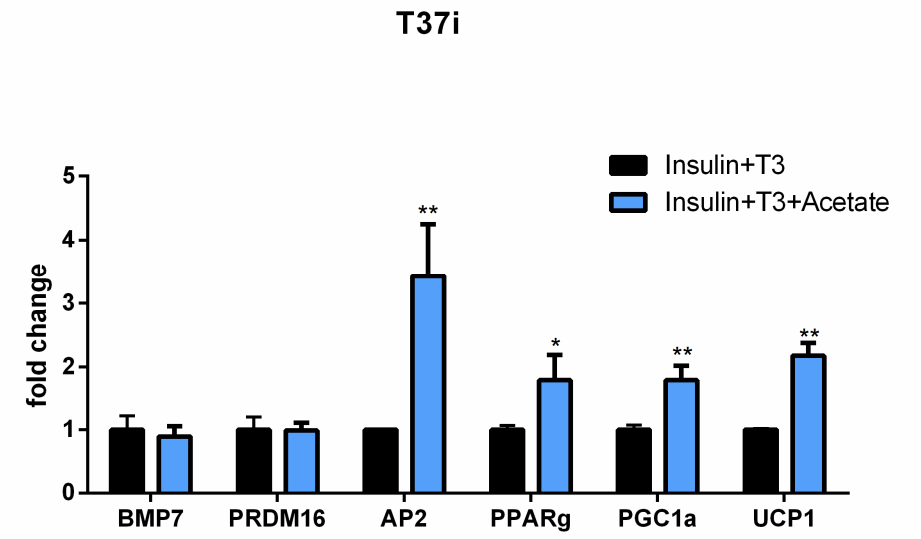

Figure 4-5 Effects of acetate treatment during differentiation on the transcription of brown adipogenesis markers in T37i cells detected by real-time PCR. The T37i cells were differentiated for 7 days with or without acetate (10 mM, from day 0 to day 7). The cells were lysed with QIAzol. The transcription levels of BMP7, PRDM16, AP2, PPARγ, PGC-1α, and UCP1 were measured by real-time PCR. Data are presented as mean ± S.E.M. *P<0.05, **P<0.01 compared to control by student's t-tests.

4.2.4 Acetate treatment affects the morphological shifts of brown adipocytes during differentiation

To further investigate the effects of acetate treatment on IM-BAT differentiation, xCELLigence system was used to monitor the Cell Index (*CI)* value of IM-BAT cells during the differentiation in real-time. As can been seen from figure 4-6 (A), the *CI* value of IM-BAT cells significantly drop after the incubation with *differentiation medium I*. A similar *CI* curve of 3T3-L1 differentiation detected by the xCELLigence system was also reported by Kramer *et al*. (Kramer et al., 2014). Interestingly, the *CI* curves of IM-BAT cells rapidly increased followed by a slightly decrease after incubation with *differentiation medium II*. Meanwhile, the acetate treatment during the incubation with *differentiation medium II* significantly decreased the augment of *CI* value compared to control group.

To find out whether acetate induced the decrease of *CI* value in IM-BAT cells was caused by change of cell numbers, the cell viability was also checked by microscopic analysis and MTS assay. The results confirmed that cell death was ruled out as a cause for this decreased *CI* values since there was almost the same cell viability in both assays (figure 4-6 (B) and (C)). Meanwhile, it also confirmed from microscopic analysis that gold sensing electrodes did not affect the differentiation (lipid accumulation) significantly (figure 4-6 (B)).

(A)

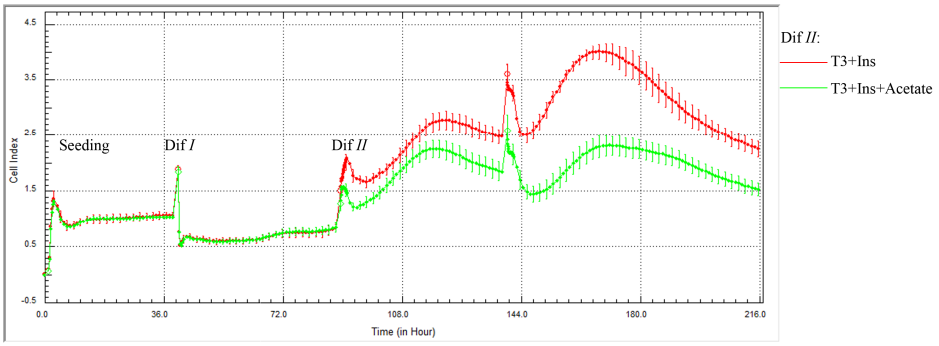

(B)

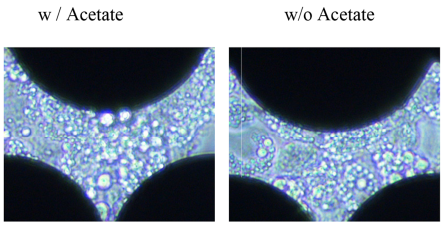

(C)

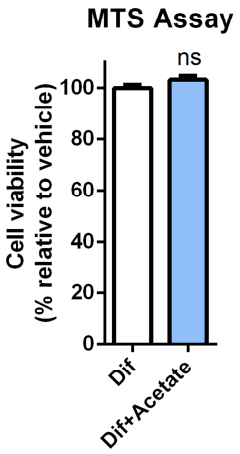

Figure 4-6 Effects of acetate treatment on morphological shifts of IM-BAT cells during differentiation. (A) **Effects of acetate treatment on IM-BAT cell growth *CI* curves during differentiation.** IM-BAT cells were treated with differential medium I followed by Insulin + T3 (control); or Insulin + T3 + Acetate (green) at the same time to compare the resulting *CI* growth curves. All curves were plotted as an average of quadruplicate treatments. Error bars show S.E.M. (n = 4). * P <0.05; ** P <0.01 compared to control by student's t-test. (B) **Terminally differentiated IM-BAT cells in E-plate were visualized by microscopy.** IM-BAT cells were differentiated in E-plate and continuously monitored the *CI* index. After measurement, the cells were checked under microscopy (40X magnification shown). (C) **Cell viability of IM-BAT cells during differentiation was measured by the MTS assay.** Values presented as mean ± S.E.M.. The IM-BAT cells were differentiated for 7 days with or without acetate (10 mM, from day 2 to day 7). The cell viability was measured by MTS assay and compared with cells without acetate treatment. Data presented as mean ± S.E.M. N.S means 'Not Significantly Different'.

4.2.5 Acetate treatment during differentiation increases mitochondrial biogenesis in brown adipocytes

Mitochondrial biogenesis has been associated with brown adipocyte differentiation and thermogenesis. PGC-1α is a key co-activator to turn on this process in brown adipocyte. Since previous results have shown the increase in PGC-1α after acetate treatment, therefore, next we examined the effects of acetate treatment on mitochondrial biogenesis in brown adipocytes. As shown in figure 4-7 (A), the mitochondrial DNA / nuclear DNA ration significantly increased after IM-BAT cells treated with acetate during the periods of differentiation from day 2 until day 7.

In agreement with this result, flowcytometry assay also indicated the augment of mitochondrial in brown adipocytes after acetate treatment during differentiation (figure 4-7 (B)).

(A)

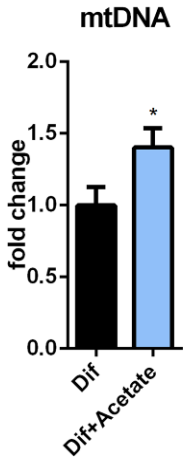

(B)

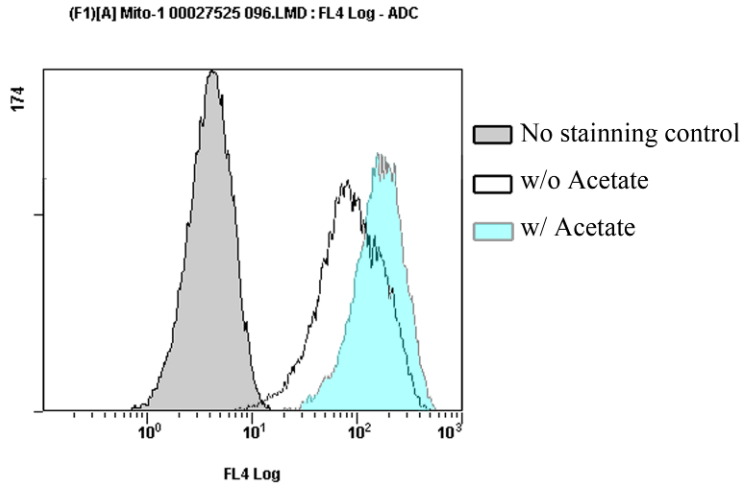

Figure 4-7 Effects of acetate treatment during differentiation on mitochondrial biogenesis of IM-BAT cells. (A) **Relative mitochondrial DNA levels in IM-BAT cells treated with or without acetate during differentiation**. DNA was isolated from IM-BAT cells using QIAamp DNA Mini Kit. The mitochondrial DNA level was measured with primers targeted for mouse mitochondrial D-Loop with 2 × SYBR green PCR master mix as described above. The mitochondrial DNA levels were normalized against the nuclear DNA level measured with 18S primers using the comparative C_T method. Data are presented as mean ± S.E.M. *P<0.05 compared to control by student's t-tests. (B) **Mitochondrial mass of IM-BAT cells treated with acetate during differentiation measured by flow cytometry.** The IM-BAT cells were differentiated for 7 days with or without acetate (10 mM, from day 2 to day 7) and stained with CytoPainter MitoNIR Indicator Reagent. The fluorescence levels (Ex/Em = 640/695 nm) were measured by flowcytometry and compared with untreated cells.

4.2.6 Acetate treatment during differentiation incrased mitochondrial basal and reserve respiratory capacity of brown adipocytes

To further assess the potential for acetate treatment during differentiation to increase mitochondrial oxidative capacity, mitochondrial respiration was measured using Seahorse XF24 Extracellular Flux Analysers and XF Cell Mito Stress Test Kit. The results showed the basal oxygen consumption rate

(OCR) and spare respiratory capacity (stimulated by FCCP) in acetate treated cells were increased by 17%, and 24%, respectively (figure 4-8).

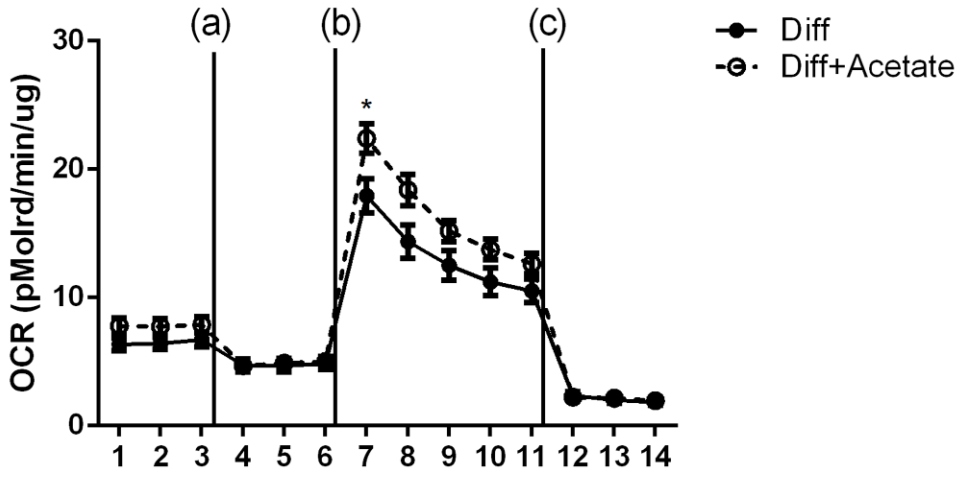

Figure 4-8 Effects of acetate treatment during differentiation on mitochondrial respiratory capacity of IM-BAT measured by the XF24 analyser. Group mean oxygen consumption rate (OCR) in pMol/min/μg protein of IM-BAT cells treated with or without acetate at 10 mM during differentiation from day 2 to day 7. Vertical lines indicate time of addition of mitochondrial inhibitors (a) oligomycin (1 μM), (b) FCCP (0.5 μM), or (c) antimycin A (1 μM) & rotenone (1 μM). Basal OCR, maximum OCR, spare capacity of cells treated as described above. Data are presented as mean ± S.E.M. * P <0.05 (Student's t-test).

4.2.7 Acetate treatment during differentiation incrased oxygen consumption rates of brown adipocytes upon β-adrenergic receptor agonist stimulation

Since β-adrenergic receptors are important regulator for energy expenditure in brown adipocytes, therefore, we also tested the effects of acetate treatment during differentiation on the response of IM-BAT cells to β-adrenergic receptors agonists. As shown in figure 4-9, both basal OCR and maximum response after CL-316,243 injection were up-regulated in cells

differentiated with acetate. This result is consistent with the increased mitochondrial biogenesis and increased mitochondrial respiratory capacity demonstrated above.

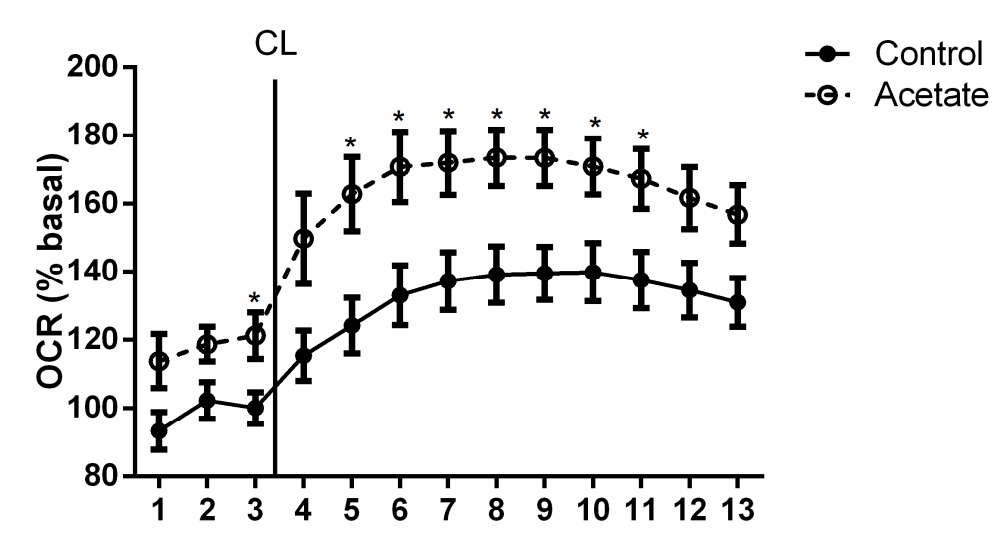

Figure 4-9 Effects of acetate treatment during differentiation on the mitochondrial respiratory capacity in IM-BAT cells in response to β-adrenergic stimulation. The x axis represents the applied XF24 protocol measurements and the vertical line indicates the time of addition of CL316,234 (CL). Data are expressed as the percentage of the basal value measured at the time point 3 (four replicates) in the control group. OCR: oxygen consumption rate. Data are presented as mean ± S.E.M. * P <0.05 (Student's t-test).

4.2.8 4-CMTB treatment during differentiation induced pro-adipogenic effects similar to acetate treatment in brown adipocytes

As shown in Chapter 3.2.2, GPR43 was successfully detected in differentiated IM-BAT cell while GPR41 was scarcely detected. Therefore, it is highly likely that GPR43, not GPR41, is mainly involved in acetate-mediated pro-adipogenic effects in brown adipocytes. To test this hypothesis,

IM-BAT cells were also treated with 4-CMTB, a synthesized selective agonist for GPR43, during the differentiation of IM-BAT cells from day 2 to day 7 post-induction. The expression of BMP7, PRDM16, AP2, PPARγ, PGC-1α and UCP1 were also measured by real-time PCR. As shown in figure 4-10 (A), similar to acetate treatment, 4-CMTB also significantly increased the transcription levels of AP2, PGC-1α and UCP1 in brown adipocytes, while PPARγ also showed an increase trend after 4-CMTB treatment. The BMP7 and PRDM16 mRNA levels were also not altered significantly by 4-CMTB treatment. Furthermore, Western blots also confirmed a significant increase of PGC-1α and UCP1 at protein level in 4-CMTB treated IM-BAT cells compared to normal differentiated cells (figure 4-10 (B) and (C)).

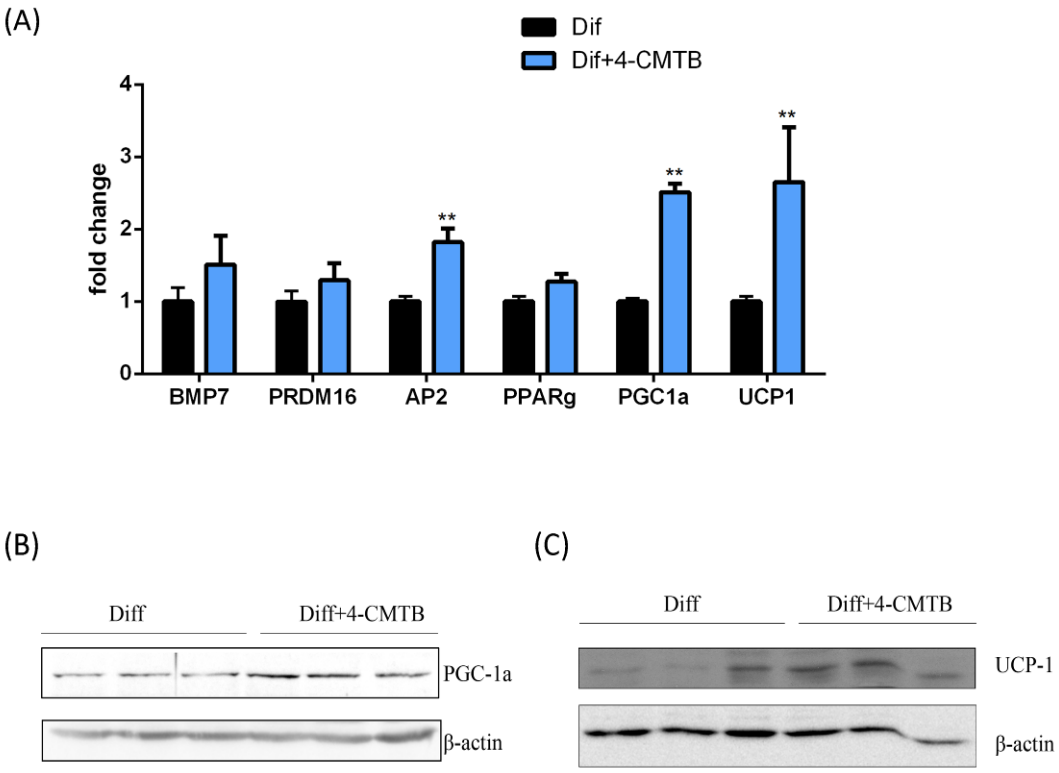

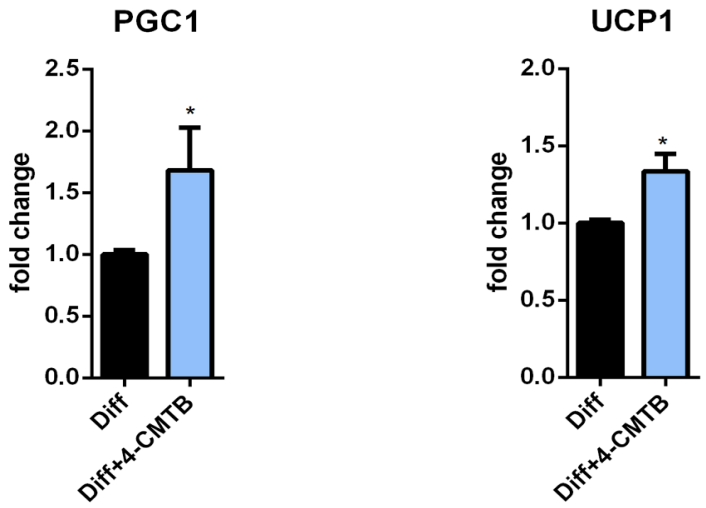

Figure 4-10 Effects of 4-CMTB treatment during differentiation on the expression of brown adipogenesis markers in immortalized brown adipocytes. (A) **The effects of 4-CMTB treatment on transcription of BMP7, PRDM16, AP2, PPAR, PGC-1α, and UCP1 in IM-BAT cells detected by real-time PCR.** (B) **The effects of 4-CMTB treatment on expression of PGC-1α in IM-BAT cells detected by Western blots.** (C) **The effects of acetate treatment on expression of UCP1 in IM-BAT cells detected by Western blots.** The IM-BAT cells were differentiated for 7 days with or without 4-CMTB (1 μM, from day 2 to day 7). The cells were lysed with QIAzol (A) or RIPA buffer (B and C). The transcription levels of GPR43 were measured by real-time PCR. The protein expression levels of PGC-1α and UCP1 were measured by Western blots. Data are presented as mean ± S.E.M. *P<0.05, **P<0.01 compared to control by student's t-tests.

Similarly, we also test the effects of 4-CMTB treatment during the differentiation on *CI* value measured by xCELLigence. The results showed 4-CMTB also elicited the similar *CI* value changes during the differentiation. The *CI* value of IM-BAT cells significantly drop after the incubation with *differentiation medium I* but rapidly increased after incubation with *differentiation medium II* followed by a slightly decrease. Meanwhile, the *CI* value is significantly lower in cells treated with *differentiation medium II* plus 4-CMTB than that in control group treated with *differentiation medium II* only

(figure 4-11 (A)). Furthermore, the cell viability and lipid accumulation after 4-CMTB treatment were also checked by MTS assay and microscopic analysis (figure 4-11 (B) & (C)). The results confirmed that cell death was not significantly increased after 4-CMTB treatment, indicating morphology change was the main reason for this decrease of *CI* values.

Mitochondrial biogenesis has also been determined in 4-CMTB treated IM-BAT cells. As shown in figure 4-12 (A), the mitochondrial DNA to nuclear DNA ratio also significantly increased after IM-BAT cells treated with 4-CMTB during the periods of differentiation from day 2 until day 7.

Furthermore, the effects of 4-CMTB treatment on mitochondrial respiration in brown adipocytes were also measured by Seahorse XF24 Extracellular Flux Analysers and XF Cell Mito Stress Test Kit. The results revealed that more pronounced increases of the basal OCR and reserve respiratory capacity were also observed after 4-CMTB treatment during the differentiation of IM-BAT cells (figure 4-12 (B)).

(A)

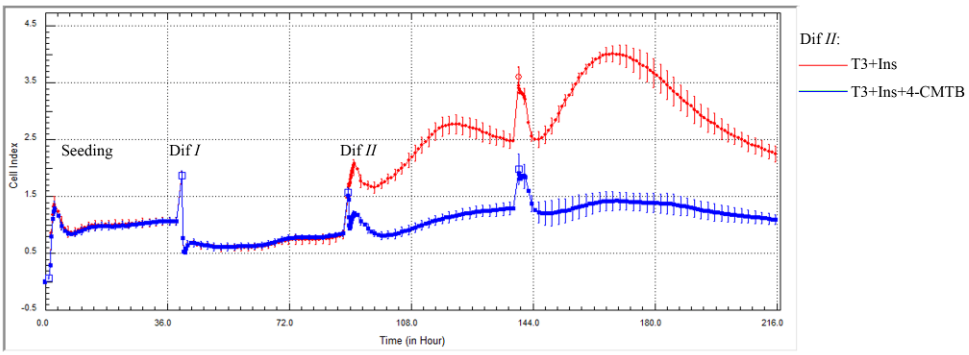

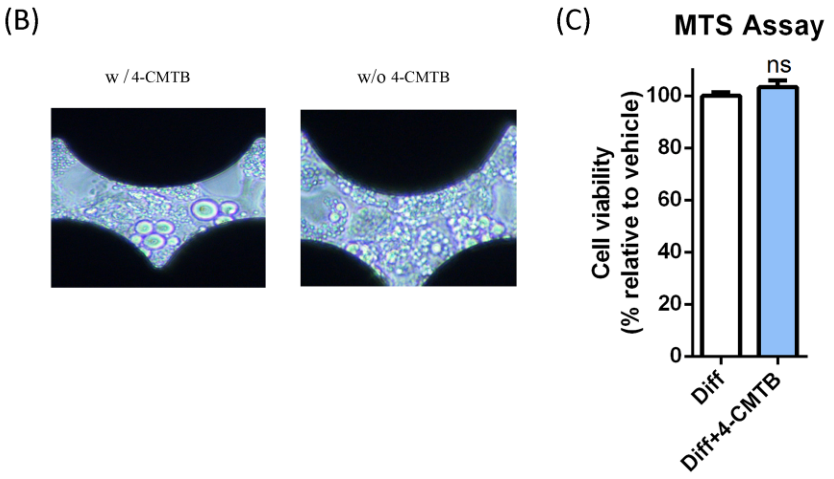

Figure 4-11 Effects of 4-CMTB treatment on morphological shifts of IM-BAT cells during differentiation. (A) Effects of 4-CMTB on IM-BAT cell growth *CI* curves during differentiation. IM-BAT cells were treated with differential medium I followed by Insulin + T3 (control); or Insulin + T3 + 4-CMTB (blue) at the same time to compare the resulting CI growth curves. All curves were plotted as an average of quadruplicate treatments. Error bars show S.E.M. (n = 4). * P <0.05; ** P <0.01 compared to control by student's t-test. (B) **Terminally differentiated IM-BAT cells in E-plate were visualized by microscopy** (40X magnification shown). (C) **Cell viability of IM-BAT cells during differentiation was measured by the MTS assay.** Values presented as mean ± S.E.M..

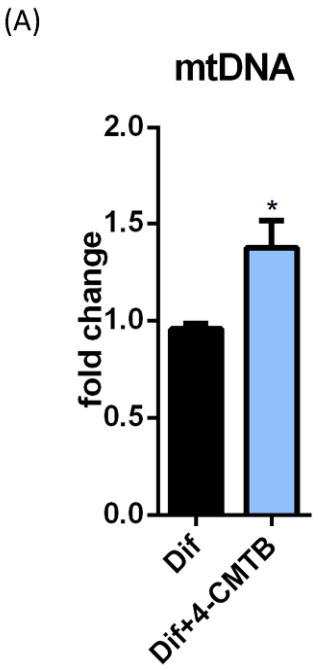

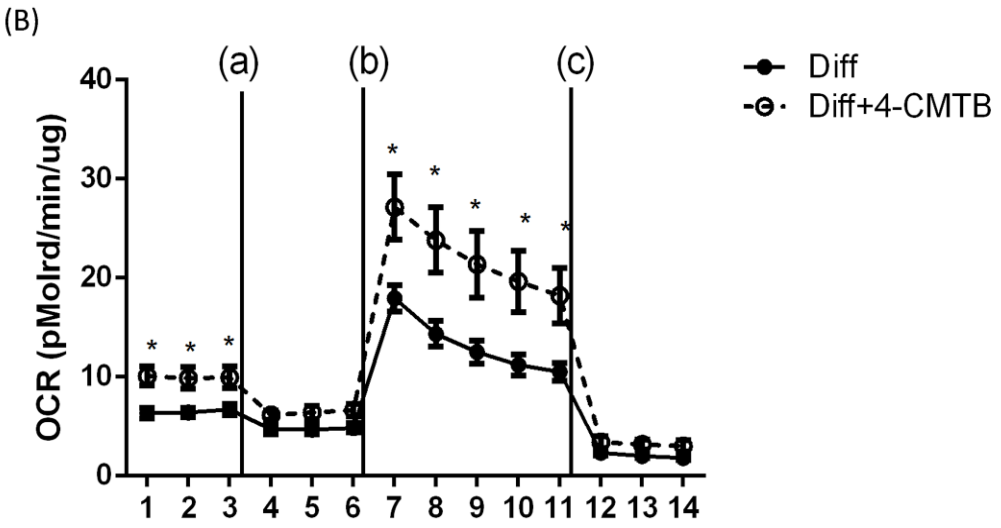

Figure 4-12 Effects of 4-CMTB treatment during differentiation on mitochondrial biogenesis and mitochondrial respiratory capacity of IM-BAT cells. (A) Relative mitochondrial DNA levels in IM-BAT cells treated with or without 4-CMTB during differentiation. DNA was isolated from IM-BAT cells using QIAamp DNA Mini Kit. The mitochondrial DNA level was measured with primers targeted for mouse mitochondrial D-Loop with 2 × SYBR green PCR master mix as described above. The mitochondrial DNA levels were normalized against the nuclear DNA level measured with 18S primers using the comparative CT method. (**B) The effect of 4-CMTB treatment on mitochondrial respiratory capacity of IM-BAT during differentiation measured by the XF24 analyser.** Group mean oxygen consumption rate (OCR) in pMol/min/μg protein of IM-BAT cells treated with or without 4-CMTB at 1 μM during differentiation from day 2 to day 7. Vertical lines indicate time of addition of mitochondrial inhibitors (a) oligomycin (1 μM), (b) FCCP (0.5 μM), or (c) antimycin A (1 μM) & rotenone (1 μM). Basal OCR, maximum OCR, spare capacity of cells treated as described above. * P <0.05 (Student's t-test).

4.2.9 Pro-adipogenic effects of acetate treatment were impired in GPR43 knock-down brown adipocytes

To further assess the role of GPR43 in acetate-induced effects on brown adipocytes, we also measured the effects of knock-down GPR43 on acetate-

induced brown adipogenic gene (UCP1) expression and mitochondria biogenesis.

IM-BAT cells were transfected with GPR43 shRNA and selected with puromycin at optimized concentration (figure 4-13(A)). Then, the cells were differentiated as described above and GPR43 expression were measured. The results showed that we successfully decreased GPR43 transcription to less than 30% of its baseline value in differentiated adipocytes by transfecting shRNA targeting GPR43 (figure 4-13(B)). While the stimulatory effect of acetate on UCP1 mRNA was apparent in control cells transfected with control shRNA, this effect was impaired in cells transfected with shRNA for GPR43 (figure 4-13(C)). Similarly, the increase of mitochondrial DNA ratio was also only observed in control cells (figure 4-13(C)).

(A)

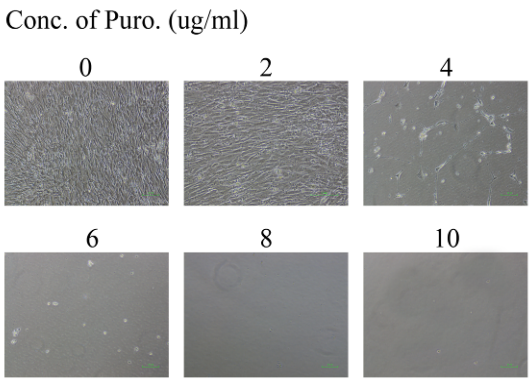

(B)

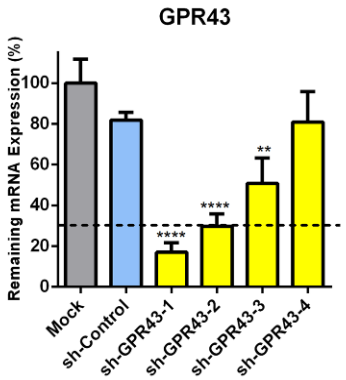

(C)

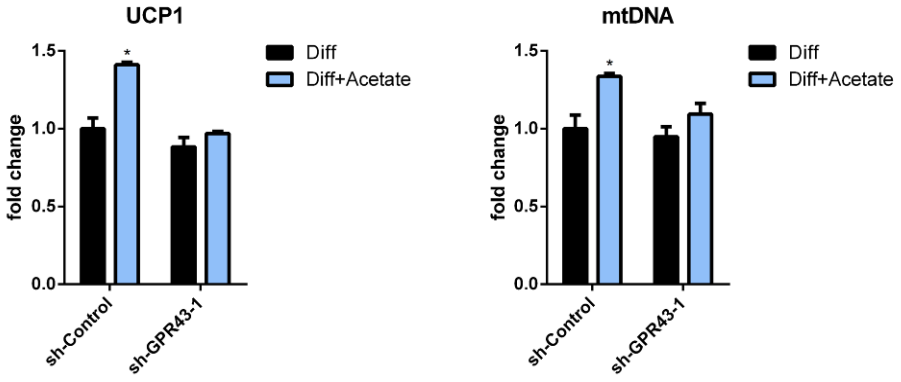

Figure 4-13 Effects of GPR43 knock-down on pro-adipogenic effects of acetate in IM-BAT cells (A) **Optimization of puromycin selection condition.** IM-BAT cells were seeded at in 96-well plates. On the next day, the culture media were replaced with DMEM:F12 containing 0-10 puromycin. After 7 days selection, the cell viability was checked by microscopy. The optimal concentration was chosen at the lowest concentration that kills 100% of non-transduced cells. (B) **Validation of shRNA-mediated knock-down of GPR43.** Undifferentiated immortalized BAT (IM-BAT) cells were transfected with shRNA non-targeting control (#RHS6848) or shRNA targeting GPR43 (sh-GPR43-1: TRCN0000027581; sh-GPR43-2: TRCN0000027541; sh-GPR43-3: TRCN0000027562 sh-GPR43-4: TRCN0000027552). Following selection by puromycin, cells were lysed with Qiazol after 7 days of differentiation and subjected to real-time PCR analysis. (C) **The effects of GPR43 knock-down on acetate induced UCP1 increase and mitochondria biogenesis.** IM-BATs transfected with non-targeting shRNA control or shRNA targeting GPR43 were treated with or without acetate during differentiation. Relative mRNA levels of UCP1 and relative mitochondrial DNA levels were analysed by real-time PCR. Data are presented as mean ± S.E.M.. *P <0.05, **P<0.01, ****P<0.0001 compared to sh-control by one-way ANOVA followed by Post-Hoc tests (A) or by student's t-test (B and C).

4.2.10 The effects of acute acetate treatment on PGC-1α and UCP1 expression in differentiated brown adipocytes

In parallel, the effect of acute acetate treatment on gene expression in mature brown adipocytes was determined. The IM-BAT cells were differentiated as described above and then treated with 10 mM acetate for 6 h. As shown in figure 4-14, acute acetate treatment (6 h) on differentiated IM-BAT cells also significantly increased PGC-1α and UCP1 transcription. Meanwhile, as positive control, CL-316,243 also elicited dramatically increase in both PGC-1α and UCP1 transcription (figure 4-14)

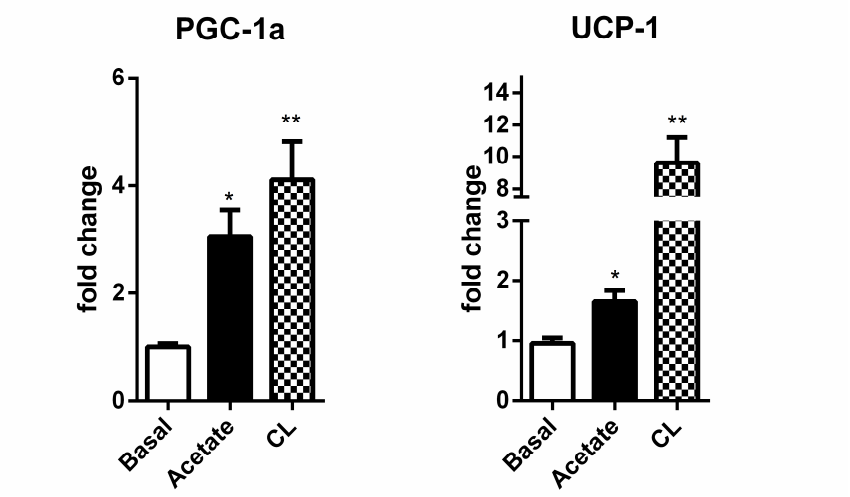

Figure 4-14 Effects of acute acetate treatment on PGC-1α and UCP1 expression in differentiated IM-BAT cells. IM-BAT cells were differentiated for 7 days followed by acetate treatment (10 mM) for 6 h. β-adrenergic receptor agonist CL-316,243 (CL) was used as positive control. The expression levels of PGC-1α and UCP1 were determined by real-time PCR. Data are presented as mean ± S.E.M.. *P <0.05, **P<0.01 by student's t-test compared with no acetate treated controls.

4.2.11 The effects of acetate administration on brown adipose tissue *in vivo*

Moreover, we also examined the effects of acetate on the expression of two thermogenesis-related genes (PGC-1α and UCP1) in brown adipose tissue *in vivo*. The results demonstrated a significant increase in PGC-1α after 6 weeks acetate administration (figure 4-15 (A)), while the increase in UCP1 expression just failed significance (figure 4-15 (B)), which might suggest the control of UCP1 expression *in vivo* is more complex than *in vitro.*

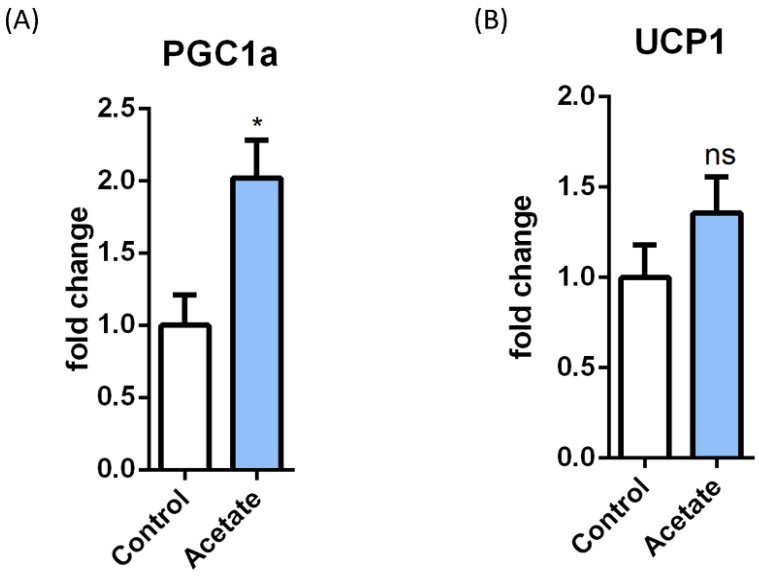

Figure 4-15 Effects of acetate administration on PGC-1α and UCP1 expression in interscapular brown adipose tissue of C57BL/6J male mice. C57BL/6J male mice were fed with sodium acetate (150 mM) in drinking water for 6 weeks (n = 5 for control, n = 5 for acetate administration). Mice were sacrificed at week 12. The expression levels of **PGC-1α** (A) and **UCP1** (B) were determined by real-time PCR. Data are presented as mean ± S.E.M.. *P <0.05 compared to control by student's t-test.

4.3 Discussion

So far, it has been discovered that plenty of transcription factors are involved in the regulation of adipogenesis. Among these transcription factors, the nuclear receptor PPARγ is a key player in transcriptional cascade during adipocyte differentiation (Siersbaek et al., 2010). Previous studies have demonstrated that PPARγ is a master regulator of adipogenesis, ectopic overexpression of PPARγ in non-adipogenic 3T3 fibroblasts cells leads to their differentiation into adipocytes with the accumulation of lipid droplets and the induction of adipogenic marker genes expression, such as C/EBPα, aP2, and GLUT4 (Hamm et al., 1999); while overexpression of PPARγ in adipogenic 3T3-L1 preadipocytes leads to increased lipid accumulation and up-regulation of adipocyte markers (Tamori et al., 2002). Furthermore, no additional factors have been found to induce adipogenesis in the absence of PPARγ (Rosen and MacDougald, 2006). In mice, PPARγ is not only critical for adipogenesis but also important for the maintenance of the fully differentiated state. However, PPARγ could not induce adipogenesis alone *in vivo* (Bastie et al., 1999). Transcription co-activators, such as C/300, PGC-1α, also mediate the activities of PPARγ *in vivo*. Among them, PGC-1α has been identified as a key molecule that stimulates brown adipocytes differentiation by interacting with PPARγ and direct gene transcription involved in both adipogenesis and mitochondrial biogenesis (Puigserver et al., 1998). Increased PGC-1α enhances the transcription of NRF-1 and NRF-2, leading to increased expression of mtTFA (Wu et al., 1999a), as well as other nuclear-encoded mitochondria subunits of the electron transport chain complex (e.g. β-ATP synthase, cytochrome c, and cytochrome c oxidase IV)

(Scarpulla, 2011). mtTFA translocates to the mitochondrion and stimulates mitochondrial DNA replication and gene expression (Larsson et al., 1998). PGC-1α also interacts with PPARγ or other nuclear hormone receptors in brown adipocytes to up-regulate the expression of brown fat-specific UCP1 (Cassard-Doulcier et al., 1994, Barbera et al., 2001). Moreover, ectopic expression of PGC-1α in white fat cells also induces expression of mitochondrial and thermogenic genes (Puigserver et al., 1998, Tiraby et al., 2003). Our results showed that increased PGC-1α and PPARγ expression, as well as increased mitochondrial mass and UCP1 expression were observed after acetate treatment in brown adipocytes, supporting the importance of PGC-1α in brown adipocyte differentiation. Based on these findings, it could be hypothesized that dietary supplementation of acetate or fibre could potentially promote brown adipose tissue by increasing the amount and/or activity of PGC-1α in brown adipose tissue, thus offering an additional target for the treatment of obesity and related metabolic diseases. Indeed, Gao et al., have demonstrated that dietary supplementation of butyric acid increase brown adipose energy expenditure in mice (Gao et al., 2009). However, further studies are needed to address this hypothesis.

Notably, PRDM16 activity is mainly mediated through protein stabilization by PPARγ in brown adipogenesis (Ohno et al., 2012), which might be another possible reason that little change of PRDM16 at transcription level was observed.

During the adipogenesis, pre-adipocyte undergoes post confluent mitosis, growth-arrest, morphology change and lipid droplets accumulation, all of

which induce the change of cell shape, adhesion, and mobility. However, traditional measurements have plenty of limitations to observe these changes continuously and in real-time. Recently, the xCELLigence system, which could measure the electrical impedance of gold sensing electrode underneath the cultured cell layer has been reported to successfully monitor the differentiation process of 3T3-L1 cells *in vitro*. Compared to the traditional ways (such MTT assay or Boyden Chamber Assays) to measure cell proliferation, invasion or migration, the biggest advantage of xCELLigence system is providing a way to monitor cell proliferation, invasion or migration and cell morphology changes in real-time. Besides, xCELLigence system is a label-free cellular analysis assay, which minimizes the effects of exogenous labels on cell growth and differentiation. Therefore, xCELLigence system can capture data throughout the entire time course of adipogenesis and reflect more physiologically relevant data. Here, we applied this system to observe brown adipocyte differentiation with different compounds treatment. Compared to the results from Kramer *et al.*, that treatment with a similar differentiation cocktail (containing insulin, IBMX, Dexamethasone, and Rosiglitazone) leads to rapid drop of *CI* curve of 3T3-L1 adipocytes (Kramer et al., 2014), a similar *CI* curve was also observed after IM-BAT being treated with *differentiation medium I* containing insulin, IBMX, Dexamethasone, and T3 in our study. Kramer *et al.* have further established that among the components of the full differentiation cocktail, treatment with IBMX is crucial to result in significant decrease of *CI* values, indicating that IBMX mainly mediates the morphological change of 3T3-L1 during the differentiation (Kramer et al., 2014). Our results are also in accordance with

this finding, since increased *CI* value was observed after the incubation with *differentiation medium II*, which does not contain IBMX. In addition, our results also demonstrated that acetate treatment could keep the *CI* value at lower levels compared to normal differentiated cells. Based on the previous data from 3T3-L1 cells, documenting that the most efficient differentiation caused by full differentiation cocktail results in the most decreased *CI* value, our results indicate that acetate promotes the differentiation of IM-BAT cells (decreased *CI* value). Meanwhile, using MTS assay, no significant difference of cell viability was observed between groups. This result strongly suggested that the changes of *CI* values after acetate treatment attribute more to the morphological shifts of IM-BAT cells instead of the difference of cell numbers. Taken together, the evidence gathered here imply IM-BAT undergo morphological shifts during the differentiation, which share high levels of similarity to that in white adipocytes, and acetate treatment could affect this process.

Since the mitochondria are key organelle for the main function of brown adipocytes (thermogenesis), therefore, functional mitochondrial measurements are useful for understanding brown adipocytes differentiation and metabolism profiles. Here, using Seahorse XF24 Analyser with XF Cell Mito Stress Test Kit, we assessed the key parameters of mitochondria in brown adipocytes differentiated with acetate. The results showed an increase in basal and maximum respiration, which is consistent to the results that increased mitochondria mass were achieved after acetate treatment during adipogenesis in IM-BAT cells.

Interestingly, the pro-adipogenic effect of short-chain fatty acids was not only found in murine adipocytes (3T3-L1), it has also been demonstrated in porcine adipose tissue that short-chain fatty acids enhance adipocyte differentiation (Li et al., 2014), suggesting pro-adipogenic effect of short-chain fatty acids might widely exits in many species, which probably indicates short-chain fatty acids could also stimulate brown adipogenesis in human, however, more clinical trials are needed to support this hypothesis.

Furthermore, we also sought to determine the effects of administration of acetate on brown adipose tissue in C57BL/6 mice. Although immortalized adipocyte cell lines provided numerous advantage for adipose tissue research, which eliminate the frequent need to re-establish fresh cultures from adipose tissue and provide a consistent homogeneity in cellular population and differentiation stage, however, during the establishment of immortalized cell lines, oncogenes such as simian virus 40 large T antigen are introduced into primary cells to overcome the normal cell cycle control points, which will inevitably affect the biological properties of normal cells. Therefore, although clonal cell lines are an important complementary tool to animal models for the study of adipocytes functions, but it still could not totally replace *in vivo* experiments to investigate brown adipose tissue functions.

Besides, as a key organ involved in the control of energy homeostasis, brown adipose tissue not only responses to the changes of energy and nutritional status by itself alone, but also incorporates all the signals from other tissue in whole body (Lee et al., 2014). Therefore, it is also worth to

investigate the function of acetate *in vivo*. Here, we deliver acetate *via* drinking water instead of traditional intravenous injection. It has been demonstrated that addition of acetic acid in drinking water can deliver acetate into circulation and significantly affects insulin sensitivities of white adipose tissue and muscle and liver *in vivo* (Kimura et al., 2013). Compared to intravenous injection, oral administration is a convenient, self-administered, and pain free route of drug administration.

It has been reported that short-chain fatty acids butyrate, an agonist for GPR43, also increase adaptive thermogenesis, mitochondrial biogenesis, and UCP-1 expression in brown adipose tissue *in vivo* (Gao et al., 2009). Meanwhile, Bjursell *et al.*, reported HFD-fed GPR43 knock-out mice demonstrated decreased lipid droplets in brown adipose compared to HFD-fed WT mice (Bjursell et al., 2011). These evidence highlights the possible role of GPR43 in brown adipose tissue. Here our findings also support the existence of GPR43 in brown adipose tissue and the possible roles for adipogenesis.

Notably, acetate treatment has been demonstrated different effects on immune system in different type of mice. For example, enhanced polyclonal antibody responses were observed in C57BL/6 mice treated with acetate (single intraperitoneal administration, 5 mg per mouse), but not in DBA/2 mice with the same treatment (Ishizaka et al., 1990). Therefore, the effects of acetate treatment on brown adipose tissue are also worth to be investigated in other models in future, which would provide better understanding towards the possible benefit of acetate administration.

Besides, most studies also revealed the protective effects of short-chain fatty acids in mice models under HFD conditions (Puddu et al., 2014, den Besten et al., 2015), which also indicated the effects of short-chain fatty acids on brown adipose tissue might be more significant when challenged by high-fat diet. However, this hypothesis also needs more evidence to support.

Chapter 5: The effects of acetate treatment on signal transduction pathways in brown adipocytes

5.1 Preamble

Protein kinases are a family of enzymes performing post-translational modification in cells, which are involved in almost all cellular processes. Protein kinases can transfer phosphate groups from ATP to their targets (normally proteins or peptides), thereby regulating the activity, localization, or other functions of the targets (Hunter, 1995, Adams, 2001). This reaction is also known as phosphorylation. Protein kinases mediated phosphorylation provides a rapid and reversible mechanism by which extracellular signals regulate intracellular responses, which in particular plays crucial roles in a wide range of cellular signalling (Cohen, 2000, Adams, 2001). Analysing the phosphorylation profiles of kinases and their protein substrates can provide important information for understanding how cells recognize and respond to extracellular stimulus (Zhong et al., 2007). Phospho-specific antibodies and mass spectrometry are both valuable tools for detection and characterization of the status of phosphoproteins (DiGiovanna et al., 2002, Salih, 2005).

GPCRs transduce a range of downstream signalling, of which the majority were mediated by kinases, such as PKA and PKC, which are the most well-known protein kinase enzymes regulated by $G\alpha_s$-, $G\alpha_{(i/o)}$- or $G\alpha_q$-coupled GPCRs, respectively (Tuteja, 2009). Protein kinases are also crucial for turning off excessive GPCRs signalling. G protein-coupled receptor kinases (GRKs) phosphorylate intracellular domains of GPCRs to recruit β-arrestin and prevent reassocitation of GPCRs with G-proteins (Ritter and Hall, 2009). β-arrestin desensitizes GRK-phosphorylated GPCRs, and causes the internalization of receptors (Pierce and Lefkowitz, 2001).

Previous studies have shown that GPR43 activation by short-chain fatty acids elicits activation of various protein kinases and phosphorylation of a range of protein substrates in different types of cells. For example, using HEK293 cells expressing GPR43, it has been demonstrated that activation of GPR43 leads to the activation of all major MAPK signalling pathways including ERK1/2, p38 and JNK (Seljeset and Siehler, 2012). Furthermore, evidence also suggested that phosphorylation of p38 is required for the anti-proliferitic effect of GPR43 in human breast cancer cell line MCF-7 and GPR43-induced neutrophilic granulocytes migration (Yonezawa et al., 2007, Sina et al., 2009). It has also been reported that short-chain fatty acids mediate CREB phosphorylation. For example, short-chain fatty acids up-regulate TH transcription *via* ERK-dependent activation of CREB (Shah et al., 2006).

Since p38, ERK1/2, CREB and Akt have been identified as key signalling pathways in adipogenesis process (Engelman et al., 1998, Reusch et al., 2000, Park et al., 2014), therefore, it is worthy to investigate the effects of acetate treatment on phosphorylation profiles of kinases and their targets in brown adipocytes, which can provide useful information for understanding the roles of acetate in brown adipogenesis.

Proteome Profiler phospho-kinase array utilized in our assays is based on the sandwich immunoassay principle. Instead of checking the relative site-specific phosphorylation of kinases by performing numerous immune-precipitations and Western blots, the Proteome Profiler phospho-kinase array detects the relative levels of phosphorylation of 43 kinase phosphorylation

sites in one assay, therefore providing a high-throughput way for detecting phosphorylation profiling semi-quantitatively.

Furthermore, there is another benefit of using Proteome Profiler phospho-kinase array since all the target proteins spotted on the membrane can be validated by phospho-specific antibodies. For example, Western bolts using phospho-specific antibodies can be applied to further determine the time-course of target protein(s) phosphorylation after acetate stimulation.

In addition, kinase inhibitors targeting various nodes of signalling pathways may also assist in elucidating the mechanisms involved in acetate-induced signalling pathways in brown adipocytes.

5.2 Results

5.2.1 Screening phospho-kinase activities after acetate stimulation in differentiated IM-BAT cells

Because phosphorylation is fundamental to many aspects of cell signalling, Proteome Profiler phospho-kinase array were applied to determine the signalling pathways activated following acetate exposure in brown adipocytes. The differentiated IM-BAT cells were treated with acetate for 10 min before lysed by lysis buffer. The lysate was incubated with Array membranes spotted with capture antibodies. The levels of phosphorylated proteins were detected by chemiluminescence. As shown in figure 5-1, of all 43 phospho-proteins interrogated in parallel, the phosphorylation of ERK1/2 and the phosphorylation of CREB (S133) increased by ~2.0 fold and ~2.6

fold vs. untreated cells, respectively, after 10 mM acetate treatment for 10 min in differentiated brown adipocytes, suggesting increased activation of these two kinases by acetate. In contrast, one spot on the membrane (Akt 1/2/3 (S473)) showed a clear decreased signal after acetate treatment, indicating acetate treatment might decrease Akt 1/2/3 phosphorylation at Ser473 in IM-BAT cells.

(A)

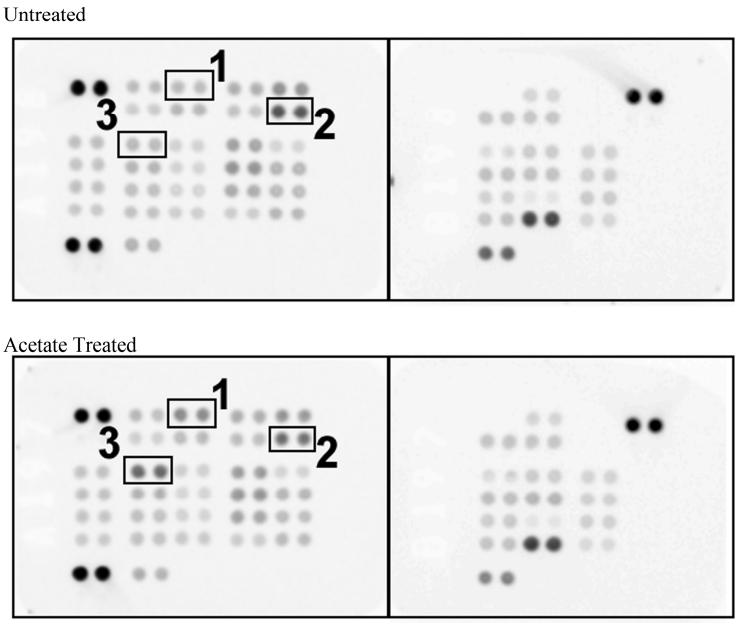

(B)

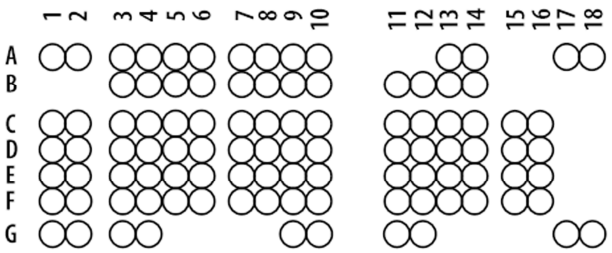

(C)

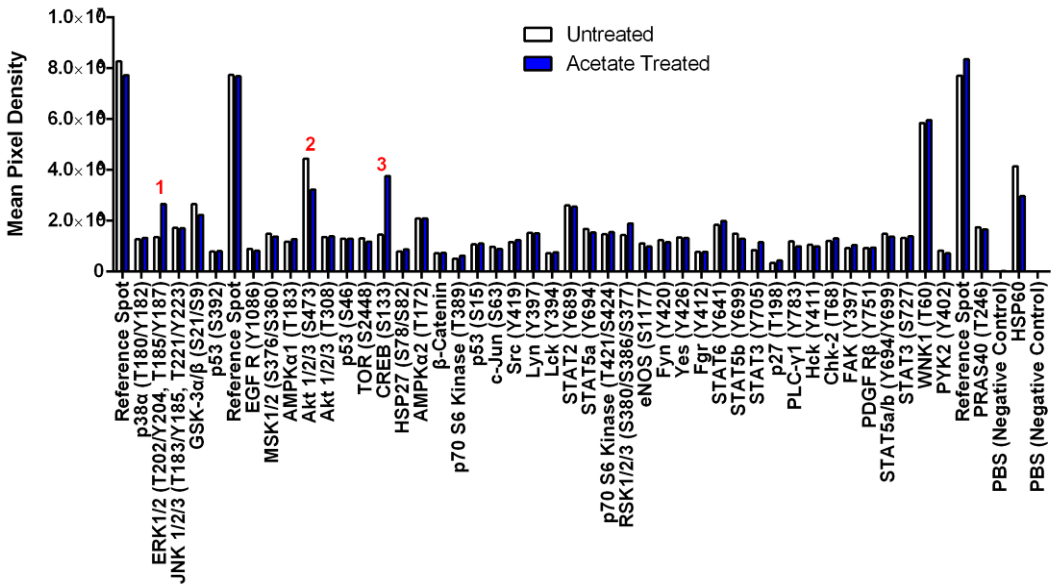

Figure 5-1 Screening protein kinase activated by acute acetate treatment in IM-BAT cells by phospho-kinase array. (A) **The effects of acetate treatment on phosphorylation of 43 protein kinase phosphorylation sites in IM-BAT cells determined by phospho-kinase array**. Differentiated immortalized BAT (IM-BAT) cells were either left untreated or treated with acetate for 10 minutes. Site-specific phosphorylation of 43 kinases were analysed by R&D Proteome Profiler Phospho-Kinase Array Kit. Data are presented as mean ± S.E.M. (B) **Phospho-Kinase Array Layout.** The location of controls and targets are listed in the table 5-1 below. (C) **Relative change in phosphorylated kinase proteins between control and acetate-treated samples.** Pixel density of the pair of duplicate spots representing phosphorylated kinase protein were quantified and subtracted the signal of negative control spots.

Table 5-1 Layout of Phospho-Kinase Array

Membrane/ Coordinate	Target/Control	Phosphorylation Site
A-A1, A2	Reference Spot	
A-A3, A4	p38α	T180/Y182
A-A5, A6	ERK1/2	T202/Y204, T185/Y187
A-A7, A8	JNK 1/2/3	T183/Y185, T221/Y223
A-A9, A10	GSK-3α/β	S21/S9
B-A13, A14	p53	S392
B-A17, A18	Reference Spot	
A-B3, B4	EGF R	Y1086
A-B5, B6	MSK1/2	S376/S360
A- B7, B8	AMPKα1	T183
A-B9, B10	Akt 1/2/3	S473
B-B11, B12	Akt 1/2/3	T308
B-B13, B14	p53	S46
A-C1, C2	TOR	S2448
A-C3, C4	CREB	S133
A-C5, C6	HSP27	S78/S82
A-C7, C8	AMPKα2	T172
A-C9, C10	β-Catenin	
B-C11, C12	p70 S6 Kinase	T389
B-C13, C14	p53	S15
B-C15, C16	c-Jun	S63
A-D1, A2	Src	Y419
A-D3, A4	Lyn	Y397
A-D5, A6	Lck	Y394
A-D7, A8	STAT2	Y689
A-D9, A10	STAT5a	Y694
B-D11, D12	p70 S6 Kinase	T421/S424
B-D13, D14	RSK1/2/3	S380/S386/S377
B-D15, D16	eNOS	S1177
A-E1, A2	Fyn	Y420
A-E3, A4	Yes	Y426
A-E5, A6	Fgr	Y412
A-E7, A8	STAT6	Y641
A-E9, A10	STAT5b	Y699
B-E11, D12	STAT3	Y705
B-E13, D14	p27	T198
B-E15, D16	PLC-γ1	Y783
A-F1, A2	Hck	Y411
A-F3, A4	Chk-2	T68
A-F5, A6	FAK	Y397
A-F7, A8	PDGF Rβ	Y751
A-F9, A10	STAT5a/b	Y694/Y699
B-F11, D12	STAT3	S727
B-F13, D14	WNK1	T60
B-F15, D16	PYK2	Y402
A-G1, G2	Reference Spot	
A-G3, G4	PRAS40	T246
A-G9, G10	PBS (Negative Control)	
B-G11, G12	HSP60	
B-G17, G18	PBS (Negative Control)	

5.2.2 Acetate treatment regulated ERK1/2 and CREB activation on differentiated IM-BAT cells

To further determine the time-course of ERK1/2 phosphorylation and CREB activation in IM-BAT cells after acetate stimulation, IM-BAT cells were treated with 10 mM of acetate from 5 to 60 min before cells were lysated with RIPA lysis buffer. The cells without acetate treatment were used as control. The ERK1/2 and CREB phosphorylation were analysed by Western blots and normalized to ERK1/2 and CREB expression, respectively.

In agreement with results from phosphor-kinase array, ERK1/2 phosphorylation increased within 5 min after acetate treatment and sustained at high levels for 30 min (figure 5-2 (A)). Furthermore, we also observed that CREB phosphorylation increased starting from 5 min and kept at peaking level at 10 min post stimulation (figure 5-2 (B)).

It has been well-established that activation of CREB enhances PGC-1α expression in a CREB-dependent manner (Wu et al., 2002). Therefore, these data consistently suggest that ERK1/2 and CREB were activated by acetate and that their activation may contribute to the increase in PGC-1α activity.

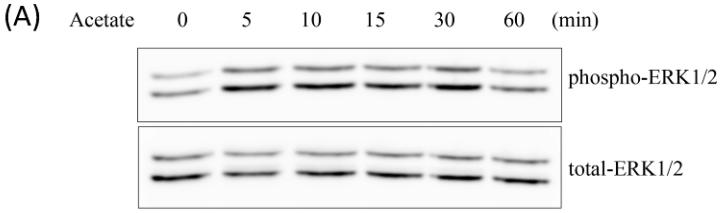

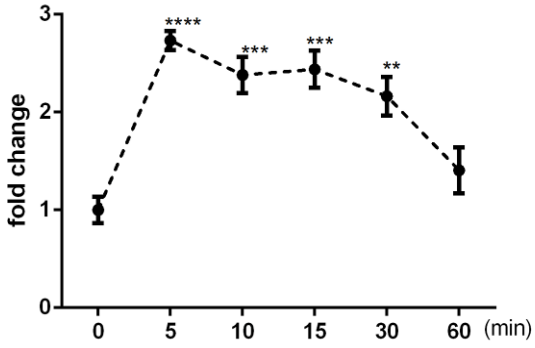

(B)

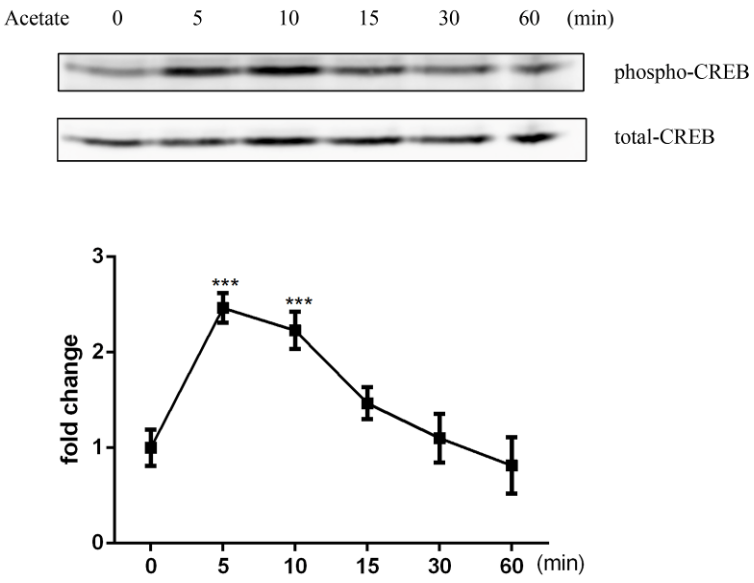

Figure 5-2 The time-course of ERK1/2 and CREB activation following treatment with acetate in IM-BAT cells. (A) **Time-course of ERK1/2 activation following treatment with acetate in IM-BAT cells.** Differentiated IM-BAT cells were either left untreated or treated with acetate for 5, 10, 15, 30 and 60 minutes. (B) **Time-course of CREB activation following treatment with acetate in IM-BAT cells.** Differentiated IM-BAT adipocytes were either left untreated or treated with acetate for 5, 10, 15, 30 and 60 minutes. Data are presented as mean ± S.E.M.. **P <0.01, ***P<0.001, ****P<0.0001 compared to control by one-way ANOVA followed by Post-Hoc tests.

5.2.3 4-CMTB stimulation evoked ERK1/2 and CREB activationin in differentiated IM-BAT cells

Similarly, we also treated differentiated IM-BAT cells with 4-CMTB (1 μM), a selective agonist for GPR43, and measured the phosphorylation of ERK1/2 and activation of CREB upon stimulation.

As shown in figure 5-3 (A), 4-CMTB treatment also elicited the phosphorylation of ERK1/2 in differentiated brown adipocytes from 5 min post-stimulation, which was similar to the effects of acetate treatment on ERK1/2 activation in IM-BAT cells.

Likewise, 4-CMTB induced phosphorylation of CREB at Ser133 was also observed from 5 min, with a peak at 10 min post-stimulation, in differentiated IM-BAT cells (figure 5-3 (B)).

Since 4-CMTB is specific for GPR43 over GPR40 and GPR41, these results also consistently support the hypothesis that GPR43, not GPR41, is mainly involved in acetate-mediated effects in IM-BAT cells.

(A)

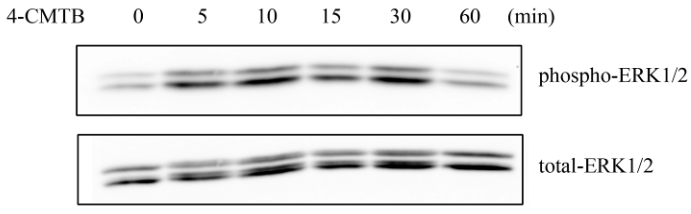

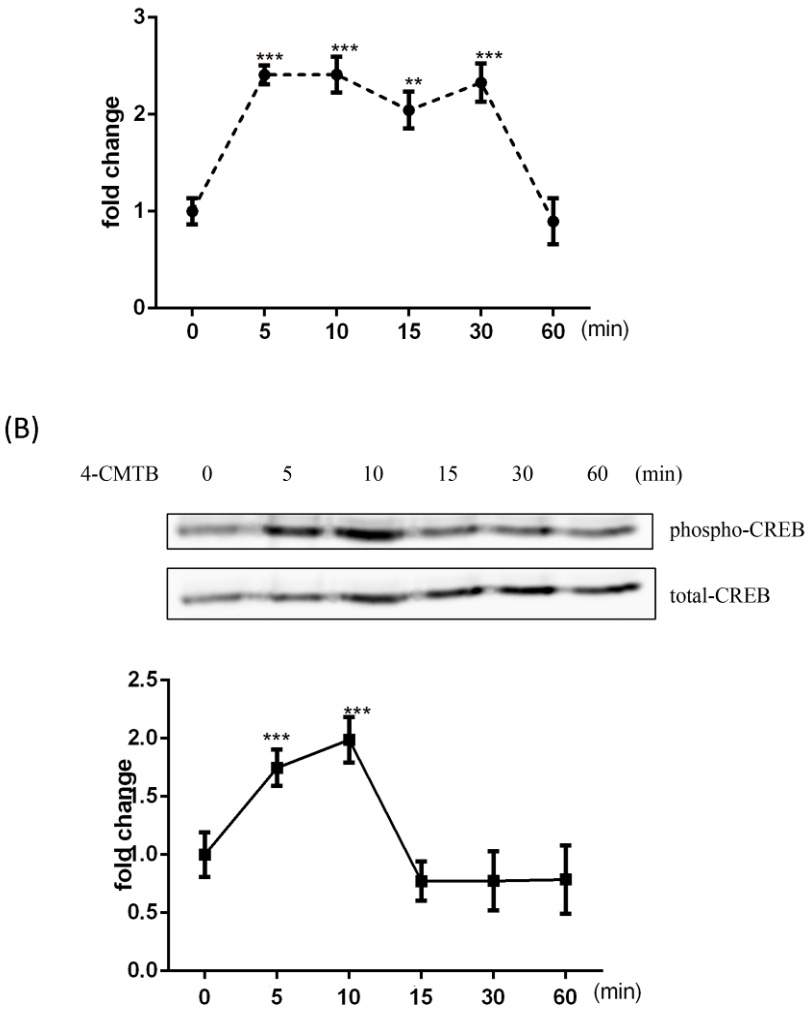

Figure 5-3 The time-course of ERK1/2 and CREB activation following treatment with 4-CMTB in IM-BAT cells. (A) **Time-course of ERK1/2 activation following treatment with 4-CMTB in IM-BAT cells.** Differentiated IM-BAT cells were either left untreated or treated with 4-CMTB for 5, 10, 15, 30 and 60 minutes. (B) **Time-course of CREB activation following treatment with 4-CMTB in IM-BAT cells.** Differentiated IM-BAT adipocytes were either left untreated or treated with 4-CMTB for 5, 10, 15, 30 and 60 minutes. Data are presented as mean ± S.E.M.. **P <0.01, ***P<0.001 compared to control by student's t-test.

5.2.4 Knock-down of GPR43 impaired acetate induced activation of ERK1/2 and CREB in brown adipocytes

To further assess the roles of GPR43 in acetate-mediated downstream signalling pathways in brown adipocytes, we also examined the effects of impaired GPR43 expression on acetate induced ERK1/2 and CREB activation.

IM-BAT cells expressing GPR43 shRNA were differentiated as described above and treated with acetate (10 mM) for 5 – 60 min. While the stimulatory effects of acetate on ERK1/2 and CREB activation have been observed in brown adipocytes, these effects were impaired in cells transfected with shRNA for GPR43 (figure 5-4 (A)).

Similarly, although 4-CMTB has been shown to enhance ERK1/2 and CREB phosphorylation in IM-BAT cells, there was no such stimulation in IM-BAT cells in which the GPR43 gene had been knocked-down by shRNA (figure 5-4 (B)).

These results also consistently support the hypothesis that GPR43, and not GPR41, is mainly involved in acetated mediated ERK1/2 and CREB activation in IM-BAT cells.

(A)

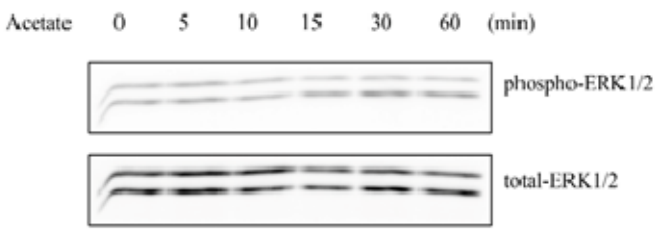

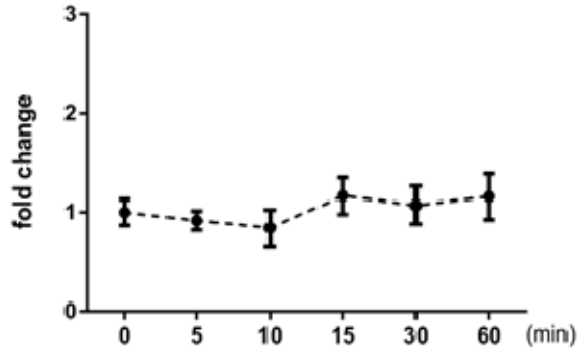

(B)

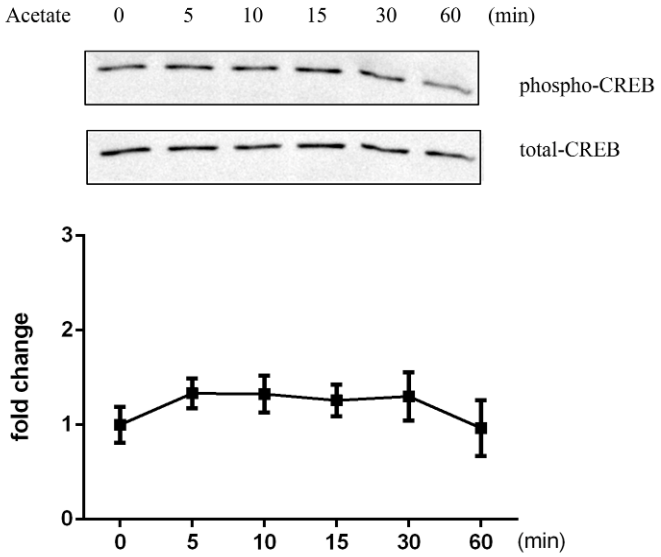

Figure 5-4 The time-course of ERK1/2 and CREB activation following treatment with acetate in IM-BAT cells stable transfected with GPR43 shRNA. (A) **Time-course of ERK1/2 activation following treatment with acetate in IM-BAT cells stable transfected with GPR43 shRNA.** Differentiated IM-BAT cells were either left untreated or treated with acetate for 5, 10, 15, 30 and 60 minutes. (B) **Time-course of CREB activation following treatment with acetate in IM-BAT cells stable transfected with GPR43 shRNA.** Differentiated IM-BAT adipocytes were either left untreated or treated with acetate for 5, 10, 15, 30 and 60 minutes. Data are presented as mean ± S.E.M..

5.2.5 ERK1/2 activation is required for short-chain fatty acids -induced CREB phosphorylation

Several studies have demonstrated that ERK1/2 is located upstream of CREB (Xing et al., 1996; Impey et al., 1998a). Having defined both ERK1/2 and CREB phosphorylation as consequence of acetate treatment, we sought next to elucidate whether ERK1/2 activation is required for short-chain fatty acid acetate evoked CREB phosphorylation.

For this purpose, U0126, a highly selective inhibitor of both MEK1 and MEK2, was used to block the phosphorylation of ERK1/2. As shown in figure 5-5, although treatment of brown adipocyte with acetate caused the expected increase in both ERK1/2 and CREB phosphorylation, acetate treatment was unable to induce CREB phosphorylation in cells pre-treated with U0126, while the ERK1/2 phosphorylation was almost completely abolished (figure 5-5). These results indicated that ERK1/2 may be an indispensable mediator of short-chain fatty acid acetate induced CREB phosphorylation.

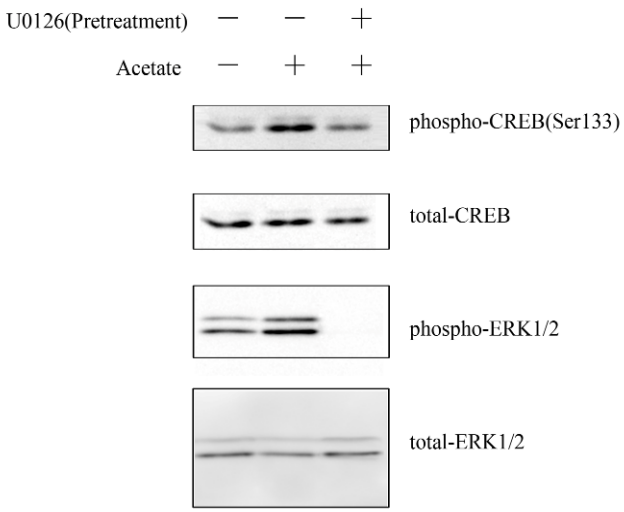

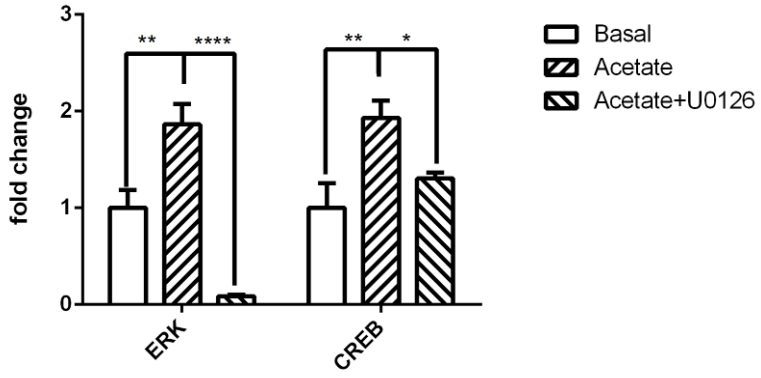

Figure 5-5 The effects of MEK inhibitor (U0126) on acetated induced ERK1/2 and CREB activation in brown adipocytes. Differentiated IM-BAT cells were either left untreated or pre-treated with U0126 followed by treatment with acetate for 15 minutes. Data are presented as mean ± S.E.M.. *P <0.05, **P<0.01, ****P<0.0001 compared to control by one-way ANOVA followed by Post-Hoc tests.

5.2.6 Phosphorylatin of ERK1/2 and CREB is dependent of $G_{(i/o)}\beta\gamma$/PLC/PKC/MEK signalling pathway

Previous research has demonstrated that GPR43 couples to both $G\alpha_q$ and $G\alpha_i$ proteins, which interact with several downstream molecules (including adenylate cyclase, phospholipase C, etc.) (Brown et al., 2003, Stoddart et al., 2008). As shown in figure 5-6, pre-treatment with pertussis toxin (PTX), a $G\alpha_{(i/o)}$-type G protein inactivator, significantly attenuated both ERK1/2 and CREB phosphorylation induced by acetate. It has been reported that $G\alpha_{(i/o)}$ mediates the PLC-PKC-ERK1/2 pathway *via* its βγ subunits (Zhou et al., 2012, Kimura et al., 2013). Therefore, we also examined the effects of pre-treatment with Gallein ($G_{(i/o)}\beta\gamma$ inhibitor), U73122 (PLC inhibitor) on acetate-induced ERK1/2 and CREB activation. Our results showed that acetate-induced CREB activation was effectively blocked by these inhibitors (figure

5-6 (B) & (C)). Taken together, these results suggested $G_{(i/o)}\beta\gamma$/PLC/PKC pathway plays a crucial role in acetate induced ERK1/2 and CREB activation in brown adipocytes.

(A)

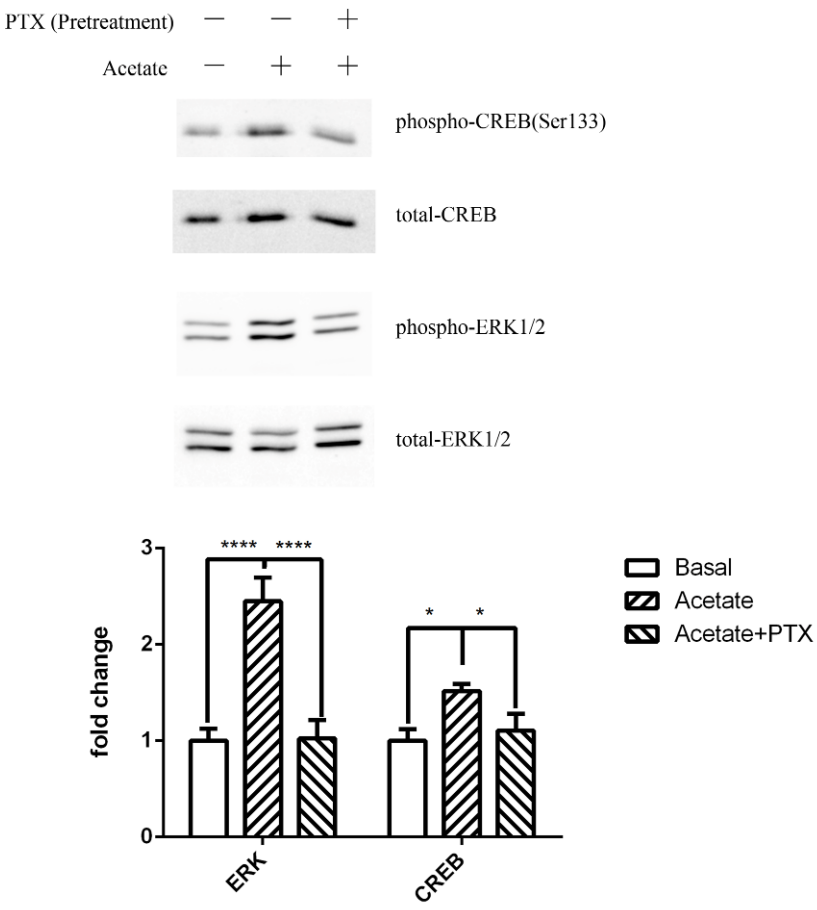

(B)

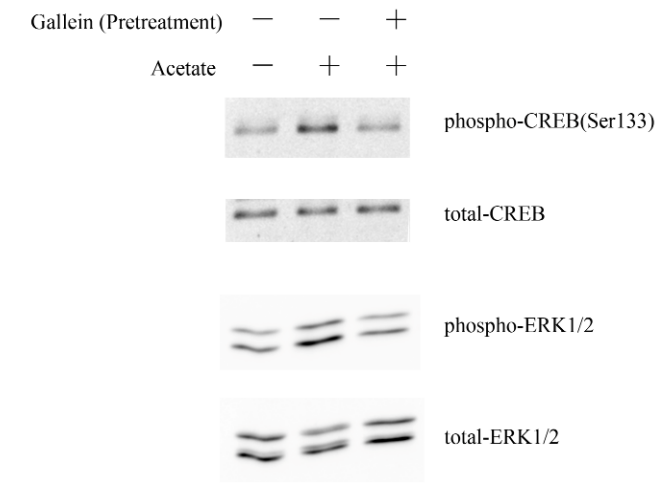
Gallein (Pretreatment) − − +
Acetate − + +
phospho-CREB(Ser133)
total-CREB
phospho-ERK1/2
total-ERK1/2

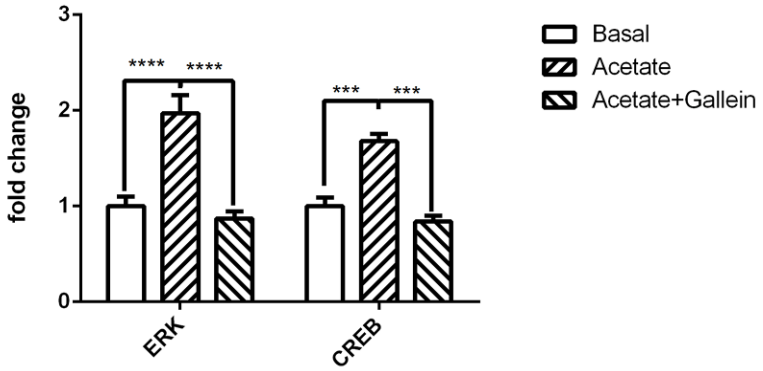
fold change
3
2
1
0
****
****
***
***
ERK
CREB
Basal
Acetate
Acetate+Gallein

(C)

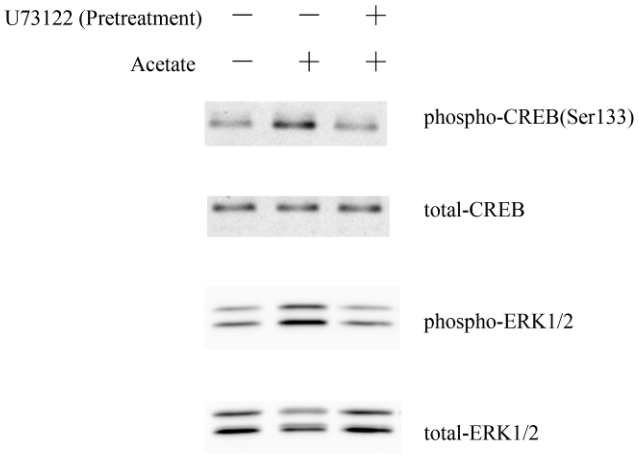
U73122 (Pretreatment) − − +
Acetate − + +
phospho-CREB(Ser133)
total-CREB
phospho-ERK1/2
total-ERK1/2

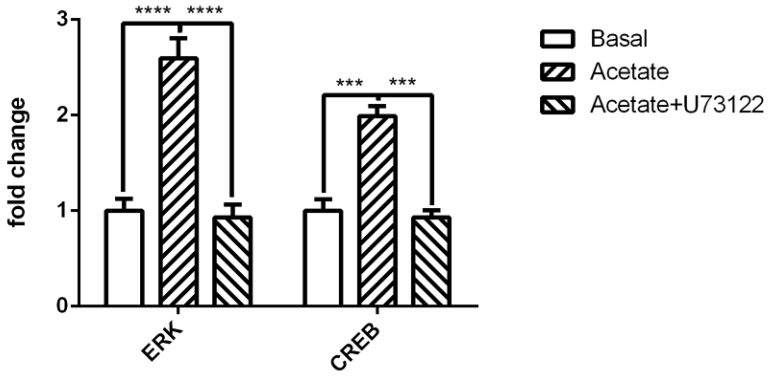

Figure 5-6 The effects of Gαi inhibitor (PTX), Gβγ inhibitor (Gallein), and PLC inhibitor (U73122) on acetated induced ERK1/2 and CREB activation in brown adipocytes. Differentiated IM-BAT cells were either left untreated or pre-treated with **PTX** (A), or **Gallein** (B), or **U73122** (C) followed by treatment with acetate for 15 minutes. Data are presented as mean ± S.E.M.. * P<0.05, ***P<0.001, ****P<0.0001 compared to control by one-way ANOVA followed by Post-Hoc tests.

5.2.7 Acute acetate treatment showed no significant effects on β-adrenergic receptors agonist induced CREB activation

To measure the effects of acute acetate treatment on the brown adipocytes response to thermogenic activator (such as β-adrenergic receptors agonist), especially the effects of acute acetate treatment on β-adrenergic receptors agonist induced the downstream signalling such as CREB, differentiated IM-BAT cells were treated with CL-316,243 with or without acetate for 10 min. The results showed no significant difference in CREB activation was observed (figure 5-7 (A)). We also measured the CL-316,243 induced CREB in GPR43 knocking down cells, the results demonstrated the significant CREB activation was still observed, suggesting β-adrenergic receptor agonist induced cAMP-PKA-CREB activation was not impaired (figure 5-7 (B)).

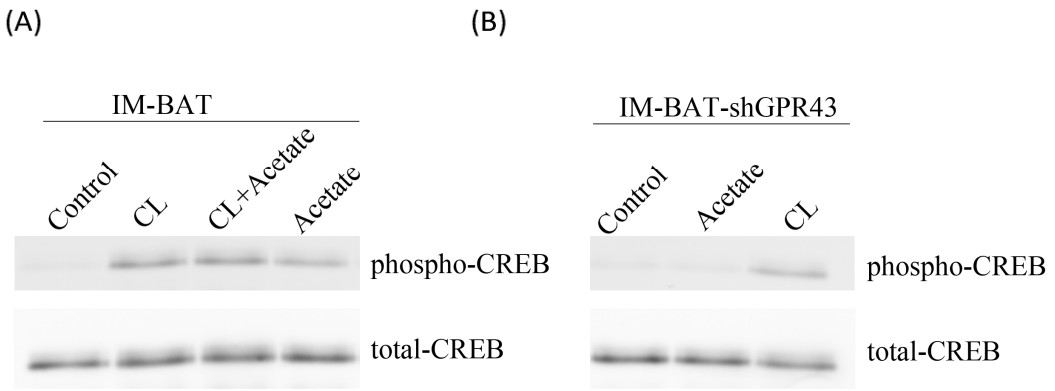

Figure 5-7 The effects of acetate treatment on β-adrenergic receptors agonist induced CREB activation. (A) Differentiated IM-BAT cells were either left untreated or treated with CL-316,234, or acetate, or CL-316,243 together with acetate for 10 minutes. Phospho-CREB and total-CREB were measured by Western blots. (B) Differentiated IM-BAT cells transfected with shGPR43 were either left untreated or treated with CL-316,243 or acetate for 10 minutes. Phospho-CREB and total-CREB were measured by Western blots.

5.2.8 Acetate or 4-CMTB stimulation decreased Akt activation in differentiated IM-BAT cells

It has also been demonstrated by phospho-kinase array that acetate treatment decreased Akt phosphorylation at Ser347. Since Akt signalling pathway is also a key mediator during the adipogenesis in brown adipocytes, therefore, we further confirmed the effects of acetate treatment on Akt activation by Western blots. IM-BAT cells were differentiated and treated with acetate for 15 min. In agreement with results from phosphor-kinase array, acetate treatment significantly decreased Akt phosphorylation (figure 5-8 (A)). Similarly, GPR43 agonist 4-CMTB treatment also elicited a reduction of Akt activation in differentiated IM-BAT cells (figure 5-8(B)).

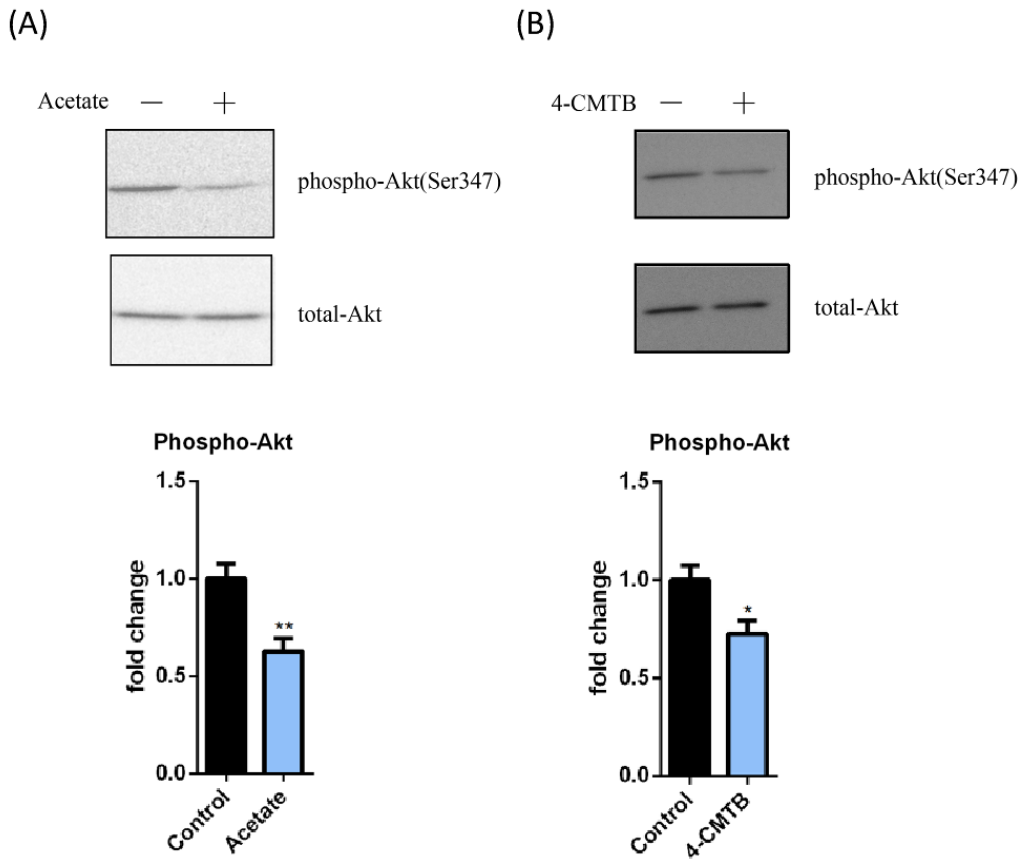

Figure 5-8 The effects of acetate and 4-CMTB treatment on Akt activation in brown adipocytes. (A) Differentiated IM-BAT cells were either left untreated or treated with acetate for 15 minutes. (B) Differentiated IM-BAT cells were either left untreated or treated with 4-CMTB for 15 minutes. Phospho-Akt and total-Akt were measured by Western blots. Data are presented as mean ± S.E.M.. *P<0.05, **P<0.01 compared to control by Student's t-tests.

5.2.9 Acetate treatment increased PTEN phosphorylation in differentiated IM-BAT cells

PTEN, a lipid phosphatase that catalyses the dephosphorisation of PIP3, is a major negative regulator of Akt signalling. It has been shown that PTEN activation positively regulates brown adipogenesis *via* decreasing Akt activity (Ortega-Molina et al., 2012). Interestingly, GPR43 activation was also found

to activate PTEN and inhibit Akt signalling in white adipocytes (Kimura et al., 2013). Therefore, to test the hypothesis that acetate decreases Akt phosphorylation at Ser347 *via* up-regulating PTEN activity, IM-BAT cells were differentiated and treated with acetate for 15 min. The results showed an increase in phosphorylation of PTEN (Ser380/Thr382 /Thr383) after acetate treatment (figure 5-9). In agreement with acetate treatment, 4-CMTB treatment also activated PTEN phosphorylation in IM-BAT cells (figure 5-9), suggesting it is highly possible that GPR43 activation decreases Akt phosphorylation *via* activation of PTEN in brown adipocytes. However, this hypothesis still needs more evidence to support.

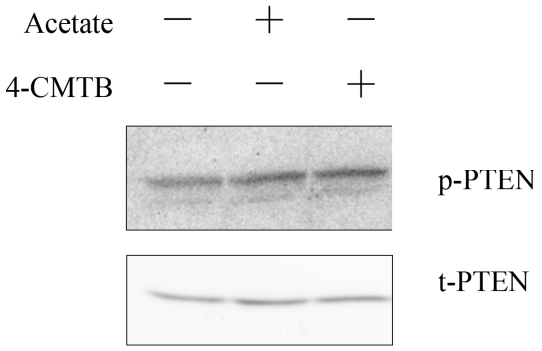

Figure 5-9 The effects of acetate and 4-CMTB treatment on PTEN activation in brown adipocytes. Differentiated IM-BAT cells were either left untreated or treated with acetate for 15 minutes. Phospho-PTEN and total-PTEN were measured by Western blots.

5.3 Discussion

It has been demonstrated by [^{35}S]GTPγS binding assay that GPR43 couples to both $G\alpha_q$ and $G\alpha_i$ G-proteins and affects second messenger molecules such as cyclic AMP and calcium *via* adenylate cyclase and phospholipase C,

respectively (Brown et al., 2003, Stoddart et al., 2008). Besides, it has also been revealed that GPR43 activation leads to downstream signalling pathways, such as PTEN activation, *via* Gβγ subunits, suggesting Gβγ subunits also play important roles in GPR43 functions (Kimura et al., 2013).

Based on the results obtained from phospho-kinase array assay, we found that acetate treatment leads to an increase in ERK1/2 and CREB activation, as well as decreased Akt phosphorylation at Ser473 in brown adipocytes. Furthermore, we also identified that CREB phosphorylation seems to be a consequence of ERK1/2 activation after acetate treatment in differentiated IM-BAT cells, suggesting that MEK1/2 - ERK1/2 is a major mediator of acetate induced CREB phosphorylation in brown adipocytes. This result is in aggreement with previous studies, which demonstrated that ERK1/2 activation is located at upstream of CREB (Xing et al., 1996, Impey et al., 1998).

Since GPR43 couples to both PTX-insensitive $G\alpha_q$ and PTX-sensitive $G\alpha_i$, therefore, using PTX pre-treatment we also explored the involvement of $G\alpha_i$ in the GPR43-regulated downstream signals in brown adipocytes. Here our results demonstrated $G\alpha_i$ is indispensable for ERK and CREB activation induced by acetate treatment *via* GPR43 in brown adipocytes. Previous studies have demonstrated that $G_{(i/o)}\beta\gamma$ mediates the PLC-PKC-ERK signalling pathway (Zhou et al., 2012, Kimura et al., 2013). Our findings also indicated that the $G_{(i/o)}\beta\gamma$ mediated PLC-PKC-ERK signalling pathway is necessary for acetate induced CREB phosphorylation.

Notably, although $G\alpha_q$ is also a classic activator for PLC-PKC signalling pathways, up to date, all GPR43 functions were found to be mediated by $G\alpha_{(i/o)}$ in adipose tissue; only in L cells GPR43 promotes GLP-1 secretion is *via* $G\alpha_q$ (Kimura et al., 2013). Hence, GPR43 might mainly interact with $G\alpha_{(i/o)}$ to exert its functions in adipocytes. Here, due to the limitation of commercial $G\alpha_q$ inhibitor, we did not explore the possibility that $G\alpha_q$ also mediates GPR43 induced PLC-PKC activation. However, based on these evidence, it seems $G\alpha_{(i/o)}$ plays crucial roles for GPR43 mediated ERK-CREB activation.

Besides, it has been well-studied that brown adipocyte differentiation requires activation of CREB-associated pathways (Reusch et al., 2000). Therefore, it is reasonable to infer that ERK/CREB signalling pathways may be the underlying mechanism by which GPR43 receptor exerts its pro-adipogenic effects in brown adipocytes.

Furthermore, it has also been well-documented that activation of CREB leads to increased PGC-1α expression in a CREB-dependent manner (Fernandez-Marcos and Auwerx, 2011). Therefore, our data consistently suggested that ERK1/2 and CREB activation may be the underlying mechanism of the increase in PGC-1α induced by acetate treatment in brown adipocytes.

Interestingly, short-chain fatty acid butyrate was also found to induce phosphorylation of CREB *via* increased the activity of PKA, and elevated the levels of cAMP in Caco-2 cells (Wang et al., 2012). Another study also reported that short-chain fatty acids inhibit growth hormone and prolactin gene transcription *via* cAMP/PKA/CREB signalling pathway in dairy cow

anterior pituitary cells, indicating short-chain fatty acids induced activation of CREB exists in a wide range of cell types (Wang et al., 2013b).

In addition, our results further identified Akt signalling pathway was decreased after acetate treatment. Recently, it has been revealed that PTEN-Akt signalling pathway plays as an important mediator for UCP1 expression in brown adipocytes (Ortega-Molina et al., 2012). Here our results also suggested acetate treatment induced PTEN activation, which might contribute to the increased expression of UCP1 in brown adipocytes.

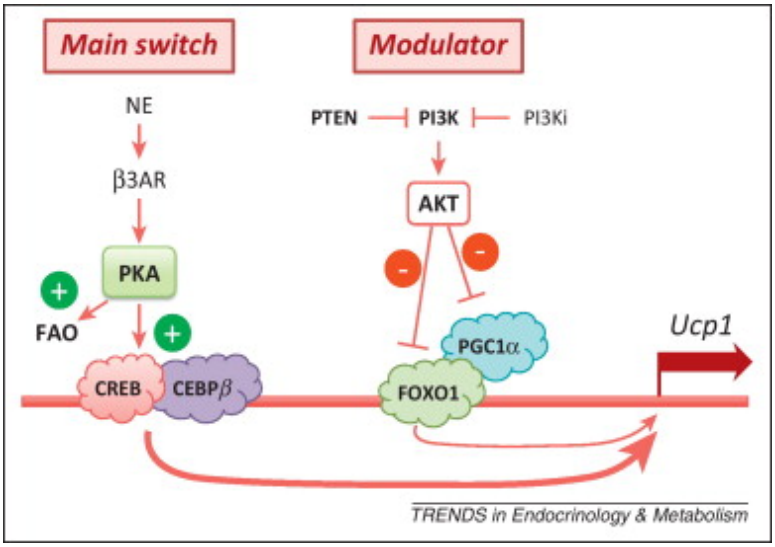

Figure 5-10 Proposed mechanisms of UCP1 transcription regulation in brown adipocytes. The main switch of UCP1 expression is cold induced norepinephrine (NE), which increases protein kinase A (PKA) activity and activates CREB/CEBPβ to elevate the levels of Ucp1 expression. The modulator of UCP1 expression is positively regulated by PTEN, which inhibits PI3K/AKT activity and activate UCP1 positive modulator FOXO1/PGC1α complex. PI3K inhibitors also positively regulate the transcription of UCP1 in this mechanism (Ortega-Molina and Serrano, 2013).

Collectively, using phospho-kinase array, we have successfully identified that several key signalling pathways (including ERK1/2, CREB, Akt) involved in

brown adipogenesis were mediated by acetate treatment. These results may provide useful information to understand underlying mechanism by which acetate exerts it pro-adipogenic effects in brown adipocytes. However, due to the limitation of antibodies spotted on the array, acetate might also elicit activation of other protein kinases. Besides, protein kinases-independent signalling may also mediate the pro-adipogenic effects of short-chain fatty acids. For example, it has been reported that short-chain fatty acids promote adipocyte differentiation *via* inhibiting histone deacetylases (Li et al., 2014). Therefore, more evidence may be needed to elucidate all the responses of brown adipocytes to the short-chain fatty acids treatment.

Chapter 6: The effects of acetate treatment on fatty acids metabolism in brown adipocytes

6.1 Preamble

As another type of adipocytes besides white adipocytes, lipid metabolism is also crucial for brown adipocytes. Free fatty acids released from triglycerides *via* lipolysis can be directly utilized as energy source by β-oxidation in brown adipocytes (Mottillo et al., 2012). Studies have shown that lipolysis-derived fatty acids are the preferred substrates oxidized in brown adipocytes, providing most of the energy to dissipate in the form of heat by UCP1-mediated mitochondrial uncoupling (Wu et al., 2006). Indeed, intracellular lipolysis of triacylglyceride into fatty acids and glycerol is indispensable for thermogenesis in brown adipocytes (Cannon and Nedergaard, 2004).

In respond to cold challenge, sympathetic nervous activity to interscapular brown adipose tissue increases (Kawate et al., 1993). Acute adrenergic stimulation up-regulates fatty acids oxidation in brown adipocytes by increasing lipolysis and enhancing fatty acids into the mitochondria. β-adrenergic receptors activation leads to increased adenylyl cyclase activity and intracellular cAMP level, which further activates PKA and phosphorylates PKA-dependent perilipin as well as hormone-sensitive lipase (HSL) (Kraemer and Shen, 2002). The increased transport of fatty acids into mitochondria after adrenergic stimulation is mainly mediated *via* carnitine palmitoyltransferase (CPT) 1 (Nedergaard and Lindberg, 1979, Kuusela et al., 1986, Zhao et al., 1994, Esser et al., 1996). Notably, up-regulation of fatty acid levels in mitochondria alone would not necessarily increase energy expenditure (Geisler, 2011). Therefore, other mechanisms must also be involved in the effects of adrenergic stimulation on energy expenditure in

brown adipocytes. Adrenergic signalling regulated UCP1 expression and mitochondrial biogenesis are also required for the increasing in thermogenesis (Golozoubova et al., 2006, Mattsson et al., 2011).

Opposite to the lipolysis, lipogenesis and triglyceride synthesis (fatty acids esterification) mediate triglyceride storage in adipocytes. Although brown adipocytes have ability to synthesize triacylglyceride from *de novo* lipogenesis using glucose, however, circulating chylomicron- and very-low-density lipoprotein (VLDL)-bound triacylglyceride are the major source of fatty acids incorporated into brown adipocytes. Since triglycerides can not cross cell membranes, triglycerides in the circulation must be break down into free fatty acids and glycerol before entering into adipocytes. Lipoprotein lipase (LPL) breaks down triglycerides carried by chylomicron and VLDL and provides fatty acids for brown adipose tissue. Cold stimulation dramatically increase LPL activity *via* downregulation angiopoietin-like 4 (ANGPTL4) and provides more plasma triglyceride-derived fatty acids for non-shivering thermogenesis in brown adipose tissue (Dijk et al., 2015). Fatty acid transport protein 1 (FATP1), an integral transmembrane fatty acid transporter, is also crucial for fatty acids uptake and thermogenesis in brown adipose tissue. Cold stimulation or adrenergic stimulation also upregulates FATP1 expression, thus increasing cellular uptake of free fatty acids for non-shivering thermogenesis. Since brown adipose tissue has great ability to uptake circulating triglyceride, therefore, brown adipose tissue activity is a major factor to mediate plasma triglyceride clearance in rodents (Bartelt et al., 2011).

In brown adipose tissue, glucose uptake is also closely linked to lipid metabolism. Glucose in brown adipocytes can be changed into glycerol-3-phosphate as well as fatty acid (palmitate) for triacylglyceride synthesis *via de novo* lipogenesis. *De novo* lipogenesis is a tightly controlled process in adipose tissue. The abnormal of *de novo* lipogenesis is often liked with a range of metabolic disorders, such as obesity, non-alcoholic fatty liver disease, etc.. Besides, glucose uptake is also crucial for non-shivering thermogenesis in brown adipocytes. Large amounts of glycogen storage are found in brown adipose tissue, which can be utilized during non-shivering thermogenesis to provide necessary energy for sustaining mitochondrial uncoupling (Farkas et al., 1999, Jakus et al., 2008).

Here, we investigated the effects of acute acetate treatment on lipid metabolism in immortalized brown adipocytes, which could provide more useful information to understand the roles of acetate in brown adipocytes metabolism.

6.2 Results

6.2.1 The effects of acute acetate or 4-CMTB treatment on lipolysis in differentiated IM-BAT cells

As shown in figure 6-1, differentiated IM-BAT cells treated with acetate for 3 h showed no significant change on lipolysis compared to cells without treatment. We also test the effects of acetate treatment on white adipocytes 3T3-L1. Similar to previous reports, a significant decrease of lipolysis was

observed after 3 h treatment, indicating acetate may demonstrate different effects on lipolysis in two types of adipocytes.

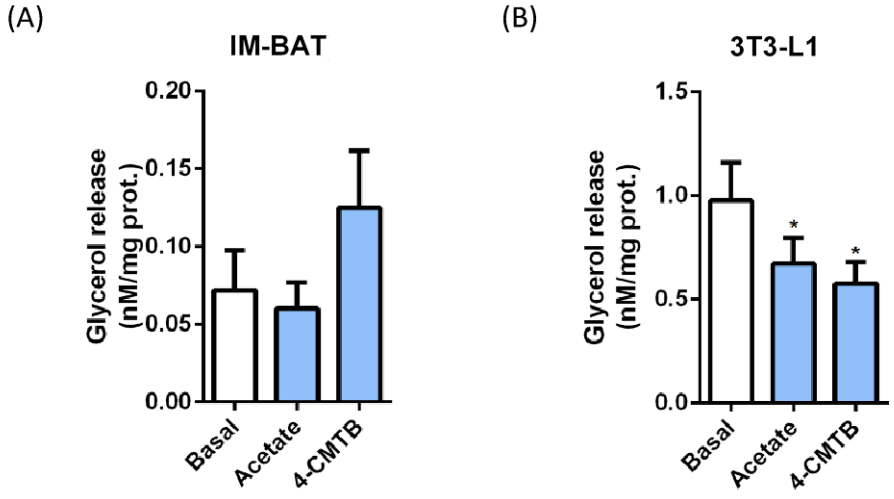

Figure 6-1 The effects of acetate and 4-CMTB treatment on lipolysis in differentiated IM-BAT cells and 3T3-L1 cells. IM-BAT cells and 3T3-L1 cells were differentiated for 7 days and seeded into 96 wells plates at 5 × 10^4 / well. The cells were treated with test compounds for 3 h and the glycerol released was measured by lipolysis assay kit (fluorometric). The protein of adipocytes was measured and used for normalization. Data are presented as mean ± S.E.M. * P <0.05 compared to control by one-way ANOVA followed by Post-Hoc tests.

6.2.2 The effects of acetate or 4-CMTB treatment on fatty acids uptake in differentiated IM-BAT cells

As shown in figure 6-2, the effects of acute acetate or 4-CMTB stimulation on fatty acids (C12:0) uptake were measured by free fatty acid uptake assay kit (ab176768, Abcam). The results demonstrated that differentiated IM-BAT cells treated with acetate or 4-CMTB had significant lower FFA uptake compared to the control adipocytes without treatment in first 20 mins after loading with TF2-C12 fatty acid solution (figure 6-2).

The FFA uptake approached normal level in later phase of experiment in cells treated with acetate. Meanwhile, the significant reduction in FFA uptake remained till 1 h post TF2-C12 fatty acid solution stimulation in 4-CMTB treated cells (figure 6-2).

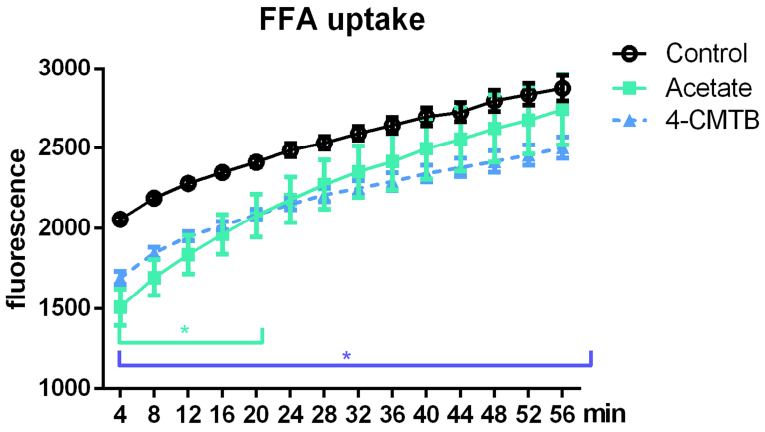

Figure 6-2 The effects of acetate and 4-CMTB treatment on FFA (TF2-C12) uptake in differentiated IM-BAT cells. IM-BAT cells were differentiated for 7 days and seeded into 96 wells plates at 5 × 10^4 / well. The cells were treated with test compounds for 30 min and the FFA uptake was measured by free fatty acid uptake assay kit (fluorometric). Data are presented as mean ± S.E.M.. * P <0.05 compared to control by two-way ANOVA followed by Post-Hoc tests.

6.2.3 The effects of acetate or 4-CMTB treatment on glucose uptake in differentiated IM-BAT cells

As shown in figure 6-3, differentiated IM-BAT cells treated with acetate or 4-CMTB showed no significant changes of fluorescent glucose analog (2-NBDG) uptake compared to the control group after 30 min of treatment, suggesting acute treatment of acetate or 4-CMTB has little effects on glucose uptake *in vitro* (figure 6-3).

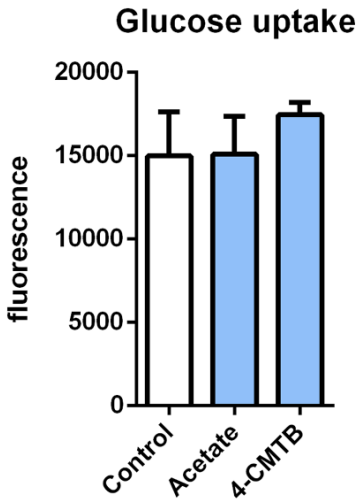

Figure 6-3 The effects of acetate and 4-CMTB treatment on glucose uptake in differentiated IM-BAT cells. IM-BAT cells were differentiated for 7 days and seeded into 96 wells plates at 5 × 10^4 / well. The cells were treated with test compounds for 30 mins and the glucose uptake was measured by glucose uptake assay kit (fluorometric). Data are presented as mean ± S.E.M..

6.3 Discussion

It has been demonstrated that GPR43 activation by short-chain fatty acids leads to a decrease in lipolysis in white adipocytes as well as in white adipose tissue without causing side effects (Ge et al., 2008). Here, as positive control, we also observed this effect in differentiated 3T3-L1 cells. However, in contrast to this anti-lipolytic effect in white adipocytes, no significant effects on lipolysis were observed in differentiated IM-BAT cells. Since the activation of thermogenesis requires increased lipolysis to provide fatty acids as substrates and no thermogenesis can be evoked without activation of lipolysis in brown adipocytes, therefore, our findings suggested acetate treatment might not be an obstacle for brown adipocytes to exert its non-shivering thermogenesis functions.

Also our results showed that differentiated white adipocytes 3T3-L1 have much higher lipolysis-released glycerol than differentiated brown adipocytes. A similar phenomenon was also reported by Klaus et al. that differentiated adipocytes isolated from white adipose tissue from Siberian dwarf hamster released 4 times as much glycerol into the medium as corresponding differentiated adipocytes isolated from brown adipose tissue (Klaus et al., 1995).

Previous studies have suggested that fatty acids with different length are absorbed by distinct routes (Dubikovskaya et al., 2014). Uptake of long-chain fatty acids is regulated by several membrane proteins including fatty acid translocase (FAT)/CD36 (Ehehalt et al., 2008), long-chain fatty acyl-CoA synthetase (LACS) (Schaffer and Lodish, 1994) and fatty acid transport proteins (FATPs) (Schroeder et al., 1998), while short-chain fatty acids (2-4 carbons) and medium-chain fatty acids (6-14 carbons) are absorbed by direct passive diffusion and active transport through a number of transporters including monocarboxylate transporters and sodium-dependent monocarboxylate transporter 1 (den Besten et al., 2013).

Here our results indicated short-chain fatty acids acetate may also influence the medium-chain fatty acids uptake. More interestingly, GPR43 agonist, 4-CMTB, provide a more sustained effects to decrease FFA uptake. The mechanism of this difference is still unclear, which might stem from the different efficacy of 4-CMTB and acetate, or GPR43-independent effects of acetate.

Furthermore, fatty acid sensing GPCRs GPR41/43 and GPR120 have been found to enhance glucose uptake *via* GLUT4 in skeletal muscle and white adipose adipocytes, respectively (Canfora et al., 2015, Oh et al., 2010). These studies hinted the potential crosstalk between fatty acids and glucose uptake (Townsend and Tseng, 2014). Although no significant changes were observed in brown adipocytes after acute acetate treatment, it is interesting to investigate the effects of long-term acetate treatment on GLUT4 expression or translocation. Besides, it is notably that acetate treatment may behave distinctively in cell models and *in vivo*. The effect of rosiglitazone on glucose uptake in brown adipose tissue is a good example of this phenomenon. Although rosiglitazone treatment leads to modest increase in glucose uptake in brown adipocytes (Hernandez et al., 2003), however, rosiglitazone reduces glucose uptake in brown adipose, the detailed mechanism is still unknown. Therefore, it is also interesting to investigate the effects of acetate on glucose tissue *in vivo* in future.

Chapter 7: Conclusion

It has been widely accepted that fatty acids serve not only as energy sources or as constituent of membrane lipids, also as important regulators of cellular signalling and metabolism. Current evidence about the roles of short-chain fatty acids in metabolic regulation has suggested their potential benefits for energy homeostasis, especially upon metabolic challenges such as high fat diet. This thesis aims to investigate the roles of acetate treatment and consequent short-chain fatty acid sensing GPCR(s) activation in the regulation of brown adipocyte differentiation and energy metabolism.

Brown adipose tissue, regarded as an important endocrine organ, has received a lot of attention recently as a potential target to combat obesity. Brown adipose tissue is a metabolically active tissue that contributes to energy expenditure by combustion of fatty acids into heat, a process called thermogenesis. Mitochondria are known to be key functional organelles in brown adipocytes, which mediate the heat dissipation *via* the unique uncoupling protein UCP1 (Golozoubova et al., 2006). Fatty acids not only provide the energy source for this process, but also mediate various aspects of thermogenesis. Since brown adipose tissue has emerged as a novel regulator for energy homeostasis, better understanding the mediating role of fatty acids may provide clues to alleviate metabolic diseases.

Induction of mitochondria biogenesis and UCP1 expression during the maturation of brown adipocytes is important for the normal thermogenic capacity in brown fat. In this research, the effects of acetate on adipogenesis in immortalized brown adipocytes derived from mice interscapular brown adipose tissue were mainly investigated. Several novel outcomes provide

mechanistic insight into the regulation of short-chain fatty acid acetate in the differentiation of immortalized brown adipocytes. Considering the pro-adipogenic property of short-chain fatty acids has also been studied in several white adipocyte models (Hong et al., 2005), our results suggested that short-chain fatty acids might exert their pro-adipogenic effects in both white and brown adipocytes.

To investigate the mechanisms governing the pro-adipogenic effects of acetate in brown adipocytes, the phosphor-kinase activities were screened. Consistence to acetate induced UCP1 expression, ERK-CREB activities were elevated while Akt activity was decreased after acetate treatment. Since it has been suggested that CREB and Akt signalling pathways serve as the main switch and modulator of UCP1 transcription, respectively (Ortega-Molina and Serrano, 2013), these findings strongly suggested that alternation of CREB and Akt activities might be the molecular mechanism underlying pro-adipogenic property of acetate.

Notably, our results also showed a great similarity between the *CI* curve of IM-BAT cells and the *CI* curve of 3T3-L1 cells during differentiation, supporting the idea that *CI* curve could be used as a novel tool to monitor the adipogenesis in real-time, which would provide great benefit for the adipocyte research.

GPR43 has been identified as one of short-chain fatty acids sensing GPCRs. In this study, the expression of GPR43 was analysed in immortalized brown adipocyte cells and interscapular brown adipose tissues of mice. The results confirmed the existence of GPR43 expression in both brown adipocytes and

brown adipose tissue. Moreover, our results also indicated that GPR43 expression levels seems to be rightly linked with the differentiation status of brown adipocytes, suggesting GPR43 might be a novel adipogenic marker in brown adipocytes. Several studies have also demonstrated GPR43 expression was influenced by diet composition and body weight. Diet-induced obesity up-regulated GPR43 expression in multiple tissues including white adipose tissue, liver, and skeletal muscles (Cornall et al., 2011, Dewulf et al., 2011). In contrast, administration of inulin-type fructans in diet lowered the body weight and counteracted HFD-fed induced GPR43 overexpression in white adipose tissue (Dewulf et al., 2011), suggesting GPR43 expression levels might reflect metabolic status in body.

Current evidence about the functions of short-chain fatty acids, especially acetate, in metabolic regulation has suggested GPR43 is an important mediator for short-chain fatty acids exerting their roles in adipose tissue. Previous studies have suggested that GPR43 is dependent for the pro-adipogenic and anti-lipolytic properties of short-chain fatty acids in white adipocytes (Hong et al., 2005). *In vivo* studies also suggested acetate treatment suppressed plasma free fatty acids without inducing the flushing side effect *via* GPR43 (Ge et al., 2008). Furthermore, GPR43 knock-out mice were demonstrated to exhibit obesity, reduced short-chain fatty acids-triggered GLP-1 secretion, impaired systemic insulin sensitivity and a parallel impairment of glucose tolerance while adipose-specific GPR43 transgenic mice were lean and showed enhanced systemic insulin sensitivity (Kimura et al., 2013, Tolhurst et al., 2012). Here, our results also suggested that GPR43

involved in pro-adipogenic effects of short-chain fatty acids. It is noteworthy that GPR43 independent mechanism (inhibiting histone deacetylases) has also been shown to mediate promotive effects of acetate on adipogenesis in white adipocytes (Li et al., 2014). Therefore, GPR43 independent mechanisms may also be mediating short-chain fatty acid-induced effects in brown adipose tissue.

GPR43 reportedly couples to either $G\alpha_{(i/o)}$ or $G\alpha_q$ signalling pathways (Brown et al., 2003). Up to date, nearly all of GPR43 roles identified in adipose tissue were found to be mediated by $G\alpha_{(i/o)}$. Our findings also indicated that $G_{(i/o)}\beta\gamma$-PLC-PKC-ERK signalling pathway was necessary for acetate induced downstream effects, which supported the importance of $G\alpha_{(i/o)}$ signalling pathway in acetate induced GPR43 activation in brown adipocytes.

Interestingly, using radioactivity-labelled acetate, it was not only demonstrated the existence of brown adipose tissue in human, but also revealed cold stimulation significantly increased the uptake of acetate in brown adipose tissue (Ouellet et al., 2012). After intravenous injection of ^{11}C-labeled acetate, radioactivity in brown adipose tissue, but not subcutaneous adipose tissue was increased throughout exposure to cold (Ouellet et al., 2012). This evidence also highlighted the possible roles of short-chain fatty acids in human brown adipose tissue upon cold stimulation. However, more evidence is needed to elucidate the links between acetate and brown adipose tissue in human.

Recently, it has also been identified that long-chain fatty acids are required for UCP1 to transport H^+ across mitochondrial inner membrane (Fedorenko

et al., 2012). This evidence together indicated that fatty acids are vital and necessary for normal physical functions of brown adipocytes and brown adipose tissue, especially their highly specific non-shivering thermogenesis.

Lastly, evidence also suggested dietary fibre leads to increased short-chain fatty acids, especially acetate, in circulation. Based on previous studies and results from this research, dietary supplementation of fibre might provide health benefits to keep energy homeostasis *via* increased brown adipogenesis and increased insulin sensitivities in muscle and liver, as well as reduced appetite.

Collectively, our finds provided useful evidence to deepen the understanding toward the functions of short-chain fatty acids on brown adipose tissue. Since brown adipose tissue has emerged as a novel regulator for energy homeostasis, better understanding the mediating role of fatty acids may provide clues to alleviate metabolic diseases as well as keep energy homeostasis. In order to examine the findings from this study in further, *in vivo* investigations as well as clinical trials are especially required.

It has been demonstrated that the amount and type of diety fiber consumed dramatic affect the composition of the intestinal microbiota and consequently on the amount of short-chain fatty acids produced in gut (den Besten et al., 2013). Analysis of the microbiota from the feces of mice fed diets revealed that fiber-rich diet increased the proportion of phyla Bacteroidaceae and Bifidobacteriaceae, which have acetate and propionate as the primary metabolic end products (Trompette et al., 2014). Further analysis also confirmed dietary fiber content alters the both local and systemic levels of

short-chain fatty acids (Trompette et al., 2014). Therefore, dietary fibre supplementary may serve as a therapeutic application to improve metabolic health and hold significant clinical potential *via* activating brown adipose tissue in human.

Of note, the majority work done in this study was to investigate the direct effects of acetate on immortalized brown adipocytes using in vitro cell models, however, the development and metabolism of brown adipose tissues were controlled by a complex network of development and metabolism of brown adipose tissues were controlled by a complex network of interorgan connections. It has been demonstrated that short-chain fatty acids also exert their functions in multiple organs. Therefore, *in vivo* assays are needed to predict the overall effects of short-chain fatty acid on development of brown adipose tissue as well as energy expenditure. Meanwhile, to test the direct effects of short-chain fatty acids on brown adipose tissue *in vivo*, novel delivery approaches are required to disassociate the central effects from peripheral actions of short-chain fatty acids in mice model since short-chain fatty acids can be transported through blood–brain barrier into brain (Frost et al., 2014). Recently, a novel delivery method using Liposome encapsulated Acetate (LITA) nanoparticle has been reported to partially overcome this obstacle since LITA nanoparticles can only reach peripheral tissues but do not cross blood–brain barrier (Sahuri-Arisoylu et al., 2016). Besides, although the circulation level of short-chain fatty acids has been measured by mass spectrometry (Opie and Walfish, 1963, Tollinger et al., 1979), the local concentration of short-chain fatty acids in brown adipose tissue is still not clear. The lack of quantitative data on actual fluxes of short-chain fatty

acids around brown adipose tissue also impaired the understanding towards the effects of short-chain fatty acids on brown adipose tissue *in vivo*. Therefore, these limitations within our study require further research to elucidate.

In conclusion, in this study we unveil short-chain fatty acids sensing machinery triggers a GPR43-dependent signalling to promote the differentiation and mitochondrial biogenesis in brown adipocytes. In addition, evidence given in this study also suggests that short-chain fatty acids treatment may affects lipid metabolism in brown adipocytes. Taken together, our findings highlight the potential to manipulate short-fatty acid sensing machinery in brown adipose tissue to regulate energy expenditure and keep energy homeostasis.

Reference

ABE, M. K., SAELZLER, M. P., ESPINOSA, R., KAHLE, K. T., HERSHENSON, M. B., LE BEAU, M. M. & ROSNER, M. R. 2002. ERK8, a New Member of the Mitogen-activated Protein Kinase Family. *Journal of Biological Chemistry,* 277**,** 16733-16743.

ACOSTA-ALVEAR, D., ZHOU, Y., BLAIS, A., TSIKITIS, M., LENTS, N. H., ARIAS, C., LENNON, C. J., KLUGER, Y. & DYNLACHT, B. D. 2007. XBP1 controls diverse cell type- and condition-specific transcriptional regulatory networks. *Mol Cell,* 27**,** 53-66.

ADAMS, J. A. 2001. Kinetic and Catalytic Mechanisms of Protein Kinases. *Chemical Reviews,* 101**,** 2271-2290.

AL-LAHHAM, S. A. H., ROELOFSEN, H., PRIEBE, M., WEENING, D., DIJKSTRA, M., HOEK, A., REZAEE, F., VENEMA, K. & VONK, R. J. 2010. Regulation of adipokine production in human adipose tissue by propionic acid. *European Journal of Clinical Investigation,* 40**,** 401-407.

ALBERTS, A. S., ARIAS, J., HAGIWARA, M., MONTMINY, M. R. & FERAMISCO, J. R. 1994. Recombinant cyclic AMP response element binding protein (CREB) phosphorylated on Ser-133 is transcriptionally active upon its introduction into fibroblast nuclei. *Journal of Biological Chemistry,* 269**,** 7623-7630.

ALEX, S., LANGE, K., AMOLO, T., GRINSTEAD, J. S., HAAKONSSON, A. K., SZALOWSKA, E., KOPPEN, A., MUDDE, K., HAENEN, D., AL-LAHHAM, S. A., ROELOFSEN, H., HOUTMAN, R., VAN DER BURG, B., MANDRUP, S., BONVIN, A. M. J. J., KALKHOVEN, E., MULLER, M., HOOIVELD, G. J. & KERSTEN, S. 2013. Short chain fatty acids stimulate Angiopoietin-like 4 synthesis in human colon adenocarcinoma cells by activating PPARγ. *Molecular and Cellular Biology*.

ALTAREJOS, J. Y. & MONTMINY, M. 2011. CREB and the CRTC co-activators: sensors for hormonal and metabolic signals. *Nat Rev Mol Cell Biol,* 12**,** 141-151.

ANDERSON, G. S. & MARTIN, A. D. 1994. Calculated thermal conductivities and heat flux in man. *Undersea Hyperb Med,* 21**,** 431-41.

ANDOH, A., TSUJIKAWA, T. & FUJIYAMA, Y. 2003. Role of dietary fiber and short-chain fatty acids in the colon. *Curr Pharm Des,* 9**,** 347-58.

ANDRISANI, O. M. 1999. CREB-mediated transcriptional control. *Crit Rev Eukaryot Gene Expr,* 9**,** 19-32.

ANG, Z., ER, J. Z. & DING, J. L. 2015. The short-chain fatty acid receptor GPR43 is transcriptionally regulated by XBP1 in human monocytes. *Sci Rep,* 5**,** 8134.

BAHAR HALPERN, K., VEPRIK, A., RUBINS, N., NAAMAN, O. & WALKER, M. D. 2012. GPR41 Gene Expression Is Mediated by Internal Ribosome Entry Site (IRES)-dependent Translation of Bicistronic mRNA Encoding GPR40 and GPR41 Proteins. *Journal of Biological Chemistry,* 287**,** 20154-20163.

BAILEY, C. J. & DAY, C. 2001. Review: Thiazolidinediones today. *The British Journal of Diabetes & Vascular Disease,* 1**,** 7-13.

BARBERA, M. J., SCHLUTER, A., PEDRAZA, N., IGLESIAS, R., VILLARROYA, F. & GIRALT, M. 2001. Peroxisome proliferator-activated receptor alpha activates transcription of the brown fat uncoupling protein-1 gene. A link between regulation of the

thermogenic and lipid oxidation pathways in the brown fat cell. *J Biol Chem,* 276**,** 1486-93.

BARTELT, A., BRUNS, O. T., REIMER, R., HOHENBERG, H., ITTRICH, H., PELDSCHUS, K., KAUL, M. G., TROMSDORF, U. I., WELLER, H., WAURISCH, C., EYCHMULLER, A., GORDTS, P. L., RINNINGER, F., BRUEGELMANN, K., FREUND, B., NIELSEN, P., MERKEL, M. & HEEREN, J. 2011. Brown adipose tissue activity controls triglyceride clearance. *Nat Med,* 17**,** 200-5.

BASTIE, C., HOLST, D., GAILLARD, D., JEHL-PIETRI, C. & GRIMALDI, P. A. 1999. Expression of Peroxisome Proliferator-activated Receptor PPARδ Promotes Induction of PPARγ and Adipocyte Differentiation in 3T3C2 Fibroblasts. *Journal of Biological Chemistry,* 274**,** 21920-21925.

BATTERHAM, R. L., LE ROUX, C. W., COHEN, M. A., PARK, A. J., ELLIS, S. M., PATTERSON, M., FROST, G. S., GHATEI, M. A. & BLOOM, S. R. 2003. Pancreatic polypeptide reduces appetite and food intake in humans. *J Clin Endocrinol Metab,* 88**,** 3989-92.

BELLAHCENE, M., O'DOWD, J. F., WARGENT, E. T., ZAIBI, M. S., HISLOP, D. C., NGALA, R. A., SMITH, D. M., CAWTHORNE, M. A., STOCKER, C. J. & ARCH, J. R. S. 2013. Male mice that lack the G-protein-coupled receptor GPR41 have low energy expenditure and increased body fat content. *British Journal of Nutrition,* 109**,** 1755-1764.

BERDEAUX, R., GOEBEL, N., BANASZYNSKI, L., TAKEMORI, H., WANDLESS, T., SHELTON, G. D. & MONTMINY, M. 2007. SIK1 is a class II HDAC kinase that promotes survival of skeletal myocytes. *Nat Med,* 13**,** 597-603.

BERRY, E. B., EYKHOLT, R., HELLIWELL, R. J., GILMOUR, R. S., MITCHELL, M. D. & MARVIN, K. W. 2003. Peroxisome proliferator-activated receptor isoform expression changes in human gestational tissues with labor at term. *Mol Pharmacol,* 64**,** 1586-90.

BIANCO, A. C., MAIA, A. L., DA SILVA, W. S. & CHRISTOFFOLETE, M. A. 2005. Adaptive activation of thyroid hormone and energy expenditure. *Biosci Rep,* 25**,** 191-208.

BINDELS, L. B., DEWULF, E. M. & DELZENNE, N. M. 2013. GPR43/FFA2: physiopathological relevance and therapeutic prospects. *Trends Pharmacol Sci,* 34**,** 226-32.

BINDELS, L. B., PORPORATO, P., DEWULF, E. M., VERRAX, J., NEYRINCK, A. M., MARTIN, J. C., SCOTT, K. P., BUC CALDERON, P., FERON, O., MUCCIOLI, G. G., SONVEAUX, P., CANI, P. D. & DELZENNE, N. M. 2012. Gut microbiota-derived propionate reduces cancer cell proliferation in the liver. *Br J Cancer,* 107**,** 1337-1344.

BINDER, H. J. 2010. Role of colonic short-chain fatty acid transport in diarrhea. *Annu Rev Physiol,* 72**,** 297-313.

BJURSELL, M., ADMYRE, T., G RANSSON, M., MARLEY, A. E., SMITH, D. M., OSCARSSON, J. & BOHLOOLY-Y, M. 2011. Improved glucose control and reduced body fat mass in free fatty acid receptor 2-deficient mice fed a high-fat diet. *American Journal of Physiology - Endocrinology And Metabolism,* 300**,** E211-E220.

BLOEMEN, J. G., VENEMA, K., VAN DE POLL, M. C., OLDE DAMINK, S. W., BUURMAN, W. A. & DEJONG, C. H. 2009. Short chain fatty acids exchange across the gut and liver in humans measured at surgery. *Clinical Nutrition,* 28**,** 657-661.

BODEN, G. 2011. Obesity, insulin resistance and free fatty acids. *Curr Opin Endocrinol Diabetes Obes,* 18**,** 139-43.

BODEN, G., CHEUNG, P., STEIN, T. P., KRESGE, K. & MOZZOLI, M. 2002. FFA cause hepatic insulin resistance by inhibiting insulin suppression of glycogenolysis. *American Journal of Physiology - Endocrinology And Metabolism,* 283**,** E12-E19.

BONKOVSKY, H. L., AZAR, R., BIRD, S., SZABO, G. & BANNER, B. 2002. Severe cholestatic hepatitis caused by thiazolidinediones: risks associated with substituting rosiglitazone for troglitazone. *Dig Dis Sci,* 47**,** 1632-7.

BORDICCHIA, M., LIU, D., AMRI, E.-Z., AILHAUD, G., DESS, XEC, FULGHERI, P., ZHANG, C., TAKAHASHI, N., SARZANI, R. & COLLINS, S. 2012. Cardiac natriuretic peptides act via p38 MAPK to induce the brown fat thermogenic program in mouse and human adipocytes. *The Journal of Clinical Investigation,* 122**,** 1022-1036.

BOST, F., AOUADI, M., CARON, L. & BIN TRUY, B. 2005a. The role of MAPKs in adipocyte differentiation and obesity. *Biochimie,* 87**,** 51-56.

BOST, F., AOUADI, M., CARON, L., EVEN, P., BELMONTE, N., PROT, M., DANI, C., HOFMAN, P., PAG S, G., POUYSS GUR, J., LE MARCHAND-BRUSTEL, Y. & BIN TRUY, B. 2005b. The Extracellular Signal–Regulated Kinase Isoform ERK1 Is Specifically Required for In Vitro and In Vivo Adipogenesis. *Diabetes,* 54**,** 402-411.

BOSTROM, P., WU, J., JEDRYCHOWSKI, M. P., KORDE, A., YE, L., LO, J. C., RASBACH, K. A., BOSTROM, E. A., CHOI, J. H., LONG, J. Z., KAJIMURA, S., ZINGARETTI, M. C., VIND, B. F., TU, H., CINTI, S., HOJLUND, K., GYGI, S. P. & SPIEGELMAN, B. M. 2012. A PGC1-alpha-dependent myokine that drives brown-fat-like development of white fat and thermogenesis. *Nature,* 481**,** 463-8.

BOUCHARD, C., PAG , J., B DARD, A., TREMBLAY, P. & VALLI RES, L. 2007. G protein-coupled receptor 84, a microglia-associated protein expressed in neuroinflammatory conditions. *Glia,* 55**,** 790-800.

BOUCHARD, C., TREMBLAY, A., DESPRES, J. P., NADEAU, A., LUPIEN, P. J., THERIAULT, G., DUSSAULT, J., MOORJANI, S., PINAULT, S. & FOURNIER, G. 1990. The response to long-term overfeeding in identical twins. *N Engl J Med,* 322**,** 1477-82.

BOURGUET, W., RUFF, M., CHAMBON, P., GRONEMEYER, H. & MORAS, D. 1995. Crystal structure of the ligand-binding domain of the human nuclear receptor RXR-[alpha]. *Nature,* 375**,** 377-382.

BRAUNER-OSBORNE, H., WELLENDORPH, P. & JENSEN, A. A. 2007. Structure, pharmacology and therapeutic prospects of family C G-protein coupled receptors. *Curr Drug Targets,* 8**,** 169-84.

BREHM, B. J., SPANG, S. E., LATTIN, B. L., SEELEY, R. J., DANIELS, S. R. & D'ALESSIO, D. A. 2005. The role of energy expenditure in the differential weight loss in obese women on low-fat and low-carbohydrate diets. *J Clin Endocrinol Metab,* 90**,** 1475-82.

BRISCOE, C. P., PEAT, A. J., MCKEOWN, S. C., CORBETT, D. F., GOETZ, A. S., LITTLETON, T. R., MCCOY, D. C., KENAKIN, T. P., ANDREWS, J. L., AMMALA, C., FORNWALD, J. A., IGNAR, D. M. & JENKINSON, S. 2006. Pharmacological regulation of insulin secretion in MIN6 cells through the fatty acid receptor GPR40: identification of agonist and antagonist small molecules. *British Journal of Pharmacology,* 148**,** 619-628.

BRISCOE, C. P., TADAYYON, M., ANDREWS, J. L., BENSON, W. G., CHAMBERS, J. K., EILERT, M. M., ELLIS, C., ELSHOURBAGY, N. A., GOETZ, A. S., MINNICK, D. T., MURDOCK, P. R., SAULS, H. R., SHABON, U., SPINAGE, L. D., STRUM, J. C., SZEKERES, P. G., TAN, K. B., WAY, J. M., IGNAR, D. M., WILSON, S. & MUIR, A. I. 2003. The Orphan G Protein-coupled Receptor GPR40 Is Activated by Medium and Long Chain Fatty Acids. *Journal of Biological Chemistry,* 278**,** 11303-11311.

BROTT, B. K., PINSKY, B. A. & ERIKSON, R. L. 1998. Nlk is a murine protein kinase related to Erk/MAP kinases and localized in the nucleus. *Proceedings of the National Academy of Sciences,* 95**,** 963-968.

BROWN, A. J., GOLDSWORTHY, S. M., BARNES, A. A., EILERT, M. M., TCHEANG, L., DANIELS, D., MUIR, A. I., WIGGLESWORTH, M. J., KINGHORN, I., FRASER, N. J., PIKE, N. B., STRUM, J. C., STEPLEWSKI, K. M., MURDOCK, P. R., HOLDER, J. C., MARSHALL, F. H., SZEKERES, P. G., WILSON, S., IGNAR, D. M., FOORD, S. M., WISE, A. & DOWELL, S. J.

2003. The Orphan G Protein-coupled Receptors GPR41 and GPR43 Are Activated by Propionate and Other Short Chain Carboxylic Acids. *Journal of Biological Chemistry,* 278**,** 11312-11319.

BROWN, L., ROSNER, B., WILLETT, W. W. & SACKS, F. M. 1999. Cholesterol-lowering effects of dietary fiber: a meta-analysis. *Am J Clin Nutr,* 69**,** 30-42.

BUKOWIECKI, L. J. 1985. Regulation of energy expenditure in brown adipose tissue. *Int J Obes,* 9 Suppl 2**,** 31-41.

BURRI, L., THORESEN, G. H. & BERGE, R. K. 2010. The Role of PPARalpha Activation in Liver and Muscle. *PPAR Res,* 2010.

CABRERA-VERA, T. M., VANHAUWE, J., THOMAS, T. O., MEDKOVA, M., PREININGER, A., MAZZONI, M. R. & HAMM, H. E. 2003. Insights into G protein structure, function, and regulation. *Endocr Rev,* 24**,** 765-81.

CALDER, P. C. 2015. Functional Roles of Fatty Acids and Their Effects on Human Health. *JPEN J Parenter Enteral Nutr,* 39**,** 18S-32S.

CANFORA, E. E., JOCKEN, J. W. & BLAAK, E. E. 2015. Short-chain fatty acids in control of body weight and insulin sensitivity. *Nat Rev Endocrinol,* 11**,** 577-591.

CANNON, B. & NEDERGAARD, J. 2004. Brown adipose tissue: function and physiological significance. *Physiol Rev,* 84**,** 277-359.

CAO, W., DANIEL, K. W., ROBIDOUX, J., PUIGSERVER, P., MEDVEDEV, A. V., BAI, X., FLOERING, L. M., SPIEGELMAN, B. M. & COLLINS, S. 2004. p38 Mitogen-Activated Protein Kinase Is the Central Regulator of Cyclic AMP-Dependent Transcription of the Brown Fat Uncoupling Protein 1 Gene. *Molecular and Cellular Biology,* 24**,** 3057-3067.

CAREY, A. L., VORLANDER, C., REDDY-LUTHMOODOO, M., NATOLI, A. K., FORMOSA, M. F., BERTOVIC, D. A., ANDERSON, M. J., DUFFY, S. J. & KINGWELL, B. A. 2014. Reduced UCP-1 content in in vitro differentiated beige/brite adipocytes derived from preadipocytes of human subcutaneous white adipose tissues in obesity. *PLoS One,* 9**,** e91997.

CARGNELLO, M. & ROUX, P. P. 2011. Activation and Function of the MAPKs and Their Substrates, the MAPK-Activated Protein Kinases. *Microbiology and Molecular Biology Reviews,* 75**,** 50-83.

CARTONI, C., YASUMATSU, K., OHKURI, T., SHIGEMURA, N., YOSHIDA, R., GODINOT, N., LE COUTRE, J., NINOMIYA, Y. & DAMAK, S. 2010. Taste Preference for Fatty Acids Is Mediated by GPR40 and GPR120. *The Journal of Neuroscience,* 30**,** 8376-8382.

CASAS-TINTO, S., ZHANG, Y., SANCHEZ-GARCIA, J., GOMEZ-VELAZQUEZ, M., RINCON-LIMAS, D. E. & FERNANDEZ-FUNEZ, P. 2011. The ER stress factor XBP1s prevents amyloid-beta neurotoxicity. *Hum Mol Genet,* 20**,** 2144-60.

CASPAR-BAUGUIL, S., COUSIN, B., BOUR, S., CASTEILLA, L., PENICAUD, L. & CARPENE, C. 2009. Adipose tissue lymphocytes: types and roles. *J Physiol Biochem,* 65**,** 423-36.

CASSARD-DOULCIER, A. M., LAROSE, M., MATAMALA, J. C., CHAMPIGNY, O., BOUILLAUD, F. & RICQUIER, D. 1994. In vitro interactions between nuclear proteins and uncoupling protein gene promoter reveal several putative transactivating factors including Ets1, retinoid X receptor, thyroid hormone receptor, and a CACCC box-binding protein. *J Biol Chem,* 269**,** 24335-42.

CAUSEY, J. L., FEIRTAG, J. M., GALLAHER, D. D., TUNGLAND, B. C. & SLAVIN, J. L. 2000. Effects of dietary inulin on serum lipids, blood glucose and the gastrointestinal environment in hypercholesterolemic men. *Nutrition Research,* 20**,** 191-201.

CHOI, S. H., CHUNG, K. Y., JOHNSON, B. J., GO, G. W., KIM, K. H., CHOI, C. W. & SMITH, S. B. 2013. Co-culture of bovine muscle satellite cells with preadipocytes increases PPARγ and C/EBPβ gene expression in differentiated myoblasts and increases

GPR43 gene expression in adipocytes. *The Journal of nutritional biochemistry,* 24**,** 539-543.

CHOO, H. J., KIM, J. H., KWON, O. B., LEE, C. S., MUN, J. Y., HAN, S. S., YOON, Y. S., YOON, G., CHOI, K. M. & KO, Y. G. 2006. Mitochondria are impaired in the adipocytes of type 2 diabetic mice. *Diabetologia,* 49**,** 784-91.

CHRISTY, R. J., KAESTNER, K. H., GEIMAN, D. E. & LANE, M. D. 1991. CCAAT/enhancer binding protein gene promoter: binding of nuclear factors during differentiation of 3T3-L1 preadipocytes. *Proceedings of the National Academy of Sciences,* 88**,** 2593-2597.

CHU, Z.-L., CARROLL, C., CHEN, R., ALFONSO, J., GUTIERREZ, V., HE, H., LUCMAN, A., XING, C., SEBRING, K., ZHOU, J., WAGNER, B., UNETT, D., JONES, R. M., BEHAN, D. P. & LEONARD, J. 2010. N-Oleoyldopamine Enhances Glucose Homeostasis through the Activation of GPR119. *Molecular Endocrinology,* 24**,** 161-170.

CHUNG, S., BROWN, J. M., PROVO, J. N., HOPKINS, R. & MCINTOSH, M. K. 2005. Conjugated Linoleic Acid Promotes Human Adipocyte Insulin Resistance through NFκB-dependent Cytokine Production. *Journal of Biological Chemistry,* 280**,** 38445-38456.

CHUNG, W. K. 2012. An overview of mongenic and syndromic obesities in humans. *Pediatr Blood Cancer,* 58**,** 122-8.

CINTI, S. 2009. Transdifferentiation properties of adipocytes in the adipose organ. *American Journal of Physiology - Endocrinology And Metabolism,* 297**,** E977-E986.

CINTI, S. 2012. The adipose organ at a glance. *Disease Models & Mechanisms,* 5**,** 588-594.

CLAPHAM, D. E. & NEER, E. J. 1993. New roles for G-protein ([beta][gamma]-dimers in transmembrane signalling. *Nature,* 365**,** 403-406.

CLARK, M. D., KUMAR, G. S., MARCUM, R., LUO, Q., ZHANG, Y. & RADHAKRISHNAN, I. 2015. Molecular Basis for the Mechanism of Constitutive CBP/p300 Coactivator Recruitment by CRTC1-MAML2 and Its Implications in cAMP Signaling. *Biochemistry,* 54**,** 5439-46.

COHEN, P. 2000. The regulation of protein function by multisite phosphorylation – a 25 year update. *Trends in Biochemical Sciences,* 25**,** 596-601.

COLLINS, S., YEHUDA-SHNAIDMAN, E. & WANG, H. 2010. Positive and negative control of Ucp1 gene transcription and the role of [beta]-adrenergic signaling networks. *Int J Obes,* 34**,** S28-S33.

COLOMBO, J., KANNASS, K. N., JILL SHADDY, D., KUNDURTHI, S., MAIKRANZ, J. M., ANDERSON, C. J., BLAGA, O. M. & CARLSON, S. E. 2004. Maternal DHA and the Development of Attention in Infancy and Toddlerhood. *Child Development,* 75**,** 1254-1267.

CONKLIN, B. R. & BOURNE, H. R. 1993. Structural elements of Gα subunits that interact with Gβγ, receptors, and effectors. *Cell,* 73**,** 631-641.

CONNOLLY, E., MORRISEY, R. D. & CARNIE, J. A. 1982. The effect of interscapular brown adipose tissue removal on body-weight and cold response in the mouse. *Br J Nutr,* 47**,** 653-8.

CORNALL, L. M., MATHAI, M. L., HRYCIW, D. H. & MCAINCH, A. J. 2011. Diet-induced obesity up-regulates the abundance of GPR43 and GPR120 in a tissue specific manner. *Cellular physiology and biochemistry : international journal of experimental cellular physiology, biochemistry, and pharmacology,* 28**,** 949-958.

CORNALL, L. M., MATHAI, M. L., HRYCIW, D. H., SIMCOCKS, A. C., O'BRIEN, P. E., WENTWORTH, J. M. & MCAINCH, A. J. 2013. GPR119 regulates genetic markers of fatty acid oxidation in cultured skeletal muscle myotubes. *Molecular and Cellular Endocrinology,* 365**,** 108-118.

CORNELIUS, P., MACDOUGALD, O. A. & LANE, M. D. 1994. Regulation of adipocyte development. *Annu Rev Nutr,* 14**,** 99-129.

COWLEY, M. A., SMART, J. L., RUBINSTEIN, M., CERDAN, M. G., DIANO, S., HORVATH, T. L., CONE, R. D. & LOW, M. J. 2001. Leptin activates anorexigenic POMC neurons through a neural network in the arcuate nucleus. *Nature,* 411**,** 480-484.

CUNNANE, S. C. 2003. Problems with essential fatty acids: time for a new paradigm? *Prog Lipid Res,* 42**,** 544-68.

CYPESS, A. M., LEHMAN, S., WILLIAMS, G., TAL, I., RODMAN, D., GOLDFINE, A. B., KUO, F. C., PALMER, E. L., TSENG, Y. H., DORIA, A., KOLODNY, G. M. & KAHN, C. R. 2009. Identification and importance of brown adipose tissue in adult humans. *New England Journal of Medicine,* 360**,** 1509-1517.

DARLINGTON, G. J., ROSS, S. E. & MACDOUGALD, O. A. 1998. The Role of C/EBP Genes in Adipocyte Differentiation. *Journal of Biological Chemistry,* 273**,** 30057-30060.

DASHTY, M. 2013. A quick look at biochemistry: carbohydrate metabolism. *Clin Biochem,* 46**,** 1339-52.

DAVENPORT, A. P., ALEXANDER, S. P., SHARMAN, J. L., PAWSON, A. J., BENSON, H. E., MONAGHAN, A. E., LIEW, W. C., MPAMHANGA, C. P., BONNER, T. I., NEUBIG, R. R., PIN, J. P., SPEDDING, M. & HARMAR, A. J. 2013. International Union of Basic and Clinical Pharmacology. LXXXVIII. G protein-coupled receptor list: recommendations for new pairings with cognate ligands. *Pharmacol Rev,* 65**,** 967-86.

DAWKINS, M. J. R. & SCOPES, J. W. 1965. Non-shivering Thermogenesis and Brown Adipose Tissue in the Human New-born Infant. *Nature,* 206**,** 201-202.

DEFRONZO, R. A., JACOT, E., JEQUIER, E., MAEDER, E., WAHREN, J. & FELBER, J. P. 1981. The effect of insulin on the disposal of intravenous glucose. Results from indirect calorimetry and hepatic and femoral venous catheterization. *Diabetes,* 30**,** 1000-7.

DELERIS, P., TROST, M., TOPISIROVIC, I., TANGUAY, P. L., BORDEN, K. L., THIBAULT, P. & MELOCHE, S. 2011. Activation loop phosphorylation of ERK3/ERK4 by group I p21-activated kinases (PAKs) defines a novel PAK-ERK3/4-MAPK-activated protein kinase 5 signaling pathway. *J Biol Chem,* 286**,** 6470-8.

DEN BESTEN, G., BLEEKER, A., GERDING, A., VAN EUNEN, K., HAVINGA, R., VAN DIJK, T. H., OOSTERVEER, M. H., JONKER, J. W., GROEN, A. K., REIJNGOUD, D. J. & BAKKER, B. M. 2015. Short-Chain Fatty Acids Protect Against High-Fat Diet-Induced Obesity via a PPARgamma-Dependent Switch From Lipogenesis to Fat Oxidation. *Diabetes,* 64**,** 2398-408.

DEN BESTEN, G., VAN EUNEN, K., GROEN, A. K., VENEMA, K., REIJNGOUD, D.-J. & BAKKER, B. M. 2013. The role of short-chain fatty acids in the interplay between diet, gut microbiota, and host energy metabolism. *Journal of Lipid Research,* 54**,** 2325-2340.

DEWULF, E. M., CANI, P. D., NEYRINCK, A. M., POSSEMIERS, S., HOLLE, A. V., MUCCIOLI, G. G., DELDICQUE, L., BINDELS, L. B., PACHIKIAN, B. D., SOHET, F. M., MIGNOLET, E., FRANCAUX, M., LARONDELLE, Y. & DELZENNE, N. M. 2011. Inulin-type fructans with prebiotic properties counteract GPR43 overexpression and PPARγ-related adipogenesis in the white adipose tissue of high-fat diet-fed mice. *The Journal of Nutritional Biochemistry,* 22**,** 712-722.

DI SABATINO, A., MORERA, R., CICCOCIOPPO, R., CAZZOLA, P., GOTTI, S., TINOZZI, F. P., TINOZZI, S. & CORAZZA, G. R. 2005. Oral butyrate for mildly to moderately active Crohn's disease. *Aliment Pharmacol Ther,* 22**,** 789-94.

DIAZ, E. O., PRENTICE, A. M., GOLDBERG, G. R., MURGATROYD, P. R. & COWARD, W. A. 1992. Metabolic response to experimental overfeeding in lean and overweight healthy volunteers. *Am J Clin Nutr,* 56**,** 641-55.

DIGIOVANNA, M. P., ROUSSEL, R. R. & STERN, D. F. 2002. Production of antibodies that recognize specific tyrosine-phosphorylated peptides. *Curr Protoc Cell Biol,* Chapter 16**,** Unit 16.6.

DIJK, W., HEINE, M., VERGNES, L., BOON, M. R., SCHAART, G., HESSELINK, M. K., REUE, K., VAN MARKEN LICHTENBELT, W. D., OLIVECRONA, G., RENSEN, P. C., HEEREN, J. & KERSTEN, S. 2015. ANGPTL4 mediates shuttling of lipid fuel to brown adipose tissue during sustained cold exposure. *eLife*.

DORSAM, R. T. & GUTKIND, J. S. 2007. G-protein-coupled receptors and cancer. *Nat Rev Cancer,* 7**,** 79-94.

DOWNWARD, J. 1998. Mechanisms and consequences of activation of protein kinase B/Akt. *Curr Opin Cell Biol,* 10**,** 262-7.

DUBIKOVSKAYA, E., CHUDNOVSKIY, R., KARATEEV, G., PARK, H. M. & STAHL, A. 2014. Measurement of long-chain fatty acid uptake into adipocytes. *Methods Enzymol,* 538**,** 107-34.

DUDLEY, D. T., PANG, L., DECKER, S. J., BRIDGES, A. J. & SALTIEL, A. R. 1995. A synthetic inhibitor of the mitogen-activated protein kinase cascade. *Proc Natl Acad Sci U S A,* 92**,** 7686-9.

DULLOO, A. G., STOCK, M. J., SOLINAS, G., BOSS, O., MONTANI, J.-P. & SEYDOUX, J. 2002. Leptin directly stimulates thermogenesis in skeletal muscle. *FEBS Letters,* 515**,** 109-113.

EBLEN, S. T., SLACK-DAVIS, J. K., TARCSAFALVI, A., PARSONS, J. T., WEBER, M. J. & CATLING, A. D. 2004. Mitogen-activated protein kinase feedback phosphorylation regulates MEK1 complex formation and activation during cellular adhesion. *Mol Cell Biol,* 24**,** 2308-17.

EDFALK, S., STENEBERG, P. & EDLUND, H. 2008. Gpr40 Is Expressed in Enteroendocrine Cells and Mediates Free Fatty Acid Stimulation of Incretin Secretion. *Diabetes,* 57**,** 2280-2287.

EHEHALT, R., SPARLA, R., KULAKSIZ, H., HERRMANN, T., FULLEKRUG, J. & STREMMEL, W. 2008. Uptake of long chain fatty acids is regulated by dynamic interaction of FAT/CD36 with cholesterol/sphingolipid enriched microdomains (lipid rafts). *BMC Cell Biol,* 9**,** 45.

ELIAS, C. F., LEE, C., KELLY, J., ASCHKENASI, C., AHIMA, R. S., COUCEYRO, P. R., KUHAR, M. J., SAPER, C. B. & ELMQUIST, J. K. 1998. Leptin activates hypothalamic CART neurons projecting to the spinal cord. *Neuron,* 21**,** 1375-85.

ELKINS, R. 1999. *Essential Fatty Acids*, Midpoint Trade Books Incorporated.

ELLISCLARE 2004. The state of GPCR research in 2004. *Nat Rev Drug Discov,* 3**,** 577-626.

ENGELMAN, J. A., LISANTI, M. P. & SCHERER, P. E. 1998. Specific inhibitors of p38 mitogen-activated protein kinase block 3T3-L1 adipogenesis. *J Biol Chem,* 273**,** 32111-20.

EROL, A. 2007. Muscle-Specific PPARbeta/delta Agonism May Provide Synergistic Benefits with Life Style Modifications. *PPAR Res,* 2007**,** 30578.

ESSER, V., BROWN, N. F., COWAN, A. T., FOSTER, D. W. & MCGARRY, J. D. 1996. Expression of a cDNA Isolated from Rat Brown Adipose Tissue and Heart Identifies the Product as the Muscle Isoform of Carnitine Palmitoyltransferase I (M-CPT I): M-CPT I IS THE PREDOMINANT CPT I ISOFORM EXPRESSED IN BOTH WHITE (EPIDIDYMAL) AND BROWN ADIPOCYTES. *Journal of Biological Chemistry,* 271**,** 6972-6977.

FAN, J. Y., CARPENTIER, J. L., VAN OBBERGHEN, E., GRUNFELD, C., GORDEN, P. & ORCI, L. 1983. Morphological changes of the 3T3-L1 fibroblast plasma membrane upon differentiation to the adipocyte form. *J Cell Sci,* 61**,** 219-30.

FARKAS, V., KELENYI, G. & SANDOR, A. 1999. A dramatic accumulation of glycogen in the brown adipose tissue of rats following recovery from cold exposure. *Arch Biochem Biophys,* 365**,** 54-61.

FARMER, S. R. 2008. Molecular determinants of brown adipocyte formation and function. *Genes Dev,* 22**,** 1269-75.

FAROOQI, I. S. & O'RAHILLY, S. 2005. Monogenic obesity in humans. *Annu Rev Med,* 56**,** 443-58.

FAVATA, M. F., HORIUCHI, K. Y., MANOS, E. J., DAULERIO, A. J., STRADLEY, D. A., FEESER, W. S., VAN DYK, D. E., PITTS, W. J., EARL, R. A., HOBBS, F., COPELAND, R. A., MAGOLDA, R. L., SCHERLE, P. A. & TRZASKOS, J. M. 1998. Identification of a novel inhibitor of mitogen-activated protein kinase kinase. *J Biol Chem,* 273**,** 18623-32.

FEDORENKO, A., LISHKO, POLINA V. & KIRICHOK, Y. 2012. Mechanism of Fatty-Acid-Dependent UCP1 Uncoupling in Brown Fat Mitochondria. *Cell,* 151**,** 400-413.

FELINSKI, E. A. & QUINN, P. G. 2001. The coactivator dTAF(II)110/hTAF(II)135 is sufficient to recruit a polymerase complex and activate basal transcription mediated by CREB. *Proc Natl Acad Sci U S A,* 98**,** 13078-83.

FELTON, C. V., CROOK, D., DAVIES, M. J. & OLIVER, M. F. 1994. Dietary polyunsaturated fatty acids and composition of human aortic plaques. *Lancet,* 344**,** 1195-6.

FERNANDEZ-MARCOS, P. J. & AUWERX, J. 2011. Regulation of PGC-1alpha, a nodal regulator of mitochondrial biogenesis. *Am J Clin Nutr,* 93**,** 884s-90.

FILLINGAME, R. H. 1997. Coupling H+ transport and ATP synthesis in F1F0-ATP synthases: glimpses of interacting parts in a dynamic molecular machine. *J Exp Biol,* 200**,** 217-24.

FINK, H., REX, A., VOITS, M. & VOIGT, J. P. 1998. Major biological actions of CCK--a critical evaluation of research findings. *Exp Brain Res,* 123**,** 77-83.

FLODGREN, E., OLDE, B., MEIDUTE-ABARAVICIENE, S., WINZELL, M. S., AHR N, B. & SALEHI, A. 2007. GPR40 is expressed in glucagon producing cells and affects glucagon secretion. *Biochemical and Biophysical Research Communications,* 354**,** 240-245.

FONSECA-ALANIZ, M. H., TAKADA, J., ALONSO-VALE, M. I. & LIMA, F. B. 2007. Adipose tissue as an endocrine organ: from theory to practice. *J Pediatr (Rio J),* 83**,** S192-203.

FOROUHI, N. G., KOULMAN, A., SHARP, S. J., IMAMURA, F., KROGER, J., SCHULZE, M. B., CROWE, F. L., HUERTA, J. M., GUEVARA, M., BEULENS, J. W., VAN WOUDENBERGH, G. J., WANG, L., SUMMERHILL, K., GRIFFIN, J. L., FESKENS, E. J., AMIANO, P., BOEING, H., CLAVEL-CHAPELON, F., DARTOIS, L., FAGHERAZZI, G., FRANKS, P. W., GONZALEZ, C., JAKOBSEN, M. U., KAAKS, R., KEY, T. J., KHAW, K. T., KUHN, T., MATTIELLO, A., NILSSON, P. M., OVERVAD, K., PALA, V., PALLI, D., QUIROS, J. R., ROLANDSSON, O., ROSWALL, N., SACERDOTE, C., SANCHEZ, M. J., SLIMANI, N., SPIJKERMAN, A. M., TJONNELAND, A., TORMO, M. J., TUMINO, R., VAN DER, A. D., VAN DER SCHOUW, Y. T., LANGENBERG, C., RIBOLI, E. & WAREHAM, N. J. 2014. Differences in the prospective association between individual plasma phospholipid saturated fatty acids and incident type 2 diabetes: the EPIC-InterAct case-cohort study. *Lancet Diabetes Endocrinol,* 2**,** 810-8.

FREDRIKSON, G., TORNQVIST, H. & BELFRAGE, P. 1986. Hormone-sensitive lipase and monoacylglycerol lipase are both required for complete degradation of adipocyte triacylglycerol. *Biochim Biophys Acta,* 876**,** 288-93.

FREDRIKSSON, R., H GLUND, P. J., GLORIAM, D. E. I., LAGERSTR M, M. C. & SCHI TH, H. B. 2003. Seven evolutionarily conserved human rhodopsin G protein-coupled receptors lacking close relatives. *FEBS Letters,* 554**,** 381-388.

FROST, G., SLEETH, M. L., SAHURI-ARISOYLU, M., LIZARBE, B., CERDAN, S., BRODY, L., ANASTASOVSKA, J., GHOURAB, S., HANKIR, M., ZHANG, S., CARLING, D., SWANN, J.

R., GIBSON, G., VIARDOT, A., MORRISON, D., LOUISE THOMAS, E. & BELL, J. D. 2014. The short-chain fatty acid acetate reduces appetite via a central homeostatic mechanism. *Nat Commun,* 5**,** 3611.

FYFE, M. C., MCCORMACK, J. G., OVERTON, H. A., PROCTER, M. J. & REYNET, C. 2008. GPR119 agonists as potential new oral agents for the treatment of type 2 diabetes and obesity. *Expert Opin Drug Discov,* 3**,** 403-13.

GAILLARD, I., ROUQUIER, S. & GIORGI, D. 2004. Olfactory receptors. *Cell Mol Life Sci,* 61**,** 456-69.

GALE, S. M., CASTRACANE, V. D. & MANTZOROS, C. S. 2004. Energy Homeostasis, Obesity and Eating Disorders: Recent Advances in Endocrinology. *The Journal of Nutrition,* 134**,** 295-298.

GANGULY, J. 1960. Studies on the mechanism of fatty acid synthesis: VII. Biosynthesis of fatty acids from malonyl CoA. *Biochimica et Biophysica Acta,* 40**,** 110-118.

GANTNER, M. L., HAZEN, B. C., CONKRIGHT, J. & KRALLI, A. 2014. GADD45gamma regulates the thermogenic capacity of brown adipose tissue. *Proc Natl Acad Sci U S A,* 111**,** 11870-5.

GAO, C.-L., ZHU, C., ZHAO, Y.-P., CHEN, X.-H., JI, C.-B., ZHANG, C.-M., ZHU, J.-G., XIA, Z.-K., TONG, M.-L. & GUO, X.-R. 2010. Mitochondrial dysfunction is induced by high levels of glucose and free fatty acids in 3T3-L1 adipocytes. *Molecular and Cellular Endocrinology,* 320**,** 25-33.

GAO, Z., YIN, J., ZHANG, J., WARD, R. E., MARTIN, R. J., LEFEVRE, M., CEFALU, W. T. & YE, J. 2009. Butyrate improves insulin sensitivity and increases energy expenditure in mice. *Diabetes,* 58**,** 1509-17.

GARRIDO, D. M., CORBETT, D. F., DWORNIK, K. A., GOETZ, A. S., LITTLETON, T. R., MCKEOWN, S. C., MILLS, W. Y., SMALLEY JR, T. L., BRISCOE, C. P. & PEAT, A. J. 2006. Synthesis and activity of small molecule GPR40 agonists. *Bioorganic & Medicinal Chemistry Letters,* 16**,** 1840-1845.

GE, H., LI, X., WEISZMANN, J., WANG, P., BARIBAULT, H., CHEN, J.-L., TIAN, H. & LI, Y. 2008. Activation of G Protein-Coupled Receptor 43 in Adipocytes Leads to Inhibition of Lipolysis and Suppression of Plasma Free Fatty Acids. *Endocrinology,* 149**,** 4519-4526.

GEISLER, J. G. 2011. Targeting energy expenditure via fuel switching and beyond. *Diabetologia,* 54**,** 237-244.

GESTA, S. & KAHN, C. R. 2012. White Adipose Tissue. *In:* SYMONDS, M. E. (ed.) *Adipose Tissue Biology.* Springer New York.

GHORBANI, M., CLAUS, T. H. & HIMMS-HAGEN, J. 1997. Hypertrophy of brown adipocytes in brown and white adipose tissues and reversal of diet-induced obesity in rats treated with a β3-adrenoceptor agonist. *Biochemical Pharmacology,* 54**,** 121-131.

GLATZ, G., GOGL, G., ALEXA, A. & REMENYI, A. 2013. Structural mechanism for the specific assembly and activation of the extracellular signal regulated kinase 5 (ERK5) module. *J Biol Chem,* 288**,** 8596-609.

GODDARD, A. & WATTS, A. 2012. Regulation of G protein-coupled receptors by palmitoylation and cholesterol. *BMC Biology,* 10**,** 27.

GOLDSMITH, Z. G. & DHANASEKARAN, D. N. 2007. G Protein regulation of MAPK networks. *Oncogene,* 26**,** 3122-3142.

GOLOZOUBOVA, V., CANNON, B. & NEDERGAARD, J. 2006. UCP1 is essential for adaptive adrenergic nonshivering thermogenesis. *Am J Physiol Endocrinol Metab,* 291**,** E350-7.

GONCALVES, P. & MARTEL, F. 2013. Butyrate and colorectal cancer: the role of butyrate transport. *Curr Drug Metab,* 14**,** 994-1008.

GOTO, T., LEE, J. Y., TERAMINAMI, A., KIM, Y. I., HIRAI, S., UEMURA, T., INOUE, H., TAKAHASHI, N. & KAWADA, T. 2011. Activation of peroxisome proliferator-activated receptor-alpha stimulates both differentiation and fatty acid oxidation in adipocytes. *J Lipid Res,* 52**,** 873-84.

GOTOH, C., HONG, Y.-H., IGA, T., HISHIKAWA, D., SUZUKI, Y., SONG, S.-H., CHOI, K.-C., ADACHI, T., HIRASAWA, A., TSUJIMOTO, G., SASAKI, S.-I. & ROH, S.-G. 2007. The regulation of adipogenesis through GPR120. *Biochemical and Biophysical Research Communications,* 354**,** 591-597.

GREGOR, M. F., MISCH, E. S., YANG, L., HUMMASTI, S., INOUYE, K. E., LEE, A. H., BIERIE, B. & HOTAMISLIGIL, G. S. 2013. The role of adipocyte XBP1 in metabolic regulation during lactation. *Cell Rep,* 3**,** 1430-9.

GREGOR, M. F., YANG, L., FABBRINI, E., MOHAMMED, B. S., EAGON, J. C., HOTAMISLIGIL, G. S. & KLEIN, S. 2009. Endoplasmic reticulum stress is reduced in tissues of obese subjects after weight loss. *Diabetes,* 58**,** 693-700.

GROSSO, G., PAJAK, A., MARVENTANO, S., CASTELLANO, S., GALVANO, F., BUCOLO, C., DRAGO, F. & CARACI, F. 2014. Role of omega-3 fatty acids in the treatment of depressive disorders: a comprehensive meta-analysis of randomized clinical trials. *PLoS One,* 9**,** e96905.

GUERRA, C., KOZA, R. A., YAMASHITA, H., WALSH, K. & KOZAK, L. P. 1998. Emergence of brown adipocytes in white fat in mice is under genetic control. Effects on body weight and adiposity. *J Clin Invest,* 102**,** 412-20.

GUNSTONE, F. D. 1996. *Fatty Acid and Lipid Chemistry*, Springer.

GUO, W., WONG, S., XIE, W., LEI, T. & LUO, Z. 2007. Palmitate modulates intracellular signaling, induces endoplasmic reticulum stress, and causes apoptosis in mouse 3T3-L1 and rat primary preadipocytes. *American Journal of Physiology - Endocrinology And Metabolism,* 293**,** E576-E586.

HAMILTON, M. T., HAMILTON, D. G. & ZDERIC, T. W. 2007. Role of low energy expenditure and sitting in obesity, metabolic syndrome, type 2 diabetes, and cardiovascular disease. *Diabetes,* 56**,** 2655-67.

HAMM, J. K., EL JACK, A. K., PILCH, P. F. & FARMER, S. R. 1999. Role of PPARγ in Regulating Adipocyte Differentiation and Insulin-Responsive Glucose Uptake. *Annals of the New York Academy of Sciences,* 892**,** 134-145.

HAN, J., MURTHY, R., WOOD, B., SONG, B., WANG, S., SUN, B., MALHI, H. & KAUFMAN, R. J. 2013. ER stress signalling through eIF2alpha and CHOP, but not IRE1alpha, attenuates adipogenesis in mice. *Diabetologia,* 56**,** 911-24.

HANADA, M., FENG, J. & HEMMINGS, B. A. 2004. Structure, regulation and function of PKB/AKT--a major therapeutic target. *Biochim Biophys Acta,* 1697**,** 3-16.

HANOUNE, J. & DEFER, N. 2001. Regulation and role of adenylyl cyclase isoforms. *Annu Rev Pharmacol Toxicol,* 41**,** 145-74.

HANSEN, H. S., ROSENKILDE, M. M., HOLST, J. J. & SCHWARTZ, T. W. 2012. GPR119 as a fat sensor. *Trends Pharmacol Sci,* 33**,** 374-81.

HARA, T., HIRASAWA, A., SUN, Q., SADAKANE, K., ITSUBO, C., IGA, T., ADACHI, T., KOSHIMIZU, T.-A., HASHIMOTO, T., ASAKAWA, Y. & TSUJIMOTO, G. 2009. Novel selective ligands for free fatty acid receptors GPR120 and GPR40. *Naunyn-Schmiedeberg's Archives of Pharmacology,* 380**,** 247-255.

HARDING, H. P., NOVOA, I., ZHANG, Y., ZENG, H., WEK, R., SCHAPIRA, M. & RON, D. 2000. Regulated translation initiation controls stress-induced gene expression in mammalian cells. *Mol Cell,* 6**,** 1099-108.

HARDING, H. P., ZHANG, Y., ZENG, H., NOVOA, I., LU, P. D., CALFON, M., SADRI, N., YUN, C., POPKO, B., PAULES, R., STOJDL, D. F., BELL, J. C., HETTMANN, T., LEIDEN, J. M. &

RON, D. 2003. An integrated stress response regulates amino acid metabolism and resistance to oxidative stress. *Mol Cell,* 11**,** 619-33.

HARIG, J. M., SOERGEL, K. H., KOMOROWSKI, R. A. & WOOD, C. M. 1989. Treatment of diversion colitis with short-chain-fatty acid irrigation. *N Engl J Med,* 320**,** 23-8.

HE, Y., SUN, S., SHA, H., LIU, Z., YANG, L., XUE, Z., CHEN, H. & QI, L. 2010. Emerging roles for XBP1, a sUPeR transcription factor. *Gene Expr,* 15**,** 13-25.

HENDERSON, S., VOGEL, J., BARR, L., GARVIN, F., JONES, J. & COSTANTINI, L. 2009. Study of the ketogenic agent AC-1202 in mild to moderate Alzheimer's disease: a randomized, double-blind, placebo-controlled, multicenter trial. *Nutrition & Metabolism,* 6**,** 31.

HENRIKSON, R. C., KAYE, G. I. & MAZURKIEWICZ, J. E. 1997. *Histology*, Lippincott Williams & Wilkins.

HERNANDEZ, R., TERUEL, T. & LORENZO, M. 2003. Rosiglitazone produces insulin sensitisation by increasing expression of the insulin receptor and its tyrosine kinase activity in brown adipocytes. *Diabetologia,* 46**,** 1618-28.

HERZIG, S., HEDRICK, S., MORANTTE, I., KOO, S.-H., GALIMI, F. & MONTMINY, M. 2003. CREB controls hepatic lipid metabolism through nuclear hormone receptor PPAR-[gamma]. *Nature,* 426**,** 190-193.

HEYMSFIELD, S. 2005. *Human Body Composition*, HUMAN KINETICS PUB Incorporated.

HEYTLER, P. G. & PRICHARD, W. W. 1962. A new class of uncoupling agents--carbonyl cyanide phenylhydrazones. *Biochem Biophys Res Commun,* 7**,** 272-5.

HINNEY, A. & HEBEBRAND, J. 2008. Polygenic obesity in humans. *Obes Facts,* 1**,** 35-42.

HIRASAWA, A., TSUMAYA, K., AWAJI, T., KATSUMA, S., ADACHI, T., YAMADA, M., SUGIMOTO, Y., MIYAZAKI, S. & TSUJIMOTO, G. 2005. Free fatty acids regulate gut incretin glucagon-like peptide-1 secretion through GPR120. *Nat Med,* 11**,** 90-94.

HOHENEGGER, M., WALDHOER, M., BEINDL, W., BOING, B., KREIMEYER, A., NICKEL, P., NANOFF, C. & FREISSMUTH, M. 1998. Gsalpha-selective G protein antagonists. *Proc Natl Acad Sci U S A,* 95**,** 346-51.

HOLLENSTEIN, K., DE GRAAF, C., BORTOLATO, A., WANG, M. W., MARSHALL, F. H. & STEVENS, R. C. 2014. Insights into the structure of class B GPCRs. *Trends Pharmacol Sci,* 35**,** 12-22.

HONG, Y.-H., NISHIMURA, Y., HISHIKAWA, D., TSUZUKI, H., MIYAHARA, H., GOTOH, C., CHOI, K.-C., FENG, D. D., CHEN, C., LEE, H.-G., KATOH, K., ROH, S.-G. & SASAKI, S. 2005. Acetate and Propionate Short Chain Fatty Acids Stimulate Adipogenesis via GPCR43. *Endocrinology,* 146**,** 5092-5099.

HOUZE, J. B., ZHU, L., SUN, Y., AKERMAN, M., QIU, W., ZHANG, A. J., SHARMA, R., SCHMITT, M., WANG, Y., LIU, J., LIU, J., MEDINA, J. C., REAGAN, J. D., LUO, J., TONN, G., ZHANG, J., LU, J. Y.-L., CHEN, M., LOPEZ, E., NGUYEN, K., YANG, L., TANG, L., TIAN, H., SHUTTLEWORTH, S. J. & LIN, D. C. H. 2012. AMG 837: A potent, orally bioavailable GPR40 agonist. *Bioorganic & Medicinal Chemistry Letters,* 22**,** 1267-1270.

HUNTER, T. 1995. Protein kinases and phosphatases: the yin and yang of protein phosphorylation and signaling. *Cell,* 80**,** 225-36.

ICHIMURA, A., HIRASAWA, A., HARA, T. & TSUJIMOTO, G. 2009. Free fatty acid receptors act as nutrient sensors to regulate energy homeostasis. *Prostaglandins & Other Lipid Mediators,* 89**,** 82-88.

IMCHEN, T., MANASSE, J., MIN, K. W. & BAEK, S. J. 2013. Characterization of PPAR dual ligand MCC-555 in AOM-induced colorectal tumorigenesis. *Exp Toxicol Pathol,* 65**,** 919-24.

IMPEY, S., OBRIETAN, K., WONG, S. T., POSER, S., YANO, S., WAYMAN, G., DELOULME, J. C., CHAN, G. & STORM, D. R. 1998. Cross Talk between ERK and PKA Is Required for Ca2+ Stimulation of CREB-Dependent Transcription and ERK Nuclear Translocation. *Neuron,* 21**,** 869-883.

INNIS, S. M. 2007. Dietary (n-3) fatty acids and brain development. *J Nutr,* 137**,** 855-9.

ISHIZAKA, S., KIKUCHI, E., HIGASHINO, T., KINOSHITA, K. & TSUJII, T. 1990. Effects of acetate on the immune system of mice. *Int J Immunopharmacol,* 12**,** 135-43.

ITANI, S. I., RUDERMAN, N. B., SCHMIEDER, F. & BODEN, G. 2002. Lipid-Induced Insulin Resistance in Human Muscle Is Associated With Changes in Diacylglycerol, Protein Kinase C, and IκB-α. *Diabetes,* 51**,** 2005-2011.

ITOH, Y., KAWAMATA, Y., HARADA, M., KOBAYASHI, M., FUJII, R., FUKUSUMI, S., OGI, K., HOSOYA, M., TANAKA, Y., UEJIMA, H., TANAKA, H., MARUYAMA, M., SATOH, R., OKUBO, S., KIZAWA, H., KOMATSU, H., MATSUMURA, F., NOGUCHI, Y., SHINOHARA, T., HINUMA, S., FUJISAWA, Y. & FUJINO, M. 2003. Free fatty acids regulate insulin secretion from pancreatic [beta] cells through GPR40. *Nature,* 422**,** 173-176.

JAKUS, P. B., SANDOR, A., JANAKY, T. & FARKAS, V. 2008. Cooperation between BAT and WAT of rats in thermogenesis in response to cold, and the mechanism of glycogen accumulation in BAT during reacclimation. *J Lipid Res,* 49**,** 332-9.

JANG, M., MISTRY, A., SWICK, A. G. & ROMSOS, D. R. 2000. Leptin rapidly inhibits hypothalamic neuropeptide Y secretion and stimulates corticotropin-releasing hormone secretion in adrenalectomized mice. *J Nutr,* 130**,** 2813-20.

JENKINS, C. M., MANCUSO, D. J., YAN, W., SIMS, H. F., GIBSON, B. & GROSS, R. W. 2004. Identification, Cloning, Expression, and Purification of Three Novel Human Calcium-independent Phospholipase A2 Family Members Possessing Triacylglycerol Lipase and Acylglycerol Transacylase Activities. *Journal of Biological Chemistry,* 279**,** 48968-48975.

JHALA, U. S., CANETTIERI, G., SCREATON, R. A., KULKARNI, R. N., KRAJEWSKI, S., REED, J., WALKER, J., LIN, X., WHITE, M. & MONTMINY, M. 2003. cAMP promotes pancreatic beta-cell survival via CREB-mediated induction of IRS2. *Genes Dev,* 17**,** 1575-80.

JIN, D.-H., PARK, J. & KIM, D.-H. 2015. MAPK15 is an attractive therapeutic target for gastric cancer. *Cancer Cell & Microenvironment,* 2.

JONES, R. M., LEONARD, J. N., BUZARD, D. J. & LEHMANN, J. 2009. GPR119 agonists for the treatment of type 2 diabetes. *Expert Opin Ther Pat,* 19**,** 1339-59.

JOOST, P. & METHNER, A. 2002. Phylogenetic analysis of 277 human G-protein-coupled receptors as a tool for the prediction of orphan receptor ligands. *Genome Biol,* 3**,** Research0063.

KAGAWA, Y. & RACKER, E. 1966. Partial resolution of the enzymes catalyzing oxidative phosphorylation. 8. Properties of a factor conferring oligomycin sensitivity on mitochondrial adenosine triphosphatase. *J Biol Chem,* 241**,** 2461-6.

KAKU, K., ARAKI, T. & YOSHINAKA, R. 2013. Randomized, Double-Blind, Dose-Ranging Study of TAK-875, a Novel GPR40 Agonist, in Japanese Patients With Inadequately Controlled Type 2 Diabetes. *Diabetes Care,* 36**,** 245-250.

KARAKI, S.-I., MITSUI, R., HAYASHI, H., KATO, I., SUGIYA, H., IWANAGA, T., FURNESS, J. & KUWAHARA, A. 2006. Short-chain fatty acid receptor, GPR43, is expressed by enteroendocrine cells and mucosal mast cells in rat intestine. *Cell and Tissue Research,* 324**,** 353-360.

KARAKI, S., TAZOE, H., HAYASHI, H., KASHIWABARA, H., TOOYAMA, K., SUZUKI, Y. & KUWAHARA, A. 2008. Expression of the short-chain fatty acid receptor, GPR43, in the human colon. *J Mol Histol,* 39**,** 135-42.

KARLSSON, M., CONTRERAS, J. A., HELLMAN, U., TORNQVIST, H. & HOLM, C. 1997. cDNA cloning, tissue distribution, and identification of the catalytic triad of monoglyceride lipase. Evolutionary relationship to esterases, lysophospholipases, and haloperoxidases. *J Biol Chem,* 272**,** 27218-23.

KASER, A., LEE, A. H., FRANKE, A., GLICKMAN, J. N., ZEISSIG, S., TILG, H., NIEUWENHUIS, E. E., HIGGINS, D. E., SCHREIBER, S., GLIMCHER, L. H. & BLUMBERG, R. S. 2008. XBP1 links ER stress to intestinal inflammation and confers genetic risk for human inflammatory bowel disease. *Cell,* 134**,** 743-56.

KATZ, M., AMIT, I. & YARDEN, Y. 2007. Regulation of MAPKs by growth factors and receptor tyrosine kinases. *Biochim Biophys Acta,* 1773**,** 1161-76.

KAUFMAN, R. J., BACK, S. H., SONG, B., HAN, J. & HASSLER, J. 2010. The unfolded protein response is required to maintain the integrity of the endoplasmic reticulum, prevent oxidative stress and preserve differentiation in beta-cells. *Diabetes Obes Metab,* 12 Suppl 2**,** 99-107.

KAUR, N., CHUGH, V. & GUPTA, A. K. 2014. Essential fatty acids as functional components of foods- a review. *J Food Sci Technol,* 51**,** 2289-303.

KAWASAKI, N., ASADA, R., SAITO, A., KANEMOTO, S. & IMAIZUMI, K. 2012. Obesity-induced endoplasmic reticulum stress causes chronic inflammation in adipose tissue. *Sci Rep,* 2**,** 799.

KAWATE, R., TALAN, M. I. & ENGEL, B. T. 1993. Aged C57BL/6J mice respond to cold with increased sympathetic nervous activity in interscapular brown adipose tissue. *J Gerontol,* 48**,** B180-3.

KEIPERT, S. & JASTROCH, M. 2014. Brite/beige fat and UCP1 - is it thermogenesis? *Biochim Biophys Acta,* 1837**,** 1075-82.

KERSHAW, E. E., HAMM, J. K., VERHAGEN, L. A., PERONI, O., KATIC, M. & FLIER, J. S. 2006. Adipose triglyceride lipase: function, regulation by insulin, and comparison with adiponutrin. *Diabetes,* 55**,** 148-57.

KERSTEN, S. 2001. Mechanisms of nutritional and hormonal regulation of lipogenesis. *EMBO Rep,* 2**,** 282-6.

KHOKHLATCHEV, A., XU, S., ENGLISH, J., WU, P., SCHAEFER, E. & COBB, M. H. 1997. Reconstitution of Mitogen-activated Protein Kinase Phosphorylation Cascades in Bacteria: EFFICIENT SYNTHESIS OF ACTIVE PROTEIN KINASES. *Journal of Biological Chemistry,* 272**,** 11057-11062.

KILROY, G., BURK, D. H. & FLOYD, Z. E. 2009. High efficiency lipid-based siRNA transfection of adipocytes in suspension. *PLoS One,* 4**,** e6940.

KIM, M. H., KANG, S. G., PARK, J. H., YANAGISAWA, M. & KIM, C. H. 2013. Short-Chain Fatty Acids Activate GPR41 and GPR43 on Intestinal Epithelial Cells to Promote Inflammatory Responses in Mice. *Gastroenterology*.

KIMURA, I., INOUE, D., MAEDA, T., HARA, T., ICHIMURA, A., MIYAUCHI, S., KOBAYASHI, M., HIRASAWA, A. & TSUJIMOTO, G. 2011. Short-chain fatty acids and ketones directly regulate sympathetic nervous system via G protein-coupled receptor 41 (GPR41). *Proc Natl Acad Sci U S A,* 108**,** 8030-5.

KIMURA, I., OZAWA, K., INOUE, D., IMAMURA, T., KIMURA, K., MAEDA, T., TERASAWA, K., KASHIHARA, D., HIRANO, K., TANI, T., TAKAHASHI, T., MIYAUCHI, S., SHIOI, G., INOUE, H. & TSUJIMOTO, G. 2013. The gut microbiota suppresses insulin-mediated fat accumulation via the short-chain fatty acid receptor GPR43. *Nat Commun,* 4**,** 1829.

KING, W. G., MATTALIANO, M. D., CHAN, T. O., TSICHLIS, P. N. & BRUGGE, J. S. 1997. Phosphatidylinositol 3-kinase is required for integrin-stimulated AKT and Raf-1/mitogen-activated protein kinase pathway activation. *Mol Cell Biol,* 17**,** 4406-18.

KJEMS, L. L., HOLST, J. J., VOLUND, A. & MADSBAD, S. 2003. The influence of GLP-1 on glucose-stimulated insulin secretion: effects on beta-cell sensitivity in type 2 and nondiabetic subjects. *Diabetes,* 52**,** 380-6.

KLAUS, S., ELY, M., ENCKE, D. & HELDMAIER, G. 1995. Functional assessment of white and brown adipocyte development and energy metabolism in cell culture. Dissociation of terminal differentiation and thermogenesis in brown adipocytes. *J Cell Sci,* 108 (Pt 10)**,** 3171-80.

KLEIN, J., FASSHAUER, M., KLEIN, H. H., BENITO, M. & KAHN, C. R. 2002. Novel adipocyte lines from brown fat: a model system for the study of differentiation, energy metabolism, and insulin action. *Bioessays,* 24**,** 382-8.

KLEUSS, C., RAW, A. S., LEE, E., SPRANG, S. R. & GILMAN, A. G. 1994. Mechanism of GTP hydrolysis by G-protein alpha subunits. *Proceedings of the National Academy of Sciences,* 91**,** 9828-9831.

KOPECKY, J., CLARKE, G., ENERB CK, S., SPIEGELMAN, B. & KOZAK, L. P. 1995. Expression of the mitochondrial uncoupling protein gene from the aP2 gene promoter prevents genetic obesity. *Journal of Clinical Investigation,* 96**,** 2914-2923.

KOTARSKY, K., NILSSON, N. E., FLODGREN, E., OWMAN, C. & OLDE, B. 2003a. A human cell surface receptor activated by free fatty acids and thiazolidinedione drugs. *Biochemical and Biophysical Research Communications,* 301**,** 406-410.

KOTARSKY, K., NILSSON, N. E., OLDE, B. & OWMAN, C. 2003b. Progress in Methodology Improved Reporter Gene Assays Used to Identify Ligands Acting on Orphan Seven-Transmembrane Receptors. *Pharmacology & Toxicology,* 93**,** 249-258.

KRAEMER, F. B. & SHEN, W.-J. 2002. Hormone-sensitive lipase: control of intracellular tri-(di-)acylglycerol and cholesteryl ester hydrolysis. *Journal of Lipid Research,* 43**,** 1585-1594.

KRAMER, A. H., JOOS-VANDEWALLE, J., EDKINS, A. L., FROST, C. L. & PRINSLOO, E. 2014. Real-time monitoring of 3T3-L1 preadipocyte differentiation using a commercially available electric cell-substrate impedance sensor system. *Biochemical and Biophysical Research Communications,* 443**,** 1245-1250.

KRINTEL, C., MORGELIN, M., LOGAN, D. T. & HOLM, C. 2009. Phosphorylation of hormone-sensitive lipase by protein kinase A in vitro promotes an increase in its hydrophobic surface area. *Febs j,* 276**,** 4752-62.

KULKARNI, A. A., WOELLER, C. F., THATCHER, T. H., RAMON, S., PHIPPS, R. P. & SIME, P. J. 2012. Emerging PPARgamma-Independent Role of PPARgamma Ligands in Lung Diseases. *PPAR Res,* 2012**,** 705352.

KUUSELA, P., NEDERGAARD, J. & CANNON, B. 1986. Beta-adrenergic stimulation of fatty acid release from brown fat cells differentiated in monolayer culture. *Life Sci,* 38**,** 589-99.

KYRIAKIS, J. M., APP, H., ZHANG, X. F., BANERJEE, P., BRAUTIGAN, D. L., RAPP, U. R. & AVRUCH, J. 1992. Raf-1 activates MAP kinase-kinase. *Nature,* 358**,** 417-21.

LAMMERS, B., CHANDAK, P. G., AFLAKI, E., VAN PUIJVELDE, G. H., RADOVIC, B., HILDEBRAND, R. B., MEURS, I., OUT, R., KUIPER, J., VAN BERKEL, T. J., KOLB, D., HAEMMERLE, G., ZECHNER, R., LEVAK-FRANK, S., VAN ECK, M. & KRATKY, D. 2011. Macrophage adipose triglyceride lipase deficiency attenuates atherosclerotic lesion development in low-density lipoprotein receptor knockout mice. *Arterioscler Thromb Vasc Biol,* 31**,** 67-73.

LAMMERT, O., GRUNNET, N., FABER, P., BJORNSBO, K. S., DICH, J., LARSEN, L. O., NEESE, R. A., HELLERSTEIN, M. K. & QUISTORFF, B. 2000. Effects of isoenergetic overfeeding of either carbohydrate or fat in young men. *Br J Nutr,* 84**,** 233-45.

LARSSON, N.-G., WANG, J., WILHELMSSON, H., OLDFORS, A., RUSTIN, P., LEWANDOSKI, M., BARSH, G. S. & CLAYTON, D. A. 1998. Mitochondrial transcription factor A is necessary for mtDNA maintance and embryogenesis in mice. *Nat Genet,* 18**,** 231-236.

LATTIN, J. E., SCHRODER, K., SU, A. I., WALKER, J. R., ZHANG, J., WILTSHIRE, T., SAIJO, K., GLASS, C. K., HUME, D. A., KELLIE, S. & SWEET, M. J. 2008. Expression analysis of G Protein-Coupled Receptors in mouse macrophages. *Immunome Res,* 4**,** 5.

LE POUL, E., LOISON, C., STRUYF, S., SPRINGAEL, J.-Y., LANNOY, V., DECOBECQ, M.-E., BREZILLON, S., DUPRIEZ, V., VASSART, G., VAN DAMME, J., PARMENTIER, M. & DETHEUX, M. 2003. Functional Characterization of Human Receptors for Short Chain Fatty Acids and Their Role in Polymorphonuclear Cell Activation. *Journal of Biological Chemistry,* 278**,** 25481-25489.

LEAN, M. E. J. & JAMES, W. P. T. 1983. Uncoupling protein in human brown adipose tissue mitochondria: Isolation and detection by specific antiserum. *FEBS Letters,* 163**,** 235-240.

LEE, A. H., CHU, G. C., IWAKOSHI, N. N. & GLIMCHER, L. H. 2005. XBP-1 is required for biogenesis of cellular secretory machinery of exocrine glands. *Embo j,* 24**,** 4368-80.

LEE, A. H., SCAPA, E. F., COHEN, D. E. & GLIMCHER, L. H. 2008. Regulation of hepatic lipogenesis by the transcription factor XBP1. *Science,* 320**,** 1492-6.

LEE, A. S. 2005. The ER chaperone and signaling regulator GRP78/BiP as a monitor of endoplasmic reticulum stress. *Methods,* 35**,** 373-381.

LEE, Y. H., JUNG, Y. S. & CHOI, D. 2014. Recent advance in brown adipose physiology and its therapeutic potential. *Exp Mol Med,* 46**,** e78.

LEFTEROVA, M. I., ZHANG, Y., STEGER, D. J., SCHUPP, M., SCHUG, J., CRISTANCHO, A., FENG, D., ZHUO, D., STOECKERT, C. J., LIU, X. S. & LAZAR, M. A. 2008. PPARγ and C/EBP factors orchestrate adipocyte biology via adjacent binding on a genome-wide scale. *Genes & Development,* 22**,** 2941-2952.

LEHMANN, D. M., SENEVIRATNE, A. M. & SMRCKA, A. V. 2008. Small molecule disruption of G protein beta gamma subunit signaling inhibits neutrophil chemotaxis and inflammation. *Mol Pharmacol,* 73**,** 410-8.

LEVINE, J. A., EBERHARDT, N. L. & JENSEN, M. D. 1999. Role of nonexercise activity thermogenesis in resistance to fat gain in humans. *Science,* 283**,** 212-4.

LI, G., YAO, W. & JIANG, H. 2014. Short-chain fatty acids enhance adipocyte differentiation in the stromal vascular fraction of porcine adipose tissue. *J Nutr,* 144**,** 1887-95.

LIANG, H. & WARD, W. F. 2006. PGC-1α: a key regulator of energy metabolism. *Advances in Physiology Education,* 30**,** 145-151.

LIAO, G.-Y., AN, J. J., GHARAMI, K., WATERHOUSE, E. G., VANEVSKI, F., JONES, K. R. & XU, B. 2012. Dendritically targeted Bdnf mRNA is essential for energy balance and response to leptin. *Nat Med,* 18**,** 564-571.

LIAW, C. W. & CONNOLLY, D. T. 2009. Sequence polymorphisms provide a common consensus sequence for GPR41 and GPR42. *DNA Cell Biol,* 28**,** 555-60.

LIEBERMAN, S., ENIG, M. G. & PREUSS, H. G. 2006. A Review of Monolaurin and Lauric Acid:Natural Virucidal and Bactericidal Agents. *Alternative and Complementary Therapies,* 12**,** 310-314.

LIN, D. C., ZHANG, J., ZHUANG, R., LI, F., NGUYEN, K., CHEN, M., TRAN, T., LOPEZ, E., LU, J. Y., LI, X. N., TANG, L., TONN, G. R., SWAMINATH, G., REAGAN, J. D., CHEN, J. L., TIAN, H., LIN, Y. J., HOUZE, J. B. & LUO, J. 2011. AMG 837: a novel GPR40/FFA1 agonist that enhances insulin secretion and lowers glucose levels in rodents. *PLoS One,* 6**,** e27270.

LINDBERG, O., DE PIERRE, J., RYLANDER, E. & AFZELIUS, B. A. 1967. Studies of the mitochondrial energy-transfer system of brown adipose tissue. *J Cell Biol,* 34**,** 293-310.

LIOU, H., BOOTHBY, M., FINN, P., DAVIDON, R., NABAVI, N., ZELEZNIK-LE, N., TING, J. & GLIMCHER, L. 1990. A new member of the leucine zipper class of proteins that binds to the HLA DR alpha promoter. *Science,* 247**,** 1581-1584.

LOBB, K. & CHOW, C. K. 2007. Fatty acid classification and nomenclature. *Fatty acids in foods and their health implications, 3rd edn. CRC Press, New York***,** 1-15.

LOEKEN, M. R. 1993. Effects of mutation of the CREB binding site of the somatostatin promoter on cyclic AMP responsiveness in CV-1 cells. *Gene Expr,* 3**,** 253-64.

LOPER, H. B., LA SALA, M., DOTSON, C. & STEINLE, N. 2015. Taste perception, associated hormonal modulation, and nutrient intake. *Nutrition Reviews,* 73**,** 83-91.

LOWE, M. R. & BUTRYN, M. L. 2007. Hedonic hunger: a new dimension of appetite? *Physiol Behav,* 91**,** 432-9.

LU, Z. L., SALDANHA, J. W. & HULME, E. C. 2002. Seven-transmembrane receptors: crystals clarify. *Trends Pharmacol Sci,* 23**,** 140-6.

MA, Y. & HENDERSHOT, L. M. 2003. Delineation of a negative feedback regulatory loop that controls protein translation during endoplasmic reticulum stress. *J Biol Chem,* 278**,** 34864-73.

MA, Y. & HENDERSHOT, L. M. 2004. ER chaperone functions during normal and stress conditions. *J Chem Neuroanat,* 28**,** 51-65.

MAALOUF, M., RHO, J. M. & MATTSON, M. P. 2009. The neuroprotective properties of calorie restriction, the ketogenic diet, and ketone bodies. *Brain Res Rev,* 59**,** 293-315.

MAEHAMA, T. & DIXON, J. E. 1999. PTEN: a tumour suppressor that functions as a phospholipid phosphatase. *Trends Cell Biol,* 9**,** 125-8.

MANDRUP, S. & LANE, M. D. 1997. Regulating Adipogenesis. *Journal of Biological Chemistry,* 272**,** 5367-5370.

MANGMOOL, S. & KUROSE, H. 2011. G(i/o) protein-dependent and -independent actions of Pertussis Toxin (PTX). *Toxins (Basel),* 3**,** 884-99.

MANN, A., THOMPSON, A., ROBBINS, N. & BLOMKALNS, A. L. 2014. Localization, identification, and excision of murine adipose depots. *J Vis Exp*.

MARIK, P. E. & VARON, J. 2009. Omega-3 dietary supplements and the risk of cardiovascular events: a systematic review. *Clin Cardiol,* 32**,** 365-72.

MARIMAN, E. C. & WANG, P. 2010. Adipocyte extracellular matrix composition, dynamics and role in obesity. *Cell Mol Life Sci,* 67**,** 1277-92.

MARTIN, C., PASSILLY-DEGRACE, P., CHEVROT, M., ANCEL, D., SPARKS, S. M., DRUCKER, D. J. & BESNARD, P. 2012. Lipid-mediated release of GLP-1 by mouse taste buds from circumvallate papillae: putative involvement of GPR120 and impact on taste sensitivity. *Journal of Lipid Research,* 53**,** 2256-2265.

MASHIMA, T., SEIMIYA, H. & TSURUO, T. 2009. De novo fatty-acid synthesis and related pathways as molecular targets for cancer therapy. *Br J Cancer,* 100**,** 1369-72.

MASLOWSKI, K. M., VIEIRA, A. T., NG, A., KRANICH, J., SIERRO, F., DI, Y., SCHILTER, H. C., ROLPH, M. S., MACKAY, F., ARTIS, D., XAVIER, R. J., TEIXEIRA, M. M. & MACKAY, C. R. 2009. Regulation of inflammatory responses by gut microbiota and chemoattractant receptor GPR43. *Nature,* 461**,** 1282-1286.

MATSUSHITA, M., YONESHIRO, T., AITA, S., KAMEYA, T., SUGIE, H. & SAITO, M. 2014. Impact of brown adipose tissue on body fatness and glucose metabolism in healthy humans. *Int J Obes (Lond),* 38**,** 812-7.

MATTHIAS, A., OHLSON, K. B. E., FREDRIKSSON, J. M., JACOBSSON, A., NEDERGAARD, J. & CANNON, B. 2000. Thermogenic Responses in Brown Fat Cells Are Fully UCP1-dependent: UCP2 OR UCP3 DO NOT SUBSTITUTE FOR UCP1 IN ADRENERGICALLY OR FATTY ACID-INDUCED THERMOGENESIS. *Journal of Biological Chemistry,* 275**,** 25073-25081.

MATTSSON, C. L., CSIKASZ, R. I., CHERNOGUBOVA, E., YAMAMOTO, D. L., HOGBERG, H. T., AMRI, E. Z., HUTCHINSON, D. S. & BENGTSSON, T. 2011. beta(1)-Adrenergic receptors increase UCP1 in human MADS brown adipocytes and rescue cold-acclimated beta(3)-adrenergic receptor-knockout mice via nonshivering thermogenesis. *Am J Physiol Endocrinol Metab,* 301**,** E1108-18.

MAYR, B. & MONTMINY, M. 2001. Transcriptional regulation by the phosphorylation-dependent factor CREB. *Nat Rev Mol Cell Biol,* 2**,** 599-609.

MCANINCH, E. A. & BIANCO, A. C. 2014. Thyroid hormone signaling in energy homeostasis and energy metabolism. *Ann N Y Acad Sci,* 1311**,** 77-87.

MCCUDDEN, C. R., HAINS, M. D., KIMPLE, R. J., SIDEROVSKI, D. P. & WILLARD, F. S. 2005. G-protein signaling: back to the future. *Cellular and Molecular Life Sciences,* 62**,** 551-577.

MEIER, J. J. & NAUCK, M. A. 2005. Glucagon-like peptide 1(GLP-1) in biology and pathology. *Diabetes Metab Res Rev,* 21**,** 91-117.

MERCER, S. W. & TRAYHURN, P. 1987. Effect of high fat diets on energy balance and thermogenesis in brown adipose tissue of lean and genetically obese ob/ob mice. *J Nutr,* 117**,** 2147-53.

MESCHER, A. 2009. *Junqueira's Basic Histology: Text and Atlas, 12th Edition : Text and Atlas: Text and Atlas*, Mcgraw-hill.

MESSINA, G., DE LUCA, V., VIGGIANO, A., ASCIONE, A., IANNACCONE, T., CHIEFFI, S. & MONDA, M. 2013. Autonomic nervous system in the control of energy balance and body weight: personal contributions. *Neurol Res Int,* 2013**,** 639280.

MIYAJIMA, T., TSUJINO, T., SAITO, K. & YOKOYAMA, M. 2001. Effects of eicosapentaenoic acid on blood pressure, cell membrane fatty acids, and intracellular sodium concentration in essential hypertension. *Hypertens Res,* 24**,** 537-42.

MIYAMOTO, T., KANEKO, A., KAKIZAWA, T., YAJIMA, H., KAMIJO, K., SEKINE, R., HIRAMATSU, K., NISHII, Y., HASHIMOTO, T. & HASHIZUME, K. 1997. Inhibition of peroxisome proliferator signaling pathways by thyroid hormone receptor. Competitive binding to the response element. *J Biol Chem,* 272**,** 7752-8.

MONDAL, A. K., DAS, S. K., VARMA, V., NOLEN, G. T., MCGEHEE, R. E., ELBEIN, S. C., WEI, J. Y. & RANGANATHAN, G. 2012. Effect of endoplasmic reticulum stress on inflammation and adiponectin regulation in human adipocytes. *Metab Syndr Relat Disord,* 10**,** 297-306.

MORENO, M., LOMBARDI, A., SILVESTRI, E., SENESE, R., CIOFFI, F., GOGLIA, F., LANNI, A. & DE LANGE, P. 2010. PPARs: Nuclear Receptors Controlled by, and Controlling, Nutrient Handling through Nuclear and Cytosolic Signaling. *PPAR Res,* 2010.

MOTTILLO, E. P., BLOCH, A. E., LEFF, T. & GRANNEMAN, J. G. 2012. Lipolytic Products Activate Peroxisome Proliferator-activated Receptor (PPAR) α and δ in Brown Adipocytes to Match Fatty Acid Oxidation with Supply. *Journal of Biological Chemistry,* 287**,** 25038-25048.

MUST, A., SPADANO, J., COAKLEY, E. H., FIELD, A. E., COLDITZ, G. & DIETZ, W. H. 1999. THe disease burden associated with overweight and obesity. *JAMA,* 282**,** 1523-1529.

NAGASAKI, H., KONDO, T., FUCHIGAMI, M., HASHIMOTO, H., SUGIMURA, Y., OZAKI, N., ARIMA, H., OTA, A., OISO, Y. & HAMADA, Y. 2012. Inflammatory changes in adipose

tissue enhance expression of GPR84, a medium-chain fatty acid receptor: TNFα enhances GPR84 expression in adipocytes. *FEBS Letters,* 586**,** 368-372.

NAGASHIMA, Y., MISHIBA, K.-I., SUZUKI, E., SHIMADA, Y., IWATA, Y. & KOIZUMI, N. 2011. Arabidopsis IRE1 catalyses unconventional splicing of bZIP60 mRNA to produce the active transcription factor. *Scientific Reports,* 1**,** 29.

NAKAMOTO, R. K., BAYLIS SCANLON, J. A. & AL-SHAWI, M. K. 2008. The rotary mechanism of the ATP synthase. *Arch Biochem Biophys,* 476**,** 43-50.

NAPOLITANO, L. 1963. The Differentiation of White Adipose Cells. An Electron Microscope Study. *J Cell Biol,* 18**,** 663-79.

NEDERGAARD, J. & LINDBERG, O. 1979. Norepinephrine-stimulated fatty-acid release and oxygen consumption in isolated hamster brown-fat cells. Influence of buffers, albumin, insulin and mitochondrial inhibitors. *Eur J Biochem,* 95**,** 139-45.

NIELSEN, T. S., VENDELBO, M. H., JESSEN, N., PEDERSEN, S. B., JORGENSEN, J. O., LUND, S. & MOLLER, N. 2011. Fasting, but not exercise, increases adipose triglyceride lipase (ATGL) protein and reduces G(0)/G(1) switch gene 2 (G0S2) protein and mRNA content in human adipose tissue. *J Clin Endocrinol Metab,* 96**,** E1293-7.

NISSEN, S. E., WOLSKI, K. & TOPOL, E. J. 2005. Effect of muraglitazar on death and major adverse cardiovascular events in patients with type 2 diabetes mellitus. *Jama,* 294**,** 2581-6.

NOGUEIRA, V., SUNDARARAJAN, D., KWAN, J. M., PENG, X. D., SARVEPALLI, N., SONENBERG, N. & HAY, N. 2012. Akt-dependent Skp2 mRNA translation is required for exiting contact inhibition, oncogenesis, and adipogenesis. *Embo j,* 31**,** 1134-46.

NUMA, S. 1984. *Fatty acid metabolism and its regulation*, Elsevier Science.

O'CONNOR, D. L., HALL, R., ADAMKIN, D., AUESTAD, N., CASTILLO, M., CONNOR, W. E., CONNOR, S. L., FITZGERALD, K., GROH-WARGO, S., HARTMANN, E. E., JACOBS, J., JANOWSKY, J., LUCAS, A., MARGESON, D., MENA, P., NEURINGER, M., NESIN, M., SINGER, L., STEPHENSON, T., SZABO, J., ZEMON, V. & A, O. B. O. T. R. P. L. S. 2001. Growth and Development in Preterm Infants Fed Long-Chain Polyunsaturated Fatty Acids: A Prospective, Randomized Controlled Trial. *Pediatrics,* 108**,** 359-371.

OAKES, N. D., THALEN, P., HULTSTRAND, T., JACINTO, S., CAMEJO, G., WALLIN, B. & LJUNG, B. 2005. Tesaglitazar, a dual PPAR{alpha}/{gamma} agonist, ameliorates glucose and lipid intolerance in obese Zucker rats. *Am J Physiol Regul Integr Comp Physiol,* 289**,** R938-46.

OH, DA Y. & OLEFSKY, JERROLD M. 2012. Omega 3 Fatty Acids and GPR120. *Cell metabolism,* 15**,** 564-565.

OH, D. Y., TALUKDAR, S., BAE, E. J., IMAMURA, T., MORINAGA, H., FAN, W., LI, P., LU, W. J., WATKINS, S. M. & OLEFSKY, J. M. 2010. GPR120 Is an Omega-3 Fatty Acid Receptor Mediating Potent Anti-inflammatory and Insulin-Sensitizing Effects. *Cell,* 142**,** 687-698.

OHIRA, H., FUJIOKA, Y., KATAGIRI, C., MAMOTO, R., AOYAMA-ISHIKAWA, M., AMAKO, K., IZUMI, Y., NISHIUMI, S., YOSHIDA, M., USAMI, M. & IKEDA, M. 2013. Butyrate Attenuates Inflammation and Lipolysis Generated by the Interaction of Adipocytes and Macrophages. *Journal of Atherosclerosis and Thrombosis,* 20**,** 425-442.

OHISHI, T. & YOSHIDA, S. 2012. The therapeutic potential of GPR119 agonists for type 2 diabetes. *Expert Opin Investig Drugs,* 21**,** 321-8.

OHNO, H., SHINODA, K., SPIEGELMAN, B. M. & KAJIMURA, S. 2012. PPARgamma agonists induce a white-to-brown fat conversion through stabilization of PRDM16 protein. *Cell Metab,* 15**,** 395-404.

OLSEN, H. & HALDOSEN, L. A. 2006. Peroxisome proliferator-activated receptor gamma regulates expression of signal transducer and activator of transcription 5A. *Exp Cell Res,* 312**,** 1371-80.

OLSON, B. J. S. C. & MARKWELL, J. 2001. Assays for Determination of Protein Concentration. *Current Protocols in Protein Science.* John Wiley & Sons, Inc.

OPIE, L. H. & WALFISH, P. G. 1963. Plasma Free Fatty Acid Concentrations in Obesity. *New England Journal of Medicine,* 268**,** 757-760.

ORTEGA-MOLINA, A., EFEYAN, A., LOPEZ-GUADAMILLAS, E., MU OZ-MARTIN, M., G MEZ-L PEZ, G., CA AMERO, M., MULERO, F., PASTOR, J., MARTINEZ, S., ROMANOS, E., MAR GONZALEZ-BARROSO, M., RIAL, E., VALVERDE, ANGELA M., BISCHOFF, JAMES R. & SERRANO, M. 2012. Pten Positively Regulates Brown Adipose Function, Energy Expenditure, and Longevity. *Cell metabolism,* 15**,** 382-394.

ORTEGA-MOLINA, A. & SERRANO, M. 2013. PTEN in cancer, metabolism, and aging. *Trends in Endocrinology & Metabolism,* 24**,** 184-189.

OSUGA, J.-I., ISHIBASHI, S., OKA, T., YAGYU, H., TOZAWA, R., FUJIMOTO, A., SHIONOIRI, F., YAHAGI, N., KRAEMER, F. B., TSUTSUMI, O. & YAMADA, N. 2000. Targeted disruption of hormone-sensitive lipase results in male sterility and adipocyte hypertrophy, but not in obesity. *Proceedings of the National Academy of Sciences,* 97**,** 787-792.

OUELLET, V., LABBE, S. M., BLONDIN, D. P., PHOENIX, S., GUERIN, B., HAMAN, F., TURCOTTE, E. E., RICHARD, D. & CARPENTIER, A. C. 2012. Brown adipose tissue oxidative metabolism contributes to energy expenditure during acute cold exposure in humans. *J Clin Invest,* 122**,** 545-52.

OVERINGTON, J. P., AL-LAZIKANI, B. & HOPKINS, A. L. 2006. How many drug targets are there? *Nat Rev Drug Discov,* 5**,** 993-996.

OVERTON, H. A., BABBS, A. J., DOEL, S. M., FYFE, M. C. T., GARDNER, L. S., GRIFFIN, G., JACKSON, H. C., PROCTER, M. J., RASAMISON, C. M., TANG-CHRISTENSEN, M., WIDDOWSON, P. S., WILLIAMS, G. M. & REYNET, C. 2006. Deorphanization of a G protein-coupled receptor for oleoylethanolamide and its use in the discovery of small-molecule hypophagic agents. *Cell metabolism,* 3**,** 167-175.

OVERTON, H. A., FYFE, M. C. T. & REYNET, C. 2008. GPR119, a novel G protein-coupled receptor target for the treatment of type 2 diabetes and obesity. *British Journal of Pharmacology,* 153**,** S76-S81.

OZCAN, U., YILMAZ, E., OZCAN, L., FURUHASHI, M., VAILLANCOURT, E., SMITH, R. O., GORGUN, C. Z. & HOTAMISLIGIL, G. S. 2006. Chemical chaperones reduce ER stress and restore glucose homeostasis in a mouse model of type 2 diabetes. *Science,* 313**,** 1137-40.

PARK, B. H., QIANG, L. & FARMER, S. R. 2004. Phosphorylation of C/EBPbeta at a consensus extracellular signal-regulated kinase/glycogen synthase kinase 3 site is required for the induction of adiponectin gene expression during the differentiation of mouse fibroblasts into adipocytes. *Mol Cell Biol,* 24**,** 8671-80.

PARK, J. Y., KIM, Y., IM, J. A., YOU, S. & LEE, H. 2014. Inhibition of Adipogenesis by Oligonol through Akt-mTOR Inhibition in 3T3-L1 Adipocytes. *Evid Based Complement Alternat Med,* 2014**,** 895272.

PECQUEUR, C., ALVES-GUERRA, M.-C., GELLY, C., L VI-MEYRUEIS, C., COUPLAN, E., COLLINS, S., RICQUIER, D., BOUILLAUD, F. & MIROUX, B. 2001. Uncoupling Protein 2, in Vivo Distribution, Induction upon Oxidative Stress, and Evidence for Translational Regulation. *Journal of Biological Chemistry,* 276**,** 8705-8712.

PENFORNIS, P., VIENGCHAREUN, S., LE MENUET, D., CLUZEAUD, F., ZENNARO, M. C. & LOMBES, M. 2000. The mineralocorticoid receptor mediates aldosterone-induced

differentiation of T37i cells into brown adipocytes. *Am J Physiol Endocrinol Metab,* 279**,** E386-94.

PENG, X.-D., XU, P.-Z., CHEN, M.-L., HAHN-WINDGASSEN, A., SKEEN, J., JACOBS, J., SUNDARARAJAN, D., CHEN, W. S., CRAWFORD, S. E., COLEMAN, K. G. & HAY, N. 2003. Dwarfism, impaired skin development, skeletal muscle atrophy, delayed bone development, and impeded adipogenesis in mice lacking Akt1 and Akt2. *Genes & Development,* 17**,** 1352-1365.

PERRY, K. J., JOHNSON, V. R., MALLOCH, E. L., FUKUI, L., WEVER, J., THOMAS, A. G., HAMILTON, P. W. & HENRY, J. J. 2010. The G-protein-coupled receptor, GPR84, is important for eye development in Xenopus laevis. *Developmental Dynamics,* 239**,** 3024-3037.

PFANNENBERG, C., WERNER, M. K., RIPKENS, S., STEF, I., DECKERT, A., SCHMADL, M., REIMOLD, M., HARING, H. U., CLAUSSEN, C. D. & STEFAN, N. 2010. Impact of age on the relationships of brown adipose tissue with sex and adiposity in humans. *Diabetes,* 59**,** 1789-93.

PIERCE, K. L. & LEFKOWITZ, R. J. 2001. Classical and new roles of [beta]-arrestins in the regulation of G-PROTEIN-COUPLED receptors. *Nat Rev Neurosci,* 2**,** 727-733.

PIERCE, K. L., PREMONT, R. T. & LEFKOWITZ, R. J. 2002. Seven-transmembrane receptors. *Nat Rev Mol Cell Biol,* 3**,** 639-650.

PIZZONERO, M., DUPONT, S., BABEL, M., BEAUMONT, S., BIENVENU, N., BLANQUE, R., CHEREL, L., CHRISTOPHE, T., CRESCENZI, B., DE LEMOS, E., DELERIVE, P., DEPREZ, P., DE VOS, S., DJATA, F., FLETCHER, S., KOPIEJEWSKI, S., L'EBRALY, C., LEFRANCOIS, J. M., LAVAZAIS, S., MANIOC, M., NELLES, L., OSTE, L., POLANCEC, D., QUENEHEN, V., SOULAS, F., TRIBALLEAU, N., VAN DER AAR, E. M., VANDEGHINSTE, N., WAKSELMAN, E., BRYS, R. & SANIERE, L. 2014. Discovery and optimization of an azetidine chemical series as a free fatty acid receptor 2 (FFA2) antagonist: from hit to clinic. *J Med Chem,* 57**,** 10044-57.

POLLOCK, N., GROGAN, C., PERRY, M., PEDLAR, C., COOKE, K., MORRISSEY, D. & DIMITRIOU, L. 2010. Bone-mineral density and other features of the female athlete triad in elite endurance runners: a longitudinal and cross-sectional observational study. *Int J Sport Nutr Exerc Metab,* 20**,** 418-26.

PUDDU, A., SANGUINETI, R., MONTECUCCO, F. & VIVIANI, G. L. 2014. Evidence for the gut microbiota short-chain fatty acids as key pathophysiological molecules improving diabetes. *Mediators Inflamm,* 2014**,** 162021.

PUIGSERVER, P. 2005. Tissue-specific regulation of metabolic pathways through the transcriptional coactivator PGC1-[alpha]. *Int J Obes Relat Metab Disord,* 29**,** S5-S9.

PUIGSERVER, P., WU, Z., PARK, C. W., GRAVES, R., WRIGHT, M. & SPIEGELMAN, B. M. 1998. A cold-inducible coactivator of nuclear receptors linked to adaptive thermogenesis. *Cell,* 92**,** 829-39.

QI, L., SABERI, M., ZMUDA, E., WANG, Y., ALTAREJOS, J., ZHANG, X., DENTIN, R., HEDRICK, S., BANDYOPADHYAY, G., HAI, T., OLEFSKY, J. & MONTMINY, M. 2009. Adipocyte CREB promotes insulin resistance in obesity. *Cell Metab,* 9**,** 277-86.

QIAN, H. & BEARD, D. A. 2006. Metabolic futile cycles and their functions: a systems analysis of energy and control. *Syst Biol (Stevenage),* 153**,** 192-200.

RAMSEY, J. J., COLMAN, R. J., SWICK, A. G. & KEMNITZ, J. W. 1998. Energy expenditure, body composition, and glucose metabolism in lean and obese rhesus monkeys treated with ephedrine and caffeine. *Am J Clin Nutr,* 68**,** 42-51.

REED, G. W. & HILL, J. O. 1996. Measuring the thermic effect of food. *Am J Clin Nutr,* 63**,** 164-9.

REGARD, J. B., SATO, I. T. & COUGHLIN, S. R. 2008. Anatomical profiling of G protein-coupled receptor expression. *Cell,* 135**,** 561-71.

REICHERT, M. & EICK, D. 1999. Analysis of cell cycle arrest in adipocyte differentiation. *Oncogene,* 18**,** 459-66.

REIFEL-MILLER, A., OTTO, K., HAWKINS, E., BARR, R., BENSCH, W. R., BULL, C., DANA, S., KLAUSING, K., MARTIN, J. A., RAFAELOFF-PHAIL, R., RAFIZADEH-MONTROSE, C., RHODES, G., ROBEY, R., ROJO, I., RUNGTA, D., SNYDER, D., WILBUR, K., ZHANG, T., ZINK, R., WARSHAWSKY, A. & BROZINICK, J. T. 2005. A peroxisome proliferator-activated receptor alpha/gamma dual agonist with a unique in vitro profile and potent glucose and lipid effects in rodent models of type 2 diabetes and dyslipidemia. *Mol Endocrinol,* 19**,** 1593-605.

REIMOLD, A. M., ETKIN, A., CLAUSS, I., PERKINS, A., FRIEND, D. S., ZHANG, J., HORTON, H. F., SCOTT, A., ORKIN, S. H., BYRNE, M. C., GRUSBY, M. J. & GLIMCHER, L. H. 2000. An essential role in liver development for transcription factor XBP-1. *Genes Dev,* 14**,** 152-7.

REIMOLD, A. M., IWAKOSHI, N. N., MANIS, J., VALLABHAJOSYULA, P., SZOMOLANYI-TSUDA, E., GRAVALLESE, E. M., FRIEND, D., GRUSBY, M. J., ALT, F. & GLIMCHER, L. H. 2001. Plasma cell differentiation requires the transcription factor XBP-1. *Nature,* 412**,** 300-7.

RENSING, D. T., UPPAL, S., BLUMER, K. J. & MOELLER, K. D. 2015. Toward the Selective Inhibition of G Proteins: Total Synthesis of a Simplified YM-254890 Analog. *Org Lett,* 17**,** 2270-3.

REUSCH, J. E., COLTON, L. A. & KLEMM, D. J. 2000. CREB activation induces adipogenesis in 3T3-L1 cells. *Mol Cell Biol,* 20**,** 1008-20.

RICQUIER, D. & BOUILLAUD, F. 2000. Mitochondrial uncoupling proteins: from mitochondria to the regulation of energy balance. *The Journal of Physiology,* 529**,** 3-10.

RIOBO, N. A. & MANNING, D. R. 2005. Receptors coupled to heterotrimeric G proteins of the G12 family. *Trends in pharmacological sciences,* 26**,** 146-154.

RITTER, S. L. & HALL, R. A. 2009. Fine-tuning of GPCR activity by receptor-interacting proteins. *Nat Rev Mol Cell Biol,* 10**,** 819-30.

ROBERTSON, M. D., BICKERTON, A. S., DENNIS, A. L., VIDAL, H. & FRAYN, K. N. 2005. Insulin-sensitizing effects of dietary resistant starch and effects on skeletal muscle and adipose tissue metabolism. *The American Journal of Clinical Nutrition,* 82**,** 559-567.

ROEDIGER, W. E. 1980. Role of anaerobic bacteria in the metabolic welfare of the colonic mucosa in man. *Gut,* 21**,** 793-8.

RONG, J. X., QIU, Y., HANSEN, M. K., ZHU, L., ZHANG, V., XIE, M., OKAMOTO, Y., MATTIE, M. D., HIGASHIYAMA, H., ASANO, S., STRUM, J. C. & RYAN, T. E. 2007. Adipose Mitochondrial Biogenesis Is Suppressed in db/db and High-Fat Diet–Fed Mice and Improved by Rosiglitazone. *Diabetes,* 56**,** 1751-1760.

ROSEN, E. D. & MACDOUGALD, O. A. 2006. Adipocyte differentiation from the inside out. *Nat Rev Mol Cell Biol,* 7**,** 885-896.

ROSEN, E. D., WALKEY, C. J., PUIGSERVER, P. & SPIEGELMAN, B. M. 2000. Transcriptional regulation of adipogenesis. *Genes Dev,* 14**,** 1293-307.

ROSENBAUM, M. & LEIBEL, R. L. 2010. Adaptive thermogenesis in humans. *Int J Obes (Lond),* 34 Suppl 1**,** S47-55.

ROSS, E. M. 2011. G{alpha}q and Phospholipase C-{beta}: Turn On, Turn Off, and Do It Fast. *Sci. Signal.,* 4**,** pe5-.

ROUSSET, S., ALVES-GUERRA, M.-C., MOZO, J., MIROUX, B., CASSARD-DOULCIER, A.-M., BOUILLAUD, F. & RICQUIER, D. 2004. The Biology of Mitochondrial Uncoupling Proteins. *Diabetes,* 53**,** S130-S135.

SAHURI-ARISOYLU, M., BRODY, L. P., PARKINSON, J. R., PARKES, H., NAVARATNAM, N., MILLER, A. D., THOMAS, E. L., FROST, G. & BELL, J. D. 2016. Reprogramming of hepatic fat accumulation and 'browning' of adipose tissue by the short-chain fatty acid acetate. *Int J Obes (Lond)*.

SALIH, E. 2005. Phosphoproteomics by mass spectrometry and classical protein chemistry approaches. *Mass Spectrom Rev,* 24**,** 828-46.

SALON, J. A., LODOWSKI, D. T. & PALCZEWSKI, K. 2011. The Significance of G Protein-Coupled Receptor Crystallography for Drug Discovery. *Pharmacological Reviews,* 63**,** 901-937.

SANCHEZ-GURMACHES, J. & GUERTIN, D. A. 2014. Adipocyte lineages: tracing back the origins of fat. *Biochim Biophys Acta,* 1842**,** 340-51.

SAWZDARGO, M., GEORGE, S. R., NGUYEN, T., XU, S., KOLAKOWSKI JR, L. F. & O'DOWD, B. F. 1997. A Cluster of Four Novel Human G Protein-Coupled Receptor Genes Occurring in Close Proximity to CD22 Gene on Chromosome 19q13.1. *Biochemical and Biophysical Research Communications,* 239**,** 543-547.

SCARPULLA, R. C. 2011. Metabolic control of mitochondrial biogenesis through the PGC-1 family regulatory network. *Biochim Biophys Acta,* 1813**,** 1269-78.

SCHAFFER, J. E. & LODISH, H. F. 1994. Expression cloning and characterization of a novel adipocyte long chain fatty acid transport protein. *Cell,* 79**,** 427-36.

SCHERER, P. E. 2006. Adipose Tissue: From Lipid Storage Compartment to Endocrine Organ. *Diabetes,* 55**,** 1537-1545.

SCHROEDER, F., JOLLY, C. A., CHO, T. H. & FROLOV, A. 1998. Fatty acid binding protein isoforms: structure and function. *Chem Phys Lipids,* 92**,** 1-25.

SEALE, P. 2010. Transcriptional control of brown adipocyte development and thermogenesis. *Int J Obes,* 34**,** S17-S22.

SEGER, R. & KREBS, E. G. 1995. The MAPK signaling cascade. *The FASEB Journal,* 9**,** 726-35.

SELJESET, S. & SIEHLER, S. 2012. Receptor-specific regulation of ERK1/2 activation by members of the “free fatty acid receptor” family. *Journal of Receptors and Signal Transduction,* 32**,** 196-201.

SHA, H., HE, Y., CHEN, H., WANG, C., ZENNO, A., SHI, H., YANG, X., ZHANG, X. & QI, L. 2009. The IRE1alpha-XBP1 pathway of the unfolded protein response is required for adipogenesis. *Cell Metab,* 9**,** 556-64.

SHAH, P., NANKOVA, B. B., PARAB, S. & LA GAMMA, E. F. 2006. Short chain fatty acids induce TH gene expression via ERK-dependent phosphorylation of CREB protein. *Brain Res,* 1107**,** 13-23.

SHAN, T., LIANG, X., BI, P., ZHANG, P., LIU, W. & KUANG, S. 2013. Distinct populations of adipogenic and myogenic Myf5-lineage progenitors in white adipose tissues. *J Lipid Res,* 54**,** 2214-24.

SHAO, D. & LAZAR, M. A. 1997. Peroxisome Proliferator Activated Receptor , CCAAT/ Enhancer-binding Protein , and Cell Cycle Status Regulate the Commitment to Adipocyte Differentiation. *Journal of Biological Chemistry,* 272**,** 21473-21478.

SHARMA, N., LOPEZ, D. I. & NYBORG, J. K. 2007. DNA binding and phosphorylation induce conformational alterations in the kinase-inducible domain of CREB. Implications for the mechanism of transcription function. *J Biol Chem,* 282**,** 19872-83.

SHAYWITZ, A. J. & GREENBERG, M. E. 1999. CREB: a stimulus-induced transcription factor activated by a diverse array of extracellular signals. *Annu Rev Biochem,* 68**,** 821-61.

SHEN, J. & PRYWES, R. 2004. Dependence of site-2 protease cleavage of ATF6 on prior site-1 protease digestion is determined by the size of the luminal domain of ATF6. *J Biol Chem,* 279**,** 43046-51.

SHIN, S. Y., RATH, O., CHOO, S. M., FEE, F., MCFERRAN, B., KOLCH, W. & CHO, K. H. 2009. Positive- and negative-feedback regulations coordinate the dynamic behavior of the Ras-Raf-MEK-ERK signal transduction pathway. *J Cell Sci,* 122**,** 425-35.

SIEGRIST-KAISER, C. A., PAULI, V., JUGE-AUBRY, C. E., BOSS, O., PERNIN, A., CHIN, W. W., CUSIN, I., ROHNER-JEANRENAUD, F., BURGER, A. G., ZAPF, J. & MEIER, C. A. 1997. Direct effects of leptin on brown and white adipose tissue. *J Clin Invest,* 100**,** 2858-64.

SIERSBAEK, R., NIELSEN, R. & MANDRUP, S. 2010. PPARgamma in adipocyte differentiation and metabolism--novel insights from genome-wide studies. *FEBS Lett,* 584**,** 3242-9.

SIMON, M. I., STRATHMANN, M. P. & GAUTAM, N. 1991. Diversity of G proteins in signal transduction. *Science,* 252**,** 802-8.

SIMONDS, W. F. 1999. G protein regulation of adenylate cyclase. *Trends in pharmacological sciences,* 20**,** 66-73.

SINA, C., GAVRILOVA, O., F RSTER, M., TILL, A., DERER, S., HILDEBRAND, F., RAABE, B., CHALARIS, A., SCHELLER, J., REHMANN, A., FRANKE, A., OTT, S., H SLER, R., NIKOLAUS, S., F LSCH, U. R., ROSE-JOHN, S., JIANG, H.-P., LI, J., SCHREIBER, S. & ROSENSTIEL, P. 2009. G Protein-Coupled Receptor 43 Is Essential for Neutrophil Recruitment during Intestinal Inflammation. *The Journal of Immunology,* 183**,** 7514-7522.

SINGH, S., LOKE, Y. K. & FURBERG, C. D. 2007. Thiazolidinediones and Heart Failure: A teleo-analysis. *Diabetes Care,* 30**,** 2148-2153.

SIRI-TARINO, P. W., SUN, Q., HU, F. B. & KRAUSS, R. M. 2010. Meta-analysis of prospective cohort studies evaluating the association of saturated fat with cardiovascular disease. *The American Journal of Clinical Nutrition*.

SKRUMSAGER, B. K., NIELSEN, K. K., MULLER, M., PABST, G., DRAKE, P. G. & EDSBERG, B. 2003. Ragaglitazar: the pharmacokinetics, pharmacodynamics, and tolerability of a novel dual PPAR alpha and gamma agonist in healthy subjects and patients with type 2 diabetes. *J Clin Pharmacol,* 43**,** 1244-56.

SLAVIN, J. 2013. Fiber and prebiotics: mechanisms and health benefits. *Nutrients,* 5**,** 1417-35.

SONG, M. S., SALMENA, L. & PANDOLFI, P. P. 2012. The functions and regulation of the PTEN tumour suppressor. *Nat Rev Mol Cell Biol,* 13**,** 283-296.

STAMBOLIC, V., SUZUKI, A., DE LA POMPA, J. L., BROTHERS, G. M., MIRTSOS, C., SASAKI, T., RULAND, J., PENNINGER, J. M., SIDEROVSKI, D. P. & MAK, T. W. 1998. Negative regulation of PKB/Akt-dependent cell survival by the tumor suppressor PTEN. *Cell,* 95**,** 29-39.

STEPHENS, J. M., MORRISON, R. F. & PILCH, P. F. 1996. The expression and regulation of STATs during 3T3-L1 adipocyte differentiation. *J Biol Chem,* 271**,** 10441-4.

STEPHENS, M., LUDGATE, M. & REES, D. A. 2011. Brown fat and obesity: the next big thing? *Clinical Endocrinology,* 74**,** 661-670.

STEWART, W. C., PEARCY, L. A., FLOYD, Z. E. & STEPHENS, J. M. 2011. STAT5A Expression in Swiss 3T3 Cells Promotes Adipogenesis In Vivo in an Athymic Mice Model System. *Obesity,* 19**,** 1731-1734.

STODDART, L. A., SMITH, N. J., JENKINS, L., BROWN, A. J. & MILLIGAN, G. 2008. Conserved Polar Residues in Transmembrane Domains V, VI, and VII of Free Fatty Acid Receptor 2 and Free Fatty Acid Receptor 3 Are Required for the Binding and

Function of Short Chain Fatty Acids. *Journal of Biological Chemistry,* 283**,** 32913-32924.

STRAND, O., VAUGHAN, M. & STEINBERG, D. 1964. Rat Adipose Tissue Lipases: Hormone-Sensitive Lipase Activity against Triglycerides Compared with Activity against Lower Glycerides. *J Lipid Res,* 5**,** 554-62.

SUM, C. S., TIKHONOVA, I. G., NEUMANN, S., ENGEL, S., RAAKA, B. M., COSTANZI, S. & GERSHENGORN, M. C. 2007. Identification of Residues Important for Agonist Recognition and Activation in GPR40. *Journal of Biological Chemistry,* 282**,** 29248-29255.

SUZUKI, T., IGARI, S.-I., HIRASAWA, A., HATA, M., ISHIGURO, M., FUJIEDA, H., ITOH, Y., HIRANO, T., NAKAGAWA, H., OGURA, M., MAKISHIMA, M., TSUJIMOTO, G. & MIYATA, N. 2008. Identification of G protein-coupled receptor 120-selective agonists derived from PPARγ agonists. *Journal of Medicinal Chemistry,* 51**,** 7640-7644.

SWAIN, P. S. & SIGGIA, E. D. 2002. The role of proofreading in signal transduction specificity. *Biophys J,* 82**,** 2928-33.

TAKEDA, S., YAMAMOTO, A., OKADA, T., MATSUMURA, E., NOSE, E., KOGURE, K., KOJIMA, S. & HAGA, T. 2003. Identification of surrogate ligands for orphan G protein-coupled receptors. *Life Sciences,* 74**,** 367-377.

TAKEUCHI, M., HIRASAWA, A., HARA, T., KIMURA, I., HIRANO, T., SUZUKI, T., MIYATA, N., AWAJI, T., ISHIGURO, M. & TSUJIMOTO, G. 2013. FFA1-selective agonistic activity based on docking simulation using FFA1 and GPR120 homology models. *Br J Pharmacol,* 168**,** 1570-83.

TALUKDAR, S., OLEFSKY, J. M. & OSBORN, O. 2011. Targeting GPR120 and other fatty acid-sensing GPCRs ameliorates insulin resistance and inflammatory diseases. *Trends in Pharmacological Sciences,* 32**,** 543-550.

TAMORI, Y., MASUGI, J., NISHINO, N. & KASUGA, M. 2002. Role of Peroxisome Proliferator-Activated Receptor-γ in Maintenance of the Characteristics of Mature 3T3-L1 Adipocytes. *Diabetes,* 51**,** 2045-2055.

TANG, Q. Q., OTTO, T. C. & LANE, M. D. 2003. Mitotic clonal expansion: a synchronous process required for adipogenesis. *Proc Natl Acad Sci U S A,* 100**,** 44-9.

TEETER, M. E., BAGINSKY, M. L. & HATEFI, Y. 1969. Ectopic inhibition of the complexes of the electron transport system by rotenone, piericidin A, demerol and antimycin A. *Biochim Biophys Acta,* 172**,** 331-3.

TEGLUND, S., MCKAY, C., SCHUETZ, E., VAN DEURSEN, J. M., STRAVOPODIS, D., WANG, D., BROWN, M., BODNER, S., GROSVELD, G. & IHLE, J. N. 1998. Stat5a and Stat5b proteins have essential and nonessential, or redundant, roles in cytokine responses. *Cell,* 93**,** 841-50.

TESKE, B. F., WEK, S. A., BUNPO, P., CUNDIFF, J. K., MCCLINTICK, J. N., ANTHONY, T. G. & WEK, R. C. 2011. The eIF2 kinase PERK and the integrated stress response facilitate activation of ATF6 during endoplasmic reticulum stress. *Mol Biol Cell,* 22**,** 4390-405.

THATTAI, M. & VAN OUDENAARDEN, A. 2002. Attenuation of noise in ultrasensitive signaling cascades. *Biophys J,* 82**,** 2943-50.

TILLEY, D. G. 2011. G Protein–Dependent and G Protein–Independent Signaling Pathways and Their Impact on Cardiac Function. *Circulation Research,* 109**,** 217-230.

TIRABY, C., TAVERNIER, G., LEFORT, C., LARROUY, D., BOUILLAUD, F., RICQUIER, D. & LANGIN, D. 2003. Acquirement of brown fat cell features by human white adipocytes. *J Biol Chem,* 278**,** 33370-6.

TOLHURST, G., HEFFRON, H., LAM, Y. S., PARKER, H. E., HABIB, A. M., DIAKOGIANNAKI, E., CAMERON, J., GROSSE, J., REIMANN, F. & GRIBBLE, F. M. 2012. Short-chain fatty

acids stimulate glucagon-like peptide-1 secretion via the G-protein-coupled receptor FFAR2. *Diabetes,* 61**,** 364-71.

TOLLINGER, C. D., VREMAN, H. J. & WEINER, M. W. 1979. Measurement of acetate in human blood by gas chromatography: effects of sample preparation, feeding, and various diseases. *Clin Chem,* 25**,** 1787-90.

TOMITA, T., MASUZAKI, H., IWAKURA, H., FUJIKURA, J., NOGUCHI, M., TANAKA, T., EBIHARA, K., KAWAMURA, J., KOMOTO, I., KAWAGUCHI, Y., FUJIMOTO, K., DOI, R., SHIMADA, Y., HOSODA, K., IMAMURA, M. & NAKAO, K. 2006. Expression of the gene for a membrane-bound fatty acid receptor in the pancreas and islet cell tumours in humans: evidence for GPR40 expression in pancreatic beta cells and implications for insulin secretion. *Diabetologia,* 49**,** 962-968.

TOPPING, D. L. & CLIFTON, P. M. 2001. Short-chain fatty acids and human colonic function: roles of resistant starch and nonstarch polysaccharides. *Physiol Rev,* 81**,** 1031-64.

TORMOS, KATHRYN V., ANSO, E., HAMANAKA, ROBERT B., EISENBART, J., JOSEPH, J., KALYANARAMAN, B. & CHANDEL, NAVDEEP S. 2011. Mitochondrial Complex III ROS Regulate Adipocyte Differentiation. *Cell metabolism,* 14**,** 537-544.

TOWNSEND, K. L. & TSENG, Y. H. 2014. Brown fat fuel utilization and thermogenesis. *Trends Endocrinol Metab,* 25**,** 168-77.

TREMBLAY, A., DESPRES, J. P., THERIAULT, G., FOURNIER, G. & BOUCHARD, C. 1992. Overfeeding and energy expenditure in humans. *Am J Clin Nutr,* 56**,** 857-62.

TROMPETTE, A., GOLLWITZER, E. S., YADAVA, K., SICHELSTIEL, A. K., SPRENGER, N., NGOM-BRU, C., BLANCHARD, C., JUNT, T., NICOD, L. P., HARRIS, N. L. & MARSLAND, B. J. 2014. Gut microbiota metabolism of dietary fiber influences allergic airway disease and hematopoiesis. *Nat Med,* 20**,** 159-166.

TSUJI, H., KASAI, M., TAKEUCHI, H., NAKAMURA, M., OKAZAKI, M. & KONDO, K. 2001. Dietary medium-chain triacylglycerols suppress accumulation of body fat in a double-blind, controlled trial in healthy men and women. *J Nutr,* 131**,** 2853-9.

TURNER, R. M., KWOK, C. S., CHEN-TURNER, C., MADUAKOR, C. A., SINGH, S. & LOKE, Y. K. 2014. Thiazolidinediones and associated risk of bladder cancer: a systematic review and meta-analysis. *Br J Clin Pharmacol,* 78**,** 258-73.

TUTEJA, N. 2009. Signaling through G protein coupled receptors. *Plant Signaling & Behavior,* 4**,** 942-947.

UKROPEC, J., ANUNCIADO, R. V., RAVUSSIN, Y. & KOZAK, L. P. 2006. Leptin is required for uncoupling protein-1-independent thermogenesis during cold stress. *Endocrinology,* 147**,** 2468-80.

URANO, F., WANG, X., BERTOLOTTI, A., ZHANG, Y., CHUNG, P., HARDING, H. P. & RON, D. 2000. Coupling of Stress in the ER to Activation of JNK Protein Kinases by Transmembrane Protein Kinase IRE1. *Science,* 287**,** 664-666.

VALVERDE, A. M., BENITO, M. & LORENZO, M. 2005. The brown adipose cell: a model for understanding the molecular mechanisms of insulin resistance. *Acta Physiologica Scandinavica,* 183**,** 59-73.

VAUGHAN, M., BERGER, J. E. & STEINBERG, D. 1964. Hormone-sensitive Lipase and Monoglyceride Lipase Activities in Adipose Tissue. *Journal of Biological Chemistry,* 239**,** 401-409.

VELAZQUEZ, O. C., LEDERER, H. M. & ROMBEAU, J. L. 1997. Butyrate and the colonocyte. Production, absorption, metabolism, and therapeutic implications. *Adv Exp Med Biol,* 427**,** 123-34.

VERMEIRE, S., KOJECKY, V., KNOFLICEK, V., REINISCH, W., VAN KAEM, T., NAMOUR, F., BEETENS, J. & VANHOUTTE, F. 2015. DOP030. GLPG0974, an FFA2 antagonist, in

ulcerative colitis: efficacy and safety in a multicenter proof-of-concept study. *Journal of Crohn's and Colitis,* 9**,** S39-S39.

VERNIA, P., MARCHEGGIANO, A., CAPRILLI, R., FRIERI, G., CORRAO, G., VALPIANI, D., DI PAOLO, M. C., PAOLUZI, P. & TORSOLI, A. 1995. Short-chain fatty acid topical treatment in distal ulcerative colitis. *Aliment Pharmacol Ther,* 9**,** 309-13.

VILLENA, J. A., ROY, S., SARKADI-NAGY, E., KIM, K.-H. & SUL, H. S. 2004. Desnutrin, an Adipocyte Gene Encoding a Novel Patatin Domain-containing Protein, Is Induced by Fasting and Glucocorticoids: ECTOPIC EXPRESSION OF DESNUTRIN INCREASES TRIGLYCERIDE HYDROLYSIS. *Journal of Biological Chemistry,* 279**,** 47066-47075.

VINOLO, M. A. R., FERGUSON, G. J., KULKARNI, S., DAMOULAKIS, G., ANDERSON, K., BOHLOOLY-Y, M., STEPHENS, L., HAWKINS, P. T. & CURI, R. 2011. SCFAs Induce Mouse Neutrophil Chemotaxis through the GPR43 Receptor. *PLoS ONE,* 6**,** e21205.

VIRTANEN, K. A., LIDELL, M. E., ORAVA, J., HEGLIND, M., WESTERGREN, R., NIEMI, T., TAITTONEN, M., LAINE, J., SAVISTO, N. J., ENERB CK, S. & NUUTILA, P. 2009. Functional brown adipose tissue in healthy adults. *New England Journal of Medicine,* 360**,** 1518-1525.

VISWAKARMA, N., JIA, Y., BAI, L., VLUGGENS, A., BORENSZTAJN, J., XU, J. & REDDY, J. K. 2010. Coactivators in PPAR-Regulated Gene Expression. *PPAR Research,* 2010**,** 21.

VLACHAKIS, D. 2007. *Adipocyte Viability and Ldh*, Dimitrios P Vlachakis.

VO, N. & GOODMAN, R. H. 2001. CREB-binding Protein and p300 in Transcriptional Regulation. *Journal of Biological Chemistry,* 276**,** 13505-13508.

WADOSKY, K. M. & WILLIS, M. S. 2012. The story so far: post-translational regulation of peroxisome proliferator-activated receptors by ubiquitination and SUMOylation. *American Journal of Physiology - Heart and Circulatory Physiology,* 302**,** H515-H526.

WALSH, S. P., SEVERINO, A., ZHOU, C., HE, J., LIANG, G.-B., TAN, C. P., CAO, J., EIERMANN, G. J., XU, L., SALITURO, G., HOWARD, A. D., MILLS, S. G. & YANG, L. 2011. 3-Substituted 3-(4-aryloxyaryl)-propanoic acids as GPR40 agonists. *Bioorganic & Medicinal Chemistry Letters,* 21**,** 3390-3394.

WANG, A., SI, H., LIU, D. & JIANG, H. 2012. Butyrate activates the cAMP-protein kinase A-cAMP response element-binding protein signaling pathway in Caco-2 cells. *J Nutr,* 142**,** 1-6.

WANG, D., GREEN, M. F., MCDONNELL, E. & HIRSCHEY, M. D. 2013a. Oxygen Flux Analysis to Understand the Biological Function of Sirtuins. *In:* HIRSCHEY, D. M. (ed.) *Sirtuins: Methods and Protocols.* Totowa, NJ: Humana Press.

WANG, J., WU, X., SIMONAVICIUS, N., TIAN, H. & LING, L. 2006. Medium-chain Fatty Acids as Ligands for Orphan G Protein-coupled Receptor GPR84. *Journal of Biological Chemistry,* 281**,** 34457-34464.

WANG, J. F., FU, S. P., LI, S. N., HU, Z. M., XUE, W. J., LI, Z. Q., HUANG, B. X., LV, Q. K., LIU, J. X. & WANG, W. 2013b. Short-chain fatty acids inhibit growth hormone and prolactin gene transcription via cAMP/PKA/CREB signaling pathway in dairy cow anterior pituitary cells. *Int J Mol Sci,* 14**,** 21474-88.

WANG, S. P., LAURIN, N., HIMMS-HAGEN, J., RUDNICKI, M. A., LEVY, E., ROBERT, M.-F., PAN, L., OLIGNY, L. & MITCHELL, G. A. 2001. The Adipose Tissue Phenotype of Hormone-Sensitive Lipase Deficiency in Mice. *Obesity Research,* 9**,** 119-128.

WANG, Y. X., LEE, C. H., TIEP, S., YU, R. T., HAM, J., KANG, H. & EVANS, R. M. 2003. Peroxisome-proliferator-activated receptor delta activates fat metabolism to prevent obesity. *Cell,* 113**,** 159-70.

WATSON, S. 2008. *Trans Fats*, Rosen Central.

WELLE, S. & CAMPBELL, R. G. 1983. Stimulation of thermogenesis by carbohydrate overfeeding. Evidence against sympathetic nervous system mediation. *J Clin Invest,* 71**,** 916-25.

WERKMAN, S. H. & CARLSON, S. E. 1996. A randomized trial of visual attention of preterm infants fed docosahexaenoic acid until nine months. *Lipids,* 31**,** 91-7.

WESTERTERP, K. R. 2004. Diet induced thermogenesis. *Nutr Metab (Lond),* 1**,** 5.

WESTERTERP, K. R. 2013. Physical activity and physical activity induced energy expenditure in humans: measurement, determinants, and effects. *Front Physiol,* 4**,** 90.

WILLATTS, P., FORSYTH, J. S., DIMODUGNO, M. K., VARMA, S. & COLVIN, M. 1998a. Effect of long-chain polyunsaturated fatty acids in infant formula on problem solving at 10 months of age. *The Lancet,* 352**,** 688-691.

WILLATTS, P., FORSYTH, J. S., DIMODUGNO, M. K., VARMA, S. & COLVIN, M. 1998b. Influence of long-chain polyunsaturated fatty acids on infant cognitive function. *Lipids,* 33**,** 973-80.

WITTENBERGER, T., SCHALLER, H. C. & HELLEBRAND, S. 2001. An expressed sequence tag (EST) data mining strategy succeeding in the discovery of new G-protein coupled receptors. *Journal of Molecular Biology,* 307**,** 799-813.

WOLEVER, T. M., JOSSE, R. G., LEITER, L. A. & CHIASSON, J. L. 1997. Time of day and glucose tolerance status affect serum short-chain fatty acid concentrations in humans. *Metabolism,* 46**,** 805-11.

WONG, J. M., DE SOUZA, R., KENDALL, C. W., EMAM, A. & JENKINS, D. J. 2006. Colonic health: fermentation and short chain fatty acids. *J Clin Gastroenterol,* 40**,** 235-43.

WOODS, S. C., SEELEY, R. J., PORTE, D. & SCHWARTZ, M. W. 1998. Signals That Regulate Food Intake and Energy Homeostasis. *Science,* 280**,** 1378-1383.

WORTZEL, I. & SEGER, R. 2011. The ERK Cascade: Distinct Functions within Various Subcellular Organelles. *Genes Cancer,* 2**,** 195-209.

WU, H., KANATOUS, S. B., THURMOND, F. A., GALLARDO, T., ISOTANI, E., BASSEL-DUBY, R. & WILLIAMS, R. S. 2002. Regulation of mitochondrial biogenesis in skeletal muscle by CaMK. *Science,* 296**,** 349-52.

WU, J. & SPIEGELMAN, B. M. 2014. Irisin ERKs the fat. *Diabetes,* 63**,** 381-3.

WU, Q., KAZANTZIS, M., DOEGE, H., ORTEGON, A. M., TSANG, B., FALCON, A. & STAHL, A. 2006. Fatty acid transport protein 1 is required for nonshivering thermogenesis in brown adipose tissue. *Diabetes,* 55**,** 3229-37.

WU, Z., PUIGSERVER, P., ANDERSSON, U., ZHANG, C., ADELMANT, G., MOOTHA, V., TROY, A., CINTI, S., LOWELL, B. & SCARPULLA, R. C. 1999a. Mechanisms controlling mitochondrial biogenesis and respiration through the thermogenic coactivator PGC-1. *Cell,* 98**,** 115-124.

WU, Z., ROSEN, E. D., BRUN, R., HAUSER, S., ADELMANT, G., TROY, A. E., MCKEON, C., DARLINGTON, G. J. & SPIEGELMAN, B. M. 1999b. Cross-regulation of C/EBP alpha and PPAR gamma controls the transcriptional pathway of adipogenesis and insulin sensitivity. *Mol Cell,* 3**,** 151-8.

XING, J., GINTY, D. D. & GREENBERG, M. E. 1996. Coupling of the RAS-MAPK Pathway to Gene Activation by RSK2, a Growth Factor-Regulated CREB Kinase. *Science,* 273**,** 959-963.

XIONG, Y., MIYAMOTO, N., SHIBATA, K., VALASEK, M. A., MOTOIKE, T., KEDZIERSKI, R. M. & YANAGISAWA, M. 2004. Short-chain fatty acids stimulate leptin production in adipocytes through the G protein-coupled receptor GPR41. *Proceedings of the National Academy of Sciences of the United States of America,* 101**,** 1045-1050.

XUE, B., COULTER, A., RIM, J. S., KOZA, R. A. & KOZAK, L. P. 2005. Transcriptional Synergy and the Regulation of Ucp1 during Brown Adipocyte Induction in White Fat Depots. *Molecular and Cellular Biology,* 25**,** 8311-8322.

YANASE, T., YASHIRO, T., TAKITANI, K., KATO, S., TANIGUCHI, S., TAKAYANAGI, R. & NAWATA, H. 1997. Differential expression of PPAR gamma1 and gamma2 isoforms in human adipose tissue. *Biochem Biophys Res Commun,* 233**,** 320-4.

YANG, E. S., BAE, J. Y., KIM, T. H., KIM, Y. S., SUK, K. & BAE, Y. C. 2014. Involvement of endoplasmic reticulum stress response in orofacial inflammatory pain. *Exp Neurobiol,* 23**,** 372-80.

YANG, Z. Z., TSCHOPP, O., BAUDRY, A., DUMMLER, B., HYNX, D. & HEMMINGS, B. A. 2004. Physiological functions of protein kinase B/Akt. *Biochem Soc Trans,* 32**,** 350-4.

YEAMAN, S. J. 2004. Hormone-sensitive lipase--new roles for an old enzyme. *Biochem. J.,* 379**,** 11-22.

YEO, G. S. H. & HEISLER, L. K. 2012. Unraveling the brain regulation of appetite: lessons from genetics. *Nat Neurosci,* 15**,** 1343-1349.

YI, P., HADDEN, C. E., ANNES, W. F., JACKSON, D. A., PETERSON, B. C., GILLESPIE, T. A. & JOHNSON, J. T. 2007. The disposition and metabolism of naveglitazar, a peroxisome proliferator-activated receptor alpha-gamma dual, gamma-dominant agonist in mice, rats, and monkeys. *Drug Metab Dispos,* 35**,** 51-61.

YONEKURA, S., HIROTA, S., TOKUTAKE, Y., ROSE, M. T., KATOH, K. & ASO, H. 2014. Dexamethasone and acetate modulate cytoplasmic leptin in bovine preadipocytes. *Asian-Australas J Anim Sci,* 27**,** 567-73.

YONESHIRO, T., AITA, S., MATSUSHITA, M., OKAMATSU-OGURA, Y., KAMEYA, T., KAWAI, Y., MIYAGAWA, M., TSUJISAKI, M. & SAITO, M. 2011. Age-related decrease in cold-activated brown adipose tissue and accumulation of body fat in healthy humans. *Obesity (Silver Spring),* 19**,** 1755-60.

YONEZAWA, T., HAGA, S., KOBAYASHI, Y., KATOH, K. & OBARA, Y. 2009. Short-chain fatty acid signaling pathways in bovine mammary epithelial cells. *Regul Pept,* 153**,** 30-6.

YONEZAWA, T., KATOH, K. & OBARA, Y. 2004. Existence of GPR40 functioning in a human breast cancer cell line, MCF-7. *Biochemical and Biophysical Research Communications,* 314**,** 805-809.

YONEZAWA, T., KOBAYASHI, Y. & OBARA, Y. 2007. Short-chain fatty acids induce acute phosphorylation of the p38 mitogen-activated protein kinase/heat shock protein 27 pathway via GPR43 in the MCF-7 human breast cancer cell line. *Cellular Signalling,* 19**,** 185-193.

YOSHIDA, H. 2007. ER stress and diseases. *Febs j,* 274**,** 630-58.

YOSHIDA, H., HAZE, K., YANAGI, H., YURA, T. & MORI, K. 1998. Identification of the cis-Acting Endoplasmic Reticulum Stress Response Element Responsible for Transcriptional Induction of Mammalian Glucose-regulated Proteins: INVOLVEMENT OF BASIC LEUCINE ZIPPER TRANSCRIPTION FACTORS. *Journal of Biological Chemistry,* 273**,** 33741-33749.

YOSHIDA, H., MATSUI, T., YAMAMOTO, A., OKADA, T. & MORI, K. 2001. XBP1 mRNA is induced by ATF6 and spliced by IRE1 in response to ER stress to produce a highly active transcription factor. *Cell,* 107**,** 881-91.

YOUNG, P., ARCH, J. R. & ASHWELL, M. 1984. Brown adipose tissue in the parametrial fat pad of the mouse. *FEBS Lett,* 167**,** 10-4.

YOUSEFI, S., COOPER, P. R., POTTER, S. L., MUECK, B. & JARAI, G. 2001. Cloning and expression analysis of a novel G-protein-coupled receptor selectively expressed on granulocytes. *Journal of Leukocyte Biology,* 69**,** 1045-1052.

YUZEFOVYCH, L. V., MUSIYENKO, S. I., WILSON, G. L. & RACHEK, L. I. 2013. Mitochondrial DNA Damage and Dysfunction, and Oxidative Stress Are Associated with Endoplasmic Reticulum Stress, Protein Degradation and Apoptosis in High Fat Diet-Induced Insulin Resistance Mice. *PLoS ONE,* 8**,** e54059.

ZAIBI, M. S., STOCKER, C. J., O'DOWD, J., DAVIES, A., BELLAHCENE, M., CAWTHORNE, M. A., BROWN, A. J. H., SMITH, D. M. & ARCH, J. R. S. 2010. Roles of GPR41 and GPR43 in leptin secretory responses of murine adipocytes to short chain fatty acids. *FEBS Letters,* 584**,** 2381-2386.

ZHANG, Y., LI, R., MENG, Y., LI, S., DONELAN, W., ZHAO, Y., QI, L., ZHANG, M., WANG, X., CUI, T., YANG, L. J. & TANG, D. 2014. Irisin stimulates browning of white adipocytes through mitogen-activated protein kinase p38 MAP kinase and ERK MAP kinase signaling. *Diabetes,* 63**,** 514-25.

ZHAO, J., UNELIUS, L., BENGTSSON, T., CANNON, B. & NEDERGAARD, J. 1994. Coexisting beta-adrenoceptor subtypes: significance for thermogenic process in brown fat cells. *American Journal of Physiology - Cell Physiology,* 267**,** C969-C979.

ZHONG, J., MOLINA, H. & PANDEY, A. 2007. Phosphoproteomics. *Curr Protoc Protein Sci,* Chapter 24**,** Unit 24.4.

ZHOU, C., TANG, C., CHANG, E., GE, M., LIN, S., CLINE, E., TAN, C. P., FENG, Y., ZHOU, Y.-P., EIERMANN, G. J., PETROV, A., SALITURO, G., MEINKE, P., MOSLEY, R., AKIYAMA, T. E., EINSTEIN, M., KUMAR, S., BERGER, J., HOWARD, A. D., THORNBERRY, N., MILLS, S. G. & YANG, L. 2010. Discovery of 5-aryloxy-2,4-thiazolidinediones as potent GPR40 agonists. *Bioorganic & Medicinal Chemistry Letters,* 20**,** 1298-1301.

ZHOU, Q., LI, G., DENG, X. Y., HE, X. B., CHEN, L. J., WU, C., SHI, Y., WU, K. P., MEI, L. J., LU, J. X. & ZHOU, N. M. 2012. Activated human hydroxy-carboxylic acid receptor-3 signals to MAP kinase cascades via the PLC-dependent PKC and MMP-mediated EGFR pathways. *British Journal of Pharmacology,* 166**,** 1756-1773.

ZHU, X., HUANG, W. & QIAN, H. 2013. GPR119 agonists: a novel strategy for type 2 diabetes treatment. *Diabetes Mellitus–Insights and Perspectives***,** 59-82.

ZIMMERMANN, R., STRAUSS, J. G., HAEMMERLE, G., SCHOISWOHL, G., BIRNER-GRUENBERGER, R., RIEDERER, M., LASS, A., NEUBERGER, G., EISENHABER, F., HERMETTER, A. & ZECHNER, R. 2004. Fat Mobilization in Adipose Tissue Is Promoted by Adipose Triglyceride Lipase. *Science,* 306**,** 1383-1386.